AN EVALUATION OF SULFIDISATION IN THE FLOTATION RECOVERY OF HEAVILY OXIDISED SULFIDE MINERALS: WITH PARTICULAR REFERENCE TO OXIDISED MERENSKY ORES

By

Andrew James Haigh Newell
B.Eng. (Metallurgical), University of Melbourne
M.Eng.Sc., University of Melbourne

A thesis submitted to the University of Cape Town in fulfilment of the requirements for the degree of Doctor of Philosophy

Department of Chemical Engineering
University of Cape Town
March 2007

STATEMENT OF ORIGINALITY

This thesis has not been submitted whole or in part to any other institution for another degree.

Signed: _____

ACKNOWLEDGEMENTS

I would like to dedicate this thesis to my wife, Helen Swang, without her support and encouragement, this thesis would not have been possible.

I would like to acknowledge with great appreciation the guidance, inspiration and assistance in the preparation of this work by my supervisors, particularly Professor Dee Bradshaw as well as Adjunct Professor Peter Harris.

The technical contributions of those who have assisted in this work both directly and indirectly are gratefully acknowledged, particularly those of Professor Zafir Ekmekçi (electrophoresis and electrochemistry), Professor Bill Skinner (XPS), Miranda Walton (SEM/EDX), Megan Becker (XRD and mineralogy) and Helen Divey and her staff (AAS, HPLC and BET). For fruitful discussions, particularly Professor Zafir Ekmekçi as well as Professor David Bastin and Professor Janusz Laskowski. For assistance with the Russian literature, Elizaveta Burdukova.

I would also like to acknowledge and thank Professor Cyril O'Connor, Professor David Reid and Professor Graham Jackson for their invaluable insights and guidance.

Lastly but not least, to my family and friends, both new and old, for their support and encouragement.

"Success is not final,

failure is not fatal,

it is the courage to continue

that counts."

Sir Winston Churchill

SYNOPSIS

Base-metals play a key role in maintaining the economic well-being of modern society and are mainly won from ore deposits containing sulfide minerals. The separation of the base-metal sulfide minerals from non-sulfide or gangue minerals is accomplished by the exploitation of differences in surface chemistry using a technique known as flotation. With increasing oxidation of the sulfide mineral surfaces, flotation ceases to be an effective tool for their separation and recovery. Where base-metal sulfide minerals have been completely oxidised to form 'oxide' minerals, such as in the near surface levels of a sulfide mineral ore deposit, sulfidisation has been employed to convert the surfaces into a sulfide form and thus made amenable to separation and recovery by flotation.

This thesis has addressed the applicability of sulfidisation to the flotation recovery of heavily oxidised sulfide minerals and was explored in the context of oxidised Merensky ores which contain three dominant sulfide minerals in association with platinum group minerals (PGMs). This investigation used a mineralogically similar ore where the sulfide minerals are in substantially greater abundances, namely a Nkomati massive sulfide ore containing chalcopyrite, pyrrhotite and pentlandite. Two oxidation methods consisting of low temperature thermal oxidation and chemical oxidation with hydrogen peroxide were used to alter the sulfide surfaces.

The oxidation behaviour of the Nkomati ore was characterised in terms of the flotation response as well as SEM/EDX. The oxidation process resulted in the development of thick iron and oxygen rich oxidised layers for thermally oxidised samples. For chemically oxidised samples, the oxidation layer was less than 100 nm thick and no analysis was possible.

Oxidation had a significant effect upon the flotation recoveries of the Nkomati ore and the three sulfide minerals, with pyrrhotite and pentlandite displaying the most reactive behaviour under thermal oxidation and achieving the lowest flotation recoveries. With chemical oxidation there was a clear trend in terms of the recoveries of chalcopyrite > pentlandite > pyrrhotite. For convenience, two oxidised conditions were defined based on the flotation response where ~50% recovery was achieved ('moderate' oxidation) and a recovery of less than 10% ('heavy' oxidation).

The restoration of floatability of the heavily oxidised Nkomati ore and sulfide minerals was explored as a function of sulfidisation potential employing a technique known as Controlled Potential Sulfidisation (CPS). The oxidised sulfide minerals in the Nkomati ore responded well to sulfidisation and there was an optimum sulfidisation potential (Es) (namely -650 mV sulfide ion electrode potential relative to silver/silver chloride (0.01M KCl solution) reference electrode or -315 mV SHE) where maximum flotation recoveries were achieved for all the three sulfide minerals. The sulfidisation mechanisms were elucidated for both the Nkomati ore and single sulfide minerals using other techniques including electrophoresis, XPS and EDTA extraction.

Electrophoretic studies showed that the oxidised Nkomati ore and sulfide minerals adsorbed hydrosulfide ions around the sulfidisation potential where flotation recovery occurred. Moreover, XPS analyses of chalcopyrite and pyrrhotite particles after sulfidisation confirmed that base-metal sulfide species had formed on the oxidised surfaces. The nature of the sulfidisation mechanisms were deduced to be a mixture of anionic exchange and precipitation as reported for the base-metal 'oxide' minerals as well as electrochemical reactions. Sulfidisation mechanisms as a function of sulfidisation intensity have been developed for the three sulfide minerals.

In particular, oxidised chalcopyrite surfaces formed predominantly covellite-like species at lower sulfidisation intensities while a mixture of covellite-like and chalcocite-like phases was found at higher sulfidisation potentials. Mainly pyrite-like species formed on oxidised pyrrhotite surfaces with lower sulfidisation potentials which became pyrrhotite-like phases under more intense sulfidisation conditions. Anodic electrochemical reactions were principally balanced by the cathodic reactions where hydrosulfide ions were converted to elemental sulfur and dissolved oxygen into hydroxyl ions.

When pentlandite was associated with oxidised sulfide minerals, restoration occurred however for pure oxidised samples, sulfidisation did not readily happen and this was matched by a poor flotation response. It was established that the precipitation of copper and iron sulfide species onto the oxidised pentlandite surfaces was responsible for the flotation response. This outcome could be obtained by the addition of base-metal ions during sulfidisation or in situ if processed with other oxidised sulfide minerals.

The presence of calcium ions did not affect the efficacy of sulfidisation nor were the dominant Merensky ore gangue minerals, namely feldspar and pyroxene, sulfidised, demonstrating the suitability of sulfidisation for the recovery of oxidised sulfide minerals from oxidised Merensky ores.

This thesis has shown the potential of using CPS to restore the floatability of oxidised sulfide minerals and has established models to explain the sulfidisation behaviour. Additionally, a novel method for the sulfidisation of oxidised pentlandite has been developed.

LIST OF PUBLICATIONS

(1) Newell, A J H, Bradshaw, D J, Harris, P J, 2005. The effect of heavy oxidation upon flotation and potential remedies for Merensky type sulfides. In Proceedings of the Centenary of Flotation Conference, Brisbane, Australia, Ed. G. Jameson, Australasian Institution of Mining and Metallurgy (Publishers), Parkville, Australia, pp 1007-1016.

(2) Newell, A J H, Bradshaw, D J, Harris, P J, 2006. The effect of heavy oxidation upon flotation and potential remedies for Merensky type sulfides. Minerals Engineering, 19, 675–686.

(3) Newell, A J H, Ekmekçi Z, Bradshaw, D J, 2006. Sulfidisation mechanisms for heavily oxidised sulfide minerals. In Proceedings of the XXIIIrd International Mineral Processing Congress, Editors G.Önal, N. Acarkan, M.S. Çelik, F. Arslan, G. Ateşok, A. Güney, A.A. Sirkeci, A.E. Yüce and K.T. Perek, Istanbul, Turkey, Promedadvertising Agency (Publishers), Volume 1, pp 560-565.

(4) Newell, A.J.H., Skinner, W.M., Bradshaw, D.J., 2006. Restoring the floatability of oxidised sulfides using sulfidisation, International Journal for Mineral Processing, accepted for publication.

(5) Newell, A J H and Bradshaw, D J, 2006. The application of sulfidisation in the flotation recovery of heavily oxidised pentlandite. In Proceedings of Reagents 06, Cape Town, South Africa., submitted to MEI for publication.

(6) Newell, A J H and Bradshaw, D J, 2006. The development of a sulfidisation technique to restore the flotation of oxidised pentlandite, Minerals Engineering, submitted for publication.

LIST OF PATENTS

(1) Newell, A J H and Bradshaw, D J, 2006. The application of sulfidisation to oxidised and surface oxidised base and precious metal minerals, South African Provisional Patent Application No. 142989.

CONFERENCE PRESENTATIONS

(1) The evaluation of sulphidisation in the flotation of surface oxidised sulphide minerals: with special reference to Merensky ores. Part One: The effect of oxidation upon sulfide mineral flotation. Chemical Engineering R&D 2004, SAIChE, May 2004, Peninsula Technikon, Cape Town, South Africa. Also Poster.

(2) The effect of heavy oxidation upon flotation and potential remedies for Merensky type sulfides. Mineral Processing 2004, SAIMM, August 2004, Lord Charles Hotel, Somerset West, South Africa.

(3) The effect of heavy oxidation upon flotation and potential remedies for Merensky type sulfides. The Centenary of Flotation Conference, AusIMM/SME, June 2005, Brisbane, Australia. Also Poster.

(4) Restoring the floatability of oxidised sulfides using sulfidisation. Mineral Processing 2006, SAIMM, August 2006, Vineyard Hotel, Newlands, Cape Town, South Africa.

(5) Sulfidisation mechanisms for heavily oxidised sulfide minerals. XXXIIIrd International Minerals Processing Congress, September 2006, Ankara, Turkey.

(6) The application of sulfidisation in the flotation recovery of heavily oxidised pentlandite. Reagents 06, MEI, November 2006, Mount Nelson Hotel, Cape Town, South Africa.

TABLE OF CONTENTS

LIST OF FIGURES

PAGE NO

LIST OF TABLES

PAGE NO

LIST OF ELECTRONIC APPENDICES

APPENDIX A: CALCULATIONS

A1: D \ Appendix A \ Sulfide mineral calculations.pdf

A1: D \ Appendix A \ Oxidation calculations.pdf

A3: D \ Appendix A \ Electrochemical calculations.xls

APPENDIX B: OXIDATION STUDIES

B1: D \ Appendix B \ Nkomati ore.xls

B2: D \ Appendix B \ Pentlandite.xls

B3: D \ Appendix B \ Merensky ore gangue minerals.xls

APPENDIX C: SULFIDISATION STUDIES

C1: D \ Appendix C \ Nkomati ore.xls

C2: D \ Appendix C \ Pentlandite.xls

C3: D \ Appendix C \ Merensky ore gangue minerals.xls

APPENDIX D: CHARACTERISATION STUDIES

D1: D \ Appendix D \ Photomicrographs and XRD.pdf

D2: D \ Appendix D \ Electrophoresis.xls

D3: D \ Appendix D \ XPS.pdf

D4: D \ Appendix D \ Electrochemistry.xls

D5: D \ Appendix D \ EDTA extraction.xls

D6: D \ Appendix D \ QEM*SEM.pdf

APPENDIX E: OTHER STUDIES

E1: D \ Appendix E \ Hydrosulfide ion adsorption.xls

E2: D \ Appendix E \ Hydrolysis.xls

E2: D \ Appendix E \ Reagents.pdf

NOMENCLATURE

Es	Sulfide ion electrode potential (mV)
Eh	Standard hydrogen electrode potential (mV)
Γ	amount of adsorbed species

UNITS

Å	Angstrom (10^{-10} m)
g	grams
IS	Ionic strength
L	litre
L/min	litres/minute @ 101 kPa and 20°C
min	minute
M	molarity (moles/litre)
m^2	square metres
mL	millilitre
mV	millivolts
µm	micrometres or microns
nm	nanometres
s	second
t	time
V	volts

LIST OF ABBREVIATIONS

Cpy	chalcopyrite
EDX	Energy dispersive spectroscopy
HSO	hydrosulfide oxidation
ORP	Oxidation reduction potential (mV)
pH_{IEP}	pH at which the iso-electric potential occurs
Pn	pentlandite
Po	pyrrhotite
SCE	Saturated calomel electrode

SEM	Scanning electron microscope
SHE	Standard hydrogen electrode
SIBX	Sodium isobutyl xanthate
XPS	X-ray photo-electron spectroscopy
XRD	X-ray diffraction

GLOSSARY

Within the context of this thesis, the following meanings and definitions apply.

Base-metal

Defined as a metal that oxidises when heated in the air, the group of *base-metals* include iron, copper, nickel, cobalt, zinc and lead.

Concentrate

One of the two product streams of the flotation process, the other being the flotation *tails*. The concentrate stream contains the *valuable minerals* which is processed typically by smelting and refining for metal recovery.

Conditioning

Conditioning is the contact time between the slurry and a reagent and is generally between 3 and 10 minutes long.

Controlled Potential Sulfidisation (CPS)

A sulfidisation technique which employs a *sulfide ion specific electrode* to control the addition rate of the *sulfidising reagent* and maintain a constant Es value during *conditioning*.

Floatability

Floatability describes the tendency of a *mineral* to float and be recovered as a *concentrate*.

Flotation cell

A vessel where the flotation separation is conducted. Industrially, *flotation cells* are cylindrical or rectangular tanks containing an impeller mechanism to maintain solids suspension, disperse the air as fine bubbles and achieve mineral particle-bubble contact.

Gangue minerals

Gangue minerals are *minerals* that are not considered *valuable* and are often silicates. These minerals report to the flotation *tailings* with good *liberation* and separation efficiencies.

Grade

The mass fraction of a *valuable mineral* present in a process stream such as the feed or concentrate. Typically expressed in terms of a *base-metal* as a percentage.

Liberation

The degree to which *valuable minerals* are separated from each other and particularly *gangue minerals*. Poorly liberated particles consist of a mixture of the *valuable* and *gangue* minerals and are often termed composites.

Mechanism

A thermodynamically favoured equation that describes the chemical interaction between two chemical species, particularly gaseous and aqueous species with mineral surfaces.

Ore

A mixture of *gangue* and *valuable* minerals that is mined from a deposit or orebody.

Oxidation

The reaction between sulfide *minerals* and an oxidant, such as oxygen, whereby the surface becomes chemically altered and *oxidation* products form.

'Oxide' minerals

Minerals that contain a *base-metal* either as an oxide, hydroxide, oxy-hydroxide, carbonates, hydroxy-carbonate, sulfate, silicate, etcetera. Better known base-metal 'oxide' minerals include cuprite, azurite, malachite, chrysocolla, cerussite, anglesite, smithsonsite, willemite and zincite. They are found in the near surface regions of sulfide ore bodies as a result of in-situ oxidation or weathering of the sulfide minerals.

Platinum group elements (PGEs)

The elements platinum, palladium, rhodium, ruthenium, osmium and iridium.

Platinum group minerals (PGMs)

The minerals that contain the *PGEs*, typically sulfides, arsenides and alloys.

Pulp/slurry

A mixture of fine (<100μm) *mineral* particles and gas bubbles suspended in water containing dissolved *reagents*.

Reagents

Collector

A *collector* selectively adsorbs onto the surface of *valuable minerals* and confers *floatability*.

Sulfidising reagent

A *sulfidising reagent* can create or regenerate a sulfide surface on *base-metal 'oxide' minerals* and thus permit adsorption of *sulfide mineral collectors*. Typical *sulfidising reagents* include sodium sulfide and sodium hydrosulfide.

Recovery

The mass percentage of a *valuable mineral* or element in the feed that reports to the *concentrate*.

Sulfide ion electrode

An ion specific electrode that is sensitive to only sulfide ions. It consists of a silver/silver sulfide electrode and a reference electrode.

Sulfide minerals

A *mineral* typically composed of two base-metals (one is typically iron) and sulfur. Typical *sulfide minerals* include, pyrrhotite, chalcopyrite, and pentlandite.

Tails

The waste stream from the *flotation cell*, which ideally contains all of the *gangue* material and none of the *valuable minerals*.

Valuable minerals

Valuable minerals are commonly *base-metal sulfide or 'oxide' minerals* as well as precious metal *minerals* or alloys (see *PGEs*) that occur in the *ore* in economic quantities.

CHAPTER 1

INTRODUCTION

The general impact of surface oxidation upon the flotation behaviour of sulfide minerals is well known and a poor flotation response is associated with oxidised surfaces. The ability to improve the flotation recovery of oxidised sulfide minerals present in oxidised Merensky ores offers significant economic benefits to the platinum industry in terms of increased revenue and the opportunity to maximise the recovery of both base-metals and platinum group elements (PGEs) from these unique resources.

The nature of the oxidation levels examined in this thesis reflected those that arise from the in-situ weathering processes that occur when sulfide ore-bodies are located near the surface. This happens due to the reactive nature of the sulfide mineral surfaces in the presence of oxygen and water. Physical abrasion processes, such as further milling, fail to restore fresh sulfide surfaces and thus floatability. The surface oxidation that occurs during processing is necessarily difficult to avoid since the mining and processing stages utilise water and do not exclude air. This aspect has not been addressed in this thesis.

While the general effect of oxidation upon the flotation response of sulfide minerals is well known, it has not been previously quantified nor explored for sulfide mineral assemblages such as that found in Merensky ores, where the main sulfide minerals are chalcopyrite, pyrrhotite, and pentlandite. In particular, the effect of heavy oxidation on these sulfide minerals has been examined. The restoration of the floatability of the oxidised sulfide minerals has been explored employing a technique that has been successfully applied to the flotation recovery of base-metal 'oxide' minerals, namely sulfidisation.

1.1 Objectives

The overall objective of this thesis is to investigate the differences in flotation response between chalcopyrite, pyrrhotite, and pentlandite sulfide minerals in terms of the deleterious effect of oxidation and the restoration by sulfidisation. Additionally the applicability of sulfidisation in the treatment of oxidised Merensky ores is examined.

The primary research objectives of this thesis are to characterise the effect of oxidation upon sulfide mineral floatability, to determine the suitability of sulfidisation to restore the flotation recovery of oxidised sulfide minerals, to compare the sulfidisation characteristics of oxidised sulfide minerals with those of base-metal 'oxide' mineral counterparts and to develop sulfidisation models for each of the three sulfide minerals.

Secondary research objectives arising from the primary objectives include a comparison of oxidation techniques, an assessment of the effect of calcium ions during sulfidisation, the development of a novel technique to sulfidise oxidised pentlandite and to determine whether the sulfidisation process had any effect upon the flotation behaviour of Merensky ore gangue minerals.

1.2 Scope of the thesis

This thesis presents the results of a study of the oxidation and subsequent sulfidisation of a pyrrhotite-pentlandite-chalcopyrite mixed ore as well as pure mineral samples where appropriate and Merensky ore gangue minerals. A massive sulfide ore from Nkomati with similar mineralogy to the Merensky ore sulfide suite was used as the study material and oxidised both chemically and thermally. Two levels of oxidation are specifically addressed, namely 'moderate' and 'heavy' oxidation which were defined based on the flotation response. The change in the floatability of the oxidised and sulfidised samples was evaluated as a function of the degree of oxidation as well as the sulfidisation intensity. Sulfidisation was conducted using the Controlled Potential Sulfidisation (CPS) technique (Jones and Woodcock, 1978a and 1978b) as a function of the sulfide ion electrode potential (Es) and the subsequent flotation response measured using micro-flotation. A number of techniques were employed to elucidate the sulfidisation mechanisms and included scanning electron microscopy (SEM), energy dispersive spectroscopy (EDX), X-ray photo-electron spectroscopy (XPS), electrophoresis, electrochemistry as well as EDTA extractions.

The location of the thesis within base-metal Mineral Processing Research is presented in Figure 1-1.

BASE-METAL MINERAL PROCESSING

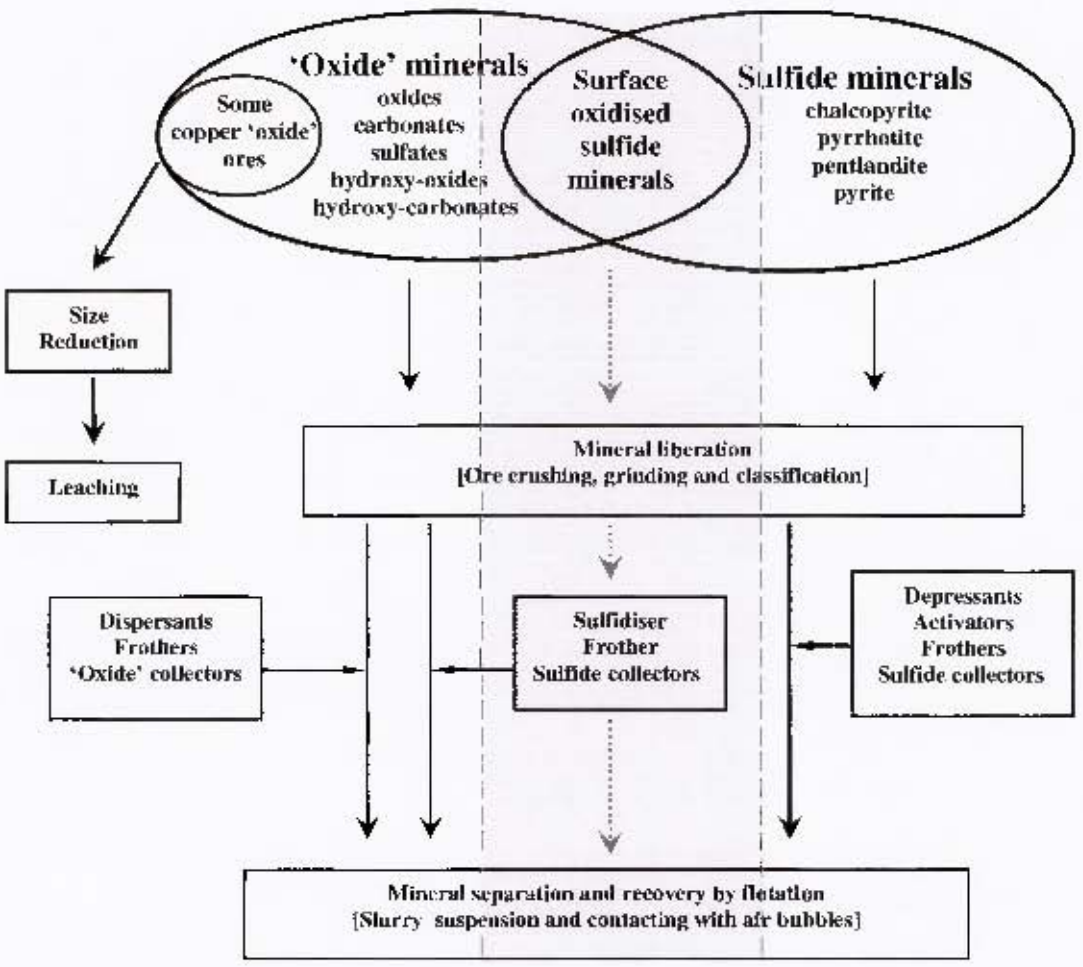

Figure 1-1: Location of the thesis (in shaded area) in base-metal Mineral Processing Research

This thesis has focussed on the sulfide mineral behaviour that occurs within a specific electrochemical window as shown in Figure 1-2, which reflects the typical range of the sulfidisation parameters used in practice. The electrochemical window defines a moderately reducing and alkaline environment where the sulfidisation of base-metal 'oxide' minerals such as malachite and cerussite and their subsequent flotation recovery under more oxidising conditions has been successful.

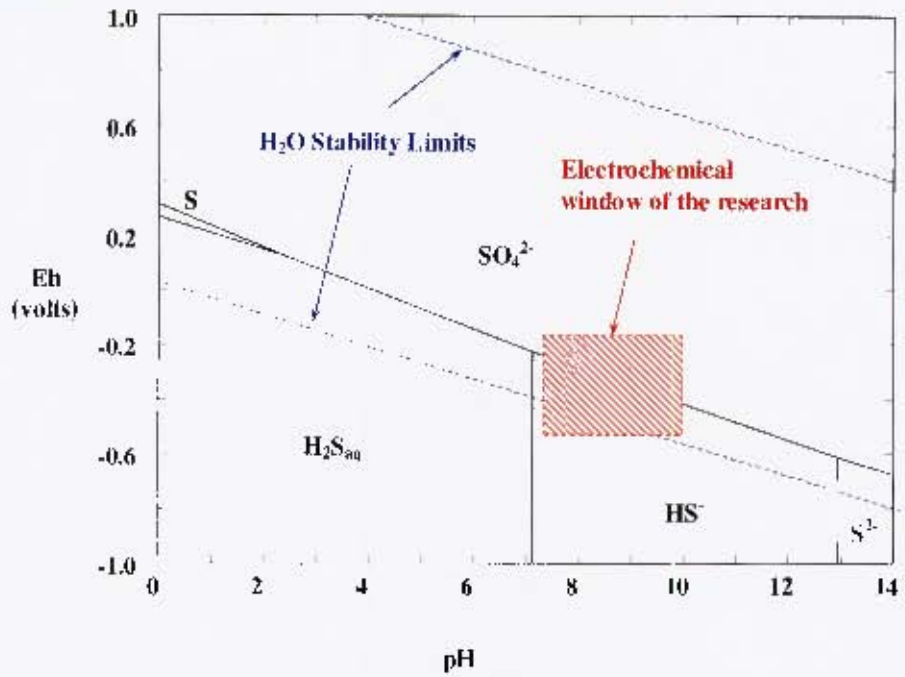

Figure 1-2: Location of the research in the electrochemical domain (based on the S-H_2O system at 25°C and 10^{-4}M total dissolved sulfur) (after Poinc, 2002)

In this electrochemical window, hydrosulfide ions are the dominant sulfur species and the alkalinity limits the nature of the species that may be present. CPS is an electrochemical technique that measures and controls the sulfidisation process to maintain conditions within this window.

1.3 Organisation of the thesis

The literature is reviewed in Chapter 2 where the pre-existing knowledge base regarding sulfide mineral oxidation and the sulfidisation process is explored and provides a context for the research. Chapter 2 ends with the list of key questions and the associated hypotheses. The experimental methodology, techniques and equipment details are provided in Chapter 3.

Chapter 4 presents the results of the testwork that addressed the oxidation of and subsequent flotation response of sulfide and Merensky ore gangue minerals. The results of the testwork that examined the effect of sulfidisation upon the flotation of oxidised sulfide minerals as well as Merensky ore gangue minerals are given in Chapter 5. The results are discussed in Chapter 6, including the sulfidisation mechanisms for each of the three oxidised sulfide minerals. Chapter 7 presents the conclusions and recommendations regarding the outcomes of the research.

CHAPTER 2

LITERATURE REVIEW

2.1 Flotation overview

The flotation separation process represents the largest and most spectacular application of surface chemistry in the world today with over several billion tonnes of material processed annually. With humble beginnings at the turn of the 20th century, where it was developed to separate lead and zinc sulfide minerals from non-sulfide minerals, flotation remains the dominant separation process for the recovery of a wide range of base-metals such as copper and nickel as well as precious metals including the platinum group elements (PGEs). The process has been successfully applied to the separation of non-sulfide minerals from each other and in waste treatment and environmental remediation.

The flotation separation process is based upon exploiting the differences in surface chemical properties between liberated mineral particles in an aqueous environment. In particular, the ability of sulfide mineral surfaces to adsorb a specific chemical or reagent known as a collector allows their surfaces to become hydrophobic and attach to air bubbles. The sulfide mineral-laden bubbles rise to the surface of the flotation vessel and form a froth phase which is consequently removed, thus effecting a separation from the non-floating or gangue minerals. Important factors include the nature and the condition of the mineral surfaces as well as the type and concentration of the solution species, particularly the chemicals or reagents employed to achieve the mineral separation.

2.2 Sulfide minerals

Sulfide minerals are a major source of base-metals and commonly found with non-sulfide or gangue minerals as an orebody. Exploitation of the orebody occurs through mining, mineral liberation, separation and concentration activities, typically flotation. In Merensky ores, the PGEs are predominately associated with the iron-bearing sulfide minerals chalcopyrite, pyrrhotite and pentlandite. These three sulfide minerals and their subsequent process behaviours are the focus of this research.

2.2.1 Properties

Most sulfide minerals exhibit poor or absent cleavage, resulting in surfaces that are typically very topographically irregular with defects induced by fracture. Although the effect of bulk defects and impurities are poorly understood, they do affect the chemical reactivity of the mineral surface (Rosso and Vaughan, 2006).

Table 2-1 summarises the important properties of the three sulfide minerals studied in this research, including the three forms of pyrrhotite. Unlike the other two sulfide minerals, pentlandite has a cubic cleavage while pyrrhotite is characterised by cationic vacancies which significantly impacts the mineral reactivity. All the sulfide minerals are highly conducting, with chalcopyrite exhibiting the greatest resistivity and classified as a semiconductor. While the other two minerals display metallic conduction, the cationic vacancies in metal deficient pyrrhotite structures result in p-type behaviour. Of the three sulfide minerals, only monoclinic pyrrhotite exhibits any significant magnetic properties.

Table 2-1: Important properties of the three sulfide minerals at 25°C
(after Pearce *et al*, 2006)

Sulfide Mineral	Chemical Formula	Crystal Structure	Conductivity Type	Electrical Resistivity (ohm-cm)	Magnetic Property	Magnetic Susceptibility (10^{-6} mole^{-1}cgs)
Chalcopyrite	$CuFeS_2$	Tetragonal	Semiconductor : n-type	10^{-5} – 150	Antiferromagnetic	~32
Pyrrhotite	Fe_7S_8	Monoclinic	Metal : p-type	10^{-6} – 10^{-1}	Ferrimagnetic	Av. 125,000
Pyrrhotite	$Fe_{1-x}S$	Hexagonal	Metal		Antiferromagnetic	
Troilite	FeS	Hexagonal	Metal : p-type	10^{-6} – 10^{-1}	Antiferromagnetic	5,187
Pentlandite	$(Fe,Ni)_9S_8$	Face centred cubic	Metal		Pauli paramagnetic	

2.2.1.1 Chalcopyrite

Chalcopyrite ($CuFeS_2$) is the most important ore mineral of copper and consists of 30.43 wt% iron, 34.63 wt.% copper and 34.94 wt.% sulphur. Chalcopyrite has a brassy to honey yellow colour and displays a tetragonal crystal structure. Copper is present as Cu(I) while iron is in the Fe(III) form, giving a formula of $Cu^{+}Fe^{3+}S_2$ (Pearce *et al*, 2006).

Chalcopyrite does not display any ordered magnetic properties at room temperature and behaves as a typical narrow band gap n-type semiconductor at room temperature (Pearce *et al*, 2006). The top two layers of fractured chalcopyrite apparently have a 50 wt.% pyritic content (Rosso and Vaughan, 2006).

Pearce *et al* (2006) noted that in the absence of any cleavage, the limitations associated with a definitive interpretation of XPS data as well as the relative complexity of the electronic structure of chalcopyrite, have all contributed to an incomplete and controversial understanding of the chalcopyrite surface.

2.2.1.2 Pyrrhotite

Pyrrhotite is the second most abundant iron sulfide mineral after the ubiquitous pyrite. Pyrrhotite exhibits a range of compositions represented by the general formula $Fe_{1-x}S$ (where x varies from 0 to 0.17). The changing amount of iron in the structure is balanced by the ratio of Fe(II) to Fe(III). The presence of Fe(III) defects in pyrrhotite surfaces has been studied by Pratt *et al* (1994). Pyrrhotite is bronze to dark brown in colour and has a nominal chemical composition of 62.33 wt.% iron and 37.67 wt.% sulfur. In mineral processing, pyrrhotite is generally an unwanted mineral, unless it is associated with or hosts precious metals, such as in Merensky ores.

Pyrrhotite consists of a family of mineral phases with structures based on the hexagonal NiAs-type structure. Complex superstructures arise from the ordering of iron atom vacancies in layers parallel to the basal plane. Troilite (FeS) and the intermediate phases (Fe_9S_{10} and $Fe_{10}S_{11}$) are mostly hexagonal while monoclinic pyrrhotite (Fe_7S_8) exhibits the maximum iron deficiency. Given the complexity of these materials, it is not surprising that there have been few detailed studies of the surface structure and surface chemistry of pyrrhotite (Rosso and Vaughan, 2006).

Only monoclinic pyrrhotite displays any significant magnetic behaviour and is classified as ferromagnetic. The value of the saturation magnetisation varies between 6 and 18 $Am^{-2}kg^{-1}$ depending upon the particle size (O'Reilly *et al*, 2000).

2.2.1.3 Pentlandite

Pentlandite is a primary source of nickel and consists of 32.56 wt.% iron, 34.21 wt.% nickel and 33.23 wt. % sulfur. It is brown to bronze in colour and displays a cubic crystalline habit. Pentlandite is a metallic conductor with Pauli paramagnetic magnetic character and can be considered an alloy of nickel, iron and sulfur, with a molar excess of metal (Warner *et al*, 1992).

Pentlandite is ubiquitously found in an intimate textural association with pyrrhotite. It may occur as grains along fractures and boundaries of pyrrhotite grains or as smaller irregular, flame-like, ex-solution structures within the pyrrhotite grains. Subsequently, while granular pentlandite tends to liberated, the flame variety is more commonly found as composites in mineral processing operations. Pyrrhotite formed in association with pentlandite can carry nickel in solid solution (Kelly and Vaughan, 1983).

2.2.2 Oxidation

The instability of sulfide minerals when exposed to the Earth's atmosphere or oxygenated surface waters makes redox reactions, particularly oxidation, of great importance in determining the behaviour of sulfide minerals. In mineral processing, other oxidants (notably Fe(III) ions) are important and factors such as temperature and pH make major contributions to the rates of these redox reactions. The roles played by a range of bacteria are also important (Rosso and Vaughan, 2006).

Sulfide mineral surfaces undergo significant changes in the surface layers due to structural and chemical rearrangements after exposure to oxidants. The mild oxidation of iron-bearing sulfides, such as those found in Merensky ores, in the presence of either air or air and water proceed through a similar mechanism. Iron is preferentially lost from the lattice to form surface iron hydroxides and oxy-hydroxides while the underlying mineral lattice becomes enriched in sulfur (Smart *et al*, 2003). Smart (1994) proposed the following generic oxidation reaction for both pyrrhotite and pentlandite under aqueous conditions:

$$MS + xH_2O + 1/2xO_2 \rightarrow M_{1-x}S + xM(OH)_2 \quad \text{.....(2-1)}$$

where MS represents a metal sulfide.

2.2.2.1 Chalcopyrite

The oxidation of chalcopyrite in air was reported to have formed mainly iron oxy-hydroxide and hydrated iron oxide surface products as well as copper oxides (Smart, 1991; Zachwieja *et al*, 1989 and Buckley and Woods, 1984). Copper and sulfur enrichment in the underlying surface resulted in the formation of CuS (Luttrell and Yoon, 1984) as well as the compositional phase CuS_2 (Buckley and Woods, 1984). After 10 minutes exposure to air, the oxidised layer had an average thickness of 1.5 nm while after 100 minutes it had increased to around 4.5 nm (Yin *et al*, 1995). The surface oxidation products on the chalcopyrite surfaces were readily removed (Zachwieja *et al*, 1989).

Similar results have been reported for the aqueous oxidation of chalcopyrite. Under mildly reducing conditions at pH 9.2, using electrochemical techniques Yin *et al* (2000) proposed the following reaction:

$$2CuFeS_2 + 6xOH^- \rightarrow CuFe_{1-x}S_2 + xFe_2O_3 + 3xH_2O + 6xe^- \quad \text{.....(2-2)}$$

At higher oxidation potentials, two further reactions occurred:

$$2CuFeS_2 + 6OH^- \rightarrow 2CuS_2^* + Fe_2O_3 + 3H_2O + 6e^- \quad \text{.....(2-3)}$$

$$CuFeS_2 + 3OH^- \rightarrow CuS_2^* + Fe(OH)_3 + 6e^- \quad \text{.....(2-4)}$$

At potentials just above the rest potential of chalcopyrite, a monolayer of $Fe_2O_3/Fe(OH)_3$ was reported to form which passivated the surface. Copper and sulfur were left unoxidised as a metastable phase of CuS_2 stoichiometry (CuS_2^*). With increasing potentials, the reactions continued, removing iron from deeper within the chalcopyrite, with the solid-state diffusion of the iron being the rate-controlling mechanism (Yin *et al*, 2000). This is depicted in Figure 2-1 in a simplified model of the aqueous oxidation of chalcopyrite (Vaughan *et al*, 1995).

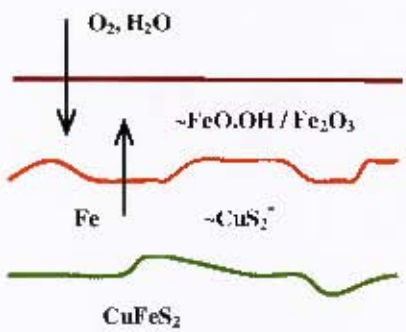

Figure 2-1: Aqueous oxidation model for chalcopyrite (based on Vaughan *et al*, 1995)

Electrochemical oxidation of chalcopyrite under alkaline conditions produced a superficial layer of heterogeneous oxidised materials with 'islands' of oxide, hydroxide and sulfate species (Velasquez *et al*, 2005).

2.2.2.2 Pyrrhotite

Oxidation products such as iron hydroxides, oxy-hydroxides and oxides were reported to form a coating on pyrrhotite under a variety of oxidising conditions (Buckley and Woods, 1985a and b; Pratt *et al*, 1994 and Jones *et al*, 1992). Using XPS, Buckley and Woods (1985a) studied the oxidation of pyrrhotite in air over 50 hours and reported that a

chemically stratified structure ($FeO_{1.5}$, FeS_2, Fe_2S_3 and Fe_7S_8) had formed due to the outward diffusion of iron from the bulk lattice. This oxidation mechanism for pyrrhotite has been corroborated by other researchers (Pratt *et al*, 1994 and Mycroft *et al*, 1995). The thickness of the oxidised layer was 5 Å while the S-depleted sulfide layer was 30 Å (Mycroft *et al*, 1995). Janzen *et al* (2000) reported no significant difference in the relative rates of oxidation although more recent work suggests that the monoclinic form may be less reactive (Belzile *et al*, 2004).

Pyrrhotite samples ground under pure water were considered heavily oxidised, with a significant sulfate presence in the surface products (Jones *et al*, 1992). Following ultrasonic treatment, decantation and washing of the samples, the principal entities remaining detected by XPS were carbonates and FeO.OH. The abundance of Fe(III) hydroxide was much greater after aqueous oxidation compared to air oxidised samples.

EDX analyses of pyrrhotite oxidised for 3 hours in an alkaline solution formed oxidation layers which were about 10 nm thick. Auger analyses of these oxidised samples identified a thin iron and oxygen rich surface layer covering an iron depleted and sulfur enriched subsurface. Further analyses of these samples with XPS confirmed that Fe(III) oxides and hydroxides dominated the surface while sulfur was present as a large array of species, mainly as S^{2-} (unoxidised pyrrhotite), sulfate, polysulfides, disulfides (pyrite) and thiosulfates (Legrand *et al*, 2005b).

Cyclic voltammetric studies of pyrrhotite electrodes under alkaline conditions identified hydrated iron oxide and sulfur as well as sulfate as the products of anodic oxidation (Hamilton and Woods, 1981). The cathodic peak was considered to be iron sulfide that formed from the iron oxide and the sulfur product as well as the reduction of the remaining ferric oxide to ferrous oxide. On the subsequent positive-going scan, the anodic peak was associated with the oxidation of the ferrous oxide.

Pyrrhotite reacted with 0.2M acetic acid (~pH 2.4) for 15 minutes was found to have a severely iron-depleted surface as a result of the formation of a soluble Fe(II) species. Elemental sulfur but no sulfate was reported, however at a higher oxidation potential under acidic conditions sulfate would be expected to form (Buckley and Woods, 1985b). The reaction of 0.05M perchloric acid with ground pyrrhotite surfaces was studied under a range of conditions (Jones *et al*, 1992). The major effect was an increased exposure of

Fe(II) oxide/hydroxides and iron sulfides with a decreased abundance of sulfates, carbonates and Fe(III) species. The iron-deficient surface was found to have re-ordered to form Fe_2S_3 with the potential for pyrite formation with greater iron losses while the oxidation layer was considered discontinuous and patchy.

Pyrrhotite has been reported to be particularly susceptible to oxidation compared to other sulfide minerals (Isihara and Kagamai, 1964). The oxidation of pyrrhotite progressed more rapidly than that of pentlandite in aerated aqueous environments (Broomhead and Layers, 1976, Legrand *et al*, 2005a and Heiskanen *et al*, 1991). Continued oxidation of the two minerals caused the conversion of Fe(II) to Fe(III) and increased the acidity of the solution, which attacked both minerals (Broomhead and Layers, 1976). The reaction rates of the two minerals as well as the degree of surface oxidation were proportional to the dissolved oxygen concentration (Broomhead and Layers, 1976 and Legrand *et al*, 2005b). Based on the degree of surface alteration, five minutes of oxidation of pyrrhotite was equal to thirty minutes of pentlandite. Only Fe(III)S and polysulfides were reported in the oxidation layer on the pyrrhotite surfaces (Legrand *et al*, 2005b). The enhanced reactivity of pyrrhotite was attributed to the presence of vacancies in the pyrrhotite crystal structure.

2.2.2.3 Pentlandite

After an hour of contact with air, pentlandite surfaces were reported to be covered in hydrated iron oxides and nickel oxides (Buckley and Woods, 1991). With increased exposure to a day, considerably more oxidation resulted. Beneath the oxide layer, the pentlandite was considered to be metal deficient and present as a restructured nickel-iron sulfide species as follows:

$$Fe_4Ni_5S_8 + 0.75xO_2 + 0.5xH_2O \rightarrow Fe_{4-x}Ni_5S_8 + 0.5xFe_2O_3.H_2O \quad \text{.....(2-5)}$$

A number of surface techniques were used to study the aqueous oxidisation of pentlandite under alkaline conditions. A 10 nm thick oxide layer had formed after 3 hours and significant enrichment in oxygen and iron was reported to have occurred at the surface while the subsurface had experienced substantial depletion in nickel and sulfur (Legrand *et al*, 1997 and 2005b). With greater exposure, the presence of FeO.OH was reported with nickel sulfate as the dominant surface species while violarite had formed in the subsurface region (Legrand *et al*, 1997, 2005a and 2005b). Other oxidation products included $Ni(OH)_2$, Fe(III)S and polysulfide species in the oxidised layer. Legrand *et al* (1997)

concluded that the oxidation of pentlandite in either air or water followed a similar trend to that of pyrrhotite.

Cyclic voltammograms of a pentlandite electrode under alkaline conditions confirmed that the major process in the oxidation of pentlandite was the selective removal of iron, while elemental sulfur was the primary sulfur oxidation product. Minor quantities of sulfate were formed that increased in quantity with greater oxidation potentials. Like pyrrhotite, the cyclic voltammogram of a pentlandite electrode displayed anodic and cathodic peaks that were identified with the oxidation and reduction of iron oxide and sulfur products. It was therefore concluded that the aqueous oxidation products of pentlandite were similar to those of pyrrhotite. An hour of aqueous oxidation produced a considerably thicker oxidised layer than that after a day of exposure to air and was not readily dislodged. Although the same oxidation mechanism was observed, pentlandite samples from different deposits varied in reactivity towards oxygen (Buckley and Woods, 1991).

Thornber (1983) studied the mineralogical and electrochemical stability of pentlandite and violarite. In an assemblage consisting of pentlandite, pyrrhotite and pyrite, pentlandite was the first sulfide mineral to react at the lowest oxidation potential. Pentlandite oxidised to violarite by releasing nickel and iron into solution:

$$Fe_{4.5}Ni_{4.5}S_8 \rightarrow 2FeNi_2S_4 + 0.5Ni^{2+} + 2.5Fe^{2+} + 6e^- \quad \text{.....(2-6)}$$

The increased nickel activity caused the pyrrhotite to become unstable, reacting with nickel from solution to form violarite:

$$Fe_7S_8 + 4Ni^{2+} \rightarrow 2FeNi_2S_4 + 5Fe^{2+} + 2e^- \quad \text{.....(2-7)}$$

The effect of a number of different oxidants, including air, steam and hydrogen peroxide, upon the surface of synthetic pentlandite has been reported (Richardson and Vaughan, 1989). Like the other studies, the oxidation layer was considered to consist of iron oxy-hydroxide species as well as nickel oxide and iron sulfate. The strength of the oxidant used, as well as the thermodynamic stability of the phases, governed the proportions of the phases present in the oxide layer. The mineral subsurface was observed to become enriched in nickel after oxidation, which then restructured to form violarite ($FeNi_2S_4$) as reported by other researchers.

Warner *et al* (1996) prepared Eh-pH diagrams for the Fe-Ni-S aqueous system showing many of these features such as the co-existence of violarite and pentlandite with the species

FeO.OH and $Ni(OH)_2$. Under strong acidic conditions (e.g. 1M HCl), pentlandite was observed to adopt a steady-state potential at 80°C of -168 mV SHE and decomposed oxidatively with the liberation of aqueous metal ions and hydrogen sulfide (Warner *et al*, 1992).

2.2.2.4 Oxidation of sulfide mineral ore bodies

Base-metal sulfide mineral orebodies in contact with aerated ground waters experience oxidation. Iron-bearing sulfide minerals preferentially lose iron (Smart, 1994) while lattice bound sulfur is sequentially oxidised to polysulfides, elemental sulfur and then through a series of sulfoxy species. The acidity of the ground water becomes greater, which in turn attacks the minerals. With increasing oxidation, the primary sulfide minerals oxidise through a series of secondary sulfide minerals and eventually to 'oxide' minerals (Garrels, 1953 and Sato, 1960a), the nature of which is dependent upon the weathering environment and oxidising conditions (Sato, 1960a and b, Blain and Andrew, 1977, de Waal, 1978 and Thornber, 1983). For ore bodies that contain significant quantities of sulfide minerals, the electrical properties of the sulfide minerals allow a large galvanic cell to form over the surface of the orebody, which maintains the continuity of the oxidation process (Thornber, 1983). The effect of oxidation on a sulfide mineral orebody is shown schematically in Figure 2-2.

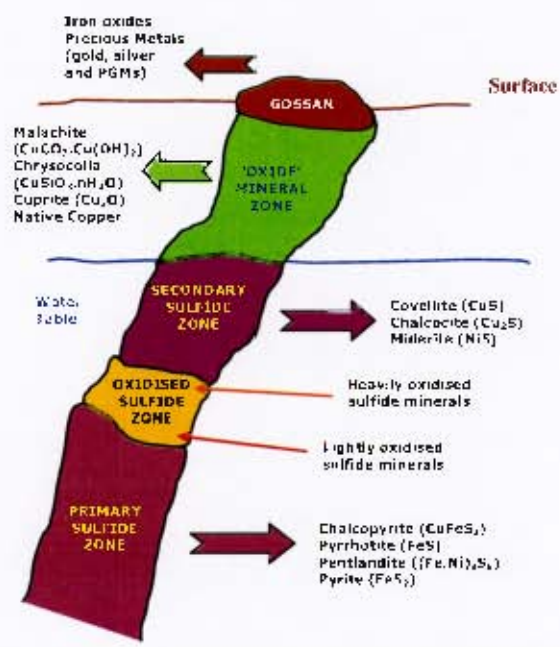

Figure 2-2: Schematic representation of the oxidation of a sulfide mineral ore body (based on Guilbert and Park, 1986)

2.2.2.5 Base-metal 'oxide' minerals

The continued oxidation of base-metal sulfide minerals, such as that which occurs during the weathering of the upper regions of a base-metal sulfide ore body, results in the formation of base-metal 'oxide' minerals, where all of the iron and generally all of the sulfur has been removed. The most commonly encountered base-metal 'oxide' minerals consist of oxides, oxy-hydroxides, carbonates, sulfates and silicates of copper, lead and zinc.

The electrophoretic behaviours of the copper 'oxide' minerals malachite, tenorite and chrysocolla were found to be very similar and the pH value of the iso-electric point (pH_{IEP}) was the same as $Cu(OH)_2$ (Gonzalez,1974). Based on a solubility diagram, this species was shown to be the equilibrium surface species for malachite over the pH range 6 to10 (Gonzalez *et al*, 1975). Zinc hydroxide was reported to form on the surfaces of zinc oxide particles (Wang *et al*, 2002). Overall, this is a feature of 'oxide' minerals in the presence of water, particularly where some degree of solubility exists (Schindler and Stumm, 1996). As can be seen from Table 2-2, many of the base-metal 'oxide' minerals are moderately soluble, noting that the surface of tenorite, with a K_{sp} of $10^{-20.5}$, was found to be covered with copper hydroxide. Thus it is expected that most base-metal 'oxide' mineral surfaces in contact with water would be covered in the corresponding base-metal hydroxide.

Table 2-2: Solubility products for base-metal 'oxide' minerals

Base-Metal	Mineral Species	Log K_{sp}
Copper	Malachite	-6.49[a]
	Azurite	-6.47[a]
	Tenorite	-20.5[a]
	Cuprite	-14.7[b]
Zinc	Smithsonite	-9.7[b]
Lead	Cerussite	-12.96[b]
	Anglesite	-7.89[b]

[a] Attia (1975)
[b] Garrels and Christ (1990)

The more commercially important iron 'oxide' minerals consist of oxides, oxy-hydroxides and carbonates and due to the high grade nature of such ore bodies, exploitation rarely involves mineral separation. The oxy-hydroxides display excellent adsorbent properties

and this aspect has been widely studied (Cornell and Schwertmann, 1996) as well as their electrophoretic behaviour (Parks, 1965, Rubio and Matijevic, 1979 and Fokkink, 1987). They also exhibit a wide range of magnetic properties, from the poorly magnetic (goethite and hematite) to the oxy-hydroxides (such as δFeO.OH) with intermediate saturation magnetisation properties to that of the highly magnetic minerals magnetite and maghemite (Pankhurst and Pollard, 1992 and Cornell and Schwertmann, 1996).

Little has been reported about the nickel 'oxide' minerals, which appear to be limited to oxy-hydroxides and carbonates.

2.2.3 Sulfide mineral flotation behaviour

The tendency to float without collector followed approximately the opposite ranking as the ease of oxidation: chalcopyrite > pyrrhotite > pentlandite (Guy and Trahar, 1984). Rand (1977) found that the relative ranking of rest potentials of sulfide minerals corresponded to the mineral requirement for oxygen during flotation with xanthate collectors, namely pentlandite > chalcopyrite > pyrrhotite. The higher rest potential of pentlandite compared to that of pyrrhotite has been reported by other researchers (Buswell and Nicol, 2002 and Kirjavainen *et al*, 2002).

Under both aerated and oxygen deficient conditions, pentlandite was reported to float more readily than pyrrhotite, based on massive nickel-copper ores from Sudbury. The order of floatability under aerated conditions was found to be chalcopyrite > pentlandite > pyrrhotite, while under an oxygen deficient environment, the order became pentlandite > chalcopyrite > pyrrhotite. This behaviour was correlated with the catalytic activity of the minerals for oxygen reduction (Kelebek, 1993).

Senior *et al* (1990) studied the flotation behaviour of pentlandite and pyrrhotite under a number of conditions. Under aerated, alkaline conditions, collector-less flotation was found to be greater for pentlandite than that of pyrrhotite after milling with iron media. With collector (ethyl xanthate at ~10^{-4}M), pentlandite flotation recoveries were similar at pH 7 and 9 however decreased significantly at pH 11 with sodium hydroxide as the pH regulator. At both pH 7 and 9, nearly 100 wt.% flotation recovery was observed over the size range from 20 to 90 microns, with a slight drop in recovery above 90 microns. At 106 microns, the flotation recovery at pH 9 was around 95 wt.%.

The flotation of pyrrhotite with ethyl xanthate (~10^{-4}M) after milling with iron media was strongly affected by pH. The optimum flotation recovery of just over 80 wt.% was achieved at pH 7 and fell significantly to just 20 wt.% at pH 9. This highlights a significant difference in the floatability between pyrrhotite and pentlandite at pH 9 after milling with iron media.

The floatability of pyrrhotite was found to decrease with increasing particle size. At pH 9, the optimum flotation recovery (~45 wt.%) was found between 20 and 40 microns. At 80 microns, flotation recovery had fallen to below 20 wt.% and at 106 microns, it was below 10 wt.%. In comparison, nearly full flotation recovery of pentlandite at pH 9 had been achieved over these size ranges in 8 minutes of flotation. The addition of copper sulfate had no effect on the pentlandite size-recovery curve, however significantly increased the recovery of pyrrhotite, particularly the finer sized particles (12 to 30 microns).

2.2.3.1 Solution ion effects

At a typical process pH of 9, electrochemical studies have shown that calcium, thiosulfate and sulfate ions were surface active and interacted strongly with pentlandite and pyrrhotite surfaces (Hodgson and Agar, 1989). It was concluded that these ions would influence the extent of xanthate adsorption and thus the degree of hydrophobicity. For pentlandite, both calcium and thiosulfate ions competed with xanthate for adsorption, whereas only the calcium ion affected the collector requirement.

The depressive effect of calcium ions upon the flotation recovery of synthetic pentlandite at pH 9 was quantified with SIBX ($5x10^{-5}$M) (Malysiak *et al*, 2002). The flotation recovery fell from 50 wt.% to 40 wt.% in an 80 ppm (~$2x10^{-3}$M) calcium solution and to around 17 wt.% with a 500 ppm solution.

In contrast to Hodgson and Agar (1989), both calcium and thiosulfate ions were found to improve the flotation of pentlandite and chalcopyrite at pH 9 after milling with mild steel media. These observations were interpreted to be strongly related to galvanic coupling effects. Not only did the calcium ions activate the two sulfide minerals, they also increased ethyl xanthate adsorption onto the mineral surfaces. On the other hand, the thiosulfate ion improved floatability by reducing the effect of surface hydrophilic species, which offset an associated decrease in the xanthate adsorption (Kirjavainen *et al*, 2002).

2.2.4 Effect of sulfide mineral oxidation

2.2.4.1 Surface charge

Electrophoresis has been widely used to measure the zeta potentials of metal oxide and hydroxide minerals as a function of the pH (Parks, 1965). This technique has been applied to sulfide minerals such as chalcopyrite (McGlashen *et al*, 1969, Ney, 1973 and Salatic *et al*, 1975), pyrrhotite (Ney, 1973) and nickel sulfide (Healy and Moignard, 1976). More recently it has been used to characterise the degree of oxidation for chalcopyrite (Fullston *et al*, 1999).

With oxidation, the sulfide mineral surfaces become covered in metal oxides/hydroxides, causing the surfaces to become less negative and even positive (Fullston *et al*, 1999). Healy and Moignard (1976) noted that the zeta potential profiles of the sulfide minerals lay between that of elemental sulfur and the corresponding metal oxide/hydroxide. They concluded that the pH value where the isoelectric point occurred (pH_{IEP}) gave a good indication of the extent of surface oxidation or surface coverage by metal oxides or hydroxides.

2.2.4.2 Flotation behaviour

Heavily oxidised surfaces on chalcopyrite were replicated by conditioning with ferric nitrate prior to flotation to form Fe (III) oxy-hydroxides (Grano *et al*, 1997). XPS analyses of the surfaces after treatment indicated that there was an increased contribution of Fe(III) oxy-hydroxides compared to the untreated chalcopyrite surfaces.

Using oxygen as the flotation gas, the collectorless flotation recovery was found to fall by 40 wt.% to below 10 wt.% after treatment with $5x10^{-6}$M Fe(III). Thus it was concluded that Fe(III) species such as $Fe(OH)_3$ would adsorb onto the chalcopyrite surfaces and cause subsequent depression.

2.3 Sulfidisation

2.3.1 Overview

The sulfidisation process was patented early in the history of flotation to enable the recovery of base-metal 'oxide' minerals by flotation, which did not respond to the recently

developed sulfide mineral flotation technology (Schwarz, 1905). It was initially employed in 1912 at Broken Hill (Australia) to recover lead 'oxide' minerals such as cerussite and anglesite. Since then, sulfidisation has been applied to the flotation recovery of a range of base-metal 'oxide' minerals, most notably malachite and heterogeneite (Shungu *et al*, 1988, John *et al*, 1991, Mwema and Mpoyo, 2001 and Bastin *et al*, 2003). Sulfidisation has also been used in the remediation of soils contaminated by base-metals (Vanthuyne and Maes, 2002).

The sulfidisation process is an aqueous based method, where soluble sulfide salts are used to create sulfide surfaces on base-metal 'oxide' minerals that are then amenable to conventional sulfide flotation practice. Another method is thermal sulfidisation, where the sulfide surfaces are formed at high temperatures in the presence of sulfur. While this approach has proved successful in the laboratory, particularly for chrysocolla (Queirolo and Castro, 1976) as well as lead and zinc 'oxide' minerals (Luganov and Bitimbaev, 2000), it has not been adopted in practice.

Soluble sulfide salts have been used in a number of contrasting roles in base-metal sulfide flotation. At low concentrations, the floatability of sulfide minerals is improved by the removal of surface oxidation products (Luttrell and Yoon, 1984) while at strong concentrations, sulfide minerals are depressed (Sutherland and Wark, 1955). In the sulfidisation of base-metal 'oxide' minerals, the range of concentrations used varies from moderate to strong.

2.3.2 Sulfidising reagents

2.3.2.1 Sources

The sulfidising reagent most commonly employed in practice is sodium hydrosulfide, although sodium sulfide is still widely used (refer to Table 2-9). Most of the sulfidisation research conducted upon base-metal 'oxide' minerals, particularly malachite, has utilised sodium sulfide (refer to Table 2-4). Calcium sulfide, used out of necessity, was reported to be a suitable replacement for sodium sulfide based upon metallurgical outcomes (Zhang, 1993). Barium sulfide has been used successfully in the sulfidisation and flotation of smithsonite, however it was not recommended for cerussite ores (Rey *et al*, 1950 and Rey, 1954).

Ammonium sulfide has been used industrially in the flotation of copper 'oxide' minerals (mainly chrysocolla and brochanite) (Raghavan *et al*, 1984) with variable results (Crozier, 1992). At the same sulfidising reagent addition rates, significantly lower pH and sulfidisation potential values were found with ammonium sulfide compared to sodium sulfide (Bastin *et al*, 2003).

Polysulfides, such as disulfide, tetrasulfide and pentasulfide, have been explored as sulfidising reagents. The pentasulfide, in particular, was reported to show marked improvements in flotation recovery with chrysocolla over that found with sodium sulfide (Glazunov *et al*, 1993). Similar findings were reported for the flotation recovery of malachite with a polysulfide sulfidising reagent (Quast *et al*, 2005).

2.3.2.2 Solution chemistry

The nature of the active species present in soluble sulfide salt solutions is a function of pH and is described by the following reactions:

$$H_2S_{aq} \leftrightarrow HS^- + H^+ \quad \text{.....(2-8)}$$

where the first dissociation constant, K_1, is given by :

$$K_1 = [HS^-].[H^+]/[H_2S_{aq}] \quad \text{.....(2-8a)}$$

$$\text{with } K_1 = 1.02 \times 10^{-7} \ (pK_1 = -6.99)$$

$$HS^- \leftrightarrow S^{2-} + H^+ \quad \text{.....(2-9)}$$

and the second dissociation constant, K_2, is :

$$K_2 = [S^{2-}].[H^+]/[HS^-] \quad \text{.....(2-9a)}$$

$$\text{with } K_2 = 1.20 \times 10^{-13} \ (pK_2 = -12.92).$$

There is some debate about the pK_2 value, with some researchers reporting values around –17.4 (e.g. Migdisov *et al*, 2002). However, it was argued that the value settled upon by Rao and Hepler (1977), namely -12.92, yielded more realistic sulfide ion concentrations (Jones and Woodcock, 1978a).

As equations 2-8 and 2-9 show, the speciation of soluble sulfide salts is controlled by the solution pH. Figure 2-3 shows the sulfur ion speciation in the $H_2S/HS^-/S^{2-}$ system as a function of pH for a pK_2 of -12.92. Aqueous hydrogen sulfide is the principal species below pH 5, while above pH 12, the chief species is the sulfide ion. Between pH 8.5 and 10, the common range for sulfidisation, the hydrosulfide ion is the dominant species and

thus considered to be the active species during sulfidisation (Crozier, 1992).

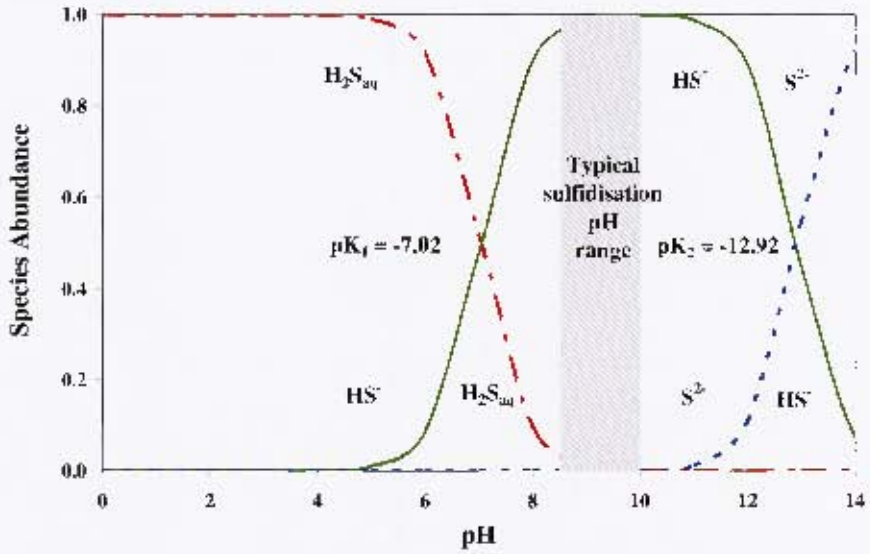

Figure 2-3: Sulfur solution speciation as a function of pH (pK_2 of -12.92, based on Crozier, 1992)

The sulfide ion concentration can be measured with a silver/silver sulfide electrode relative to a standard reference electrode such as saturated calomel (SCE) (Jones and Woodcock, 1978a). It is very sensitive to low sulfide ion concentration levels (as low as 10^{-9}M (Orion, 1996)) and is relatively free of interfering ions (Jones and Woodcock, 1978a).

The sulfide ion electrode potential, often referred to as Es, is a function of both the sulfide ion concentration and pH as presented in Figure 2-4. A 10 fold change in the concentration of the sulfide ion concentration causes a change in the electrode potential Es of 29 mV as does a pH change of one unit (Jones and Woodcock, 1979a).

In addition to these species, polyhydrosulfide (HS_n^-) and polysulfide (S_n^{2-}) species, where n = 2 to 5, have been detected in sulfide solutions (Rickard and Luther, 2006). The hydrodisulfide ion (HS_2^-) is the dominant polysulfide ion and below pH 7, may account for up to 1 wt.% of the total dissolved sulfide species in the system (Rickard and Luther, 2006). Polyhydrosulfide ions decompose to form the counterpart polysulfide ion and hydrogen ions.

The polysulfide species are thermodynamically unstable and decompose to thiosulfate ($S_2O_3^{2-}$) and hydrosulfide ions (Licht and Davis, 1997). Polysulfides with increasing chain length become more abundant under more highly alkaline conditions and can make up to

20% of the sulfide ion concentration under certain conditions. However, in the presence of trace levels of oxygen, this falls to around 5% (Rickard and Luther, 2006).

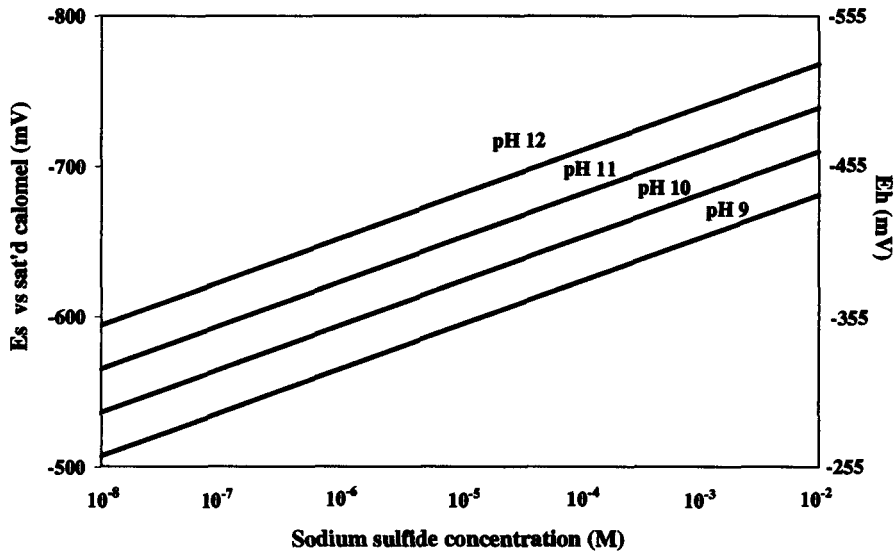

Figure 2-4: Sulfide ion electrode potential as a function of sodium sulfide concentration and pH (after Jones and Woodcock, 1979a)

A number of sulfide and hydrosulfide ion complexes can form with base-metal ions, particularly copper, silver and antimony (Rickard and Luther, 2006). Although not as extensive, cadmium, mercury, nickel, iron, manganese and cobalt exhibit a modest array of such complexes. The dissolution of nickel, cobalt and copper sulfide precipitates in 10^{-6}M hydrosulfide concentrations, possibly as polysulfide complexes, has been reported (Shea and Helz, 1988 and Lewis and van Hille, 2006).

2.3.2.3 Role of dissolved oxygen

Dissolved oxygen also plays a very significant role in the consumption of sulfidising reagent species. Removing the dissolved oxygen from the sulfidisation conditioning stages significantly reduced the consumption of sulfidising reagent by up to 70% (Cantrell, 1996, Clark and Newell, 1996 and Clark *et al*, 2000).

Dissolved oxygen reacts readily with sulfidising reagent solutions, particularly sulfide ions, although an induction period is often found (Chen and Morris, 1972a). The oxidation rate displayed maxima at pH 8 and 11. The presence of base-metal cations in small quantities (10^{-4} to 10^{-5}M) rapidly catalysed the oxidation of sulfidising reagent solutions, forming colloidal sulfur and a range of sulfoxy compounds. Nickel ions were the most effective

catalyst, followed by iron and lastly copper (Krebs, 1929, Chen and Morris, 1972b, and Zhang and Millero, 1994).

The oxidation of sulfide and hydrosulfide ions by dissolved oxygen is electrochemical and occurs rapidly on the surface of sulfide minerals (Klassen and Mokrousov, 1963, Tolun and Kitchener 1964 and Woods *et al*, 1989). The order of reactivity followed that found by Rand (1977) where pyrite was the most reactive sulfide surface for the oxidation of hydrosulfide ions (Woods *et al*, 1989). Polysulfides were also reported to be very unstable in the presence of dissolved oxygen (Steudel, 2000) and the products of oxidation were mainly sulfate ions (Klassen and Mokrousov, 1963), which like thiosulfate ions, may depress sulfidised minerals (Castro *et al*, 1974b and Soto and Laskowski, 1973).

2.3.3 Controlled potential sulfidisation (CPS)

Like other reagents commonly used in flotation, the sulfidisation technique originally employed a fixed rate of addition. Due to variability in both the 'oxide' mineral type and the associated abundance in the ore, ores were either 'under' or 'over' sulfidised and the subsequent flotation metallurgy was often erratic and occasionally unpredictable (Crozier, 1992).

Boyard (1954) had suggested that the sulfidisation process would be significantly improved by controlling the process through the measurement of the solution potential (ORP). The development of a more specific potential detection system, namely the sulfide ion selective electrode, finally lead to the development of a technique (Jones and Woodcock, 1978a, 1978b, 1979a and 1979b and Jones, 1990). It was demonstrated that better and more reliable metallurgy was achievable by conditioning at a fixed sulfide ion electrode potential (Es) with a number of copper and lead 'oxide' ores. The technique was termed Controlled Potential Sulfidisation (CPS) and not only addressed the variability in the sulfidising reagent requirements but provided a characterisation technique that could be successfully applied in practice. Important developments included the use of a number of stages of sulfidisation (Jones and Woodcock, 1979b), the application to cleaning stages (Jones *et al*, 1986) and the utilisation of nitrogen during sulfidisation (Clark *et al*, 2000). Lewis (1990) described a successful plant application with four stages of CPS as well as a CPS cleaning stage treating a gold-bearing ore containing copper 'oxide' minerals.

2.3.4 Additives to the sulfidisation process

Ammonium sulfate has been used in the sulfidisation of copper 'oxide' minerals (predominantly malachite) (Zhang and Poling, 1989 and 1991) and copper/cobalt 'oxide' minerals (malachite and heterogeneite) (Bastin *et al*, 2003). The significant improvement in copper metallurgy reported by Zhang and Poling (1991) was only found for heterogeneite (Bastin *et al*, 2003). While some authors ascribe any benefits to the surface cleansing effects, Zhang and Poling (1991) reported that the ammonium species catalysed the sulfidisation reaction and caused a more coherent copper sulfide surface to form. However, the effect of ammonium salts may be either ore or technique specific, since other researchers have not been able to reproduce these results (Mwema and Mpoyo, 2001).

2.3.5 Use of sulfidisation with base-metal 'oxide' minerals

Both the study and application of sulfidisation has concentrated predominately on the family of minerals commonly referred to as base-metal 'oxide' minerals (refer to Section 2.2.3.5). The base-metal 'oxide' minerals that have been sulfidised are summarised in Table 2-3.

Table 2-3: Base-metal 'oxide' minerals amenable to sulfidisation

Base-metal	Carbonates/ Hydroxy-Carbonates	Sulphates/ Hydroxy-Sulphates	Silicates/ Hydroxy-Silicates	Oxides/ Oxy-Hydroxides	Other
Copper	Malachite Azurite	Brochanite	Chrysocolla	Tenorite Cuprite	
Lead	Cerussite	Anglesite			Crocoite Wulfenite Vanadinite Descloizite Pyromorphite
Zinc	Smithonsite/ Hydrozincite		Willemite/ Hemimorphite		
Cobalt				Heterogenite	
Iron				Goethite Fe(III) oxy-hydroxide	

Sulfidisation followed by flotation has been used in practice to recover the 'oxide' minerals of the major base-metals, such as copper (malachite, azurite, cuprite and tenorite),

lead (cerussite and anglesite) and zinc (smithsonite and willemite). A large body of research and operational details have been reported for these minerals (refer to Tables 2-4 and 2-9).

Amongst the iron 'oxide' minerals, goethite (FeO.OH) has been successfully sulfidised (Mitrofanov *et al*, 1957). A hydrated ferric oxy-hydroxide (generically ferrihydrite: $FeO.OH._nH_2O$) was reported to have produced Fe(II) species upon contact with solutions containing hydrosulfide ions, which subsequently precipitated as FeS onto the surfaces (Poulton *et al*, 2003). Hematite was not affected during the sulfidisation of a malachite bearing ore (Hu *et al*, 1986).

A summary of the sulfidisation research conducted on these base-metal 'oxide' minerals is presented in Table 2-4, highlighting the mineral type, sulfidisation and flotation conditions as well as the subsequent metallurgical results.

2.3.5.1 Sulfidisation mechanisms

Wright and Prosser (1965) proposed that the sulfidisation mechanism for copper 'oxide' minerals were similar and based on the precipitation of covellite (CuS) onto the surfaces and pores. The rate of reaction was controlled by diffusion of species through the product layers and driven by the substantial insolubility of the copper sulfide product.

$$CuSiO_{3(s)} + H_2O \rightarrow H_2SiO_{3(s)} + 2OH^- + Cu^{2+}_{(aq)} \quad (2\text{-}10)$$

$$Cu^{2+}_{(aq)} + HS^- \rightarrow CuS_{(s)} + H^+ \quad (2\text{-}11)$$

Similarly, Zhou and Chander (1993) considered that the precipitation of copper sulfide was the precursor to the formation of the sulfide layer on the surface of malachite, based on the presence of colloidal copper sulfides during sulfidisation. They considered that the copper ions diffused through the primary sulfidised layer and form copper precipitates:

$$CuCO_3.Cu(OH)_2 + HS^- \rightarrow Cu^{2+} + CuS + HCO_3^- + 2OH^- \quad (2\text{-}12)$$

For lead 'oxide' minerals in moderate sulfide ion concentrations (~10^{-4}M), lead sulfide precipitates were reported in both solution and adhered to the mineral surfaces (Fuerstenau *et al*, 1985). At higher concentrations, however, sulfide surfaces were formed directly after the strong adsorption of hydrosulfide ions and maximum flotation recoveries were achieved. Leppinen and Mielczarski (1986) also reported similar findings for the sulfidisation of lead 'oxide' minerals.

Table 2-4: Summary of selected base-metal 'oxide' mineral sulfidisation research

Mineral(s)	Sulfidiser type	Solution strength mg/l [M]	Sulfidisation conditions: pH	Sulfidisation conditions: Eh[a] (mV)	Sulfidisation conditions: Time (min)	Collector details M (mg/l)	Flotation recovery (%)	Reference
Chrysocolla	$Na_2S.9H_2O$		N.R.[b]	N.R.	10	Ethyl xanthate Amyl xanthate	N.R	Wright & Prosser (1965)
Chrysocolla	$Na_2S.9H_2O$	48 [$2.00x10^{-4}$] 200 [$8.33x10^{-4}$] 960 [$4.00x10^{-3}$]	8.5 8.5 8.5	-630[c] -648[c] -638[c]	10	>$1.88x10^{-5}$ (3) >$3.44x10^{-5}$ (5.5) >$6.25x10^{-6}$ (1) AX	~100 Decant ~ 95 Decant ~ 0	Castro *et al* (1974b)
Willemite	$Na_2S.9H_2O$	60 [$2.50x10^{-4}$] 80 [$3.33x10^{-4}$] 150 [$6.24x10^{-4}$]	10.2 10.4 10.8	-682[c] -691[c] -711[c]	2	$1x10^{-5}$ Amine	~85	Salum *et al* (1992)
Hemimorphite	$Na_2S.9H20$	60 [$2.50x10^{-4}$] 80 [$3.33x10^{-4}$] 150 [$6.24x10^{-4}$]	10.2 10.4 10.8	-682[c] -691[c] -711[c]	4	$1x10^{-5}$ Amine	~90	Salum *et al* (1992)
Malachite	$Na_2S.9H_2O$	1000 [$4.16x10^{-3}$]	8	-639[c]	5	3.13×10^{-4} (50) Amyl xanthate	Decant ~100	Bustamante & Castro (1975)
Malachite	$Na_2S.9H_2O$	48 [$2.00x10^{-4}$] 48 [$2.00x10^{-4}$] 960 [$4.00x10^{-3}$] 960 [$4.00x10^{-3}$] 960 [$4.00x10^{-3}$]	N.R.	N.R.	10	$1.38x10^{-4}$ (22) $1.75x10^{-4}$ (28) $3.13x10^{-5}$ (5) $7.5x10^{-5}$ (12) <$2.5x10^{-4}$ (< 40)	Decant ~100 ~100 Decant ~100 Aerate ~100 <5	Soto & Laskowski (1973)
Chrysocolla Ore (Chrysocolla)	NaHS $Na_2S.9H_2O$	$2x10^{-4}$ gm/m^2 consumption $1x10^{-4}$ M/m^2 $2.5x10^{-4}$ M/m^2 ~$1x10^{-4}$ M/m^2 Chrys. (2.27 kg/t)	N.R. 9.5	N.R.	N.R. 6	Ethyl xanthate $0.5x10^{-4}$ M/m^2 $0.5x10^{-4}$ M/m^2 $0.25x10^{-4}$ M/m^2 Chrys.(0.23 kg/t) Amyl xanthate	No reaction/ no flotation 95 99 ~78	Wright & Prosser (1965)
Cerussite	Na_2S	10^{-4} to $4x10^{-4}$ M	9.5	-650 to -687[c]	10 5 (Coll)	$5x10^{-5}$ Amyl xanthate	90 to 100 Colour change	Fuerstenau *et al* (1985)
Anglesite	Na_2S	$6x10^{-4}$ to $2x10^{-3}$	9.5	-673 to -688[c]	10 5 (Coll)	$5x10^{-5}$ Amyl xanthate	100	Fuerstenau *et al* (1985)
Ore (Anglesite)	Na_2S	$1.2x10^{-2}$ CPS 1 $8.9x10^{-3}$ CPS 2 $6.3x10^{-3}$ CPS 3	N.R.	-600	3	$1.6x10^{-4}$ per stage Amyl xanthate	52 3 CPS stages	Jones & Woodcock (1979a)
Various Ores (Chalcocite/ Malachite)	Na_2S	$3.4x10^{-3}$ CPS 1 $5.3x10^{-4}$ CPS 2 $1.3x10^{-4}$ CPS 3 $1.6x10^{-4}$ CPS 4	~8.8-9.2	-500	3 2 (Coll) CPS 1 only	$3.9 x10^{-5}$ per stage Amyl xanthate	96 Total Cu 4 CPS stages	Jones *et al* (1986)
Various mixed ores (Malachite/ Chalcopyrite)	Na_2S	$1.7-2.4 x10^{-3}$ CPS 1 $3.3-6.6x10^{-4}$ CPS 2 $2.3-5.3x10^{-4}$ CPS 3 $1.7-4.4x10^{-4}$ CPS 4	~8.8-9.2	-500	3	$1.3x10^{-4}$ CPS 1 $5.2x10^{-5}$ CPS 2-4 Amyl xanthate	81-88 Total Cu 4 CPS stages	Jones & Woodcock (1978b)
Two mixed ores : Bornite/Chalcopyrite Digenite/Chalcocite Malachite/Cuprite	NaHS	$7.48-6.4x10^{-3}$ total consumption	9.8 - 10.6	-400 to -600	5 2 (Coll)	$1.5-7.7 x 10^{-5}$ CPS 1-3 DTC, DTP & Acrophine	70 to 85 'oxide' Cu 3 CPS stages	Nagaraj & Gorken (1991)
Cerussite and Smithsonite	Na_2S H_2S Na_2S	350 -16250 (20 - 60°C) 160 g/t	N.R. 5 10 12	N.R. N.R. N.R. N.R.	15 15 2 2	10^{-5}-10^{-3}M Ethyl Xanthate/DAA 80 g/t Amyl Xanthate 100 g/t DAA	XPS/adsorption studies 85 % Pb 92 % Zn	Marabini *et al* (1984)
Cerussite Smithsonite	Na_2S Na_2S	4 kg/t N.R.	N.R. N.R.	N.R. N.R.	N.R. N.R.	300 g/t Amyl xanthate Dodecylamine	71% Pb grade. 75% 14% Zn grade. 49%	Ozbayoglu *et al* (1994)
Smithsonite	Na_2S	5 kg/t consumption	N.R.	N.R.	N.R.	$3.0 x 10^{-5}$ Dodecylamine	> 98% (pH > 7.5)	Cases *et al* (1979)
Zinc 'oxide' ore (mainly smithsonite)	Na_2S	N.R.	N.R.	-800	N.R.	$3.0 x 10^{-5}$ Amine	50-75%	Tian (2003)
Zinc 'oxide' ores (smithsonite, hydrozincite, hemimorphite & willemite)	Na_2S	4.66-5 kg/t	12	N.R.	12	115-127 g/t Amine Petroleum	60-65%	Billi & Quai (1963)
Zinc 'oxide' ore (mainly hemiphorite)	Na_2S	2.6-6.8 kg/t	~12	N.R.	N.R.	235-664 g/t Amine Diesel	84-95% Zn	Pereira & Peres (2005)
Malachite/ heterogenite	NaHS	2.5-20 kg/t	N.R.	N.R.	N.R.	Amyl xanthate Gasoil & tall oil 6 stages (sulfidis.)	63-92% Cu 60-87% Co	Bastin *et al* (2003)

[a] Relative to SCE [b] N.R. : Not Reported [c] Calculated

Bustamante and Castro (1975) also considered that an anionic exchange mechanism occurred between the hydrosulfide ion and malachite.The reaction involved more than the surface layers and continued within the bulk of the mineral to form copper sulfide coatings:

$$CuCO_3.Cu(OH)_2 + HS^- \rightarrow Cu(OH)_2.CuS + CO_3^{2-} + H_2O \quad \text{.....(2-13)}$$

During the sulfidisation of cerussite, it was reported that carbonate ions were released from the surface (Rey *et al*, 1950 and Rey 1954), indicating an exchange mechanism.

Castro *et al* (1974a) postulated that the adsorption of sulfide ions preceded the formation of copper sulfide during sulfidisation of a synthetic tenorite surface while Bustamante and Shergold (1983a) considered that a direct sulfidisation mechanism occurred for zinc 'oxide' minerals. As proposed by other researchers, the driving force was the lower solubility of zinc sulfide while rate of sulfidisation was controlled by the diffusion of hydrosulfide ions and reaction products through the sulfidised layer:

$$ZnCO_{3(S)} + HS^- \rightarrow ZnS_{(S)} + HCO_3^- \quad \text{.....(2-14)}$$

The formation of both covellite and sulfur on the chrysocolla surfaces was considered the primary mechanism by Glazunov *et al* (1993):

$$CuSiO_3 + 2HS^- \rightarrow CuS + S^o + SiO_2 + H_2O \quad \text{.....(2-15)}$$

With polysulfides as the sulfidising species, Zhou and Chander (1993) proposed the following mechanism:

$$CuCO_3.Cu(OH)_2 + S_4^{2-} \rightarrow CuS_4 + Cu^{2+} + CO_3^{2-} + 2OH^- \quad \text{.....(2-16)}$$

Based on solubility products and Eh-pH diagrams (Garrels and Christ, 1990), FeS and NiS would be expected to form on the surfaces of oxidised iron and nickel minerals respectively. In the formation of pyrite, FeS is considered to be the precursor (Rickard, 1969 and Berner, 1970). The rate of formation only progressed at a significant rate if intermediate sulfur species were present, such as polysulfides (Schoonen and Barnes, 1991 and Wei and Osseo-Asare, 1995). Additionally, the presence of an oxidising agent would rapidly promote the formation of pyrite.

2.3.5.2 Surface species after sulfidisation

XRD has been used to identify covellite (CuS) on sulfidised malachite (Castro *et al*, 1974b and Bessiere *et al*, 1991) and chalcocite (Cu_2S) on sulfidised chrysocolla (Raghavan *et al*, 1984). No copper sulfides were identified on sulfidised brochanite (Raghavan *et al*, 1984).

Based on solubility considerations, chalcocite would be expected to form on both minerals (refer to Table 2-5). Based on Eh-pH diagrams, Cu_2S is the thermodynamically favoured (Garrels and Christ, 1990) however covellite can form under more intense sulfidisation conditions (Zhang, 1994). Copper tends to occur as Cu(I) in a sulfide environment. For covellite (CuS), sulfur appears to be in the disulfide form and the composition can be Cu_2S_2 (Fleet, 2006 and Rickard and Luther, 2006).

Lead sulfide was reported on cerussite surfaces after sulfidisation (Fleming, 1953, Marabini *et al*, 1984 and Marabini and Rinelli, 1986) while zinc sulfide formed on the surface of smithonsite (Cases *et al*, 1979, Marabini *et al*, 1984 and Marabini and Rinelli, 1986). Bastin *et al* (2003) reported that divalent cobalt sulfide formed on heterogeneite.

Table 2-5: Solubility products for base-metal sulfides

Base-metal	Sulfide species	Log K_{sp}[a]
Iron	FeS	-17.35
	FeS_2	-36.15[b]
Nickel	NiS	-20.55
	NiS_2	-18.5
	Ni_3S_2	-36.86
Cobalt	CoS	-20.64
	Co_2S_3	-125.9
Copper	CuS	-35.05
	Cu_2S	-47.7
Lead	PbS	-27.03
Zinc	ZnS	-24.05

[a] Garrels and Christ (1990)
[b] Helgeson (1969)

The sulfidisation reaction was reported to occur quickly (less than 30 seconds) for lead 'oxide' minerals in very strong solutions and indicated a direct reaction (Marabini *et al*, 1984). The sulfidising layers were calculated to be several monolayers thick for both copper 'oxide' (Castro *et al*, 1974a and b) and lead 'oxide' minerals (Bustamante and Shergold, 1983a and Marabini *et al*, 1984). Sulfidisation products were reported to not fully cover the surface (Zhou and Chander, 1993) and a surface coverage of 30% for smithsonite in equilibrium with 3.5×10^{-5} M Na_2S solution was reported (Cases *et al*, 1979).

The lowering of the zeta potential of base-metal 'oxide' mineral surfaces in the presence of hydrosulfide ions has been attributed to the adsorption of these ions (Mitrofanov *et al*, 1955a, Fuerstenau *et al*, 1985 and Salum *et al*, 1992). The adsorption of sulfide and hydrosulfide ions onto cerussite followed a Freundlich type relationship, although many monolayers of sulfide were reported (Fleming, 1953 and Marabini *et al*, 1984). For most base-metal 'oxide' minerals, the relationship $\Gamma = at^{1/n}$ holds, where Γ is the amount of adsorbed species, t is the adsorption time, a and 1/n are constants (Mitrofanov *et al*, 1955a and 1957, Mitrofanov and Kushnikova, 1958 and Marabini *et al*, 1984). For malachite the kinetic isotherm was $\Gamma = a \log t + b$, where a and b are constants, with b varying between 0.25 and 0.65 (Mitrofanov *et al*, 1955a, Mitrofanov, 1958 and Klassen and Mokrousov, 1963).

2.3.5.3 Other factors affecting sulfidisation

2.3.5.3.1 Sulfidisation conditioning period

It has been reported in many studies that an optimum conditioning period existed, as reflected in the subsequent flotation metallurgy (Billi and Quai, 1963, Jones and Woodcock, 1978b, Pereira and Peres, 2005 and Newell *et al*, 2006). The sulfidising period was a compromise between developing a sufficiently thick sulfide surface to enable flotation in an agitated environment and the onset of antagonistic processes such as oxidation and mineral dissolution (Marabini and Rinelli, 1986). This period was typically around three minutes (Jones and Woodcock, 1978a and 1978b) although up to 10 minutes may be required, depending upon the mineral type.

The thickness of the sulfide layer formed during the sulfidisation of malachite increased with time, decreasing particle size and increasing sulfide ion concentration (Bessiere *et al*, 1991). While longer conditioning times form thicker sulfide surfaces, they also result in greater sulfidising reagent consumption, and in the case of cerussite, this can be excessive (Rey *et al*, 1961).

2.3.5.3.2 pH

The effect of pH during sulfidisation is predominantly related to the solubility of the base-metal 'oxide' mineral surfaces, with lower pH values releasing considerably more metallic

ions for sulfidisation. Not surprisingly, the sulfidisation intensity was reported to be greater at lower pH values for most base-metal 'oxide' minerals, including malachite and goethite, and a thicker layer appeared to be developed with often better flotation metallurgy (Mitrofanov *et al*, 1955a, 1955b, 1957 and 1958, Mitrofanov and Kushnikova, 1958 and 1959 and Castro *et al*, 1974b). Klassen and Mokrousov (1963) reported that the pH affected the thickness of the sulfide film by controlling the rate of diffusion through the layer. However for cerussite, the maximum rate of formation occurred in the pH range 9 to 10. Although a thicker film was detected under these conditions the attachment of the sulfide product to the surface was reported to be poorer (Mitrofanov *et al*, 1955b).

2.3.5.3.3 Temperature

Higher temperatures are reported to improve the rate of sulfidisation for most base-metal 'oxide' minerals including malachite and goethite (Mitrofanov *et al*, 1955a, 1955b, 1957 and Mitrofanov and Kushnikova, 1958, 1959). As a consequence, the consumption rate of the sulfidising reagent also increases, and with increased temperatures, much shorter sulfidising periods are recommended (Rey *et al*, 1961)

Temperature also affected the rate of diffusion through the sulfide film and thus the growth of this layer, with thicker sulfide layers observed with increasing temperature for most base-metal 'oxide' minerals (Mitrofanov *et al*, 1957 and Klassen and Mokrousov, 1963).

2.3.5.3.4 Solution species

Rey *et al* (1950) reported that calcium ions significantly affected the flotation of sulfidised cerussite due to the precipitation of calcium carbonate upon the mineral surfaces. Fleming (1953) found that chloride ions significantly affected the sulfidisation of lead and vanadium 'oxide' minerals. During flotation, thiosulfates were reported to depress sulfidised malachite (Soto and Laskowski, 1973) whereas sulfate ions had little effect on the flotation of sulfidised cerussite (Fleming, 1953).

2.3.5.3.5 Consumption of sulfide species

A feature of the sulfidisation of base-metal 'oxide' minerals is the high consumption rate of the sulfidising reagent, which arises due to precipitation by metallic cations, oxidation by dissolved oxygen and the sulfidisation reaction. Both mineral solubility and surface area

play a significant role in driving these reactions (Klassen and Mokrousov, 1963). A significant amount of sulfidising reagent, up to 50%, is consumed within the few minutes of sulfidisation by the formation of colloidal precipitates with the cations released by hydrolysis of the base-metal 'oxide' mineral surface (Monks and Weiss, 1930, Jones and Woodcock, 1979b and Bessiere *et al*, 1991). Conditioning with sodium carbonate significantly reduced sulfidising reagent consumption (Rey *et al*, 1954 and Bessiere *et al*, 1991).

Another factor is the nature of the sulfidised surfaces, which can be fragile and readily removed by abrasion within the flotation cell (Mitrofanov *et al*, 1955b). The sulfidised surfaces can also become oxidised (Fleming, 1953) and, along with sulfide precipitates, experience a cyclic existence where they are continuously oxidised and re-sulfidised (Jones and Woodcock, 1979a).

2.3.5.3.6 Collectors

Three collector types have been employed after sulfidisation: long chained xanthates, dithiophosphates and amines. Amyl xanthate is the most widely used collector in practice (refer to Table 2-9).

Freshly formed sulfide surfaces were found to form strong attachments with sulfydryl collectors such as xanthate (Castro *et al*, 1974b). While short chained thiols such as ethyl xanthate were found to adsorb onto these surfaces, possibly as dixanthogen, flotation did not result (Wright and Prosser, 1965, Marabini *et al*, 1984 and Leppinen and Mielczarski, 1986). This may be caused by the strong reducing properties of sulfide ions, which were reported to form polysulfides and S_2^{2-} with dixanthogen (Tolun and Kitchener, 1964). Amyl xanthate was required to achieve satisfactory flotation. Sulfide ions were also reported to convert previously surface precipitated base-metal thiolates into an adsorbed surface form (Bustamante and Castro, 1975, Castro *et al*, 1976, Marabini *et al*, 1984 and Leppinen and Mielczarski, 1986).

Xanthates and non-xanthate sulfydryl collectors were reported to be effective in the nitrogen flotation of sulfidised copper 'oxide' and sulfide minerals (Nagaraj and Gorken, 1991 and Kongolo *et al*, 1995). Dithiophosphates (particularly the Cyanamid proprietary product R238) have been widely used in conjunction with amyl xanthate in the flotation of

copper/gold 'oxide' ores in a number of Australian sulfidisation operations to increase the flotation of free gold particles.

Unlike thiol collectors, amine collectors are unaffected by high levels of residual sulfidising reagent species where more intense levels of sulfidisation are required e.g. lead and zinc 'oxide' minerals (Rey, 1954, Cases *et al*, 1979 and Salum *et al*, 1992). Other potential collectors such as chelating agents have not shown promise (Bustamante and Shergold, 1983b). Oil has been used as an adjunct to collectors in order to the enhance flotation recovery of partially sulfidised coarser particles (Rosas and Poling, 1975 and Shungu *et al*, 1988).

2.3.6 Use of sulfidisation for base-metal sulfide minerals

Sulfidisation has been advocated for the flotation recovery of oxidised sulfide minerals (Klassen and Mokrousov, 1963), particularly oxidised copper sulfides (Malghan, 1986). The use of sodium sulfide during milling was reported to have significantly improved the flotation recovery of 'tarnished' chalcopyrite from weathered copper-zinc ores (Bulatovic and Wyslouzil, 1985). Sulfidisation was used in a plant trial to recover surface oxidised or tarnished chalcopyrite with some success (Hunt, 2000). There are reports of sulfidisation being employed to recover tarnished copper sulfide ores by flotation in the USA during the 1940s. Oxidised chalcopyrite was reported to be successfully recovered during the sulfidisation of copper 'oxide' minerals in a Zambian operation (John *et al*, 1991).

Sulfidisation was used in an attempt to recover refractory nickel minerals of unknown mineralogy at the Trojan mine in Botswana, however was abandoned (Barker *et al*, 1982). On the other hand, fine galena responded favourably to sulfidisation along with the accompanying lead 'oxide' minerals at low sulfide ion concentrations (Lord and Markovic, 1970). A number of mainly secondary copper sulfide minerals have been reported to respond well to sulfidisation (refer to Table 2-6).

In ores containing both copper 'oxide' and sulfide minerals, it was reported that the two different mineral types could be successfully floated together under the correct sulfidisation conditions (Jones and Woodcock, 1978b and Jones *et al*, 1986, Nagaraj and Gorken, 1991, Clark and Newell, 1996 and Clark *et al*, 2000). The copper sulfide minerals had improved kinetics and recoveries, which was possible because the potential for the

depression of copper sulfides had not been reached (-650 mV to -750 mV Es (SCE) (Nagaraj and Gorken, 1991)).

Table 2-6: Base-metal sulfide minerals amenable to sulfidisation

Base-metal	Secondary Sulfide	Primary Sulfide	Arsenide/ Sulfo-arsenide
Copper	Chalcocite Digenite Covellite	Bornite Chalcopyrite Tarnished chalcopyrite	
Cobalt		Carrollite	Cobaltite Maucherite
Lead		Galena	
Iron		Oxidised Pyrite	

The use of CPS was reported to improve the flotation recovery of very fine digenite as well as chalcopyrite (Orwe *et al*, 1998). The mechanism involved the re-sulfidisation of the oxidised digenite surfaces and the formation of a sulfur enriched copper mineral (Orwe *et al*, 1997). A similar finding was also reported for chalcocite (Walker *et al*, 1986). Sulfidisation is used in the Northparkes operation to improve the flotation recovery of fine bornite, which does oxidise readily (Freeman *et al*, 2000).

Sulfidisation has been used to recover fine cobalt arsenides including cobaltite (CoAsS) employing copper sulfate and amyl xanthate (Formanek and Lauvernier, 1963 and de Cuyper, 1981). The only reported use of sulfidisation with nickel was where a similar strategy was employed in the flotation recovery of readily oxidisable nickel arsenide minerals such as maucherite (Iwasaki *et al*, 1988).

A number of Russian authors have reported the deposition of sulfur from sulfide solutions onto chalcopyrite and pyrite surfaces (Buckley *et al*, 1988). Substantial quantities of elemental sulfur were detected on chalcopyrite and pyrite surfaces in the presence of oxygenated sulfide solutions (Buckley *et al*, 1988 and McCarron *et al*, 1990). However, at very high concentrations (10^{-2}M), no sulfur was found on chalcopyrite surfaces and a metal-deficient surface like a secondary sulfide copper mineral was reported to have formed (McCarron *et al*, 1990). Polysulfides were proposed to form when hydrosulfide ions were oxidised at sulfide mineral electrodes:

$$xHS^- + 0.5\,(x-1)O_2 \rightarrow S_x^{2-} + H_2O + (x-2)OH^- \quad \text{.....(2-17)}$$

which combines the anodic oxidation of hydrosulfide ion to polysulfide and the simultaneous cathodic reduction of oxygen (Buckley *et al*, 1988).

2.3.7 Comparison of sulfidised and sulfide surfaces

Differences in the collector requirement for satisfactory flotation between base-metal sulfides and their sulfidised 'oxide' counterparts have been reported. Comparing sulfidised malachite (amyl xanthate) with chalcocite and covellite (butyl xanthate), it was noted that there were up to three orders of magnitude in the difference in collector requirements (Soto and Laskowski, 1973). A similar trend was reported for galena and the lead 'oxide' minerals (Fuerstenau *et al*, 1985 and Herrera-Urbina *et al*, 1998). Short chained thiol collectors were ineffective and longer chained collectors were required and, in greater quantities, in order to realise the benefit of sulfidisation, compared to sulfide mineral counterparts. Additionally, there was a tendency for the sulfidised minerals to float more slowly.

2.3.8 Sulfidisation intensity

The potential or intensity under which sulfidisation has been conducted for various base-metal 'oxide' minerals are presented in Table 2-7. The sulfide ion electrode potential (Es) is referenced to the saturated calomel electrode (245 mV SHE).

Table 2-7: Range of Es values used to achieve sulfidisation of base metal minerals

Es (mV) (calomel)	Malachite	Anglesite	Cerussite	Willemite	Digenite	Bornite	Tarnished chalcopyrite
Range	-400 to -600[a] -400 to 650[b]	-400 to -700[c] -670 to -690[d]	-650 to -677[d]		-350 to -400[f]	-350 to -400[f]	-500[g] -350[h]
Optimum	-500[a] -600[b]	-600[c] -682 to -690[d]	-673 to -677[d]	-700[e]			

[a]Jones and Woodcock (1978b) [b]Nagaraj and Gorken (1991) [c]Jones and Woodcock (1979b)
[d]Fuerstenau *et al* (1985) [e]Tian (2003) [f]Estimate [g]John *et al* (1991) [h]Hunt (2000)

The sulfidisation potential is dependent upon the mineral solubility and the sulfidisation mechanism. For more soluble minerals, such as malachite and cerussite, the sulfidisation

process not only releases base-metal ions into solution, which consumes more sulfide species, but progresses deeply into the mineral surfaces. Less soluble surfaces (e.g. smithsonite) require very strong concentrations simply to form a sulfide surface (Es = -700 mV). Consequently, there is a critical range of hydrosulfide ion concentrations (i.e. Es values) whereby a suitable sulfide surface can be readily established without excessive sulfidising reagent consumption. The spectrum of sulfidisation potentials for various base-metal minerals is summarised in Table 2-8.

Table 2-8: Spectrum of sulfidisation potentials for base-metal minerals

Reference Electrode	Sulfide Ion Electrode Potential (Es, mV)						
Sat'd Calomel	-300	-350	-400	-500		-600	-700
Ag/AgCl (0.01M KCl)	-393	-443	-493	-593		-693	-793
Role	Removal of oxidation products	← Sulfidisation →					
Base-metal 'oxide' minerals				Carbonates Malachite Cerussite	Oxides Cuprite Tenorite	Sulfates Anglesite	Silicates Willemite Hydrozincite Heterogenite
Base-metal sulfide minerals	Lightly oxidised	Primary Galena Chalcopyrite	Secondary Bornite Digenite Chalcocite	Heavily oxidised Tarnished chalcopyrite			
Sulfidiser consumption	Very low	Very low	Low	High / low	Moderate	High	High

The flotation recovery of base-metal 'oxide' minerals as a function of sulfidisation potential is characterised by a bell-shaped response where, after an optimum sulfidisation potential has been reached, the recovery falls away with increasing sulfide concentration (Jones and Woodcock, 1978b, 1979b and Fuerstenau *et al*, 1985). Since flotation is typically conducted after sulfidisation in the same solution, depression of the freshly formed sulfide surfaces will occur after a certain hydrosulfide ion concentration has been reached. Marabini *et al* (1984) found that for cerussite there was an optimum Na_2S/ethyl xanthate ratio for maximum flotation which was directly related to amount of chemisorbed collector on the surface.

2.3.9 Industrial practice

The adoption of the CPS technique does not appear to have occurred outside Australia, Russia (Abramov and Avdohin, 1997) and Zambia (John *et al*, 1991), although a somewhat

similar process appears to have been developed for a low grade copper operation in Mexico (Ealy, 1973). Zhang (1993) makes no mention of CPS being used in Chinese plants while the degree of adoption was not apparent for several operations in Central Africa. During the 1980's, a new generation of sulfidisation plants with three to four CPS stages were installed in Australia to treat copper 'oxide' and copper sulfide-gold ores. A summary of selected sulfidisation/flotation plants, highlighting the pertinent features, is presented in Table 2-9.

Table 2-9: Summary of selected plant sulfidisation practice

Operation	Feed details	Recoveries (%)	Sulfidising details (kg/t)	Collector details (g/t)	Method (nos of stages)
Telfer, WA Australia (Bartels, 1990)	Supergene (chalcocite) copper/gold ores	90% Cu 96% Au	Na_2S : 3 ORP (Pt) -150 mV 3 min. cond.	PAX : R238 (2:1) 3 min. cond.	CPS : Ro/Scav (3) Cl (1)
Boddington, WA Australia (Ehm & Hill, 1992)	Copper/gold ores : 'Oxide' (malachite) Supergene (chalcocite)	 44-65% Cu 62-77% Au 84% Cu 87% Au	Na_2S : Es -300 mV 2.0-2.5 4/5 min cond 1.2 4/5 min cond	3 min cond PAX 320-420 R238 120-150 PAX 1040 R238 170	CPS : Ro 2&3 Scav Flotation pH 9.8
Red Dome, QLD Australia (Lewis, 1990)	'Oxide' (malachite) copper/gold ores	83.2% Cu (CN sol) 68% Au	Na_2S/NaHS Es -500 mV 20% solids	PAX R 238	CPS : Ro 2&3 Scav & Cl (1)
Mineral Hill, NSW Australia (Clay, 1993)	Oxide (malachite) & supergene (chalcocite) copper/gold ores	N.R.	Na_2S/NaHS	PAX R 238	CPS : Ro/Scav (4) Cl (4)
Nchanga, Zambia (John *et al*, 1991)	Mixed oxide/sulfide copper ores : malachite chalcopyrite & 'oxidised' chalcopyrite	45 -55% Cu (Acid sol)	NaHS Sulfide Ro : 0.40 Sulfide Cl : N.R. Both Es -300 mV Oxide Ro 0.21 Es -500 mV	Xanthate	CPS : Sulfide Ro (2) Sulfide Cl (1) Oxide Ro (1)
Kakanda, DRC (Shungu *et al*, 1988)	Mixed oxide/sulfide copper/cobalt ores : malachite,heterogeneite and chalcocite	81% Cu 46% Co	NaHS : 2.47	SNBX 240 Gas oil 323 Palm oil 33 KAX 19	Fixed addition prior to Ro
Kamoto, DRC (Shungu *et al*, 1988)	Sulfide copper/cobalt ores chalcocite and carrollite ('oxide' minerals not stated)	86% Total Cu 90% Sulf. Cu 77% Co	NaHS : 0.36	SIPX 52 SNBX 70 Gas oil 51	Fixed addition prior to Ro
Kolwezi, DRC, (Anon, 1957)	Mixed 'oxide'/sulfide copper/cobalt ores : malachite,heterogeneite chalcocite and carrollite	82-85% Cu 70% Co	NaHS : 1.2 Conditioning time minimal	KAX 50 SEX 80 Gas oil 100 Tall oil 10	Fixed addition to each flotation cell
San Diego Mexico (Monks & Weiss, 1930)	'Oxide' lead ores : cerussite (60%) and anglesite (10%)	79.3% Pb	Na_2S : 1.82	Petroleum 600 Creosote 100 Gasoline 40 Kerosene 25	Fixed addition to flotation feed

2.4 Merensky ores

Merensky ores are a valuable source of PGEs that are found in the Bushveld Complex in South Africa. It is a preferred ore type, due to the ease of mining and processing as well as the presence of base-metal sulfide minerals. The PGEs are intimately associated with sulfide minerals, both as solid solutions within the sulfide mineral lattices and as discrete platinum group minerals (PGMs) either on grain boundaries or locked within the sulfide minerals (Snodgrass *et al*, 1994 and Lee, 1996). The sulfide mineral suite typically forms approximately 1 wt.% of the ore and consists of predominately pyrrhotite followed by pentlandite, chalcopyrite and pyrite (Viljoen *et al*, 1986). The sulfide mineral proportions vary greatly, and for an ore from the Rustenburg section of the reef, the sample contained 44 wt.% pyrrhotite, 27 wt.% pentlandite, 19 wt.% chalcopyrite and 10 wt.% pyrite (Cawthorn *et al*, 2002). In another part of the reef, the sulfide mineral proportions were 50-56 wt.% pyrrhotite, 23-32 wt.% pentlandite, 17 wt.% chalcopyrite and 1-2 wt. % pyrite (Wiese *et al*, 2005). The nature of the pyrrhotite is not well documented, however the composition is known to vary between the hexagonal and monoclinic forms (Liebenberg, 1970).

The remainder of the ore consists of mainly gangue silicate minerals and includes pyroxene (52 to 59 wt.%), feldspar (24 to 40 wt.%) and talc (0.5 to 5 wt.%) as well as chromite (3 to 4.5 wt.%). The pyroxene is present as two forms in approximately equal quantities, namely *ortho*pyroxene and the calcium-rich *clino*pyroxene. Although neither pyroxene nor feldspar show any natural flotation tendencies, they can become activated by base-metal ions and subsequently float after interaction with collectors (Malysiak *et al*, 2002, Malysiak *et al*, 2004 and O'Connor *et al*, 2006). Talc, a naturally floating mineral, can also rim the pyroxene particles, resulting in flotation (Becker *et al*, *2006*). Amongst the gangue minerals, feldspar is the most readily affected by weathering and forms kaolinite clays after heavy weathering. Under intense weathering, pyroxene can break down into smectite clays (Hey, 1999).

In the treatment of Merensky ores, the base-metal sulfide minerals and associated PGMs are recovered from the non-sulfide gangue minerals using conventional sulfide ore flotation practice to produce a bulk concentrate. The treatment strategy involves multiple stage grinding followed by flotation, where the ore is coarsely milled and floated and the

flotation tailings milled to a finer size and re-floated. This is known as the Mill-Float-Mill-Float or MF2 approach. Typical sequential grind sizes are 60% and 75% passing 74 microns respectively while SIBX features amongst the flotation reagent suite.

In order to maximise PGE flotation recoveries, it is particularly important to maximise the flotation recoveries of the sulfide minerals (Snodgrass *et al*, 1994). During processing, the gangue minerals release calcium and magnesium ions into solution (IS of 10^{-2}M or $3x10^{-3}$M Ca^{2+}), which buffers the slurry around pH 9. Typical flotation recoveries for a Merensky ore are 82-85% PGEs, 82-85% nickel and 85% copper (de Villiers *et al*, 1978).The order of flotation was chalcopyrite > pentlandite > pyrrhotite (Bradshaw *et al*, 1999).

The study of ores containing more than one sulfide mineral adds another level of complexity since the sulfide minerals may well interact with each other as well as with the chemical species present or generated during each stage of the process separation (Kocaberg and Smith, 1985). The nature of these potential interactions and any impact upon the efficacy of flotation separation has significant relevance in the potential treatment of oxidised Merensky ores.

2.5 OBJECTIVES AND HYPOTHESES

2.5.1 Introduction

The primary research objectives of this thesis are to characterise the effect of oxidation upon sulfide mineral floatability, to determine the suitability of sulfidisation in the flotation recovery of oxidised sulfide minerals, to compare the sulfidisation characteristics of oxidised sulfide minerals with those of base-metal 'oxide' mineral counterparts, to develop sulfidisation models for each of the three sulfide minerals and to determine the effect of sulfidisation upon Merensky ore gangue minerals.

Secondary research objectives, arising from the primary research objectives, include a comparison of oxidation techniques, an assessment of the effect of calcium ions during sulfidisation and the development of a novel technique to sulfidise pentlandite.

These research objectives are addressed by two hypotheses that focus on three themes, namely the oxidation of sulfide minerals, the sulfidisation of oxidised sulfide minerals and

the effect of sulfidisation on non-sulfide minerals. Key questions are developed to test these hypotheses through the development of appropriate experimental methodologies using Nkomati massive ore as the test material. Methods are established to oxidise the sulfide minerals, to characterise the degree of oxidation and assess the impact upon floatability. The oxidised sulfide minerals are sulfidised, analysed and the floatability measured under modified Merensky ore flotation conditions. To support these findings, oxidised and sulfidised samples of the three sulfide minerals are also analysed and characterised to develop mechanistic models of the sulfidisation process.

2.5.2 The effect of oxidation upon sulfide mineral flotation

2.5.2.1 Background

Based on the literature, primarily due to the mineral properties, a difference in floatability would be expected between the individual sulfide minerals in terms of the extent of oxidation under both thermal and chemical oxidation conditions. Chalcopyrite would be the most resistant to oxidation, while pyrrhotite the least. Specifically, pyrrhotite would be expected to be nearly an order of magnitude more reactive than pentlandite, while pentlandite would be considered to be more reactive than chalcopyrite.

Literature indicates that the general oxidation pathway for the iron bearing sulfide minerals, such as chalcopyrite, pyrrhotite and pentlandite, is through the loss of iron, with the partial loss of other base-metal species and subsequent surface enrichment of sulfur. The oxidation products consist of mainly base-metal oxide and oxy-hydroxides, which would be expected to share many similarities with the base-metal 'oxide' minerals. All of these conclusions, however, are based on mild oxidation with air or air and water and have not been examined for conditions of heavy oxidation. Moreover the flotation response of the sulfide minerals after oxidation was not tested.

Thermal oxidation may be different to chemical oxidation in that there may be greater loss of sulfur through the formation of sulfoxy compounds such as sulfate. While this aspect is minimised by keeping temperatures low (85°C), it would also diminish the possibility of forming magnetite and hematite, which are not amenable to aqueous sulfidisation. In the presence of water, the surfaces of base-metal 'oxide' minerals are covered with the base-metal hydroxides. Additionally, sulfates were reported as oxidation products after air,

aqueous and chemical oxidation. Moreover, since the sulfide mineral surfaces would be heavily oxidised in both methods and that the thermally oxidised surfaces would be hydrolysed, a significant convergence in the nature of surface species would be expected. Thus, very similar sulfide mineral surface responses to flotation and sulfidisation for the two oxidation methods would be expected.

SEM/EDX and XPS have been both used as techniques to study the oxidation of the iron-bearing sulfide minerals. The analysis offered by EDX was more qualitative in nature and identified elements while that of XPS was more quantitative and identified chemical species and specific bonds. These techniques were able to determine the thickness and chemical makeup of the oxidation layers on oxidised sulfide mineral surfaces. Additionally, electrophoresis and electrochemical techniques have significant potential as characterisation tools.

2.5.2.2 Hypothesis

It is hypothesised that increasing levels of surface oxidation would adversely affect the flotation response of sulfide minerals, particularly pyrrhotite, pentlandite, and to a lesser extent, chalcopyrite. Further, a secondary postulate is that there would be no significant difference between oxidation methods, such as thermal and chemical, as measured by the behaviour of the sulfide minerals.

2.5.2.3 Key Questions

The following key questions have been formulated as a basis for the experimental methodology that will test the hypothesis:

1.1 Nature of the flotation response

- What is the relationship between the degree of sulfide mineral oxidation and floatability for the three sulfide minerals present in Merensky ores?
- Is there a difference between the three sulfide minerals in terms of oxidation and the subsequent flotation behaviour?

1.2 Nature of oxidation

- Can the nature of the oxidation of the sulfide minerals be characterised?
- Is there a difference between chemical and thermal oxidation treatments?

2.5.3 The effect of sulfidisation upon oxidised sulfide mineral surfaces

2.5.3.1 Background

While the nature of the surface species has only been reported for mildly oxidised sulfide minerals, similar species are expected to be present after exposure to more highly oxidising conditions. Under aqueous conditions, heavily oxidised sulfide mineral surfaces would be expected to be covered in base-metal hydroxides as well as remanent base-metal oxides and oxy-hydroxides and thus comparable to those found on hydrolysed base-metal 'oxide' surfaces. Based on both solubility product and thermodynamic considerations, base-metal sulfides would be expected to form on these surfaces. Since the aqueous sulfidisation process has been successfully applied to base-metal 'oxide' minerals, it would therefore be expected to be effective with oxidised base-metal sulfide minerals. More specifically, the sulfidisation of oxidised chalcopyrite has been reported and the conditions for effective sulfidisation would be expected to occur around an Es of -500 mV (SCE). However, the nature of any sulfidisation mechanism has not been reported.

On the other hand, the sulfidisation of oxidised sulfide minerals such as pyrrhotite and pentlandite has received little attention in the literature. Iron oxide and oxy-hydroxide species are excellent adsorbents and they would be expected to adsorb hydrosulfide ions. Goethite (FeO.OH) was reported to respond to sulfidisation and subsequently floated while hematite did not. Hydrated ferric oxy-hydroxides, such as ferrihydrite, react with hydrosulfide ions which result in the formation of iron sulfide precipitates. It is significant that amongst the commercially important base-metals, there have been no reported sulfidisation studies on nickel 'oxide' minerals. However, sulfidisation has been used to recover an oxidised nickel arsenide mineral. Based on reported chemical and thermodynamic factors, nickel sulfide species would be expected to form. In summary, it would be expected that chalcopyrite would be the most readily sulfidised oxidised sulfide mineral followed by pyrrhotite and pentlandite.

Based on the literature, the sulfidisation mechanism for base-metal 'oxide' minerals is associated with the strong adsorption of hydrosulfide ions onto the mineral surface followed by the formation of a sulfide surface through anionic exchange and the precipitation of base-metal sulfides. Due to the hydrolysed 'oxide' nature of the surface layers of oxidised sulfide minerals, similar mechanisms would be expected to operate

during sulfidisation. As a result of sulfidisation, the respective base-metal sulfide would be expected to form and restore the sulfide mineral character to the oxidised sulfide surfaces. Electrochemical reactions would also be expected most likely due to the requirements of some of the sulfidisation reactions as well as the semiconductor nature of the parent sulfide mineral.

It is important to understand whether the sulfidisation process is selective between oxidised sulfide and non-sulfide minerals and thus has potential for the treatment of oxidised Merensky ores. Little has been reported about the response of non-sulfide gangue minerals to sulfidisation. Unlike the base-metal 'oxide' minerals, most non-sulfide gangue minerals encountered in mineral processing are of a siliceous nature and generally exhibit low aqueous solubility. Where solubility does occur, such as the release of alkali or alkaline earth cations from a mineral surface (e.g. pyroxene), the subsequent sulfides that would form are soluble (e.g. sodium sulfide and calcium sulfide). Therefore, unless chemically active base-metal species are present on the non-sulfide gangue mineral surfaces, it is unlikely that sulfidisation would have any effect upon the subsequent floatability of gangue minerals.

An industrially important consideration is that the sulfidisation process would not be affected by the presence of calcium ions at the levels encountered during the processing of Merensky ores. Based on the points made in the previous paragraph, calcium ions would not be expected to affect the sulfidisation of oxidised Merensky ores.

The preferred method of sulfidisation is Controlled Potential Sulfidisation (CPS) and the primary sulfidisation variable is the sulfide ion electrode potential (Es). A suitable range of investigative sulfidisation potentials would be -400 to -700 mV (relative to SCE) with a conditioning period of 5 minutes. Sulfidisation is conducted at the 'natural' pH of the system and at ambient temperatures in the presence of air. The flotation of the sulfidised oxidised sulfide minerals requires a strong collector and the SIBX used in the flotation of Merensky ores meets this criterion. However, a high dosage would be expected.

Electrophoresis and electrochemical techniques have significant potential as tools to elucidate possible mechanisms, while XPS analysis, although not been reported in this application, would be well suited to the identification of any sulfidised surface species.

2.5.3.2 Hypothesis

It is proposed that sulfidisation would restore the sulfide mineral character to oxidised sulfide mineral surfaces and thus their floatability, particularly pyrrhotite and chalcopyrite. It is hypothesised that the sulfidisation mechanisms of oxidised sulfide minerals would be similar to those proposed for their base-metal 'oxide' counterparts. Additionally, electrochemical mechanisms are expected.

In contrast, it is postulated that the floatability of Merensky gangue minerals, specifically feldspar and pyroxene, would not be enhanced by sulfidisation process and that sulfidisation of oxidised sulfide minerals can be conducted successfully in the presence of high levels of calcium ions.

2.5.3.3 Key Questions

The following key questions have been formulated as a basis for the experimental methodology that will test the hypothesis:

2.1 Nature of the sulfidisation response

- Can sulfidisation restore the sulfide mineral structure to the surfaces of the oxidised sulfide minerals?
- Is there a difference between chemical and thermal oxidation treatments in terms of sulfidisation and the subsequent flotation response?
- Is there a difference between the three sulfide minerals in terms of sulfidisation and subsequent flotation behaviour?
- How effective is the sulfidisation process in the presence of calcium ions in solution i.e. under Merensky flotation conditions?

2.2 Nature of the sulfidisation mechanism

- What species are present on the oxidised sulfide mineral surfaces before and after sulfidisation?
- What are the sulfidisation mechanisms for the three oxidised sulfide minerals?

2.3 Effect of sulfidisation upon floatability of non-sulfide minerals

- Does sulfidisation and the subsequent intensity affect the floatability of non-sulfide minerals present in Merensky ores such as feldspar and pyroxene?

2.4 Potential sulfidisation mechanism for non-sulfide minerals

- If sulfidisation does cause subsequent flotation of these non-sulfide minerals, what are the mechanisms?

CHAPTER 3

EXPERIMENTAL DETAILS

3.1 Introduction

The first stage of the experimental programme involved the preparation and characterisation of mineral samples and included chemical, XRD, mineralogical and liberation (QEM*SEM) analyses. Due to uncertainty concerning the nature of oxidised species present on oxidised Merensky ore sulfide surfaces, a number of oxidation approaches were evaluated and two methods settled upon, namely low temperature thermal oxidation followed by hydrolysis and chemical oxidation with hydrogen peroxide. The progress of the oxidation, particularly for thermally oxidised mineral samples, was tracked and characterised with both SEM/EDX and flotation. Corroborative studies were conducted with electrophoresis, electrochemistry and XPS. For input into other studies, additional data were collected with surface area measurements as well as chemical analyses of solutions after both EDTA extraction and hydrolysis.

In the second stage, the primary focus was the sulfidisation and flotation of oxidised mineral samples, particularly heavily oxidised Nkomati ore samples. Techniques such as XPS, electrophoresis and electrochemistry were used to gain an insight into the nature of the sulfidisation mechanisms and applied to both single sulfide mineral and Nkomati ore samples. The unexpected behaviour of oxidised pentlandite required further study and a specific flotation testwork programme was designed to elucidate the nature of the sulfidisation mechanism.

Finally, an experimental programme was formulated to clarify two practical issues regarding the sulfidisation of oxidised Merensky ores. This testwork examined the effect of calcium ions during sulfidisation and the effect of the sulfidisation process upon the flotation response of Merensky ore gangue minerals.

3.2 Minerals

The research programme was based on Nkomati massive sulfide ore samples as a proxy for Merensky ore sulfide minerals due to mineralogical similarities and significantly greater

sulfide mineral abundance (86 wt.% versus ~1 wt.%). Single sulfide minerals, such as chalcopyrite, pyrrhotite and pentlandite, were sourced for specific sulfidisation studies. Unweathered and weathered Merensky gangue ore minerals were also prepared for testwork.

3.2.1 Nkomati ore

Nkomati massive sulfide ores contain the same base-metal sulfide minerals as Merensky ores and was thus selected as the study material. Although this ore sample did not contain exactly the same sulfide mineral proportions, the investigation of the behaviour and subsequent trends of the sulfide minerals is nonetheless possible. Based on several samples, the head grade of the Nkomati ore sample was determined by AAS analysis to be 55.3 wt.% iron, 31.4 wt.% sulfur, 2.93 wt.% nickel and 1.85 wt.% copper (refer to Table 3-1).

Table 3-1: Chemical analyses of sulfide mineral samples

Mineral Sample	Ni (wt.%)	Cu (wt.%)	Fe (wt.%)	S (wt.%)	Other
Nkomati (-106μm/+38μm)	2.9	1.9	55.3	31.4	Iron oxides
Nkomati (-11μm)	2.8	1.9	55.4	31.8	(~13.6 wt.%)
Synthethic Pentlandite	34.1	-	32.5	33.2	-
Natural Pentlandite	34.0	0.1	32.4	33.1	-
Chalcopyrite	-	33.8	30.1	34.8	Minor lead, zinc
Pyrrhotite	0.2	-	56.0	33.9	Silica (~10 wt.%)

QEM*SEM analyses (refer to Section 3.7.2 and Appendix D6) determined that the Nkomati ore sample consisted of 85 wt.% sulfides (67 wt.% pyrrhotite, 9 wt.% pentlandite, 6 wt.% chalcopyrite and 3 wt.% pyrite) with mainly iron oxide minerals (13.6 wt.%). This was corroborated by chemical and mineralogical reconciliations (refer to Table 3-2). The solid solution nickel content in the pyrrhotite was estimated to be 0.05 wt.%. Using a technique developed by Arnold (1966), XRD analysis indicated that the pyrrhotite was predominantly monoclinic (77%) which is in accord with other studies on Nkomati ore samples (Becker, *pers comm*) and of Merensky ores. Based on SEM/EDX analyses of the pyrrhotite particles, the most commonly identified chemical formula was $Fe_{0.97}S$ followed by $Fe_{0.95}S$.

Table 3-2: Comparative mineral analyses of Nkomati ore samples
(errors are expressed as ± SD)

Mineral	Percent Mass		
	XRD [*1]	Chemical [*2]	Sulfide [*3]
Pyrrhotite	66.3 ± 1.1	66.7 ± 0.4	78.3
Pentlandite	8.4 ± 0.6	9.0 ± 0.4	10.5
Chalcopyrite	5.4 ± 0.5	6.1 ± 0.4	7.2
Pyrite	3.2 ± 0.1	3.5 ± 0.4	4.1
Iron Oxides	15.2 ± 1.7	13.6	-
Silicates	1.5 ± 0.03	1.3	-

[*1] Average of the three size ranges (QEM*SEM)
[*2] Reconciliation based on all test work samples
[*3] Based on sulfide minerals

Based on the QEM*SEM analyses, the sulfide minerals were relatively well liberated in each of the three size ranges used in the flotation studies. Overall liberation by mineral was pyrrhotite (90%), pentlandite (80%) and chalcopyrite (84%). Composites that existed between the sulfide minerals were primarily with pyrrhotite and are not problematic in bulk flotation. Some of the iron oxide minerals were present as composites with the sulfide minerals, in particular pyrrhotite (5%), pentlandite (3%) and chalcopyrite (2%). The relative errors in the QEM*SEM analyses were estimated as follows: pyrrhotite (1.1%), pentlandite (4.2%), chalcopyrite (6.1%) and pyrite (8.6%).

3.2.2 Single sulfide minerals

Samples of chalcopyrite, and pyrrhotite were sourced from Wards Scientific while the pentlandite sample had been synthesised by Anglo-Platinum Research Centre. When the need arose for flotation testwork, a pure pentlandite sample was prepared from a nickel-rich massive sulfide ore sample from the Raglan deposit in Canada. The chemical analyses of the sulfide minerals are presented in Table 3-1.

The chalcopyrite sample had minor quantities of lead and zinc, which were readily oxidised and subsequently sulfidised during testwork. The pyrrhotite sample contained a reasonable quantity of silica and was predominately monoclinic based on XRD studies (Arnold, 1966). XRD analysis of the natural pentlandite revealed no crystalline impurities and although it had a small copper content, it was nearly pure (>98%).

3.2.3 Mineral sample preparation

For Nkomati ore, hand picked lump samples were carefully crushed and dry ground with chrome steel media to obtain three size fractions namely, –106/+74 microns, –74/+53 microns and –53/+38 microns and wet screened on a 38 micron screen before oxidation. Unoxidised samples were sealed in plastic bags, stored under refrigeration and floated within two weeks of preparation.

The natural pentlandite sample was prepared from the Raglan ore sample where both the pentlandite and monoclinic pyrrhotite had formed as large, granular phases, which enabled magnetic separation at a relatively coarse size range. The remaining impurity, chalcopyrite, was removed by micro-flotation, employing starvation quantities (5 ppm) of a copper specific collector (Senkol 65). The subsequent flotation tailing was thoroughly washed with ethyl alcohol followed by de-ionised water before filtration and drying under vacuum. Like the Nkomati ore sample, the pure pentlandite was separated into three size fractions.

For other studies, such as electrophoresis, finely powdered samples of chalcopyrite, pyrrhotite and synthetic pentlandite were prepared by grinding in an agate mortar and pestle to below 25 microns. In the case of the Nkomati ore sample, a fine sample was prepared by wet screening the -38 micron size fraction on a Merco Industry 11 micron nylon mesh. The -11 μm size fraction was filtered, dried under vacuum, sealed under nitrogen and stored under refrigeration.

Unweathered Merensky ore gangue minerals were recovered from the tailings of a batch flotation test where virtually all the sulfide minerals had been recovered. A moderate level of gangue depressant had been employed and the talcaceous minerals were not fully depressed. The tailings were filtered, dried and screened into the three size ranges before thoroughly mixing and sub-sampling into smaller quantities. The sub-samples were washed with ethyl alcohol followed by de-ionised water before being finally dried under vacuum.

The weathered Merensky ore gangue minerals were extracted from a heavily oxidised Merensky ore after milling and flotation in the same fashion as described for the unweathered sample. The flotation stage was undertaken as a precaution to ensure that the tailing contained no sulfide minerals. Mineralogical analysis of the sample revealed that nearly all the sulfide minerals had completely been oxidised and that the base-metal values

had been captured as a manganese wad.

3.2.4 Other characterisation studies

XRD studies were conducted on finely ground samples of all the mineral samples, including the unweathered and weathered Merensky ore gangue minerals. Polished sections of the sulfide minerals were examined and photographed using a Zeiss binocular microscope. The results of the XRD studies as well as photographs of the ore and mineral samples are presented in Appendix D1.

3.3 Reagents

Analytical grade reagents were used and while the collectors were supplied by Senmin. The reagents used in this research are summarised by application in Appendix D-1. All solutions were prepared with high purity water (<0.15 μS/cm specific conductivity) such as Milli-Pore Q^{TM} water. Ten to fifteen minutes of purging with nitrogen was used to obtain de-aerated solutions for use in the adsorption, electrophoretic and electrochemical testwork as well as preparation of the EDTA solution.

3.4 Oxidation methods

3.4.1 Thermal oxidation

The first approach employed low temperature thermal oxidation where the mineral samples were placed in an oven at 85°C with circulated air. This technique has been used to study the oxidation behaviour of pentlandite at much higher temperatures (Richardson and Vaughan, 1989) while several investigators have studied the air oxidation of sulfides at ambient temperatures (Pratt *et al*, 1994, Mycroft *et al*, 1995 and Legrand *et al*, 1998), in one case, for a comparable period to that employed in this study (Buckley and Woods, 1984). For the finer sized sulfide mineral samples, the same degree of oxidation was achieved by oxidising this finer material under the same conditions for a period based on the ratio of the surface areas (refer to Table 3-3). The basis for these calculations is presented in Appendix A2.

Table 3-3: Oxidation conditions for the finer sized sulfide mineral samples

Mineral sample	Thermal oxidation		Chemical oxidation
	Moderate (days)	Heavy (days)	Oxidant volume (mL)
Nkomati ore (-11μm)	8	18	43
Pentlandite (-25μm)	12	28	27
Chalcopyrite (-25μm)	15	33	23
Pyrrhotite (-25μm)	11	25	30

3.4.2 Chemical oxidation

The second approach involved chemical oxidation with hydrogen peroxide which has been used to oxidise sulfide minerals (Sui *et al*, 1995 and Laskowski and Yuan, 2002). A systematic procedure was adopted whereby the sulfide mineral samples were agitated with hydrogen peroxide solutions of different strengths for selected periods of time. In the case of the finer sized sulfide mineral samples, the same degree of oxidation was achieved by maintaining the same oxidation intensity (moles/m^2/minute). The same solution strength and contact times were used as for the coarser material, however the amount of solution was varied based on the ratio of the surface area and the sample quantity (refer to Table 3-3). Appendix A2 outlines the basis for these calculations.

3.5 Micro-flotation

Flotation recovery was used as the primary tool to evaluate the effect of oxidation upon the sulfide mineral suite as well as the ability of sulfidisation to restore sulfide surfaces to the oxidised minerals. The flotation evaluations were conducted with the UCT micro-flotation system (Bradshaw and O'Connor, 1996) which offered a number of attractive features that were aligned with the fundamental nature of this research. Table 3-4 presents the experimental details for the micro-flotation tests based on modified Merensky ore bench flotation conditions.

The mass of the concentrate and tailing samples were used to calculate recoveries, and for Nkomati ore samples, chemical analyses for iron, nickel, copper and sulfur were made (refer to Section 3-7-2). Based on these assays, employing the technique presented in Appendix A1, the individual sulfide mineral proportions were calculated. The maximum Standard Error (SE) in the flotation results was found to be ±1.2% for unoxidised samples, ±2.5% for oxidised samples and ±2.0% for sulfidised samples.

Table 3-4: Experimental details of the micro-flotation studies

Parameter/Equipment	Experimental Details
Cell volume	365 mL
Peristaltic pump	50 rpm
Air flow-rate	7 mL/min
Air source	Synthetic air (no H_2O nor CO_2)
Sample quantity	2 g
Feed size range	Equal amounts of -106µm/+74µm,-74µm/+53µm and -53µm/+38µm
Pre flotation	Wet screened at 38µm
Collector	SIBX, 1 minute conditioning
Flotation conditions	pH 9, IS of 10^{-2} Ca^{2+}
Concentrates	1, 3 and 10 minutes
Number of replications	2

Pulp chemistry conditions for selected tests were measured and recorded with a TPS meter Model 90 FLMV and included pH, ORP (platinum electrode with a silver/silver chloride reference) and temperature. During sample conditioning, pH measurements were made with a Hanna pH 211 meter.

3.5.1 Experimental testwork

3.5.1.1 Reproducibility

The reproducibility of the flotation testwork procedure was tested with unoxidised Nkomati ore samples based on five replications and a collector concentration of 1.375×10^{-4}M. As Table 3-5 shows, almost complete flotation of the sulfide minerals was found with acceptable reproducibility.

Table 3-5: Reproducibility of micro-flotation testwork with unoxidised Nkomati ore samples

Cumulative flotation time (min)	Cumulative Flotation Mass Recovery (%)					Statistics		
						Mean	SD	SE
1	41.7	37.8	38.7	43.3	40.7	40.4	2.23	1.00
3	71.1	73.3	69.6	70.7	74.5	71.8	2.00	0.89
10	83.1	85.1	81.9	81.1	82.2	82.7	1.56	0.70

3.5.1.2 Oxidation studies

Micro-flotation tests were conducted with oxidised Nkomati samples as a function of the degree of oxidation. Initially, the effect on the collectorless flotation was examined and compared to that found for an initially unoxidised sample determined from four replications. The degree of floatability of the sample was ascertained over the first 27 days of thermal oxidation with a high collector concentration ($1.375x10^{-3}M$). The nature of the coherency of the oxidised layer was also addressed with ultrasonic treatment prior to flotation with a higher collector addition ($1.375x10^{-2}M$) over the period from 5 to 121 days. This latter approach was adopted as the standard procedure for assessing the impact of thermal oxidation upon sulfide mineral samples. The experimental details for the testwork programme are presented in Table 3-6. Appendix B1 presents the raw data arising from this testwork.

Table 3-6: Experimental details of the oxidation study with oxidised Nkomati ore samples

Parameter/Treatment	**Experimental Details**
Ultrasonic treatment and hydrolysis (thermally oxidised samples)	Pre-conditioning : Two 1 minute ultrasonic treatments (Elma Transsonic 310, 500cm^3, 0.05W/m^2 and 35kHz) followed by 10 minutes aqueous contact (hydrolysis)
Variables	
Thermal oxidation (85°C in air)	No collector: 0 and 1 day Collector ($1.375x10^{-3}M$): 2, 5, 8, 16 and 27 days Ultrasonic treatment and collector ($1.375x10^{-2}M$): 5, 16, 27, 31, 50, 60, 92 and 121 days
Chemical oxidation (H_2O_2)	Collector ($1.375x10^{-2}M$): 1 minute $10^{-8}M$, 10 minutes $10^{-5}M$, 10 minutes $10^{-3}M$ and 10 minutes $10^{-2}M$

The degree of oxidation of the sample is defined in terms of flotation recovery. Moderate oxidation describes where the flotation recovery of the sample has been reduced to 50 wt.% (27 days of thermal exposure and 1 minute with $10^{-8}M$ H_2O_2) and heavy oxidation where the flotation response has been practically removed (121 days of thermal treatment and 10 minutes with $10^{-2}M$ H_2O_2).

As background to another study, the flotation response of heavily oxidised pentlandite samples was also characterised (refer to Table 3-7). The raw data are located in Appendix B2.

The flotation behaviour of unweathered and weathered Merensky ore gangue minerals was evaluated with and without collector. Table 3-8 presents the experimental details for these tests. Appendix B3 records the raw data collected from this testwork.

Table 3-7: Experimental details of the oxidation study with heavily oxidised pentlandite samples

Parameter/Treatment	Experimental Details
Collector strength	$1.375x10^{-2}$ M
Variables	
Thermal oxidation (85°C in air)	121 days
Chemical oxidation (H_2O_2)	10 minutes 10^{-2}M

Table 3-8: Experimental details of the flotation of weathered and unweathered Merensky ore gangue minerals

Parameter/Treatment	Experimental Details
Collector strength	$1.375x10^{-2}$ M
Number of replications	5
Variables	
Collector addition	With and without
Degree of oxidation	Unweathered and weathered

3.5.1.3 Sulfidisation studies

Sulfidisation studies were conducted on oxidised sulfide mineral samples using Controlled Potential Sulfidisation (CPS) (Jones and Woodcock, 1978a). In order to determine the true flotation response, the solution was decanted and replaced with fresh solution after sulfidisation. The experimental details are presented in Table 3-9.

Table 3-9: Experimental details of the sulfidisation studies

Parameter/Equipment	Experimental Details
Potentiometric titrator	Radiometric PHM 290 pH-Stat Controller
Sulfide ion probe	Orion 9616 (Ag/Ag_2S with Ag/AgCl [0.01M KCl] reference)
Control system	Feedback with solenoid valve: ± 5 mV
Sulfidisation	NaHS, CPS 5 minutes conditioning in air
Post sulfidisation	Solution decantation, sample washing and solution replacement
Collector strength	$1.375x10^{-3}$M

The sulfide ion electrode potential was checked against known concentrations of sulfidising reagent solutions prepared with sulfide anti-oxidant buffer solution (SAOB) (Orion, 1996) and corroborated with total sulfide measurements (Clesceri and Greenberg, 1998). The measured parameters for sodium hydrosulfide solutions as a function of concentration are given in Table 3-10.

Table 3-10: Solution parameters as a function of sodium hydrosulfide concentration

[NaSH] (M)	Es (mV)	ORP (SHE, mV)	DO (ppm)	pH
10^{-2}	-792	-0.382	5.8	9.45
10^{-3}	-743	-0.315	5.4	8.80
10^{-4}	-696	-0.250	5.4	8.13
10^{-5}	-644	-0.205	5.5	7.93

3.5.1.3.1 Nkomati ore

The effect of sulfidisation was examined with heavily oxidised Nkomati ore samples and the experimental details are presented in Table 3-11. The raw data generated by this testwork are located in Appendix C1.

Table 3-11: Experimental details of the sulfidisation studies with heavily oxidised Nkomati ore samples

Variable/Treatment	Experimental Details
Oxidation method	Thermal : 121 days at 85°C in circulated air Chemical : 10 minutes 10^{-2}M H_2O_2
Sulfidisation intensity (Es)	-500,-600,-650,-700 and -800 mV

The influence of calcium ions during sulfidisation conditioning was examined with a heavily thermally oxidised Nkomati ore sample at the optimum sulfidisation potential of -650 mV. Table 3-12 presents the experimental details. The raw data from these experiments are captured in Appendix C1.

Table 3-12: Experimental details of the study of calcium ions during sulfidisation at constant Es

Variable	
Calcium ions (IS of 10^{-2})	Presence/absence during sulfidisation

3.5.1.3.2 Pentlandite

A number of sulfidisation studies was conducted with heavily oxidised pentlandite samples. The first set of tests was based on establishing the response to sulfidisation over the Es range used for the chemically and thermally heavily oxidised Nkomati samples. Table 3-13 presents the experimental details. Appendix C2 summarises the raw data collected with this experimental campaign.

Table 3-13: Experimental details of the sulfidisation studies with heavily oxidised pentlandite samples

Variables	
Oxidation method	Thermal: 121 days at 85°C in air Chemical: 10 minutes in 10^{-2}M H_2O_2

The base-metal precipitation hypothesis was tested by evaluating the effect of copper and iron ion additions upon the flotation response of heavily chemically oxidised pentlandite at the optimum sulfidisation potential (Es = -650 mV). Additional flotation time was required. Table 3-14 summarises the experimental details while the raw data are presented in Appendix C2.

Table 3-14: Experimental details of the base-metal ion additions with heavily chemically oxidised pentlandite samples at constant Es

Parameter/Treatment	**Experimental Details**
Sulfidisation intensity (Es)	-650 mV
Concentrates	1, 3, 10 and 20 minutes
Variables	
Base-metal ion	Fe(III) (500µmoles) or Cu(II) (5µmoles)
Addition point	Before or during sulfidisation

The role of iron additions during sulfidisation upon the flotation response of heavily thermally oxidised pentlandite was investigated as a function of sulfidisation potential. The experimental conditions are shown in Table 3-15. Appendix C2 captures the raw data from this testwork.

Table 3-15: Experimental details of the Fe(III) ion additions during sulfidisation with heavily thermally oxidised pentlandite samples

Parameter/Treatment	Experimental Details
Base-metal addition	Fe(III) (500µmoles) during sulfidisation
Concentrates	1, 3, 10 and 20 minutes
Variable	
Sulfidisation intensity (Es)	-500,-600,-650,-700 and -800 mV

3.5.1.3.3 Merensky ore gangue minerals

To evaluate the influence of the sulfidisation process upon the floatability of Merensky ore gangue minerals, weathered and unweathered samples were sulfidised at three selected potentials. Table 3-16 summarises the experimental details. The raw data are presented in Appendix C3.

Table 3-16: Experimental details of the sulfidisation studies with Merensky ore gangue minerals

Parameter/Treatment	Experimental Details
Number of replications	5
Variables	
Sulfidisation intensity (Es)	-500 mV,-650 mV and -800 mV
Degree of oxidation	Unweathered and weathered

3.6 Surface techniques

3.6.1 Zeta potential measurements

3.6.1.1 Experimental testwork

The details of the electrophoretic procedure are presented in Table 3-17. For thermally oxidised samples, the pH was adjusted after hydrolysis to the value found for the unoxidised sulfide mineral samples.

Table 3-18 presents the experimental details used in the electrophoretic study of the oxidised sulfide mineral samples while the raw data are collated in Appendix D2.

Table 3-17: Experimental details of the electrophoretic procedures for the sulfide minerals

Parameter/Treatment	Experimental Details
Equipment	Zeta-Meter model 3.0+ system with video display
Sample concentration	0.1 g/L
Feed size range	-11 μm : Nkomati ore sample -25μm : other sulfide minerals
Solution preparation	10 minutes de-aeration with nitrogen
Support solution	$5x10^{-2}$M NaCl under nitrogen
Initial pH adjustment	NaOH to 6.5 for oxidised samples
Measurements	10+ readings corrected for temperature (22.5°C) 5 minutes acclimatisation before each reading

Table 3-18: Experimental details of the electrophoretic study with the oxidised sulfide minerals

Parameter/Treatment	Experimental Detailss
pH adjustment	Acidic values: HCl and basic values: NaOH
Variables	
Oxidation method	Thermal and chemical
Degree of oxidation	Unoxidised, moderate and heavy
Mineral samples	Nkomati ore, chalcopyrite, pyrrhotite, and pentlandite
pH range	2 to 11 in 1 pH unit increments

The experimental details for the electrophoretic study of the sulfidisation of the oxidised sulfide minerals are shown in Table 3-19. Initially, a comparison was made between this approach and where the pH was maintained constant (pH 11) to determine the relative contributions of pH and hydrosulfide ions to the zeta potential using a heavily chemically oxidised Nkomati sample. The raw data are presented in Appendix D2.

Table 3-19: Experimental details of the electrophoretic study of the sulfidisation of oxidised sulfide minerals

Parameter/Treatment	Experimental Details
Sulfidising reagent	Na_2S under N_2
Variables	
Oxidation method	Thermal and chemical
Degree of oxidation	Moderate and heavy
Mineral samples	Nkomati ore, chalcopyrite, pyrrhotite, and pentlandite
Sulfidisation intensity (Es)	-400 to -800 mV in 50mV increments

3.6.2 X-ray photo-electron spectroscopy (XPS)

The details of the equipment, procedures and the heavily thermally oxidised sulfide mineral samples for XPS analyses are summarized in Table 3-20.

Table 3-20: Details of XPS equipment, procedures and sulfide mineral samples

Parameter/Equipment	Experimental Details
Equipment	Kratos Axis Ultra photo-electron spectrometer Hemispherical analyser with delay line detector
Irradiation source	300W monochromatic Mg Kα
Pass energy	20 eV: broad and valence band spectra 10 eV: Fe 2p and S 2p
Take-off angle	45°
Vacuum	~10^{-8} torr
Narrow scan step size	0.025 eV
Sample quantity	0.5 g
Mineral sample type	Nkomati ore, chalcopyrite and pentlandite
Feed size range	-106μm/+38μm: Nkomati ore samples -25μm: chalcopyrite, pentlandite and pyrrhotite samples

The preparation methods replicated the procedures used during testwork except that sulfidisation was conducted under nitrogen to minimise the oxidation of the sulfidised surfaces (refer to Table 3-21). Additionally, for the Nkomati ore samples, sulfidisation was also performed under air while a heavily chemically oxidised surface was examined. After treatment, the replacement solution was adjusted to pH 9 and the sample snap frozen and stored under refrigeration until analysed. Appendix D3 presents the raw data with the fitted curves.

Table 3-21: Preparation details for XPS analyses of oxidised sulfide minerals

Parameter/Treatment	Experimental Details
Oxidation method	Nkomati ore: chemical and thermal Sulfide minerals: thermal
Sulfidisation intensity (Es)	-500, -650 and -800 mV (pentlandite sample) -500 and -650 mV (Nkomati ore and chalcopyrite samples)
Sulfidisation atmosphere	Under N_2: all samples and sulfidisation conditions Under air: Nkomati ore sample at -650 mV

Details of the method used to interpret the XPS data are presented in Appendix D3. The XPS measurements were made without replication and it is difficult to assign a specific error. Hesse *et al* (2004) have studied the error associated with XPS analyses and shown that is dependent upon the BE peak separation, the count intensity and the signal/noise ratio. Based this assessment, it was concluded that the relative XPS errors fell between 5 and 15%, with most measurements having an error of 10% or less.

3.6.3 Electrochemistry

Cyclic voltammetric and chronoamperometric studies were conducted on mineral electrodes prepared from the three sulfide mineral samples used in this research, namely chalcopyrite, pyrrhotite and pentlandite. Table 3-22 presents the experimental details and Appendix D4 presents the raw results.

Table 3-22: Experimental details of the cyclic voltammetric studies of sulfide mineral electrodes

Preparation/Treatment	Experimental Details
Equipment	Gamry Instruments Potentiostat/ Galvanostat model PCI4/750 unit
CV supporting solution	Sodium tetraborate ($5x10^{-2}$M, pH 9.2) under nitrogen
Polarisation	Unoxidised electrodes:15 minutes at -500 mV (SHE)
Scanning details	Commenced at open circuit potential -500 to +500 mV (SHE) at 20mV/s
Sulfidisation	10^{-3}M (~-650mV Es), Na_2S, 15 minutes in air
Variables	
Degree of oxidation	Unoxidised and heavy chemical

Chronoamperometric experiments were performed with the sulfide mineral electrodes to observe the interaction with the hydrosulfide ion as a function of Na_2S addition under nitrogen. After heavy chemical oxidation, the mineral electrodes were exposed to two sulfidising reagent concentrations ($1x10^{-3}$M and $1x10^{-2}$M) over time. The potential of the mineral electrode was held at its open circuit value during this study, namely chalcopyrite 0.1449 V, pyrrhotite 0.1404 V and pentlandite -0.0226 V. The variation in the mineral electrode current revealed the nature of the surface electrochemical reaction: a negative current indicated a cathodic reaction while a positive current disclosed an anodic reaction. The raw data are presented in Appendix D4.

3.7 Characterisation techniques

3.7.1 EDTA extractions

EDTA extractions under nitrogen were conducted to determine the amount of chemically available species present on the oxidised surfaces of flotation sized Nkomati ore samples (Rumball and Richmond, 1996 and Vanthuyne and Maes, 2002). The experimental conditions are summarised in Table 3-23 while the raw data are presented in Appendix D5.

Table 3-23: Experimental conditions of the EDTA extractions with oxidised Nkomati ores

Treatment	Experimental details
Sample quantity	1 g
EDTA strength	3% (~0.1M) (prepared with de-aerated, de-ionised water)
Contact time	10 minutes
Solution analysis	AAS
Pre extraction treatment (thermally oxidised)	10 minutes aqueous contact (hydrolysis) pH adjustment to 6.5
Variables	
Oxidation method	Chemical and thermal
Degree of oxidation	None, moderate and heavy
Post thermal oxidation treatment	With and without ultrasonic treatment

3.7.2 Electron microscopy

Table 3-24 presents the experimental details for the SEM/EDX investigation. The limit of detection of the EDX for the lightest element detected (oxygen) was approximately 2%, with lower detection limits for the heavier elements.

QEM*SEM is a technique that employs a SEM in conjunction with 4 Gresham x-ray detectors to statistically determine the mineralogical, chemical and textural properties of an ore sample. These details for the three size ranges of the Nkomati ore sample are presented in Appendix D6.

Table 3-24: Experimental details for the SEM/EDX study

Treatment	Experimental details
Equipment	Leica Stereoscan 440 SEM and a Kevex Detector (EDX)
Sample preparation	Setting and curing in Spurr's resin Polishing of sample end to provide mineral cross-sections
EDX acceleration voltage	20 kV
EDX element analysis	O, S, Fe, Ni and Cu
EDX analysis points	Oxidation layer, near surface and bulk regions
Variables	
Mineral sample	Nkomati ore (pyrrhotite), chalcopyrite and pentlandite
Oxidation method	Chemical and thermal
Degree of oxidation	Chalcopyrite, pentlandite: moderate and heavy (thermal) heavy (chemical) Nkomati ore (pyrrhotite): 2, 10, 15, 18, 27, 30, 50, 60 and 121 days heavy (chemical)

3.7.3 Other techniques

BET surface area determinations were made using a Micrometrics Tri-star unit with a Flowprep 060 after the samples had been held in-situ at 60°C for 24 hours (Brunauer *et al*, 1938). Table 3-25 summarises the surface areas determined for the sulfide mineral samples used in this research.

Table 3-25: Surface areas of the sulfide mineral samples

Mineral sample	Surface area (m^2/g)	Error ($\pm m^2/g$)
Nkomati ore (-106μm/+38μm)[a]	0.3335	0.0058
Nkomati ore (-11μm)	1.1350	0.0113
Pentlandite (-106μm/+38μm)[a]	0.3457	0.0046
Pentlandite (-25μm)	0.7218	0.0129
Chalcopyrite (-25μm)	0.6035	0.0108
Pyrrhotite (-25μm)	0.7936	0.0234

[a] after ultrasonic treatment and wet screening at 38 microns

Mineral samples and flotation products were analysed after a HF/aqua regia digestion for copper, nickel and iron by AAS on a dual wavelength absorption Varian SpectrAA-30. Sulfur assays were determined by a Leco SC-432DR unit. The flotation recoveries of the

individual sulfide minerals were calculated using these assays although pyrrhotite and pyrite could not be reliably distinguished and are collectively referred to as pyrrhotite. The calculation method is presented in Appendix A1.

Sulfate analyses were made on solutions from the hydrolysis and chemical oxidation studies with high pressure liquid chromatography. The HPLC system consisted of a Waters 1525 binary HPLC pump, a Waters 2487 dual wavelength absorbance detector and a Waters Model 430 conductivity detector.

3.8 Other studies

3.8.1 Adsorption studies

Adsorption studies were conducted on heavily oxidised Nkomati ore samples to complete the comparison between the behaviour of oxidised sulfide minerals and base-metal 'oxide' minerals in a sulfidising environment. During adsorption, the ORP, pH and Es values were logged every 2 seconds on the TPS meter. The initial and final solution concentrations were measured for total soluble sulfide using the methylene blue method (Clesceri and Greenberg, 1998). The hydrosulfide ion and sulfide ion concentrations were calculated from the pK values for the $H_2S/HS^-/S^{2-}$ system based on the measured total sulfide and pH values (Rao and Hepler, 1977). The experimental details are shown in Table 3-26 while the raw data and associated calculations are presented in Appendix E1.

Table 3-26: Experimental details for the adsorption studies with heavily oxidised Nkomati ores

Constants	
Cell volume	50 mL
Sample quantity	0.5 g
Feed size range	-11 μm : Nkomati ore sample
Oxidation details	Heavily thermal (121 days @ 85°C in air)
Conditioning	10 minutes hydrolysis
pH adjustment	6.5
Gas details	Nitrogen at 5mL/minute
Sulfidisation details	NaHS under N_2
Solution preparation	De-aerated de-ionised water
Variables	
Sodium hydrosulfide concentration	10^{-3},10^{-4} and 10^{-5} M

3.8.2 Hydrolysis

The interaction between moderately and heavily thermally oxidised Nkomati ore samples was monitored over a ten minute period. A TPS meter was used to log the ORP and pH values every two seconds. When the reaction was complete, the solution was recovered, filtered and analysed for base-metal ion and sulfate values. Appendix E2 contains the raw data collected doing these experiments.

CHAPTER 4

RESULTS : OXIDATION OF SULFIDE MINERALS

4.1 Introduction

The results presented in this chapter were generated from the testwork programme designed to address the first hypothesis, namely *that increasing levels of surface oxidation would adversely affect the flotation response of sulfide minerals, particularly pyrrhotite, pentlandite, and to a lesser extent, chalcopyrite* and *that there would be no significant difference between oxidation methods, such as thermal and chemical, as measured by the behaviour of the sulfide minerals.*

Oxidation studies were conducted on the Nkomati ore samples and pure mineral samples in order to characterise the influence of the degree of surface oxidation upon the flotation recovery of chalcopyrite, pyrrhotite and pentlandite as measured by micro-flotation. Two oxidation methods were used. The first method consisted of low temperature thermal oxidation in air followed by hydrolysis while the second approach entailed chemical oxidation using hydrogen peroxide. Both of these methods produced suitably oxidised samples for the testwork programme. The studies were predominately carried out on the size range that was suitable for micro-flotation, namely equal quantities of -106µm/+74µm, -74µm/+53µm and -53µm/+38µm material.

Cross-sections of oxidised samples were inspected and analysed by SEM/EDX to determine the development of the oxide layers. These loose oxide layers on thermally oxidised samples were removed by ultrasonic treatment and chemically analysed. The response of the thermally oxidised samples during hydrolysis was also measured. The terms moderate and heavy oxidation are used to describe the oxidised conditions where 50% flotation recovery and a low flotation recovery were found respectively. The flotation behaviour of oxidised pentlandite as a single mineral was also studied.

Unless noted otherwise, errors bars are based on the Standard Error (±SE).

4.2 Flotation response

In this section, the results of the flotation studies with Nkomati ore samples and pentlandite samples after oxidation are presented.

4.2.1 Nkomati ore

4.2.1.1 Before oxidation

The Nkomati ore sample displayed considerable natural floatability as shown in Figure 4-1. Chalcopyrite floated the most readily, followed by pentlandite and pyrrhotite.

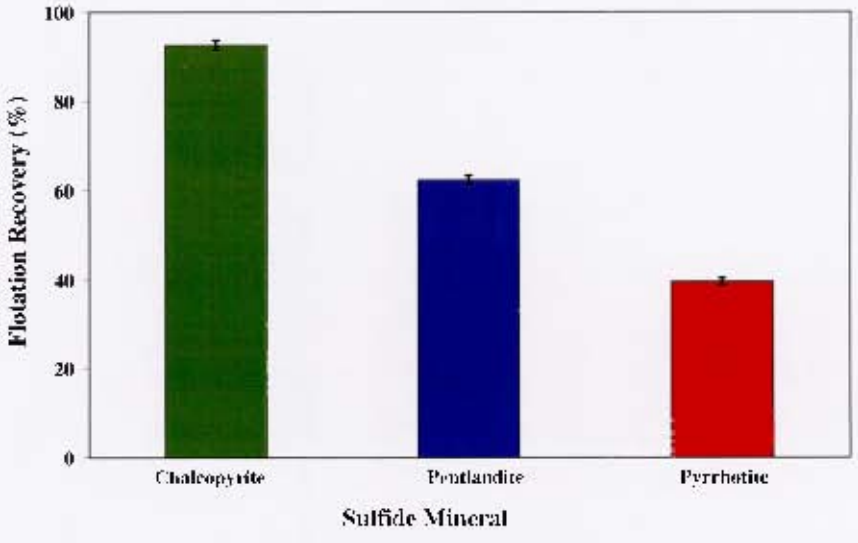

Figure 4-1: The flotation recoveries of sulfide minerals from Nkomati ore samples without collector

Figure 4-2 shows that after conditioning with SIBX at a concentration of 1.375×10^{-4}M, practically all the floatable material was recovered after 10 minutes.

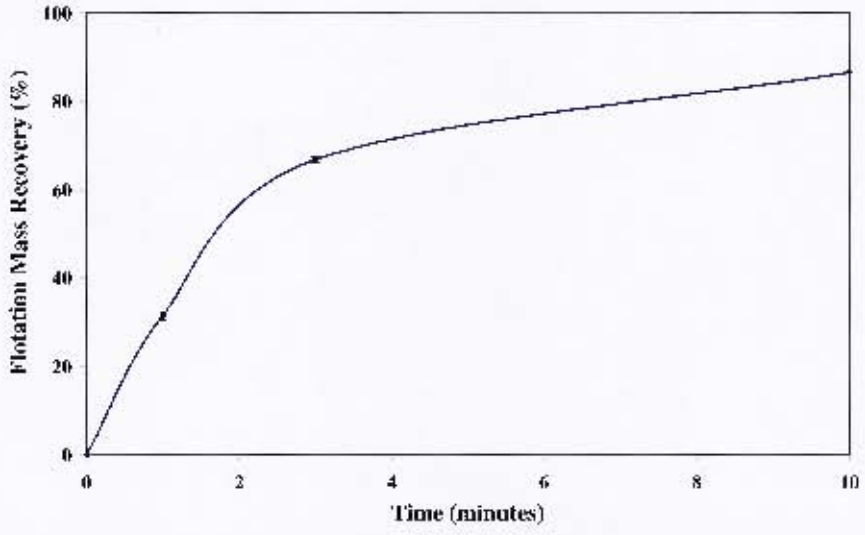

Figure 4-2: Flotation mass recovery of the Nkomati ore with 1.375×10^{-4}M SIBX

All of the sulfide minerals demonstrated good floatability under these conditions and very high flotation recoveries were achieved (refer to Figure 4-3).

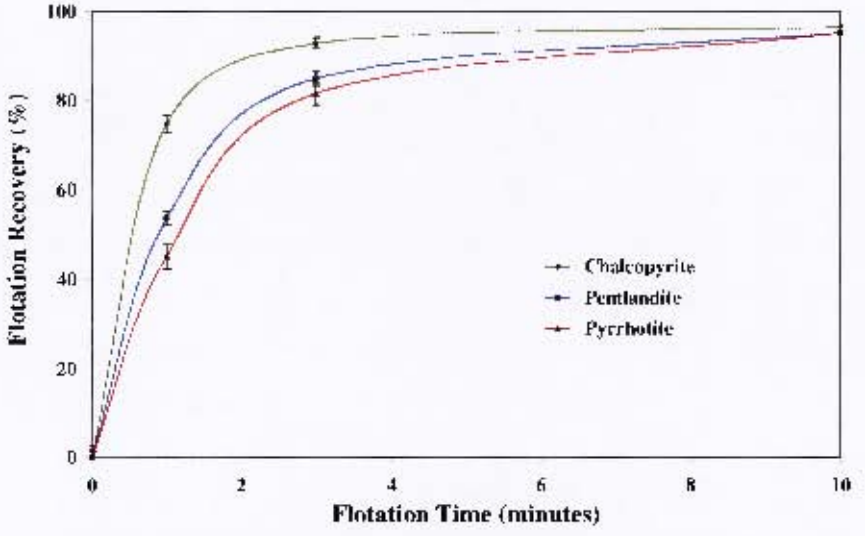

Figure 4-3: Flotation recoveries of the sulfide minerals from Nkomati ore with 1.375×10^{-4}M SIBX

Table 4-1 shows that chalcopyrite exhibited the fastest flotation, followed by pentlandite and pyrrhotite, with flotation rate constants of 1.46, 0.81 and 0.63 respectively based on a simple flotation rate model (i.e. Flotation recovery = $R_{max}(1-e^{-kt})$ (Lynch *et al*, 1981)).

Table 4-1: The flotation rates of the sulfide minerals in Nkomati ore samples with 1.375×10^{-4}M SIBX

Sulfide Mineral	Rate Parameters	
	R_{max}	k (min^{-1})
Chalcopyrite	0.96	1.46
Pentlandite	0.95	0.81
Pyrrhotite	0.96	0.63

4.2.1.2 After thermal oxidation

It was found that the thermal oxidation process produced a loose layer which would be readily abraded and removed during the mineral separation process. A surface layer that was coherent and not easily dislodged was required and this was achieved by removing this layer with ultrasonic treatment. For selected samples, the oxide layer removed by ultrasonic treatment was recovered through filtration, weighed and dried for chemical analysis.

4.2.1.2.1 Before ultrasonic treatment

Increasing exposure to thermal oxidation significantly affected the flotation mass recovery of the Nkomati ore samples based on the standard flotation period of 10 minutes (refer to Figure 4-4). After two days of oxidation the floatability without collector had all but disappeared. Flotation mass recoveries were restored with 1.37×10^{-3}M SIBX however after 16 days it was necessary to increase the collector concentrations to higher levels. While a higher concentration of SIBX (1.375×10^{-2}M) offset the effect of oxidation for a longer period, by 27 days the flotation recovery was less than 10 wt.%. The reasons for the improved flotation recoveries with substantially higher collector concentrations are two-fold. At such collector strengths, the formation of dixanthogen is more likely and may have significantly increased the particle hydrophobicity. The second role involves the displacement of surface oxidation products, which appears to have occurred for samples in the earlier stages of thermal oxidation. With increasing oxidation time, a thicker layer of oxidation products formed and the effect of these two mechanisms was significantly reduced.

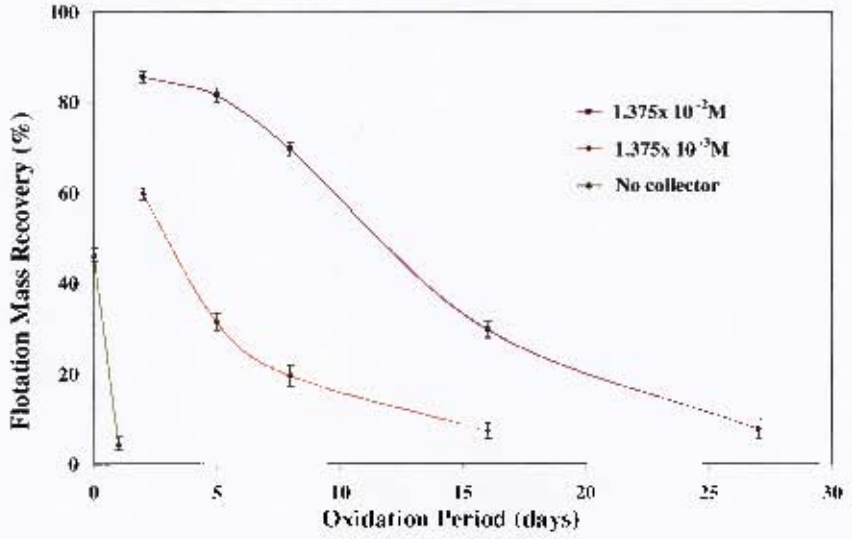

Figure 4-4: The impact of thermal oxidation upon the flotation mass recovery of Nkomati ore samples

4.2.1.2.2 After ultrasonic treatment

Ultrasonic treatment, as shown in Figure 4-5, significantly improved the flotation recovery of oxidised Nkomati ore samples. However by 60 days, a threshold had been reached and the flotation recovery remained fairly constant over the next 61 days.

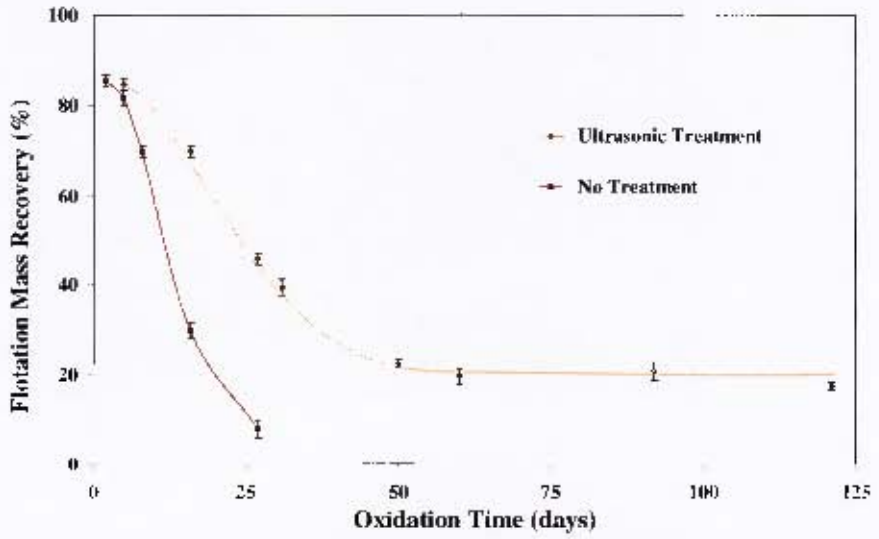

Figure 4-5: The effect of ultrasonic treatment upon the flotation mass recovery of thermally oxidised Nkomati ore samples with 1.375x10⁻²M SIBX

The surface cleansing effect of the ultrasonic treatment upon the mineral surfaces of a heavily thermally oxidised Nkomati sample can be seen in Figure 4-6, where less obscuration of the surfaces as well as fines removal are evident.

(a) before ultrasonic treatment

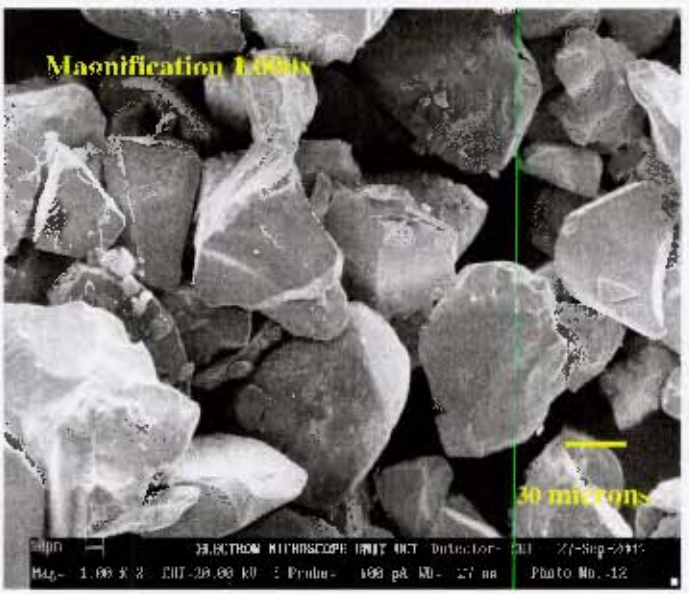

(b) after ultrasonic treatment

Figure 4-6: **Secondary** electron images of the effect of ultrasonic treatment upon on a thermally oxidised Nkomati ore sample (60 days) (20kV accoleration voltage)

Figure 4-7 shows that the thermal oxidation had a significant and similar impact upon the flotation recoveries of both pyrrhotite and pentlandite. On the other hand, although chalcopyrite is known to have a special affinity for thiol collectors, the superior flotation response for chalcopyrite does suggest a less oxidised surface. After 60 days, no further

decrease in the flotation recoveries of the sulfide minerals was observed.

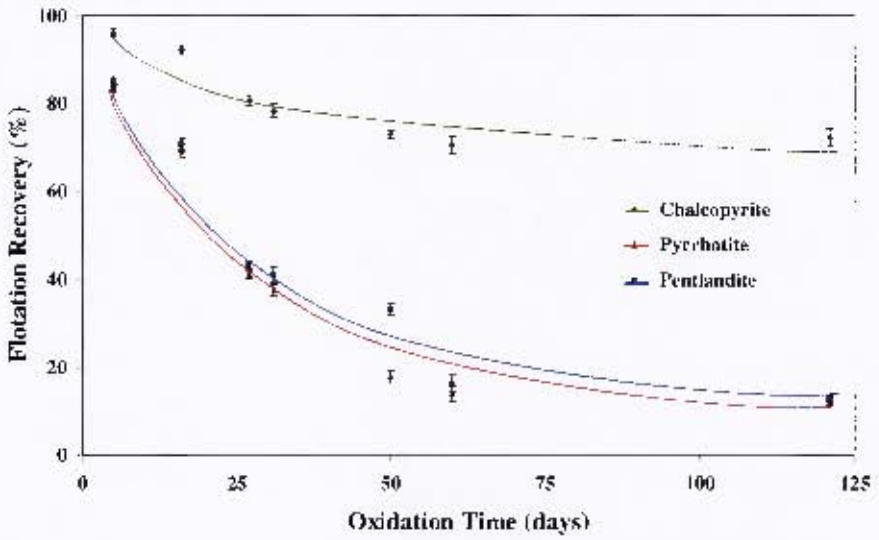

Figure 4-7: Effect of ultrasonic treatment upon the flotation recovery of sulfide minerals from thermally oxidised Nkomati ore samples with 1.375×10^{-2}M SIBX

4.2.1.3 After chemical oxidation

Figure 4-8 shows that increasing exposure to chemical oxidation by hydrogen peroxide significantly affected the flotation recovery of Nkomati ore samples. After a contact period of 1 minute with a 10^{-8}M solution, the flotation mass recovery decreased to 50%. No significant flotation was found after 10 minutes of exposure to a 10^{-2}M solution.

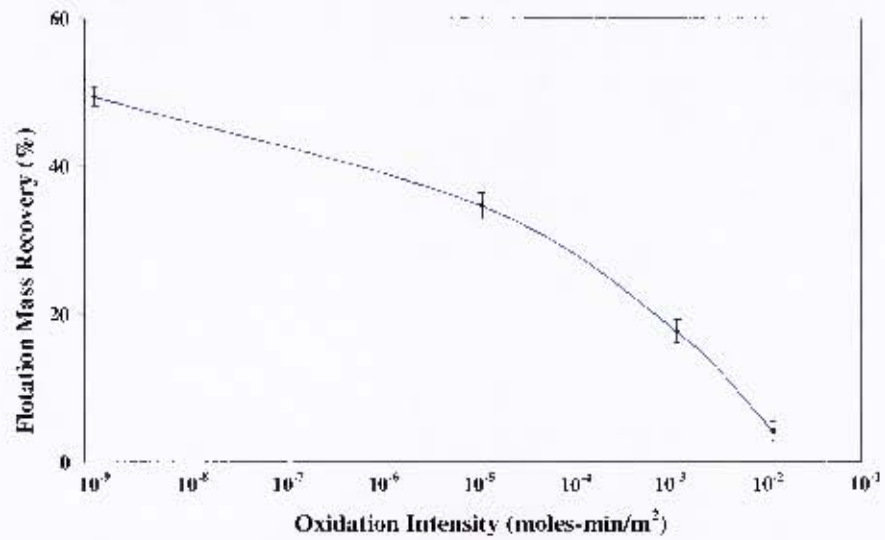

Figure 4-8: The impact of chemical oxidation upon the flotation mass recovery of Nkomati ore samples with 1.375×10^{-2}M SIBX

Chemical oxidation had a significant impact upon the flotation recoveries of all the sulfide minerals as demonstrated in Figure 4-9. As measured by the flotation response, chalcopyrite initially showed considerable resistance to oxidation by hydrogen peroxide, only succumbing to the more intensive oxidative conditions. Both pentlandite and pyrrhotite were more readily oxidised than chalcopyrite, however pentlandite was clearly less reactive than pyrrhotite under these conditions. Unlike the thermally oxidised situation, there was a clear order of reactivity with hydrogen peroxide as the oxidant: pyrrhotite > pentlandite > chalcopyrite.

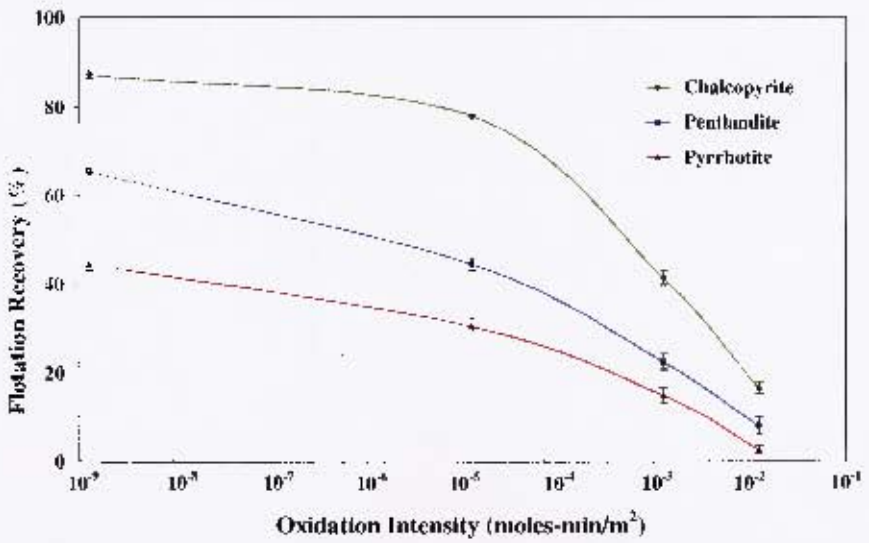

Figure 4-9: The impact of chemical oxidation upon the flotation recovery of sulfide minerals from Nkomati ore samples with 1.375×10^{-2}M SIBX

4.2.2 Pentlandite

After heavy oxidation, the flotation recovery of pentlandite samples was effectively reduced to zero (refer to Figure 4-10).

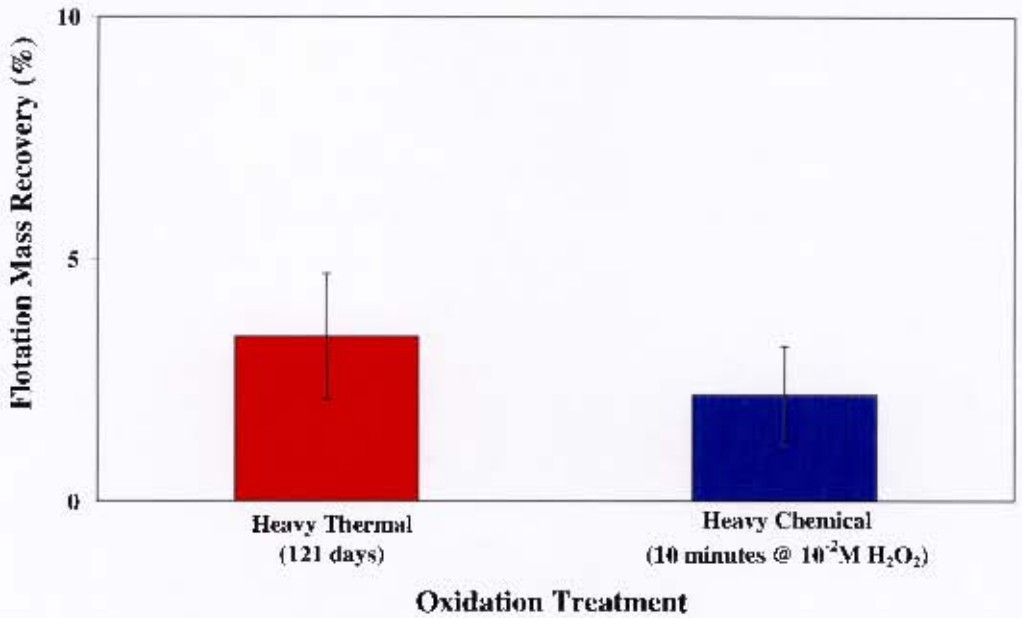

Figure 4-10: The impact of heavy oxidation upon the flotation mass recovery of pentlandite samples with 1.375x10^{-2}M SIBX

4.3 Surface characterisation by SEM/EDX

Oxidised mineral samples were prepared as described in Section 3.7.2 and the cross-sectioned oxidised mineral particles examined under a SEM. EDX analyses were made in three regions of selected particles consisting of the oxidised layer, the near-surface layer and the centre or bulk mineral. The EDX results are reported as elemental ratios and do not necessarily reflect a chemical compound.

4.3.1 Pyrrhotite

4.3.1.1 After thermal oxidation

Figure 4-11 presents back-scattered electron images of cross-sectioned thermally oxidised pyrrhotite particles from oxidised Nkomati ore samples showing a clearly defined oxide layer that increased in thickness with greater duration of oxidation. The chemical nature of the oxide layer changed with increasing oxidation as did the near surface region, with more associated iron and oxygen present.

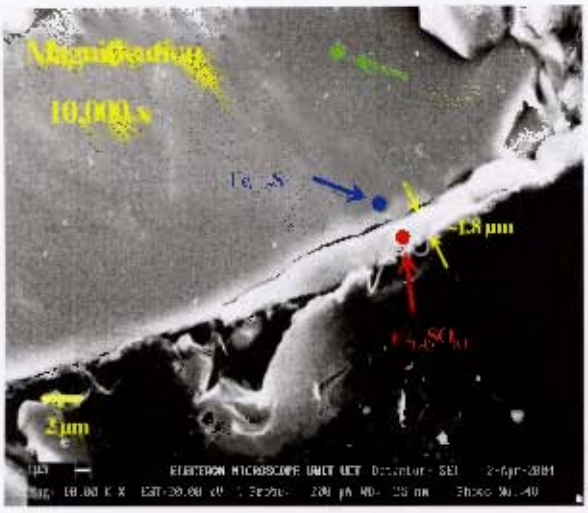

(a) 27 days

(a) 50 days

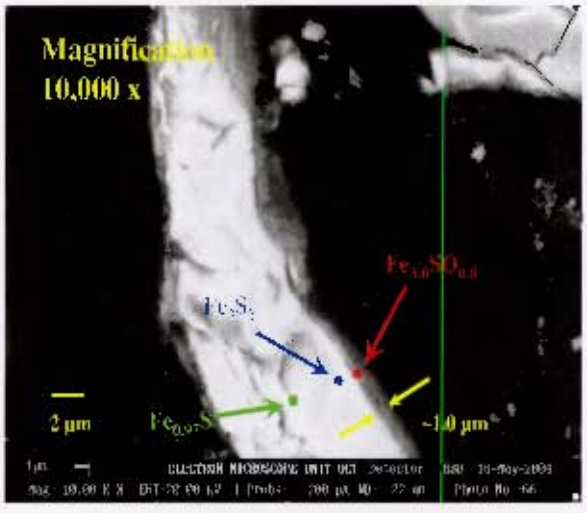

(c) 121 days

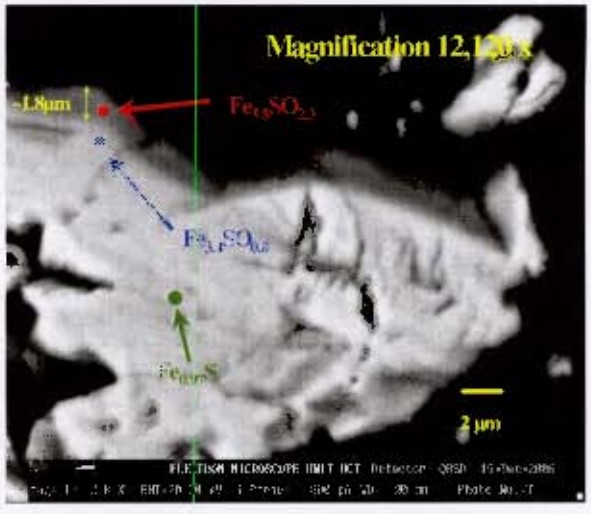

Figure 4-11: Back-scattered electron images of cross–sections of thermally oxidised pyrrhotite particles showing the development of oxidised layer with time (20 kV acceleration voltage) [red : oxide layer, blue : near surface and green : bulk mineral]

Table 4-2 summarises the oxidation trend with time as detected by SEM/EDX analyses for pyrrhotite particles in thermally oxidised Nkomati ore samples. Pyrrhotite particles, due to their greater abundance, were more consistently found. There was a strong trend in the relative elemental concentrations in the surface and near-surface regions with increased oxidation. In particular, more iron was detected in the oxide layer, while the region near the oxide layer became more depleted in iron and incorporated oxygen. Generally, the thickness of the oxidised surface layer was found to increase with greater oxidation, noting that the thickness of this layer was also a function of the particle size.

Table 4-2: Elemental ratios of surface, near surface and bulk regions as a function of oxidation time for pyrrhotite particles

Oxidation Time (days)	Surface Layer		Near Surface Elemental Ratio	Bulk Mineral Elemental Ratio
	Thickness (nm)	Elemental Ratio		
2	400	FeS	$Fe_{0.97}S$	$Fe_{0.97}S$
10	800	$FeS_{1.6}O$	$Fe_{0.97}S$	$Fe_{0.97}S$
15	600	$Fe_{1.1}SO_{0.2}$	$Fe_{0.97}S$	$Fe_{0.97}S$
18	1000	$Fe_{1.1}SO_{0.2}$	$Fe_{0.97}S$	$Fe_{0.97}S$
27	1200	$Fe_{1.3}SO_{0.2}$	$Fe_{0.97}S$	$Fe_{0.97}S$
Moderately	1000	$Fe_{1.3}SO_{0.3}$	$Fe_{0.97}S$	$Fe_{0.97}S$
Oxidised	900	$Fe_{1.4}SO_{0.2}$	$Fe_{0.97}S$	$Fe_{0.97}S$
	1000	$Fe_{1.6}SO_{0.2}$	$Fe_{0.97}S$	$Fe_{0.97}S$
	1100	$Fe_{1.5}SO_{0.2}$	$Fe_{0.97}S$	$Fe_{0.97}S$
30	1800	$Fe_{1.4}SO_{0.2}$	$Fe_{0.97}S$	$Fe_{0.97}S$
50	1000	$Fe_{2.9}SO_{0.8}$	Fe_3S_2	$Fe_{0.97}S$
60	2200	$Fe_{4.8}SO_{1.6}$	$Fe_{2.6}SO_{0.7}$	$Fe_{0.97}S$
121	1800	$Fe_{5.8}SO_{2.3}$	$Fe_{3.4}SO_{0.8}$	$Fe_{0.97}S$
Heavily	2000	$Fe_{4.9}SO_{2.1}$	$Fe_{3.2}SO_{0.7}$	$Fe_{0.97}S$
Oxidised	2200	$Fe_{4.7}SO_{2.0}$	$Fe_{3.8}SO_{0.6}$	$Fe_{0.97}S$
	1900	$Fe_{3.9}SO_{2.4}$	$Fe_{2.5}SO_{0.3}$	$Fe_{0.97}S$
	2100	$Fe_{4.8}SO_{2.2}$	$Fe_{2.7}SO_{0.5}$	$Fe_{0.97}S$

In the case of thermally oxidised Nkomati ore samples treated ultrasonically, no oxide layer was readily discernable (refer to Figure 4-12). Since the SEM resolution was less than 100 nanometres, the thickness of the thermally oxidised surface layer after ultrasonic treatment must be less than this value.

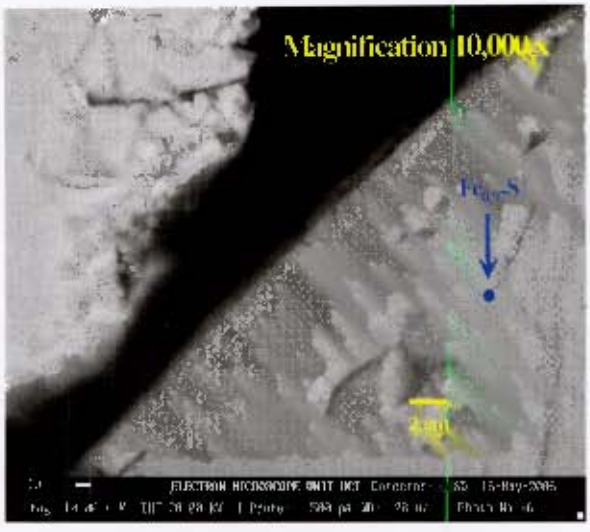

Figure 4-12: Back-scattered electron image of a cross–sectioned heavily thermally oxidised pyrrhotite particle after ultrasonic treatment (20 kV acceleration voltage)

4.3.1.2 After chemical oxidation

Figure 4-13 presents a back-scattered electron image of a cross-sectioned chemically oxidised pyrrhotite particle without any clearly defined oxide layer. As noted in the case of the thermally oxidised sample that had been treated ultrasonically, the thickness of chemically oxidised surface layer must also be less than 100 nanometres.

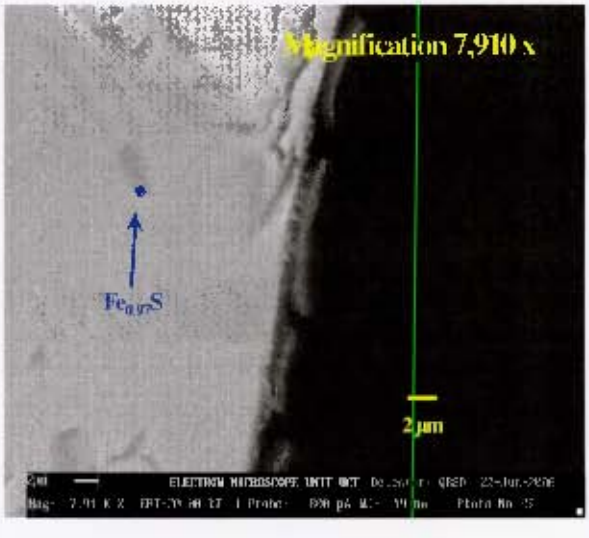

Figure 4-13: Back-scattered electron image of a cross–sectioned heavily chemically oxidised pyrrhotite particle (20 kV acceleration voltage)

4.3.2 Chalcopyrite

A comparison between moderately and heavily thermally oxidised chalcopyrite particles shows that a more substantial oxidised layer has developed (refer to Figure 4-14). More oxygen has been incorporated into the oxide layer while some sulfur depletion has occurred for the near surface regions at the higher degree of oxidation. Although the thickness of the oxide layer is smaller for the heavily oxidised sample, the difference is most likely due to particle size effects.

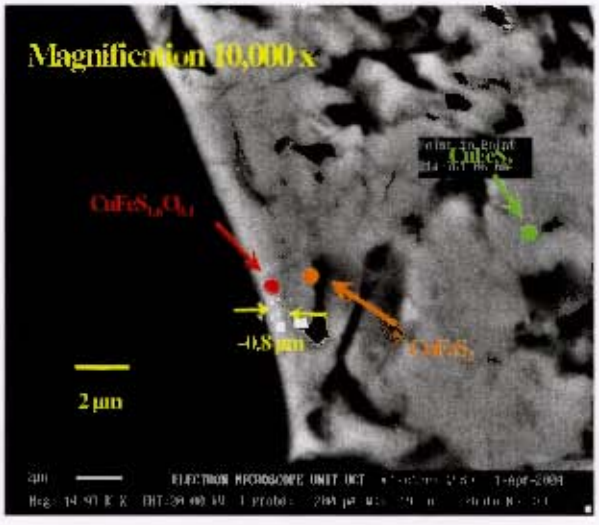

(a) moderate thermal oxidation

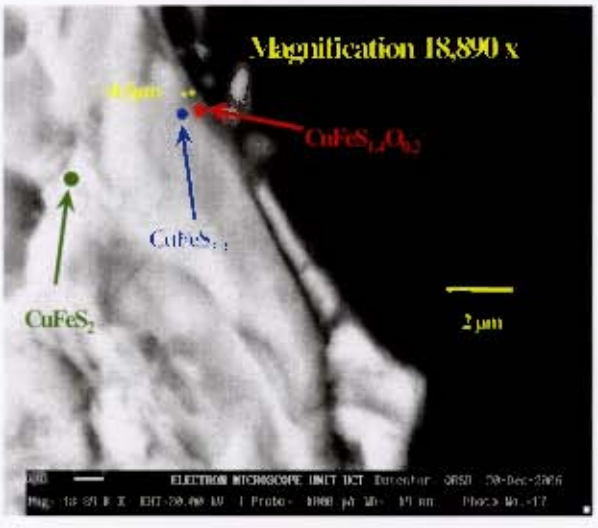

(b) heavy thermal oxidation

Figure 4-14. Back-scattered electron images of cross–sectioned thermally oxidised chalcopyrite particles (20 kV acceleration voltage)

Table 4-3 summarises the SEM/EDX analyses for moderately and heavily thermally oxidised chalcopyrite particles. There was a trend in the relative elemental concentrations in the surface and near surface regions with increasing oxidation. In particular, iron enrichment as well as the incorporation of oxygen in both regions was found over time. However neither the degree of oxidation nor the thickness of the oxidation layer was as substantial as that observed for pyrrhotite. As found with the oxidised pyrrhotite particles, the thickness of the oxidised surface layer increased with greater oxidation.

Table 4-3: Elemental ratios of surface and near surface and bulk regions for thermally oxidised chalcopyrite particles

Oxidation Time (days)	Surface Layer		Near Surface Elemental Ratio	Bulk Mineral Elemental Ratio
	Thickness (nm)	Elemental Ratio		
Moderately Oxidised (27)	700	$CuFeS_{1.6}O_{0.1}$	$CuFeS_2$	$CuFeS_2$
	400	$CuFeS_{1.6}O_{0.1}$	$CuFeS_2$	$CuFeS_2$
	600	$CuFeS_{1.8}O_{0.1}$	$CuFeS_2$	$CuFeS_2$
	500	$CuFeS_{1.8}O_{0.1}$	$CuFeS_2$	$CuFeS_2$
Heavily Oxidised (121)	700	$CuFeS_{1.4}O_{0.2}$	$CuFeS_{1.1}$	$CuFeS_2$
	800	$CuFeS_{1.5}O_{0.2}$	$CuFeS_2O_{0.1}$	$CuFeS_2$
	700	$CuFeS_{1.7}O_{0.2}$	$CuFeS_{1.5}$	$CuFeS_2$
	800	$CuFeS_{1.6}O_{0.2}$	$CuFeS_2O_{0.1}$	$CuFeS_2$

The SEM technique could not identify the presence of an oxidised layer on heavily chemically oxidised chalcopyrite particles.

4.3.3 Pentlandite

Figure 4-15 presents back-scattered electron images of cross-sectioned thermally oxidised pentlandite particles showing that a substantial oxidised layer has developed. The chemical nature of the oxide layer changed with increasing oxidation as did the near surface region, with more associated iron and oxygen. Although the thickness of the oxide layer is less for the heavily oxidised sample, this is considered to be due to particle size and shape effects. Smaller particles as well as particles with low aspect ratios tend to develop thicker oxide layers.

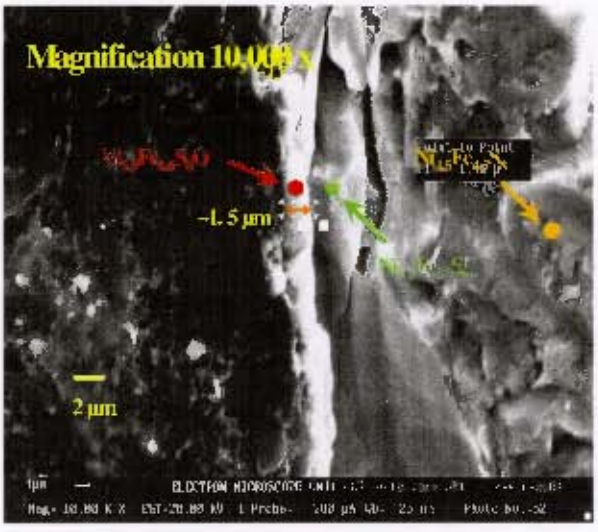

(a) moderate thermal oxidation

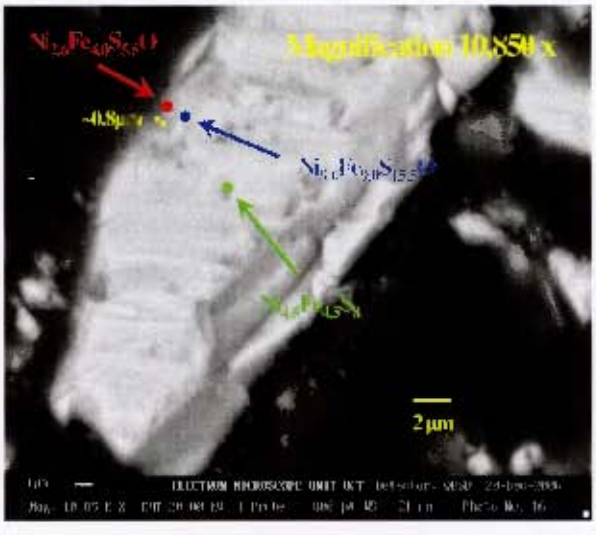

(b) heavy thermal oxidation

Figure 4-15: Back-scattered electron images of cross–sectioned thermally oxidised pentlandite particles (20 kV acceleration voltage)

The SEM/EDX analyses for moderately and heavily thermally oxidised pentlandite particles are summarised in Table 4-4. There is a trend in the relative elemental concentrations in the surface and near surface regions with increasing oxidation. In particular, iron enrichment as well as the incorporation of oxygen in both regions is found over time. The thickness of the oxidised surface layer increased with greater oxidation. The oxidation behaviour of pentlandite is more similar to that of pyrrhotite than chalcopyrite. While the degree of oxidation, as measured by elemental ratios, is not as substantial as that found for pyrrhotite, the thickness of the oxidation layer was of a similar magnitude.

Table 4-4: Elemental ratios of surface, near surface and bulk regions for thermally oxidised pentlandite particles

Oxidation Time (days)	Surface Layer		Near Surface Elemental Ratio	Bulk Mineral Elemental Ratio
	Thickness (nm)	Elemental Ratio		
Moderately Oxidised (27)	1500	$Ni_{5.9}Fe_{6.6}S_{8.0}O$	$Ni_{4.5}Fe_{4.5}S_8$	$Ni_{4.5}Fe_{4.5}S_8$
	800	$Ni_{6.6}Fe_{6.7}S_{8.3}O$	$Ni_{4.5}Fe_{4.5}S_8$	$Ni_{4.5}Fe_{4.5}S_8$
	700	$Ni_{6.6}Fe_{5.8}S_{9.3}O$	$Ni_{4.5}Fe_{4.5}S_8$	$Ni_{4.5}Fe_{4.5}S_8$
	900	$Ni_{7.4}Fe_{6.2}S_{9.1}O$	$Ni_{4.5}Fe_{4.5}S_8$	$Ni_{4.5}Fe_{4.5}S_8$
Heavily Oxidised (121)	1200	$Ni_{2.6}Fe_{4.0}S_{5.5}O$	$Ni_{9.6}Fe_{9.9}S_{15.5}O$	$Ni_{4.5}Fe_{4.5}S_8$
	1100	$Ni_{4.8}Fe_{6.3}S_{10.6}O$	$Ni_{8.9}Fe_{9.6}S_{16.2}O$	$Ni_{4.5}Fe_{4.5}S_8$
	1000	$Ni_{5.9}Fe_{6.8}S_{8.0}O$	$Ni_{9.3}Fe_{10.7}S_{16.8}O$	$Ni_{4.5}Fe_{4.5}S_8$
	1200	$Ni_{4.7}Fe_{6.5}S_{7.3}O$	$Ni_{8.9}Fe_{10.1}S_{17.6}O$	$Ni_{4.5}Fe_{4.5}S_8$

The SEM technique failed to identify oxidised layers on heavily chemically oxidised pentlandite particles.

4.4 Surface analysis with XPS

4.4.1 Pyrrhotite

Thermally and chemically oxidised Nkomati samples were prepared for XPS analysis as described in Section 3.6.2. The particles within the samples reacted strongly to the magnetic field created within the XPS analytical chamber, and spun, making analysis impossible. This was not observed with oxidised samples that had been sulfidised, indicating that an oxidised surface species was responsible for this behaviour.

4.4.2 Chalcopyrite

A heavily thermally oxidised chalcopyrite sample was analysed by XPS after hydrolysis. Table 4-5 shows that the surface species consisted of predominantly hydroxide/oxy-hydroxides and oxide species associated with iron and copper. Water was detected in moderate quantities. A reasonable exposure of unoxidised chalcopyrite was observed on the surface. Cu (I) species were detected and in greater abundance than Cu (II) species. Sulfur was present in the surface layers in an array of species such as the monosulfide ion (S^{2-}), the disulfide iron (S_2^{2-}), elemental/polysulfide as well as sulfate.

Table 4-5: XPS analysis of heavily thermally oxidised chalcopyrite surfaces after hydrolysis

Species	Abundance (%)
Oxygen	**75.6**
Oxide	25.7
OH^-	37.0
$H_2O + SO_4^{2-}$	12.9
Copper	**3.5**
Cu(I)	1.9
Cu(II)	1.6
Iron	**7.1**
Fe-S	-
Fe-O	7.1
Sulfur	**10.6**
S^{2-}	3.4
Cpy-S	2.4
S_2^{2-}	2.4
S_n/S^o	1.6
SO_4^{2-}	0.7

4.4.3 Pentlandite

Table 4-6 shows the XPS analysis of a heavily thermally oxidised synthetic pentlandite sample after hydrolysis. The results show some similarities with that observed for heavily oxidised chalcopyrite sample after hydrolysis. The surface species consisted of predominantly hydroxide/oxy-hydroxides and oxide species associated with iron and nickel. The presence of water indicates that the various metal species are hydrated. A small nickel-sulfur signal was detected which may be associated with either unoxidised pentlandite or an oxidation product such as violarite. Sulfur was present mainly in S-S bonds with some in association with nickel, however the exact nature of the speciation is not clear. A small quantity of sulphur was present as sulfoxy species, most likely as sulfate.

Table 4-6: XPS analysis of heavily thermally oxidised pentlandite surfaces after hydrolysis

Species	Abundance (%)
Oxygen	**85.6**
Oxide	18.8
OH^-	47.9
$H_2O + SO_4^{2-}$	18.8
Nickel	**3.6**
Ni-S	0.1
Ni-O	3.5
Iron	**6.5**
Fe-O	6.5
Sulfur	**4.2**
$S^{2-}/S_n/S^\circ$	3.3
Sulfoxy	0.9

4.5 Electrophoretic studies

Table 4-7 summarises the pH_{IEP} values found for the oxidised Nkomati ore and sulfide mineral samples as a function of degree of oxidation. For the Nkomati ore samples, the pH_{IEP} values reflected the major component, namely pyrrhotite.

Table 4-7: pH_{IEP} as a function of the degree of oxidation for oxidised Nkomati ore and sulfide mineral samples

Degree of Oxidation	pH_{IEP}							
	Nkomati ore		Pyrrhotite		Chalcopyrite		Pentlandite	
	Thermal	Chemical	Thermal	Chemical	Thermal	Chemical	Thermal	Chemical
None	2.0	2.0	2.0	2.0	-	-	2.0	2.0
Moderate	4.0	2.8	2.5	2.6	3.0	2.2	5.9	3.5
Heavy	5.4	3.4	3.5	3.3	3.2	3.3	5.1	4.6

Thermally oxidised Nkomati ore samples exhibited higher pH_{IEP} values than the chemically oxidised samples, indicating a greater degree of surface oxidation. Nonetheless, both types of heavy oxidation showed very poor flotation responses. The pH_{IEP} values for oxidised pyrrhotite samples were independent of the oxidation method and followed the same trend with increasing oxidation. The trend is very similar to that found for chemically oxidised Nkomati ore samples. This is not surprising since the composition of the Nkomati

ore sample is dominated by pyrrhotite. The pH_{IEP} values for the thermally oxidised Nkomati ore samples are different to those found for the thermally oxidised pyrrhotite samples. This indicates that the oxidation products from both the pentlandite and the chalcopyrite contributed to the zeta potential of thermally oxidised Nkomati ore samples.

For chalcopyrite, the pH_{IEP} values were similar for both of the thermally oxidised samples as well as the heavily chemically oxidised sample, demonstrating the rather refractory nature of chalcopyrite. However, in the case of moderately chemically oxidised chalcopyrite, the pH_{IEP} was significantly lower at 2.2.

In the case of oxidised pentlandite samples, the pH_{IEP} values were dependent upon the oxidation method. Higher pH_{IEP} values were found for thermally oxidised samples than for chemically oxidised samples, although the moderately thermally oxidised sample anomalously produced the highest pH_{IEP} value. Due to the high pH_{IEP} values associated with thermally oxidised pentlandite samples, it is likely that these oxidation products contributed to pH_{IEP} values of the thermally oxidised Nkomati samples.

4.6 Analysis of oxidation layers

Other studies were undertaken on heavily thermally oxidised Nkomati samples for the -106µm/+38µm size fraction (flotation feed) to provide corroboration as well as a basis for other testwork.

4.6.1 Oxidation products

With increasing oxidation, greater quantities of oxidation product were recovered after ultrasonic treatment (refer to Table 4-8). This indicated that the oxide layer became thicker with longer periods of oxidation and corroborates the observations made by the SEM/EDX studies.

Table 4-8: Mass of ultrasonically removed oxide layer as a function of degree of oxidation

Duration (days)	Mass (%)
31	6.20
50	7.29
60	7.05
121	12.66

With increasing thermal oxidation, the surface area of the Nkomati ore samples significantly increased (refer to Figure 4-16). After 121 days of thermal oxidation, the surface area of the sample had increased by over 200%. The decrease in surface area associated with the removal of surface oxidation products by ultrasonic treatment varied from 16 to 20% over the duration of the oxidation period.

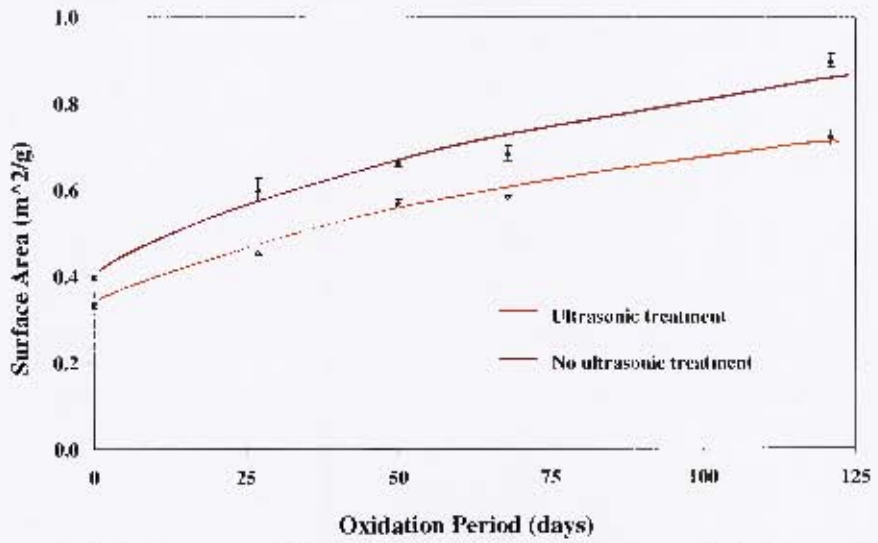

Figure 4-16: Surface area of thermally oxidised Nkomati ore samples before and after ultrasonic treatment as a function of degree of oxidation (error bars ± SD)

Figure 4-17 presents the chemical analysis of the oxidation products removed by the ultrasonic treatment. This analysis identified iron and sulfur as the principal elements with smaller quantities of nickel and copper present. Elementally, the composition of the oxidation products did not vary significantly with oxidation time, suggesting that oxidation products of similar composition were being formed during all stages of oxidation.

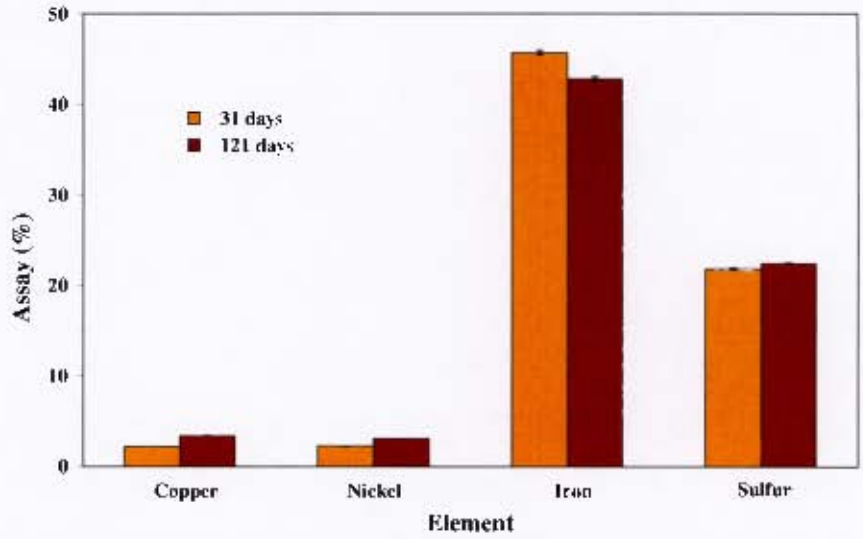

Figure 4-17: Chemical analysis of ultrasonically removed oxide layer from thermally oxidised Nkomati ore samples (error bars ±SD)

4.6.2 Hydrolysis

Figure 4-18 shows that, upon exposure of the thermally oxidised Nkomati ore samples to water, significant hydrolysis occurred. The interaction significantly decreased the solution pH while increasing the solution redox potential to more oxidising values. Based on the solution parameters, the hydrolysis had substantially dissipated after 10 minutes. The hydrolytic reactions of the moderately oxidised Nkomati ore sample appeared to be more vigorous than that of the heavily oxidised sample. However, as revealed in Table 4-9, significantly more species were released by the heavily oxidised sample, indicating a greater extent of hydrolysis.

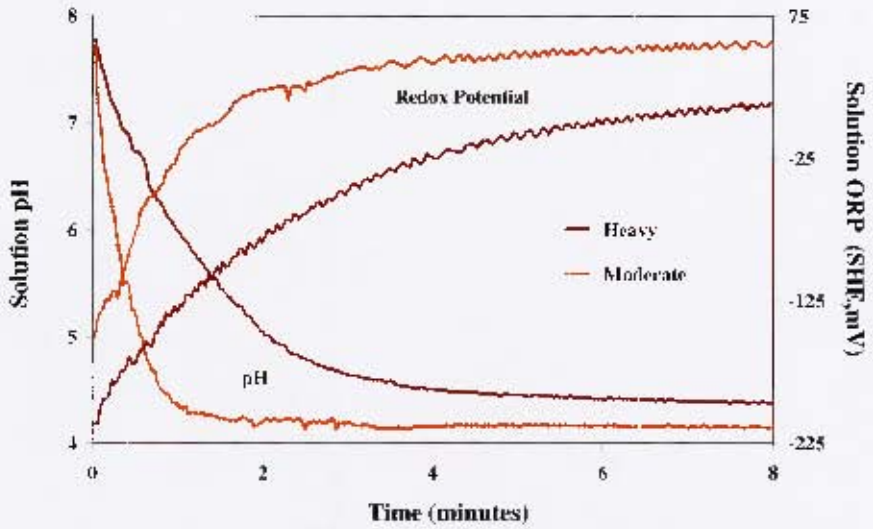

Figure 4-18: Hydrolytic behaviour of moderately (27 days) and heavily (121 days) thermally oxidised Nkomati ore samples

Table 4-9 presents the species that were released from the thermally oxidised Nkomati ore samples surfaces during hydrolysis. Relative to the amount of that 'metal' is initially present in the Nkomati ore, nickel and sulfate ions are the dominant species released. The abundance of all species significantly increased after 121 days of thermal oxidation, particularly iron and copper, followed by sulfate ions. When compared to Figure 4-17, these results suggest that both the sulphur and nickel oxidation products were predominantly present as soluble species, whereas the iron and copper appear to be mainly present as insoluble species.

Table 4-9: Species released from thermally oxidised Nkomati ore samples after hydrolysis (error bars ± SD)

Oxidation Period (days)	Species released after hydrolysis (µmole/g 'metal')			
	Cu	Ni	Fe	SO_4^{2-}
27	0.051 ± 0.001	1.28 ± 0.04	0.012 ± 0.003	0.31 ± 0.03
121	0.44 ± 0.02	3.84 ± 0.08	0.99 ± 0.07	2.04 ± 0.08

4.6.3 EDTA extractions

Figure 4-19 presents the results of the EDTA extractions as a function of degree of thermal oxidation as well as before and after ultrasonic treatment. Iron and nickel were the dominant elements extracted under all conditions, with copper values significantly lower. Generally the amounts of iron and nickel extracted were similar, except for the moderately

oxidised sample. The quantities of elements extracted from the heavily oxidised sample were approximately double the amount removed from the surfaces of the moderately oxidised sample. After ultrasonic treatment, a reasonable quantity of metals was extracted, indicating that oxidation products were still present, particularly in the case of the heavily oxidised sample. The copper and nickel values for the unoxidised sample may include some milling media which were observed during the SEM analyses of Nkomati ore samples.

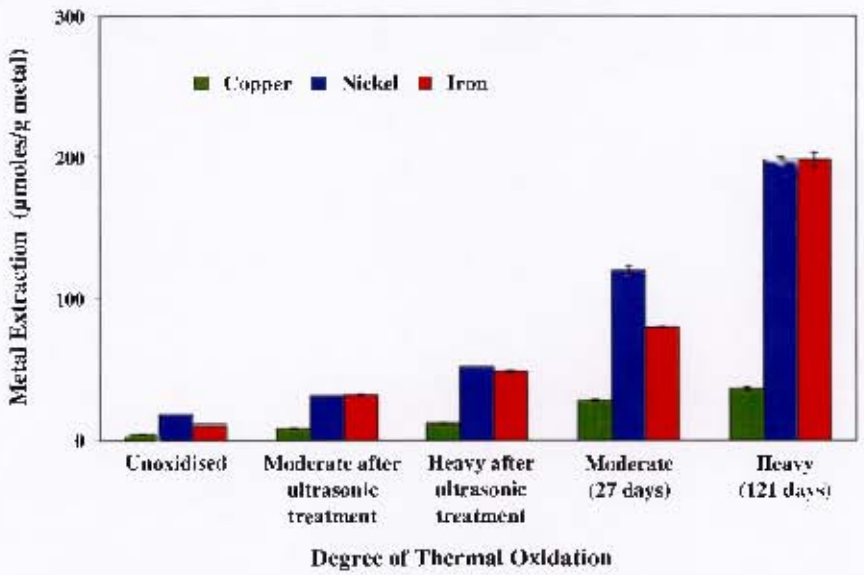

Figure 4-19: EDTA extraction results for thermally oxidised Nkomati ores samples as a function of degree of oxidation (error bars ± SD)

After chemical oxidation, only a third of the quantity of elements was extracted by EDTA as compared to the thermally oxidised samples (refer to Figure 4-20). Nickel was the dominant element extracted under all conditions, followed by iron and copper. With greater oxidation, the quantities of extracted elements significantly increased while the relative proportions between the elements remained similar.

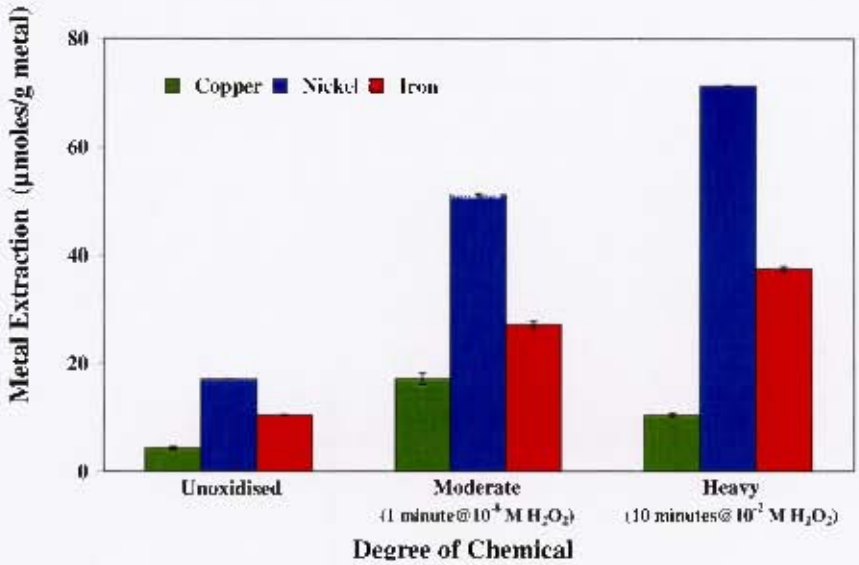

Figure 4.20: EDTA extraction results for chemically oxidised Nkomati ore samples as a function of degree of oxidation (error bars +SD)

4.7 Summary

The sulfide minerals present in Nkomati ore samples displayed considerable natural floatability with the flotation order being chalcopyrite > pentlandite > pyrrhotite. With the addition of collector, nearly complete flotation of the sulfide minerals was found. Analogously to the natural floatability situation, chalcopyrite floated the most readily followed by pentlandite and pyrrhotite. The flotation recovery of Nkomati ore samples deteriorated significantly with increasing oxidation through either chemical or thermal means, with pyrrhotite showing the greatest response, followed by pentlandite and chalcopyrite.

For thermally oxidised samples, the oxidation process depleted the sulfide mineral surfaces of iron and formed oxide layers containing iron and sulfur as well as lower levels of nickel and copper. The oxide layers became progressively thicker with increased oxidation and substantially increased the surface area of the sample. A significant proportion of this layer was readily removed with ultrasonic treatment. Even after ultrasonic treatment, a reasonable quantity of soluble base-metal ions was present as indicated by EDTA analysis.

The thermally oxidised surfaces underwent rapid hydrolysis when contacted with water which was complete after 10 minutes. The rapid drop in pH during hydrolysis indicated significant uptake of hydroxyl ions by the oxidised surfaces. This was corroborated by the

change in the pH_{IEP} values. However, the nature of the oxidation products on heavily thermally oxidised Nkomati surfaces could not be directly identified by XPS.

Chemical oxidation did not produce thick oxide layers however was effective in reducing mineral floatability. As measured by the flotation response, chalcopyrite was the most resistant to chemical oxidation followed by pentlandite and pyrrhotite. With increasing oxidation, the pH_{IEP} values of the Nkomati ore surfaces increased. Like the thermally oxidised Nkomati sample, XPS was unable to identify the nature of the surface oxidised species.

The heavily thermally oxidised chalcopyrite surfaces after exposure to water were found be covered in hydrated oxides and oxy-hydroxides of iron and copper. A reasonable exposure of chalcopyrite was observed, corroborating the resistance of this mineral to oxidation. The reasonably modest increments in pH_{IEP} values after oxidation also attest to this refractory behaviour.

Similarly, the heavily thermally oxidised pentlandite surfaces after exposure to water were found be covered in hydrated oxides and oxy-hydroxides of iron and nickel. Since only a very small exposure of nickel sulfide was observed, it was concluded that significant surface oxidation had occurred. This was corroborated by the large changes in pH_{IEP} values after oxidation.

CHAPTER 5

RESULTS : SULFIDISATION STUDIES

5.1 Introduction

The testwork results reported in this chapter addressed the second hypothesis, namely *that sulfidisation would restore the sulfide mineral character to oxidised sulfide mineral surfaces and thus their floatability, particularly pyrrhotite and chalcopyrite* and *that the sulfidisation mechanisms of oxidised sulfide minerals would be similar to those proposed for their base-metal 'oxide' counterparts* with some *electrochemical mechanisms*.

Sulfidisation studies were undertaken on heavily oxidised Nkomati ore samples to test whether floatability would be restored and that sulfide surfaces would be regenerated. Controlled potential sulfidisation (CPS) was employed as the sulfidisation technique and was conducted over a range of hydrosulfide ion concentrations to establish the optimum conditions.

The mechanistic aspects of the sulfidisation process were elucidated using a number of techniques with heavily oxidised Nkomati ore samples as well as single sulfide mineral samples. Electrophoresis was used to measure the change in the zeta potential as function of sulfidisation intensity while the nature of the subsequent surface species was determined by XPS. Cyclic voltammetry as well as chronoamperometry were also employed to reveal aspects of the sulfidisation process of the oxidised sulfide minerals.

To demonstrate the suitability of sulfidisation for the recovery of sulfide minerals from oxidised Merensky ores, the influence of calcium ions upon the efficacy of the sulfidisation process was examined. Additionally the effect of the sulfidisation process upon the floatability of the dominant Merensky ore gangue minerals, namely feldspar and pyroxene, were studied.

Finally, adsorption studies were undertaken to characterise the sulfidisation characteristics of heavily thermally oxidised Nkomati ore sulfide minerals for comparison with the well researched sulfidisation behaviour of base-metal 'oxide' minerals.

As background to interpreting the flotation recoveries as a function of sulfidisation potential, Table 5-1 summarises the solution conditions.

Table 5-1: Sulfidisation solution conditions as a function of sulfidisation potential

Es (mV)	[NaSH] (M)	Measured pH
-800	$1.91x10^{-2}$	9.62
-700	$1.70x10^{-4}$	8.21
-650	$2.4x10^{-5}$	8.00
-600	$5.7x10^{-6}$	7.80
-500	$6.0x10^{-7}$	7.51

Unless otherwise noted, errors bars are based on the Standard Error (±SE).

5.2 Nkomati ore

After settling upon the best conditions for both the sulfidisation and flotation recovery of the sulfide minerals in heavily oxidised Nkomati ore samples, electrophoresis and XPS were used to determine the nature of the sulfidisation mechanism. In the electrophoretic studies, the contribution of both pH and hydrosulfide ions to the zeta potential value was established with heavily chemically oxidised samples.

5.2.1 Flotation

5.2.1.1 Thermal oxidation

Preliminary testwork indicated that 5 minutes of conditioning time for sulfidisation in the presence of air was suitable and that $1.375x10^{-3}$M SIBX was required to achieve satisfactory flotation recoveries after sulfidisation. Longer sulfidisation conditioning periods and lower collector additions both resulted in significantly poorer flotation responses.

Figure 5-1 shows the flotation response of heavily thermally oxidised Nkomati ore samples to sulfidisation. Flotation mass recovery steadily increased until an optimum flotation recovery was achieved at a sulfidisation potential of -650 mV. After this Es value, the flotation recovery deteriorated.

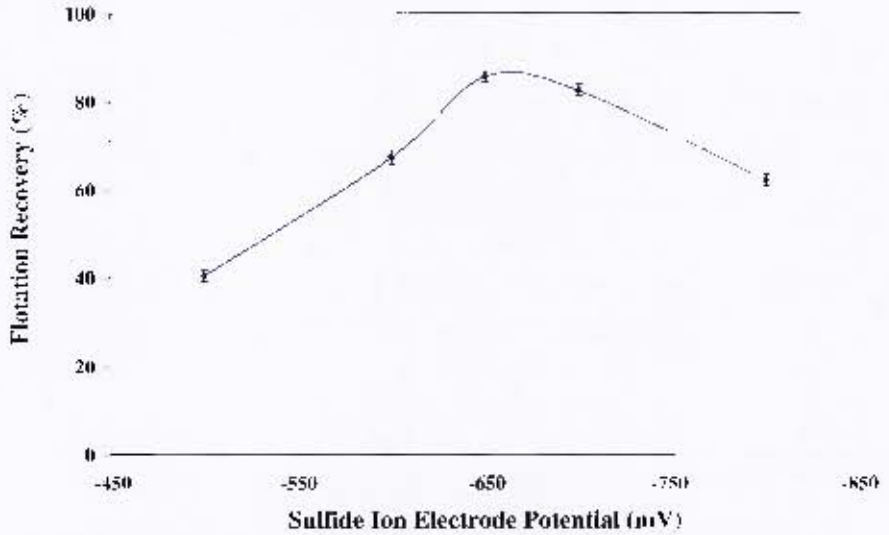

Figure 5-1: Flotation mass recovery of heavily thermally oxidised Nkomati ore samples as a function of sulfidisation potential(1.375 x10 $^{-3}$M SIBX)

Figure 5-2 presents the flotation response as a function of sulfidisation potential for each of the three sulfide minerals present in the heavily thermally oxidised Nkomati ore sample.

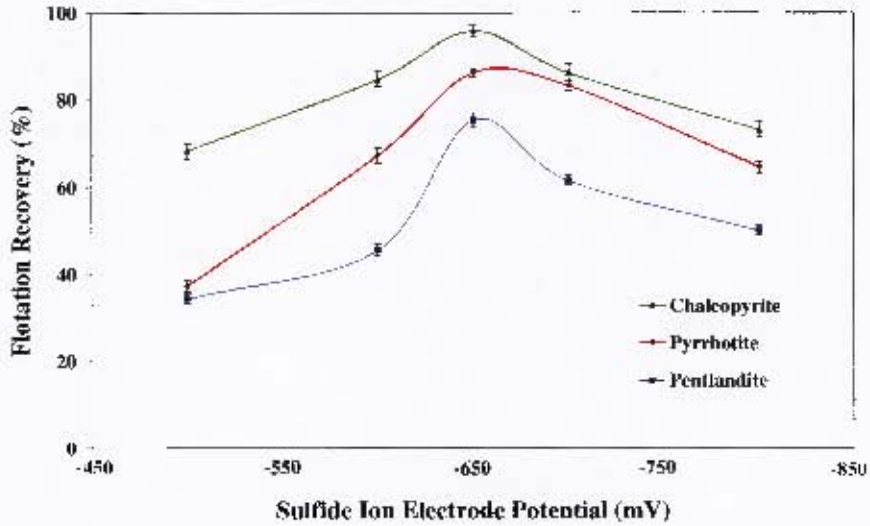

Figure 5-2: Sulfide mineral flotation recoveries from heavily thermally oxidised Nkomati ore samples as a function of sulfidisation potential (1.375 x10 $^{-3}$M SIBX)

Chalcopyrite responded most favourably to sulfidisation followed by pyrrhotite and pentlandite. Based on the flotation recovery, the response of the oxidised pentlandite to sulfidisation was not to the same degree as the other two sulfide minerals. The flotation response after sulfidisation for the three sulfide minerals had similar characteristics and the best flotation recovery for all three minerals occurred at an Es of -650 mV.

Sulfidisation was conducted in the presence of calcium ions (10^{-2} IS) with heavily thermally oxidised Nkomati ore samples. Table 5-2 shows that, as expected, there was no significant difference between the two test conditions in terms of flotation recovery for either the sample or the individual sulfide minerals.

Table 5-2: The effect of calcium ions during sulfidisation on the flotation recovery of sulfide minerals from heavily oxidised Nkomati ore samples at -650 mV Es

Nkomati Mineral Component	Flotation Recovery (%)			
	Without Ca^{2+}		With Ca^{2+}	
	Average	SE	Average	SE
Sample	86.1	±1.0	85.4	±1.5
Chalcopyrite	96.4	±1.2	96.0	±0.9
Pentlandite	75.6	±1.4	75.2	±1.1
Pyrrhotite	86.4	±1.3	86.2	±1.0

5.2.1.2 Chemical oxidation

Sulfidisation of heavily chemically oxidised Nkomati ore samples were conducted under the same sulfidisation conditions as that for the heavily thermally oxidised Nkomati ore samples. Figure 5-3 shows the flotation response of the individual sulfide minerals was similar to that found for the heavily thermally oxidised Nkomati ore sample after sulfidisation.

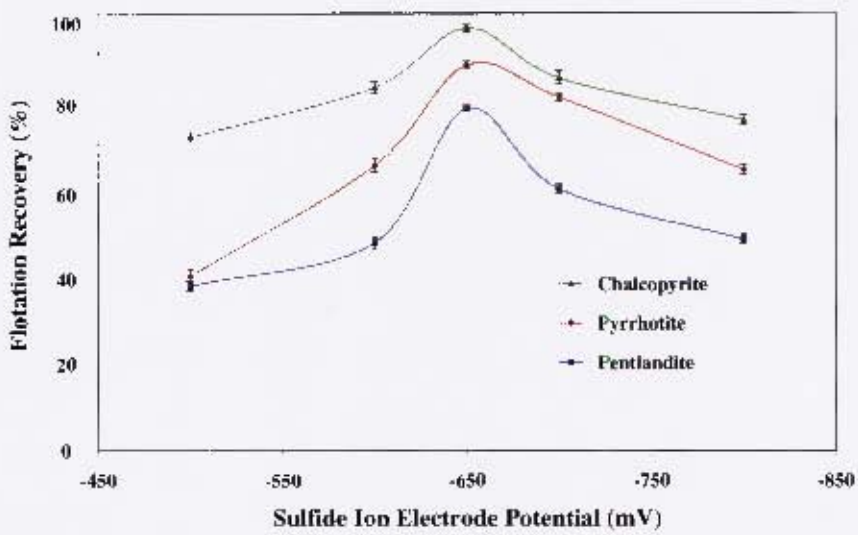

Figure 5-3: Sulfide mineral flotation recoveries from heavily chemically oxidised Nkomati ore samples as a function of sulfidisation potential ($1.375x10^{-3}$M SIBX)

5.2.2 Electrophoresis

5.2.2.1 Thermal oxidation

Figure 5-4 shows that the surface charge of the thermally oxidised Nkomati ore sulfide minerals became more negative in the presence of increasing hydrosulfide ion concentrations for both samples. Since Nkomati ore is predominantly pyrrhotite, the results reflect the behaviour of this mineral. A significant difference in the behaviour of the zeta potential between the two degrees of oxidation was found as the sulfidisation potential increased. For the moderately oxidised Nkomati ore sample, the surface charge was initially positive and became negative at around a sulfide ion electrode potential of -510 mV. As the hydrosulfide ion concentration increased, the moderately oxidised sample was characterised by three regions where the surface charge became increasingly negative, interspersed with three plateaus.

On the other hand, the surface charge of the heavily oxidised sample was negative for all sulfide ion electrode potentials. The zeta potential steadily decreased over two regions, namely from -550 to -650 mV and -700 to -750 mV. Outside these two regions, the surface charged assumed approximately constant values.

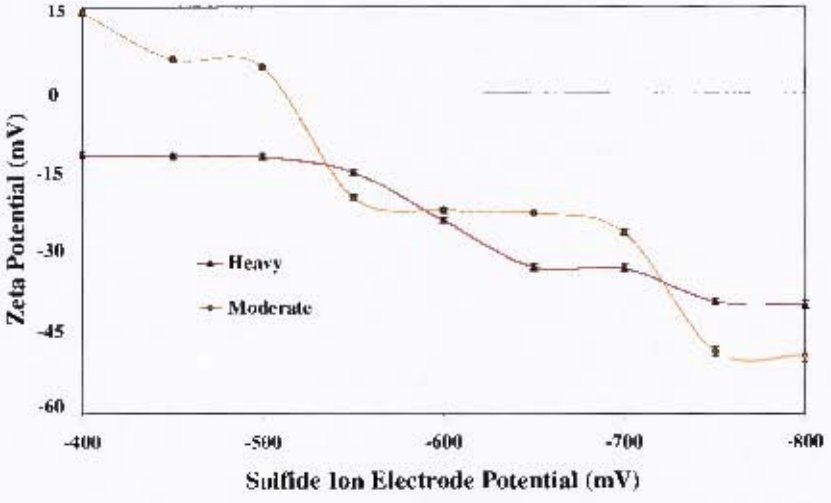

Figure 5-4: Zeta potential of thermally oxidised Nkomati ore samples as a function of degree of oxidation and sulfidisation potential

5.2.2.2 Chemical oxidation

The initial aim in this batch of electrophoretic testwork was to decouple and identify the roles of pH and hydrosulfide ion concentration in effecting changes in the zeta potential. Hydrosulfide ions were added at a constant pH (10) and compared with the situation where the pH was not controlled and determined solely by the strength of the sodium sulfide solution. Figure 5-5 shows that for both systems, the same trend in the zeta potential was observed as a function of sodium sulfide concentration and the effect of sodium sulfide concentration is more dominant than pH. The most significant change in the zeta potential occurred over the same range of sodium sulfide concentrations, namely $1x10^{-6}$M to $1.5x10^{-5}$M.

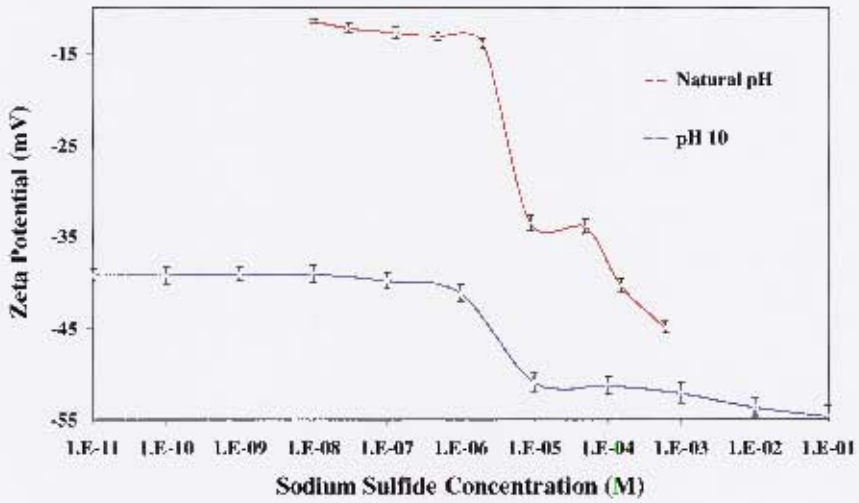

Figure 5-5: Zeta potential of heavily chemically oxidised Nkomati ore samples as a function of sulfidisation potential at natural and fixed pH values

Figure 5-6 shows the contribution of both pH and hydrosulfide ion concentration to the zeta potential values for heavily chemically oxidised Nkomati ore samples. The hydrosulfide ion concentration has the dominant effect, particularly over the sulfide ion electrode potential range -600 to -650 mV.

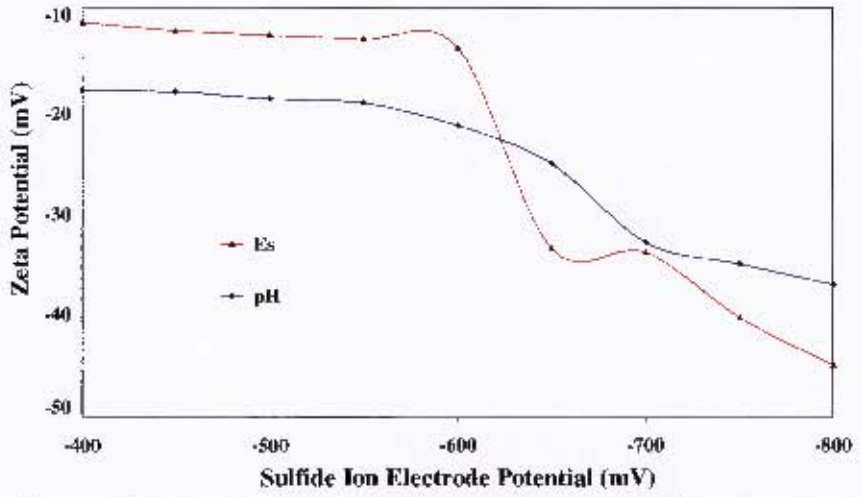

Figure 5-6: Zeta potential contributions as a function of sulfidisation potential for heavily chemically oxidised Nkomati ore samples

In Figure 5-7, the surface charge of the chemically oxidised Nkomati ore sulfide minerals became more negative in the presence of increasing hydrosulfide ion concentrations for both samples.

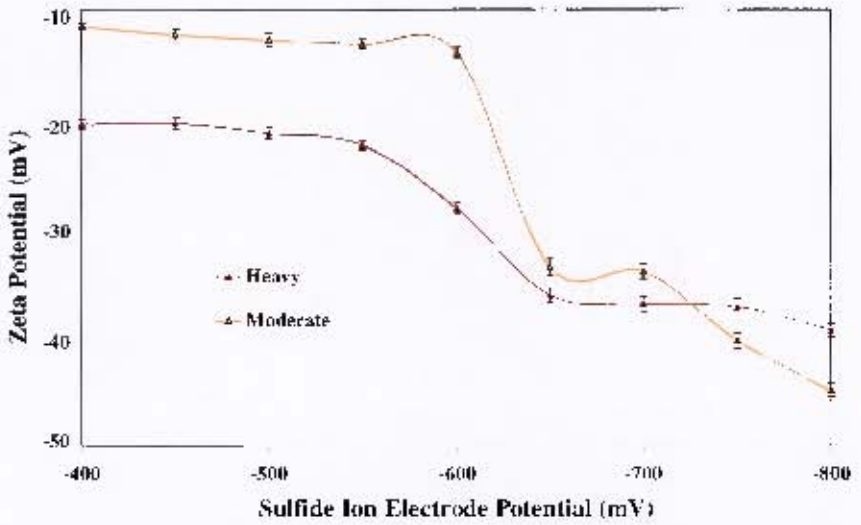

Figure 5-7: Zeta potential of chemically oxidised Nkomati ore samples as a function of degree of oxidation and sulfidisation potential

There was a difference between the two degrees of oxidation in terms of the behaviour of the zeta potential as a function of the sulfidisation potential. For the moderately oxidised Nkomati ore sample, the surface charge was initially negative and fell sharply over the sulfide ion electrode potential range of -600 to -650 mV. The zeta potential dropped again after an Es of -700 mV. In the case of the heavily oxidised sample, the zeta potential was

more negative and fell away over the sulfide ion electrode potential range -550 to -650 mV. After a plateau, the zeta potential slowly decreased again after an Es of -750 mV.

Comparison of the two zeta potential profiles for the heavily oxidised Nkomati ore samples produced by the two oxidation methods indicated similar behaviour, particularly between -550 mV and -650 mV Es.

5.2.3 XPS

Table 5-3 presents the surface speciation of sulfidised heavily thermally oxidised Nkomati ore sulfide mineral surfaces as a function of sulfide ion electrode potential under nitrogen and air.

Table 5-3: XPS analysis of sulfidised thermally oxidised Nkomati surfaces as a function of sulfidisation potential

Species	Abundance (%)		
	Sulfidisation Potential (Es,mV)		
	-500 (N_2)	-650 (N_2)	-650 (Air)
Oxygen	**60.9**	**62.2**	**61.1**
Oxide	22.6	24.6	25.7
OH^-	28.4	24.2	28.0
SO_4^{2-}	9.9	13.3	7.4
Iron	**31.9**	**29.2**	**29.8**
Fe-S	1.6	1.5	2.3
Fe-O	30.3	27.7	27.5
Sulfur	**6.6**	**7.1**	**7.4**
S^{2-}	1.4	2.6	1.8
S_2^{2-}	2.1	1.1	3.6
S_n/S^0	0.6	1.5	0.6
SO_4^{2-}/SO_3^{2-}	2.5	1.9	1.4
Copper	**0.7**	**1.5**	**1.8**
Nickel	**N.D.**	**N.D.**	**N.D.**

Figure 5-8 summarises the salient differences in the speciation and bonds observed under the three sulfidisation conditions.

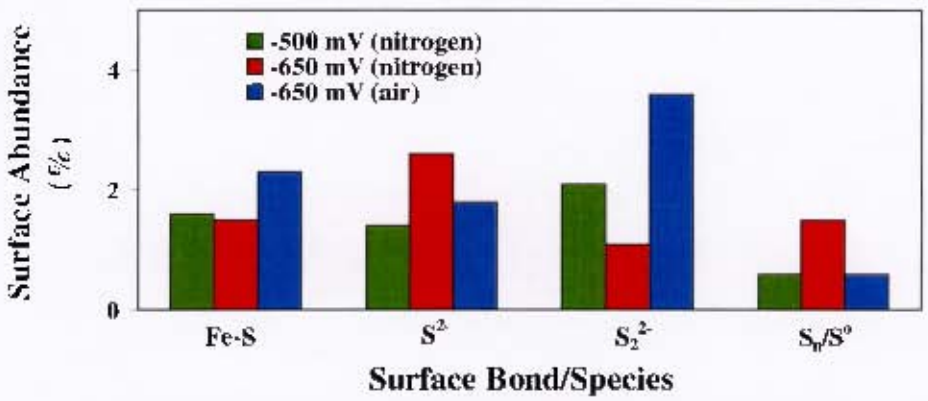

Figure 5-8: Abundances of selected species and bonds on thermally heavily oxidised Nkomati ore surfaces after sulfidisation

Under nitrogen, Fe-S bonds were detected at both sulfide ion electrode potentials while the quantity of S^{2-} increased with greater sulfidisation intensity. While both the elemental sulfur/polysulfur and copper concentrations were enhanced, the abundance of the S_2^{2-} bond was lower at the higher Es value. Under air at an Es of -650 mV, the Fe-S bond and S_2^{2-} species were found in significantly greater amounts than that at the same sulfide ion electrode potential under nitrogen. Only elemental sulfur/polysulfur and sulfoxy bonds were detected in lower quantities.

With an increase in the sulfidisation potential to -650 mV, there was a decrease in the abundance of hydroxyl species as well as the Fe-O signal. Both S^{2-} and S_2^{2-} were identified and their abundances followed opposite trends with increased sulfidisation potential. The disulfide halved in abundance while the amount of monosulfide doubled. Similar levels of Fe-S bonding were noted under both sulfidisation potentials.

Some sulfur oxidation products were found in moderate abundance as mainly polysulfides/elemental sulfur and sulfate/sulfite. As the amount of S_n/S^0 increased significantly under the more intense sulfidisation conditions, the quantity of SO_4^{2-}/SO_3^{2-} decreased. The presence of copper in both the Cu(II) and Cu(I) forms was identified on the sulfidised surfaces however could not be fully quantified (refer to Appendix D3). However, the proportion of Cu(I) increased markedly with more intense sulfidising conditions.

5.2.4 Adsorption

Hydrosulfide ion adsorption studies were conducted on thermally heavily oxidised -11 µm Nkomati ore samples as described in Section 3.7.3.1. Figure 5-9 shows that nearly complete abstraction of the hydrosulfide ion was observed at the three solution strengths, particularly at the lower initial concentrations of 10^{-4} and 10^{-5}M. At the higher hydrosulfide ion concentration, the solution became more alkaline with increasing hydrosulfide ion adsorption. In the case of the intermediate concentration, the pH initially turned more alkaline, before becoming more acidic with increased hydrosulfide ion abstraction. At the lowest hydrosulfide ion strength, the solution pH decreased as more hydrosulfide ion was adsorbed.

The adsorption of the hydrosulfide ions as a function of time can be described by the following relationship $[HS^-] = at^{1/n}$, where t is time (minutes) while a and n are constants (Mitrofanov *et al*, 1957 and Marabini *et al*, 1984). The values of these constants as well as the quality of fit (R^2) of the data to the equation are summarised in Table 5-4.

Table 5-4: Hydrosulfide ion adsorption equation parameters for heavily oxidised Nkomati ore samples

$[HS^-]_{initial}$ (M)	a	1/n	R^2
10^{-3}	$2x10^{-4}$	-0.9125	0.9464
10^{-4}	$1x10^{-4}$	-1.6061	0.9415
10^{-5}	$4x10^{-5}$	-1.4707	0.8639

Figure 5-10 presents a Langmuir plot of the hydrosulfide ion adsorption data.

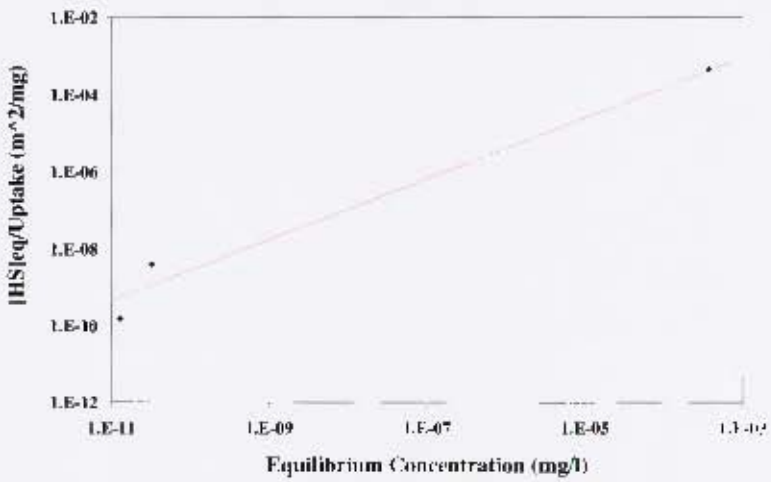

Figure 5-10: Langmuir plot of the hydrosulfide ion adsorption onto heavily thermally oxidised Nkomati ore surfaces

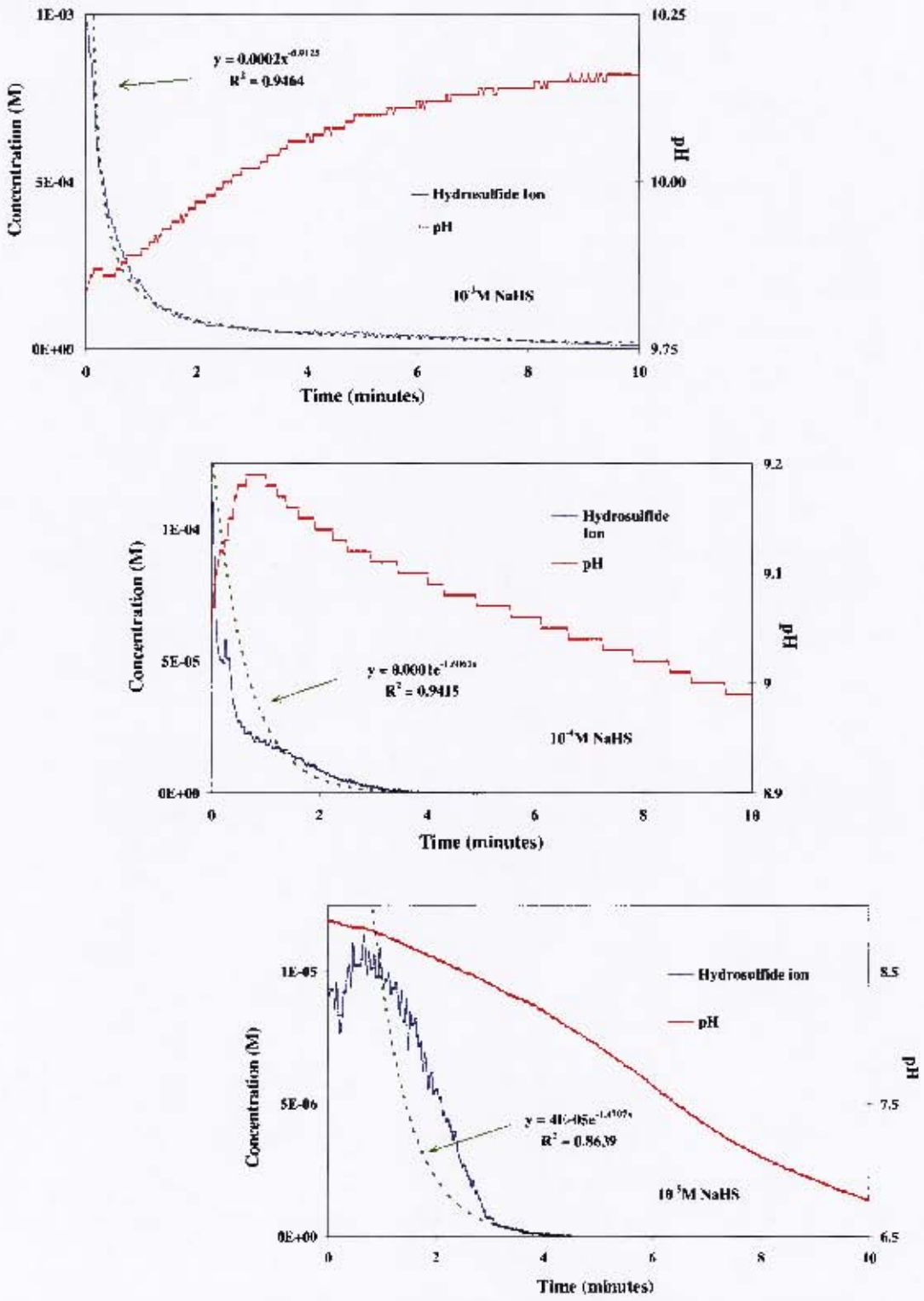

Figure 5-9: pH and HS^- concentration changes for heavily thermally oxidised Nkomati ore samples as a function of NaHS concentration

5.3 Pyrrhotite

5.3.1 Electrophoresis

5.3.1.1 Thermal oxidation

Figure 5-11 shows that the degree of thermal oxidation had a pronounced effect upon the zeta potential of oxidised pyrrhotite particles in the presence of an increasing concentration of hydrosulfide ions. Heavily oxidised samples experienced two strong regions of significant change in zeta potential values. A steady decrease in the zeta potential was observed between -500 and -650 mV Es while the second region occurred over the sulfidisation potential range of -700 to -750 mV. In the case of moderately oxidised samples, the change in the zeta potential values occurred over similar ranges of sulfidisation potentials, however not as great. Two steady changes in zeta potential were found between -500 and -550 mV Es and -600 and -650 mV while a small decrease was observed over the range -700 to -750 mV.

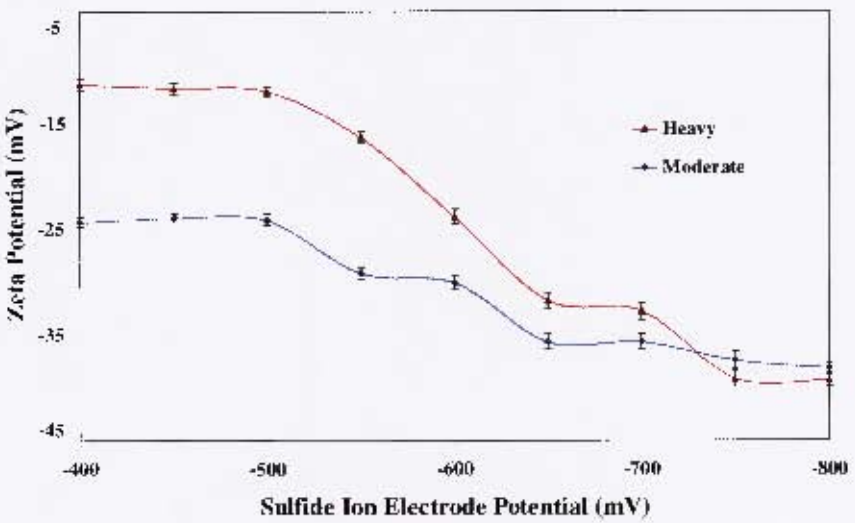

Figure 5-11: Zeta potential of thermally oxidised pyrrhotite samples as a function of degree of oxidation and sulfidisation potential

5.3.1.2 Chemical oxidation

Somewhat similar electrophoretic results were observed for chemically oxidised pyrrhotite particles with increasing concentrations of hydrosulfide ions (refer to Figure 5-12). For heavily oxidised samples, a sharp decrease in the zeta potential was observed between -600

and -650 mV Es while a second reduction started at a sulfidisation potential of -700 mV. Similarly to the moderately thermally oxidised samples, three regions with steady but significant declines in the zeta potential values were identified at Es values between -400 to -550 mV, -600 and -700 mV and from -750 to -800 mV. An interesting feature was the increase in zeta potential that occurred between the Es values of -700 and -750 mV.

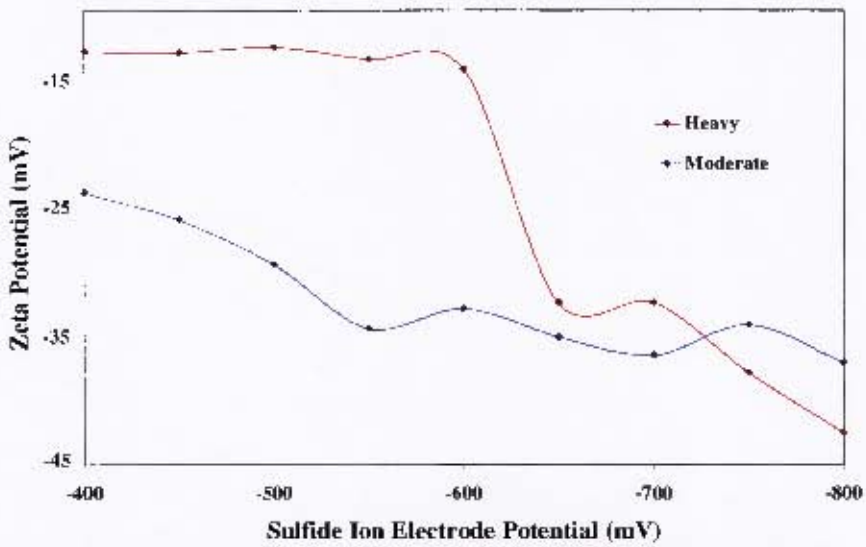

Figure 5-12: Zeta potential of chemically oxidised pyrrhotite samples as a function of degree of oxidation and sulfidisation potential

5.3.2 Electrochemistry

5.3.2.1 Cyclic voltammetry

Figure 5-13 compares the cyclic voltammograms of a pyrrhotite electrode before and after sulfidisation following heavy chemical oxidation to that of the unoxidised electrode. The comparison shows that heavy chemical oxidation produced a passivated and electrochemically inert surface without the characteristic anodic (A1) and cathodic (C1) reactions. After sulfidisation, a similar surface has been regenerated to that before oxidation although the cathodic reaction C1 was not observed.

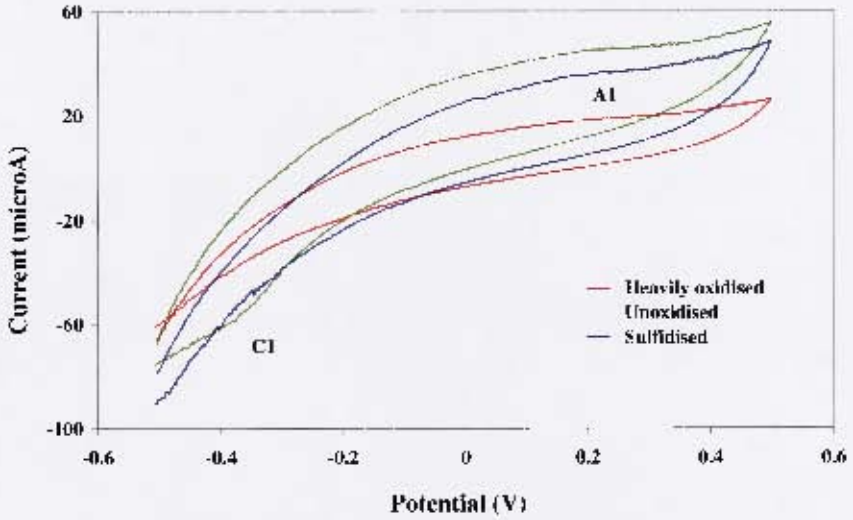

Figure 5-13: Cyclic voltammograms of pyrrhotite before and after oxidation and sulfidisation

5.3.2.2 Chronoamperometry

In Figure 5-14, the addition of sodium sulfide produced a negative current at the surface of the heavily chemically oxidised pyrrhotite electrode. A higher sodium sulfide concentration produced an even stronger cathodic reaction.

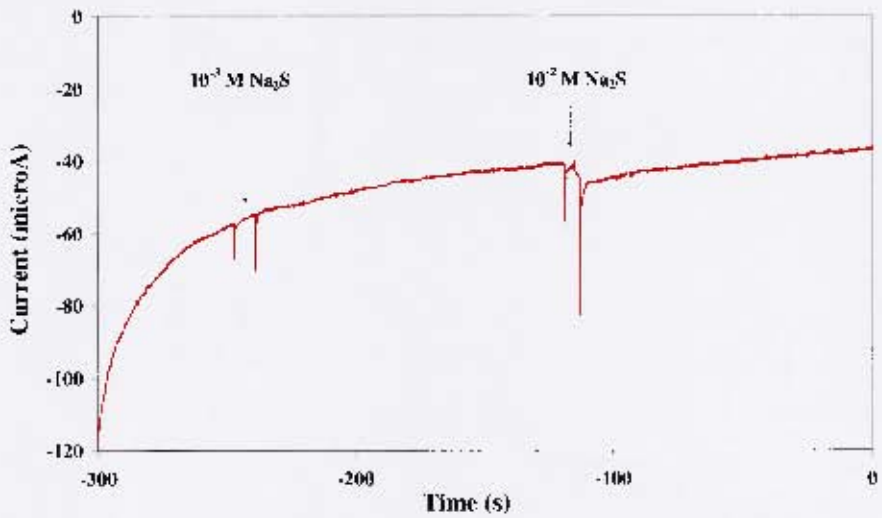

Figure 5-14: Chronoamperogram of heavily chemically oxidised pyrrhotite electrode as a function of sulfide concentration

5.4 Chalcopyrite

5.4.1 Electrophoresis

5.4.1.1 Thermal oxidation

The zeta potential of heavily thermally oxidised chalcopyrite slowly decreased over the range -400 to -500 mV Es before dropping sharply between -600 and -650 mV Es (refer to Figure 5-15). After -700 mV Es, the surface charge became increasingly negative. On the other hand, the zeta potential of moderately thermally oxidised chalcopyrite steadily decreased over the range -500 to -750 mV Es.

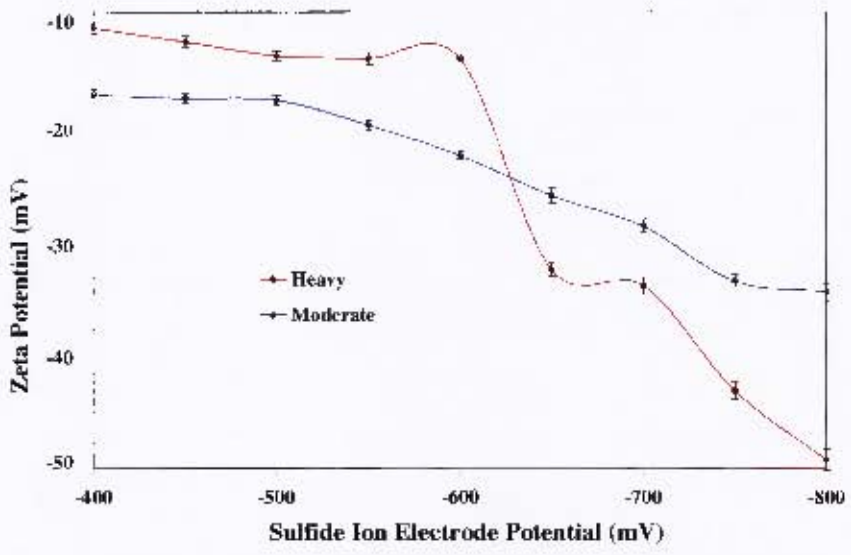

Figure 5-15: Zeta potential of thermally oxidised chalcopyrite as a function of degree of oxidation and sulfidisation potential

5.4.1.2 Chemical oxidation

Figure 5-16 shows that the electrophoretic response of heavily chemically oxidised chalcopyrite was almost identical to that displayed by the heavily thermally oxidised sample. In the case of moderately chemically oxidised chalcopyrite, a small but steady decrease in the zeta potential was found and punctuated by two plateaus between -500 to -600 mV and -650 to -700 mV Es.

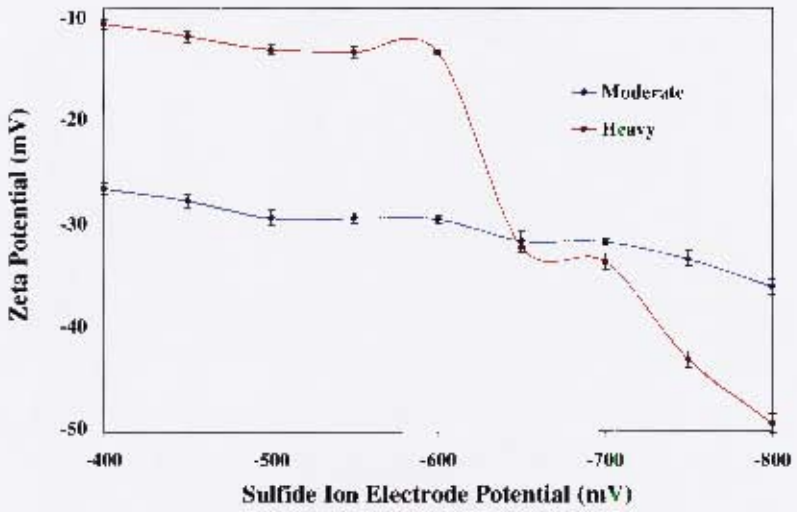

Figure 5-16: Zeta potential of chemically oxidised chalcopyrite as a function of degree of oxidation and sulfidisation potential

5.4.2 Electrochemistry

5.4.2.1 Cyclic voltammetry

The cyclic voltammograms of a chalcopyrite electrode before and after sulfidisation following heavy chemical oxidation is compared with that of the unoxidised electrode in Figure 5-17. The comparison shows that heavy chemical oxidation did not significantly change the electrochemical characteristics of the chalcopyrite surface. After sulfidisation, a very similar surface was restored to that before oxidation, noting the characteristic anodic reactions (A1 and A2) and the cathodic reaction (C1).

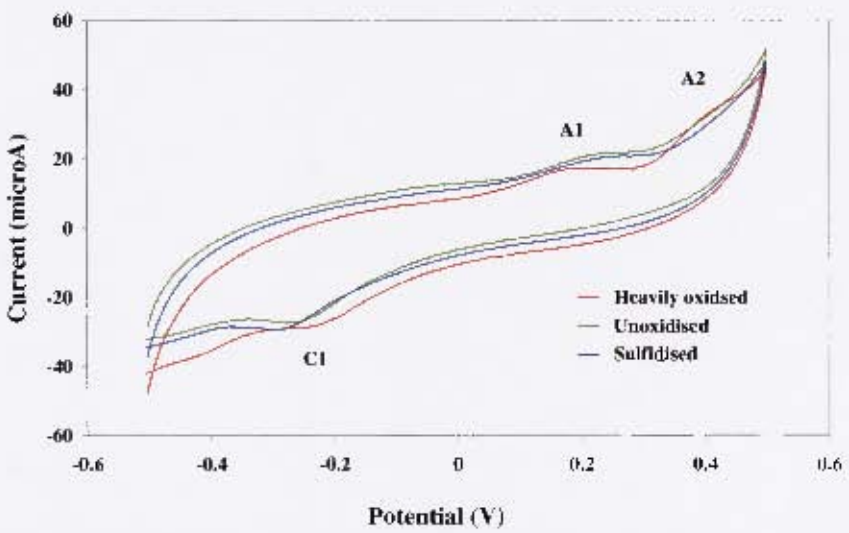

Figure 5-17: Cyclic voltammograms of chalcopyrite before and after oxidation and sulfidisation

5.4.2.2 Chronoamperometry

In Figure 5-18, the addition of sodium sulfide produced a strong negative current at the surface of the heavily chemically oxidised chalcopyrite electrode. At a higher sodium sulfide concentration, another negative current was observed.

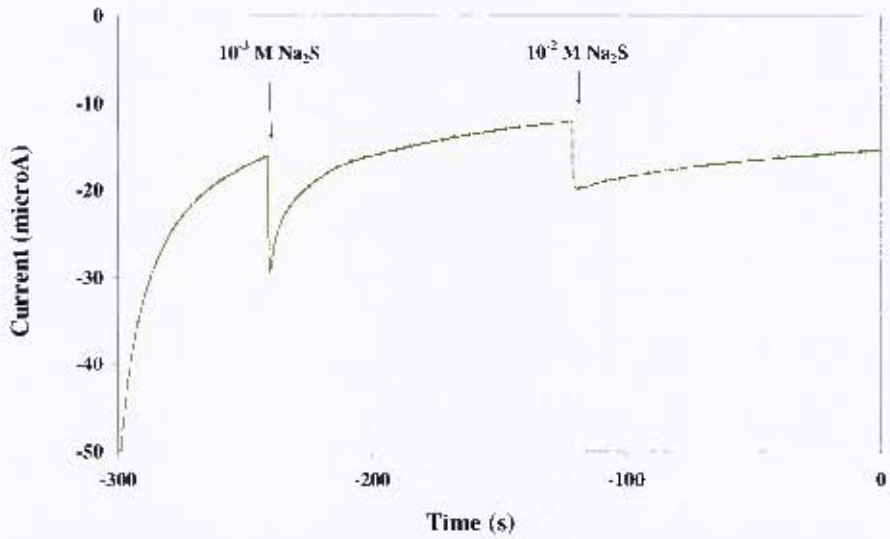

Figure 5-18: Chronoamperogram of heavily chemically oxidised chalcopyrite electrode as a function of sulfide concentration

5.4.3 XPS

The XPS analysis of a heavily thermally oxidised chalcopyrite surface after sulfidisation at two potentials is presented in Table 5-5. Figure 5-19 summarises the salient differences in the speciation and bonds identified under the two sulfidisation conditions.

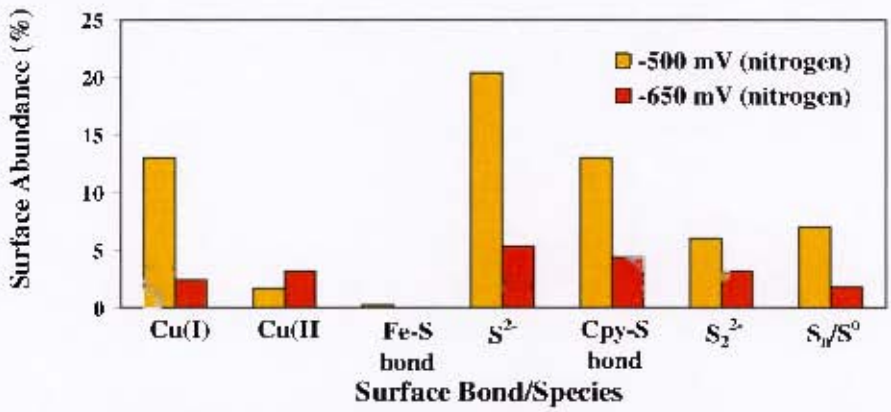

Figure 5-19: Surface abundances of selected species and bonds of thermally oxidised chalcopyrite surfaces after sulfidisation

Table 5-5: XPS analysis of sulfidised thermally oxidised chalcopyrite surfaces as a function of sulfidisation potential

Species	Abundance (%)	
	Sulfidisation Potential (mV)	
	-500 (N_2)	-650 (N_2)
Oxygen	**33.1**	**68.2**
Oxide	3.6	28.6
OH^-	21.5	30.0
$H_2O+SO_4^{2-}$	7.9	9.5
Copper	**14.7**	**5.6**
Cu(I)	13.0	2.4
Cu(II)	1.7	3.2
Iron	**4.8**	**8.2**
Fe-S	0.3	
Fe-O	4.5	8.2
Sulfur	**46.4**	**14.7**
S^{2-}	20.4	5.3
Cpy-S	13.0	4.4
S_2^{2-}	6.0	3.2
S_n/S^0	7.0	1.8
SO_4^{2-}	-	-
Lead	**1.0**	**2.0**
Zinc	**-**	**1.3**

At an Es of -500 mV, high exposures of S^{2-}, S_2^{2-}, Cu(I) and Cpy-S were observed. In addition, the Fe-O signal decreased while a Fe-S bond was detected along with a large quantity of polysulfides /elemental sulfur.

Under the stronger sulfidisation potential, a similar array of species was present however in reduced proportions compared to that observed at an Es of -500 mV. Most significantly, the proportion of Cu(II) had increased while that of the Cu(I) had substantially decreased. Both the S^{2-} and S_2^{2-} signals were reasonably strong however the exposure of polysulfides/elemental sulfur had diminished to pre-sulfidisation levels.

5.5 Pentlandite

In this Section, the behaviour of pentlandite as a single mineral is reported in contrast to the response found with the Nkomati ore sample. In particular, the flotation response of oxidised pentlandite after treatment with base-metal ions during sulfidisation is highlighted.

5.5.1 Flotation

Figure 5-20 shows that heavily oxidised pentlandite as a single mineral did not respond readily to sulfidisation as measured by flotation recovery. This was in contrast to that obtained in a mixed sulfide mineral system, where a flotation recovery of around 75% was found. At an Es of -800 mV, however, some flotation was observed, particularly for the chemically oxidised sample.

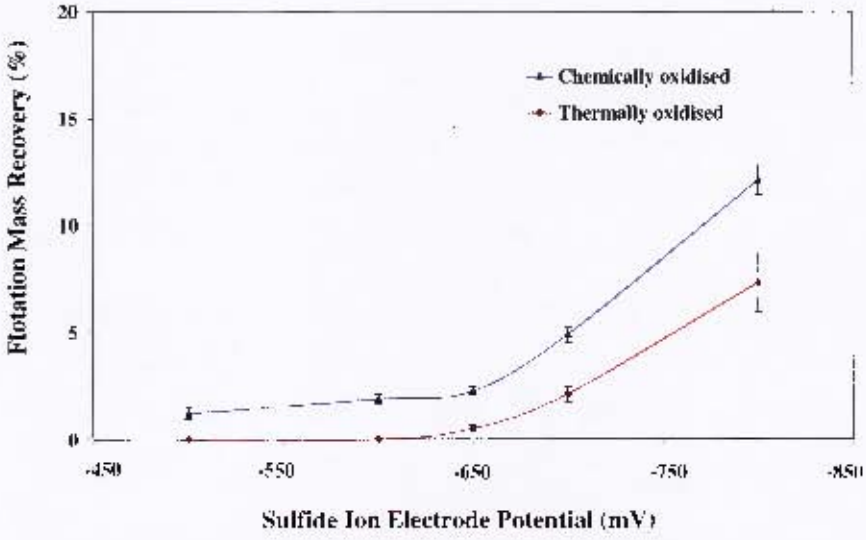

Figure 5-20: Flotation mass recovery of oxidised pentlandite surfaces as a function of sulfidisation potential (1.375×10^{-3}M SIBX)

5.5.2 Electrophoresis

5.5.2.1 Thermal oxidation

The electrophoretic behaviour of heavily thermally oxidised pentlandite in the presence of hydrosulfide ions was characterised by two sharp falls in the zeta potential (refer to Figure 5-21). Initially, a small but progressive decrease in zeta potential was observed over the sulfidisation potential range -400 to -600 mV. The first significant decrease in zeta potential occurred between -600 to -650 mV Es and after a brief plateau, it fell continuously with increasing sulfidisation potential from -700 mV Es.

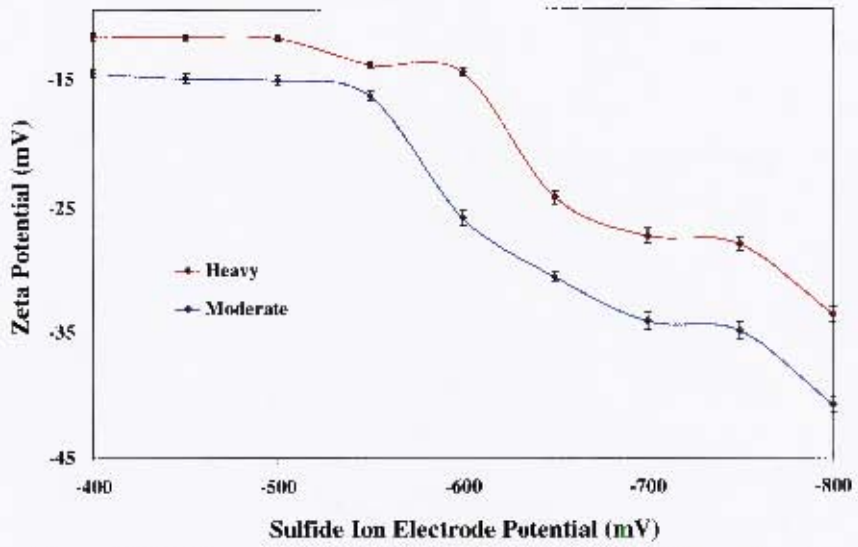

Figure 5-21: Zeta potential of thermally oxidised pentlandite as a function of degree of oxidation and sulfidisation potential

The electrophoretic behaviour of the moderately oxidised pentlandite followed a similar trend to that of the heavily oxidised sample and was characterised by a large progressive fall in the zeta potential between -550 and -700 mV Es. After a plateau between -700 and -750 mV Es, the zeta potential then sharply fell away.

5.5.2.2 Chemical oxidation

Figure 5-22 shows that for the heavily oxidised pentlandite samples, a gradual fall in the zeta potential was observed over the sulfidisation potentials of -400 to -550 mV. The zeta potential decreased significantly between -600 to -650 mV Es followed by a plateau over the 50 mV Es. After -750 mV Es, another significant fall in zeta potential occurred.

In the case of the moderately oxidised samples, a sharp fall in zeta potential occurred between -600 and -650 mV Es, with a gradual and extended decrease over the sulfidisation potential range -650 to -750 mV.

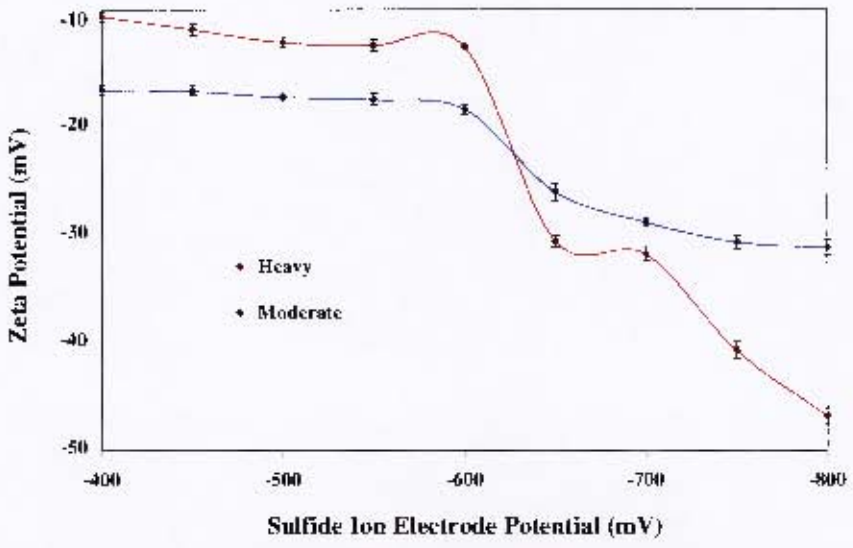

Figure 5-22: Zeta potential of chemically oxidised pentlandite as a function of degree of oxidation and sulfidisation potential

5.5.3 Electrochemistry

5.5.3.1 Cyclic voltammetry

Figure 5-23 compares the cyclic voltammograms of the unoxidised pentlandite electrode with the electrode after heavy chemical oxidisation and sulfidisation. The surface after sulfidisation is not the same as the unoxidised pentlandite surface and still retains some of the characteristics of the heavily oxidised electrode surface. However, the cathodic reaction (C1) is common to both cyclic voltammograms.

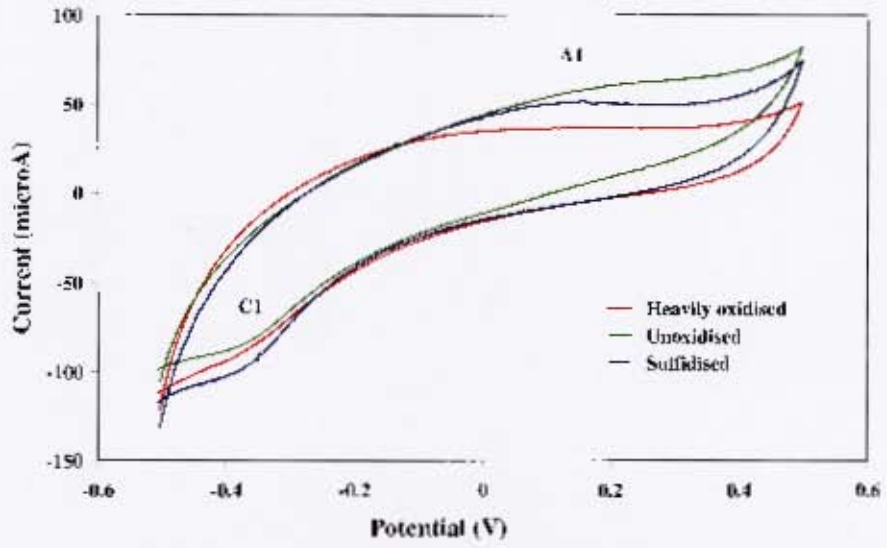

Figure 5-23: Cyclic voltammograms of pentlandite electrode before and after heavy chemical oxidation and sulfidisation

5.5.3.2 Chronoamperometry

In Figure 5-24, the addition of sodium sulfide produced a negligible current at the surface of the heavy chemically oxidised pentlandite electrode, while the presence of a higher sodium sulfide concentration generated only a very small cathodic reaction.

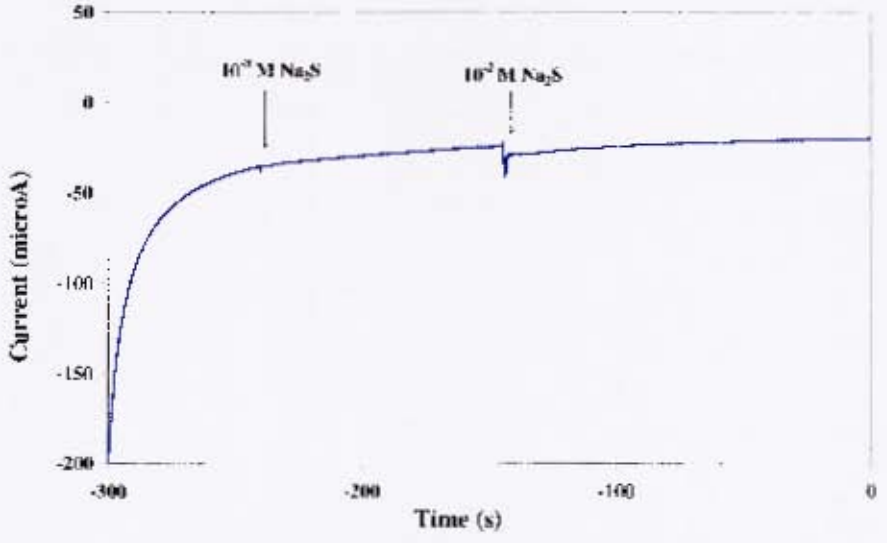

Figure 5-24: Chronoamperogram of heavily chemically oxidised pentlandite electrode as a function of sulfide concentration

5.5.4 XPS

Table 5-6 presents the full XPS analysis of the sulfidised heavily oxidised pentlandite surfaces, with the more pertinent features summarised in Figure 5-25.

Table 5-6: XPS analysis of sulfidised thermally heavily oxidised pentlandite surfaces as a function of sulfidisation potential

Species	Abundance (%)		
	Sulfidisation Potential (Es,mV)		
	-500 (N_2)	-650 (N_2)	-800 (N_2)
Oxygen	**77.4**	**86.7**	**85.7**
Oxide	26.3	52.9	25.7
OH^-	37.2	20.8	44.6
$H_2O+SO_4^{2-}$	13.9	13.0	15.4
Nickel	**7.7**	**3.1**	**3.5**
Ni-S	0.3	-	-
Ni-O	7.4	3.1	3.5
Iron	**8.5**	**6.4**	**8.4**
Fe-O	8.5	6.4	8.4
Sulfur	**6.4**	**3.9**	**2.3**
$S^{2-}/S_n/S^0/...$	4.9	2.8	1.8
Sulfoxy	1.5	1.1	0.5

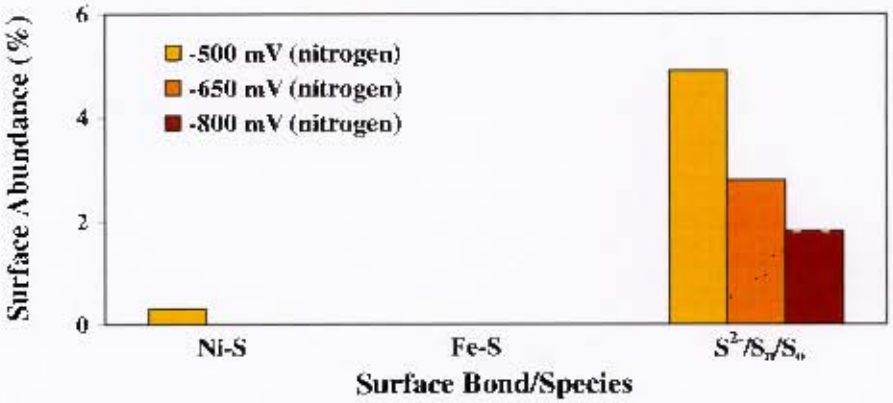

Figure 5-25: Surface abundances of selected species and bonds of thermally heavily oxidised pentlandite surfaces after sulfidisation

Under nitrogen and with increasing sulfidisation intensity (-500 to -800 mV), the abundance of the surface hydroxyl groups fell away markedly, while that of the oxide increased reflecting a redistribution of the oxygen speciation. At an Es of -500 mV, both the nickel and iron oxide/hydroxides abundances were at a maximum. Only a very small Ni-S signal was detected and no Fe-S signal was apparent. Sulfur was present in moderate quantities as $S^{2-}/S_0/S^0$, possibly as elemental sulfur/polysulfides. At a sulfidisation potential

of -650 mV, the signals for the hydroxyl, Ni-O and $S^{2-}/S_n/S^o$ species decreased significantly while that of the oxide signal increased substantially. The Fe-O signal also declined however no Ni-S or Fe-S signals were detected. The XPS speciation profile of the oxidised pentlandite surfaces under more intense sulfidisation conditions (-800 mV) was similar to that observed after sulfidisation at an Es of -500 mV. The major differences were a lower Ni-O signal and an even lower level of sulfur speciation. Significantly, signals for Ni-S and Fe-S were absent.

5.5.5 Improving the flotation response with base-metal ions

The addition of base-metal ions, such as Cu(II) [5μmoles] and Fe(III) [500μmoles], had a significant impact on the flotation response of heavily chemically oxidised pentlandite after sulfidisation at an Es of -650 mV. Figure 5-26 shows that when iron ions were added prior to sulfidisation, a moderate improvement in the flotation of oxidised pentlandite was observed. With the addition of iron ions during sulfidisation, a significant increase in the flotation recovery was observed.

The addition of copper ions displayed a similar but generally less significant impact on the flotation of oxidised pentlandite. The presence of copper ions before sulfidisation improved the flotation recovery more effectively than iron ions. However, as found with iron ions, the best flotation response occurred with addition during sulfidisation, although not as great.

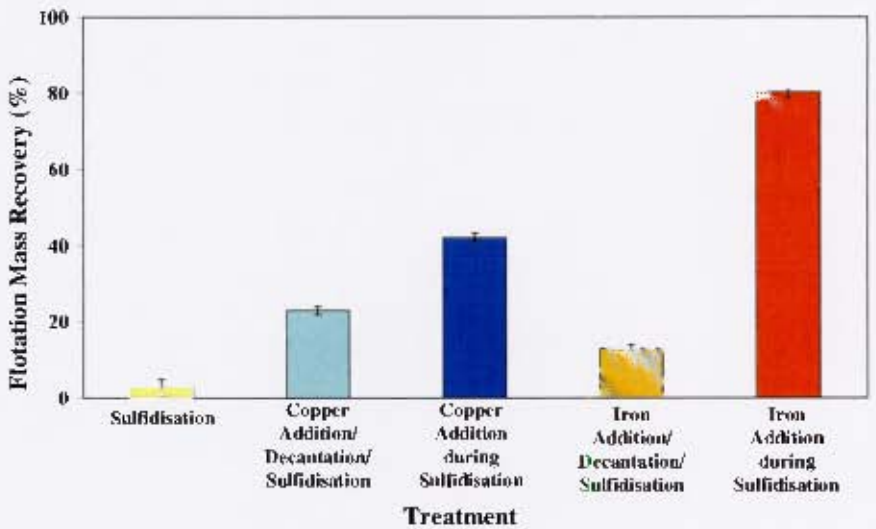

Figure 5-26: Flotation mass recovery of heavily chemically oxidised pentlandite after sulfidisation as a function of base-metal ion type and addition location (1.375×10^{-3}M SIBX)

5.5.5.1 Iron additions

Figure 5-27 shows the flotation recovery of heavily oxidised pentlandite samples after iron addition (500μmoles) during sulfidisation as a function of sulfidisation potential. The flotation response for both chemically and thermally heavily oxidised pentlandite was similar, although higher flotation recoveries were achieved with the heavily chemically oxidised samples at the higher sulfidisation potentials. Significantly, the best flotation recoveries were obtained at an Es of -650 mV.

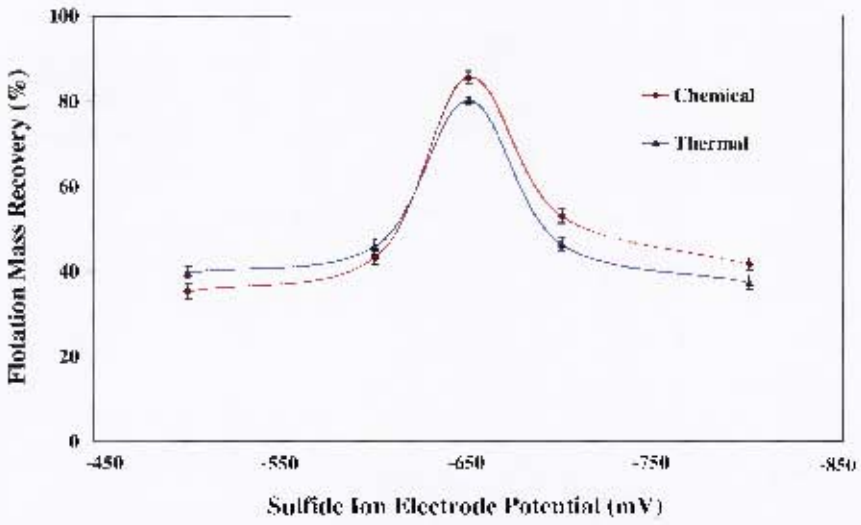

Figure 5-27: Flotation mass recovery of heavily oxidised pentlandite samples with iron addition as a function of sulfidisation potential (1.375×10^{-3} M SIBX)

The flotation rate of the sulfidised oxidised pentlandite in these tests was found to be much slower than that found during the sulfidisation of thermally oxidised Nkomati samples. Another ten minutes of flotation time was required to achieve similar flotation recoveries.

5.6 Merensky ore gangue minerals

5.6.1 Flotation

5.6.1.1 Before sulfidisation

As a baseline for comparison, the flotation behaviour of the Merensky ore gangue minerals, predominantly pyroxene and feldspar with a small quantity of talc, was examined using micro-flotation. Samples of unweathered (i.e. unoxidised) and weathered (i.e. naturally oxidised) material were compared with and without the use of a collector. As

Figure 5-28 shows, neither weathering nor the presence of collector significantly affected the flotation response of the gangue minerals.

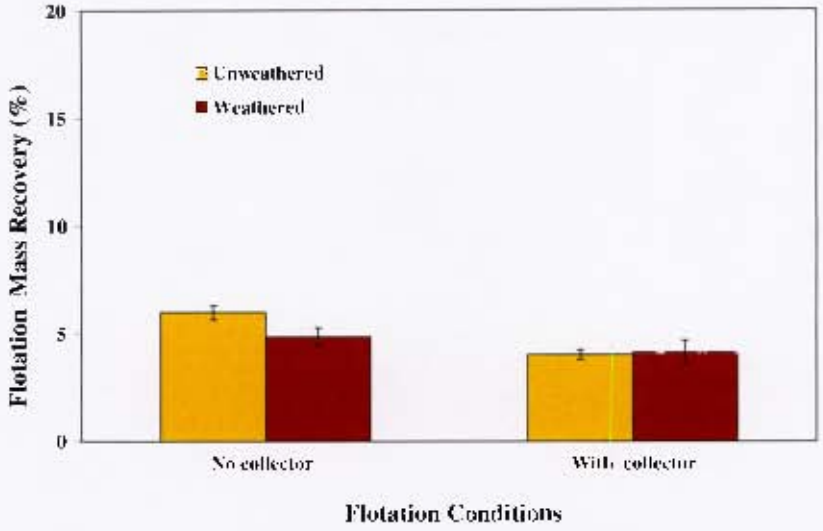

Figure 5-28: Flotation mass recovery of unweathered and weathered Merensky ore gangue minerals with and without collector

5.6.1.2 After sulfidisation

The unweathered and weathered Merensky ore gangue mineral samples were sulfidised and floated after the addition of collector. Figure 5-29 shows that neither sulfidisation nor the sulfidisation intensity had any significant effect upon the flotation of Merensky ore gangue minerals. The unweathered samples showed a tendency to be recovered in greater quantities than the weathered samples.

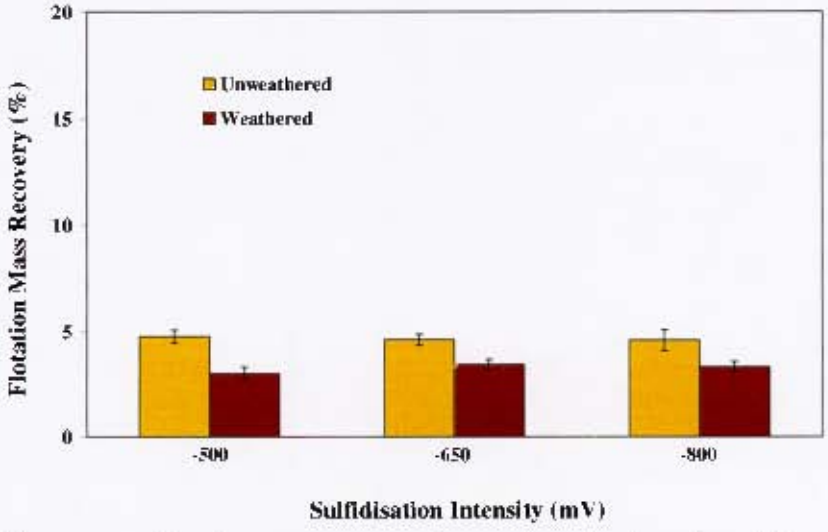

Figure 5-29: Flotation mass recovery of unweathered and weathered Merensky ore gangue minerals as a function of sulfidisation

5.7 Summary

Similar flotation responses were found after sulfidisation for the three sulfide minerals from heavily oxidised Nkomati ore samples with both oxidation methods. The optimum flotation recoveries of all the sulfide minerals occurred at moderate sulfidisation potentials (Es = -650 mV). Chalcopyrite responded the most favourably to sulfidisation followed by pyrrhotite while the response of pentlandite was the poorest. In contrast, as a single mineral, heavily oxidised pentlandite did not readily float after sulfidisation.

XPS analyses revealed the presence of base-metal sulfide species on heavily oxidised pyrrhotite and chalcopyrite surfaces after sulfidisation however, after sulfidisation, only base-metal non-sulfide species were identified on heavily oxidised pentlandite surfaces. Additionally, reasonable quantities of polysulfides/elemental sulfur were found on the sulfidised mineral surfaces, particularly chalcopyrite and pyrrhotite.

Electrophoretic studies showed that the zeta potential of the oxidised sulfide mineral surfaces in the presence of hydrosulfide ions fell away sharply over specific ranges of sulfidisation potentials. For the heavily chemically oxidised sulfide mineral samples, this occurred over the same Es range (-600 to -650 mV) while some broadening of this range was found for both the heavily thermally oxidised pyrrhotite and pentlandite samples.

Cyclic voltammetric studies showed that the sulfidisation of oxidised pyrrhotite and chalcopyrite surfaces regenerated similar surfaces to those of the unoxidised sulfide mineral surface. Sulfidisation did not restore an unoxidised surface to heavily oxidised pentlandite.

Chronoamperometric studies found that heavily oxidised pyrrhotite and chalcopyrite surfaces generated negative currents in the presence of hydrosulfide ions, indicating a cathodic electrochemical reaction. In contrast, there was effectively no interaction between heavily oxidised pentlandite surfaces and hydrosulfide ions.

The addition of base-metal ions, particularly iron, during sulfidisation significantly improved the flotation recovery of heavily oxidised pentlandite and produced a similar flotation recovery–sulfidisation potential response curve to that observed for heavily oxidised pentlandite in Nkomati ore samples after sulfidisation. The effect of base-metal additions during sulfidisation yielded a similar flotation response with both methods of

oxidation.

The presence of calcium ions during sulfidisation had no effect on the flotation recoveries of the sulfide minerals from heavily thermally oxidised Nkomati ore samples.

The flotation recoveries of both unweathered and weathered Merensky ore gangue mineral samples collector were not enhanced by sulfidisation.

CHAPTER 6

DISCUSSION

6.1 Introduction

The discussion reviews the results in terms of the two hypotheses, namely the impact of oxidation upon the flotation behaviour of sulfide minerals and the mechanistic role of sulfidisation in restoring sulfide surfaces to oxidised sulfide mineral surfaces and thus floatability. Additionally, the discussion addresses the results obtained from a specific investigation of the sulfidisation of oxidised pentlandite, which was required due to the unexpected behaviour of this mineral and develops the associated sulfidisation mechanism.

In reviewing the potential oxidation, hydrolysis and sulfidisation reactions, the possibility of such reactions has been established on thermodynamic grounds at the appropriate temperature. Where electrochemical reactions are indicated, the cell half-potential has been calculated. For base-metal cations, the standard convention of 10^{-6}M concentration has been used, while the concentration of the sulfidising reagent species has been calculated for the relevant pH and Es/Eh conditions. For hydrosulfide ion concentrations of 10^{-3}M, an activity coefficient has been used. A comparison of the calculated results is made with the measured or calculated conditions. These calculations are presented in Appendix A3.

For hydrolysis reactions, Table 6-1 summarises the values of the Eh and the corresponding pH during the hydrolysis of heavily thermally oxidised Nkomati ore sample.

Table 6-1: Summary of parameter values during hydrolysis

Measured pH	Measured Eh (SHE,V)
7.5	-0.196
7.0	-0.176
6.5	-0.154
6.0	-0.133
5.5	-0.099
5.0	-0.072
4.5	-0.020

Table 6-2 presents the values of the Eh, pH and corresponding sulfur species concentration during the sulfidisation of heavily thermally oxidised Nkomati samples.

Table 6-2: Summary of solution parameter values during sulfidisation

Es (mV)	Equivalent Eh (SHE,V)	Calculated [NaSH] (M)	Calculated [HS^-] (M)	Calculated [S^{2-}] (M)	Measured pH
-800	-0.465	$1.91x10^{-2}$	$1.91x10^{-2}$	$9.55x10^{-6}$	9.62
-700	-0.365	$1.70x10^{-4}$	$1.60x10^{-4}$	$3.13x10^{-9}$	8.21
-650	-0.315	$2.4x10^{-5}$	$2.19x10^{-5}$	$2.63x10^{-10}$	8.00
-600	-0.265	$5.7x10^{-6}$	$4.94x10^{-6}$	$3.74x10^{-11}$	7.80
-500	-0.165	$6.0x10^{-7}$	$4.61x10^{-7}$	$1.79x10^{-12}$	7.51

6.2 Chalcopyrite

6.2.1 Effect of oxidation

6.2.1.1 Flotation response

Chalcopyrite was the fastest floating component in the unoxidised Nkomati ore sample, displaying considerable natural floatability as well as excellent collector-induced flotation. Thermal oxidation had a significant impact on the flotation of chalcopyrite, however ultrasonic treatment largely restored the floatability with a high level of collector. After 60 days of oxidation, little change in the flotation recovery was observed after ultrasonic treatment. The oxidation products were easily removed and exposed a surface that interacted with the collector. This was consistent with the reported oxidation behaviour of chalcopyrite where iron oxide surface products were reported to form over a copper sulfide mineral surface (Buckley and Woods, 1984, Luttrell and Yoon, 1984 and Vaughan *et al*, 1995).

Chemical oxidation had a more significant effect on the flotation behaviour of chalcopyrite, causing nearly complete depression after exposure to 10^{-2}M hydrogen peroxide solution. This oxidative approach was more effective than thermal oxidation followed by hydrolysis in terms of depression.

6.2.1.2 Oxidation characteristics

The SEM/EDX studies showed that thermal oxidation formed moderately thick layers of oxidation product on the surfaces of the chalcopyrite particles. Iron and sulfur were increasingly abstracted into the oxidation layers with greater exposure to thermal

oxidation. With heavier oxidation, copper was also found in the oxidation layers. These observations are in agreement with other oxidation studies on the oxidation of chalcopyrite, although these studies were conducted over significantly shorter time spans (Smart, 1991, Zachwieja *et al*, 1989, Buckley and Woods, 1984 and Luttrell and Yoon, 1984).

A large number of oxidation reactions are thermodynamically possible at 85°C (refer to Table 6-3). The formation of oxides are strongly favoured, particularly CuO and FeO. With moisture in the air, FeO.OH can form particularly with Cu_2O as a co-oxidation product. Although Fe_2O_3 is thermodynamically possible at these temperatures, along with Fe_3O_4, it was not expected to form in any significant quantities. Sulfates will also form, however, not as abundantly as oxides. While all reactions have very large reaction constants, not all reactions would go to completion due to the formation of oxide layers on the particles based on the shrinking core reaction model. This layer would affect the transport of reactants to the unoxidised surfaces and was the main reason for incomplete oxidation of the sulfide minerals, as reflected by the flotation response. In summary, the expected surface products for thermally oxidised chalcopyrite include FeO, CuO, Cu_2O, FeO.OH with $CuSO_4$ and possibly $FeSO_4$.

Table 6-3: Chalcopyrite oxidation reactions in air at 85°C (after Roine, 2002)

Oxidation reaction	ΔG^o (kJ)	Log K
$CuFeS_2 + 1.5O_{2(g)} \rightarrow FeO + CuS + SO_{2(g)}$	-408.3	59.6
$CuFeS_2 + 3O_{2(g)} \rightarrow FeO + CuO + 2SO_{2(g)}$	-774.8	113.0
$2CuFeS_2 + 5.5O_{2(g)} \rightarrow 2FeO + Cu_2O + 4SO_{2(g)}$	-1447.8	211.2
$CuFeS_2 + 1.5O_{2(g)} \rightarrow FeS + CuO + SO_{2(g)}$	-334.7	48.8
$CuFeS_2 + 2O_{2(g)} \rightarrow FeSO_4 + CuS$	-670.2	97.8
$CuFeS_2 + 2O_{2(g)} \rightarrow FeS + CuSO_4$	-550.3	80.3
$CuFeS_2 + 3.5O_{2(g)} \rightarrow FeO + CuSO_4 + SO_{2(g)}$	-236.7	144.5
$CuFeS_2 + 3.5O_{2(g)} \rightarrow FeSO_4 + CuO + SO_{2(g)}$	-247.8	151.2
$2CuFeS_2 + 6O_{2(g)} + H_2O_{(g)} \rightarrow 2FeO.OH + Cu_2O + 4SO_{2(g)}$	-1689.1	246.4
$CuFeS_2 + 3.25O_{2(g)} + 0.5H_2O_{(g)} \rightarrow FeO.OH + CuO + 2SO_{2(g)}$	-214.0	130.6
$CuFeS_2 + 3.75O_{2(g)} + 0.5H_2O_{(g)} \rightarrow FeO.OH + CuSO_4 + SO_{2(g)}$	-265.5	162.1
$2CuFeS_2 + 6O_{2(g)} \rightarrow Fe_2O_3 + Cu_2O + 4SO_{2(g)}$	-1689.6	246.4
$2CuFeS_2 + 6.5O_{2(g)} \rightarrow Fe_2O_3 + 2CuO + 4SO_{2(g)}$	-428.1	261.3
$2CuFeS_2 + 7.5O_{2(g)} \rightarrow Fe_2O_3 + 2CuSO_4 + 2SO_{2(g)}$	-531.2	308.0

For chemically oxidised chalcopyrite samples, the oxidation layer was considerably thinner than that observed for the thermally oxidised samples and was less than 100 nanometres. Table 6-4 shows that thermodynamically the reaction between chalcopyrite and hydrogen peroxide predominantly forms iron and copper sulfates, however the release of Cu(II), Fe(II) and sulfate ions is also favoured. The very high half-cell potentials indicate that the electrochemical reactions are unlikely to occur and that the formation of Fe(III) ions would only occur under extreme oxidising conditions.

Table 6-4: Chalcopyrite reactions with hydrogen peroxide reactions at 25°C (Roine, 2002)

Reaction with H_2O_2	ΔG° (kJ)	Log K	E° (SHE,V)
$4H_2O_2 + CuFeS_2 \rightarrow Fe^{2+} + CuS + 4H_2O + SO_4^{2-}$	-1114.8	195.3	-
$4H_2O_2 + CuFeS_2 \rightarrow FeSO_4 + CuS + 4H_2O$	-1103.8	193.90	-
$4H_2O_2 + CuFeS_2 \rightarrow Cu^{2+} + FeS + 4H_2O + 2SO_4^{2-}$	-1003.0	175.7	-
$4H_2O_2 + CuFeS_2 \rightarrow FeSO_4 + CuS + 4H_2O$	-985.0	172.6	-
$8H_2O_2 + CuFeS_2 \rightarrow Cu^{2+} + Fe^{2+} + 8H_2O + 2SO_4^{2-}$	-2149.7	308.0	-
$4H_2O_2 + CuFeS_2 \rightarrow FeSO_4 + CuSO_4 + 4H_2O$	-2120.7	308.0	
$8H_2O_2 + CuFeS_2 \rightarrow Cu^{2+} + Fe^{3+} + 8H_2O + 2SO_4^{2-} + e^-$	-2075.4	308.0	21.5
$4H_2O_2 + CuFeS_2 \rightarrow Fe^{3+} + CuS + 4H_2O + SO_4^{2-} + e^-$	-1040.4	182.3	10.8

6.2.1.3 Aqueous exposure

After contact with water, the XPS analysis showed that the thermally oxidised chalcopyrite surfaces were covered in iron and copper oxides and hydroxides. The Pourbaix diagram for the Cu/Fe/S/H_2O system shows thermodynamically that copper and ferric hydroxides are the dominant oxidation products (Garrels and Christ, 1990) (refer to Figure 6-1). A reasonable exposure of unoxidised chalcopyrite was observed on the surface, confirming that the surface of the sample was not completely oxidised. Cu(I) species were detected and in greater abundance than Cu(II) species. As expected, little surface SO_4^{2-} was found due to the dissolution of these species.

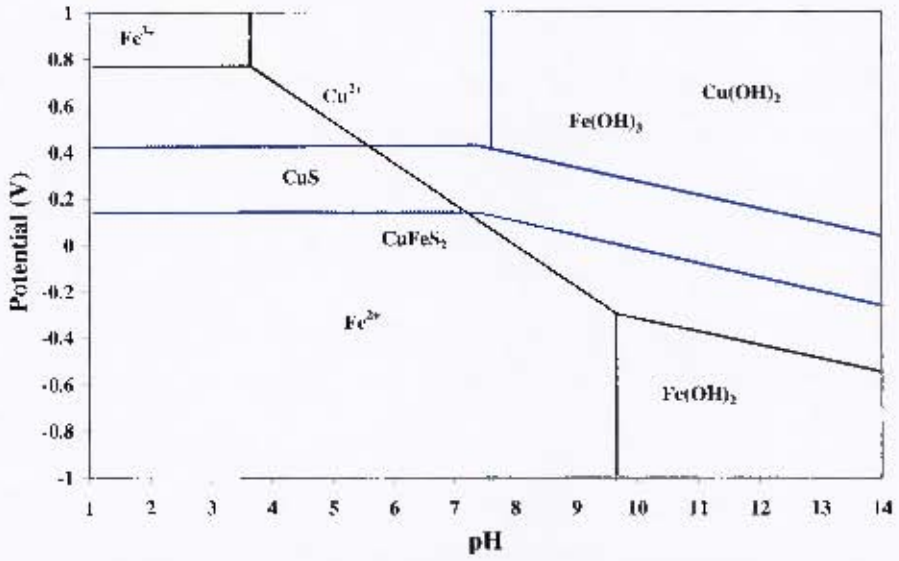

Figure 6-1: The Pourbaix diagram for the Cu/Fe/S/H_2O system (after Roine, 2002)

A number of hydrolysis reactions are possible between the oxidised chalcopyrite surfaces and water. The iron reactions are probably more dominant and discussed under pyrrhotite (refer to 6.3.1.3) and only the copper reactions are considered here (refer to Table 6-5). Besides the formation of hydroxides through Cu(II) ions, which would arise due to soluble oxidation products such as copper sulfate, no other significant hydrolysis reaction was apparent, noting that conditions for the hydrolysis of cuprite were not oxidising enough (refer to Table 6-6).

Table 6-5: Possible oxidised chalcopyrite hydrolysis reactions at 25°C

Hydrolysis reaction	ΔG° (kJ)	Log K	E° (SHE,V)
$Cu^{2+} + 2OH^- \rightarrow Cu(OH)_2$	-110.0	19.3	-
$Cu_2O + 2OH^- \rightarrow Cu(OH)_2 + CuO + 2e^-$	-25.6	4.3	0.128
$CuO + H_2O \rightarrow Cu(OH)_2$	6.2	-1.1	-
$CuO + H^+ \rightarrow Cu^{2+} + OH^-$	37.1	-6.4	-

Table 6-6: Cuprite electrochemical hydrolysis reactions at 25°C

pH	Eh (V)
7.5	0.5128
6.5	0.5720
5.5	0.6312
4.5	0.6904

The cyclic voltammetric studies indicated that the chalcopyrite surfaces were not heavily oxidised after heavy chemical oxidation which corroborates the electrophoretic measurements, which is in accord with the general literature that chalcopyrite is not readily susceptible to oxidation.

Electrophoresis showed that both thermal and chemical heavy oxidation had a significant effect on the surface charge of the chalcopyrite surfaces, particularly at low pH values. Table 6-7 summarises the reported pH_{IEP} values for a number of chalcopyrite samples as a function of the degree of oxidation.

Table 6-7: Reported pH $_{IEP}$ values for chalcopyrite

Degree of oxidation	pH_{IEP}	Reference
None	-	Fullston et al, 1999
	- 1.8	Ney, 1973
	2.2	Kelebek and Smith, 1989
	3	Salatic et al, 1975
	3	McGlashen et al, 1969
Mild	-	Fullston et al, 1999
Heavy	6.6 / 8.5	Fullston et al, 1999

The zeta potential profile found for 'unoxidised' chalcopyrite under nitrogen varied from -30 mV at pH 5 to around -55 mV at pH 11, with a significant trough around pH 6.5 (Fullston *et al*, 1999). Samples conditioned with oxygen for 60 minutes, termed mildly oxidised, developed a zeta potential that was less negative than the 'unoxidised' case and moved the zeta potential profile up by about 20 mV. Moreover the trough had disappeared. Heavily oxidised samples, produced by conditioning with ~ $7x10^{-3}$M H_2O_2 for 60 minutes, showed substantially less negative surfaces and displayed a pH_{IEP} value of 6.6 or 8.5, depending upon the direction of the pH change during measurements.

The unoxidised zeta potential profile found in this research lay between those of the 'unoxidised' and mildly oxidised chalcopyrite samples reported by Fullston *et al* (1999), indicating that the chalcopyrite sample tested had experienced some mild degree of oxidation. Under the preparation conditions for the 'unoxidised' samples (i.e. conditioning at pH 11 for 20 minutes with nitrogen) reported by Fullston *et al* (1999), it was likely that many of the oxidation products were removed. In this study, the heavily thermally oxidised

samples were hydrolysed under effectively acidic conditions before pH adjustment to 6.5. Comparing the pH_{IEP} values for the thermally and chemically oxidised samples, a similar degree of oxidation was achieved for both of the heavily oxidised samples. However, in the case of the moderately oxidised samples, the pH_{IEP} value for thermal oxidation was higher than that for chemical oxidation and similar to that of the heavily thermally oxidised samples. These values were very similar to those reported by previous researchers for unoxidised samples and actually reflect the response of heavily oxidised surfaces (Salatic *et al*, 1975 and McGlashen *et al*, 1969).

Table 6-8 summarises pH_{IEP} values for selected copper 'oxide' mineral species and compounds. The values found for the oxidised chalcopyrite samples are significantly different and indicate that the surfaces were partly oxidised and thus only partially covered. Moreover, as noted for pH_{IEP} studies with iron 'oxide' species (refer to Section 6.3.1.3), more acidic values of pH_{IEP} were reported to be associated with 'oxide' species. The most likely copper species are Cu_2O and $Cu(OH)_2$, which corroborates the XPS analyses. The iron species would include FeO, FeO.OH and $Fe(OH)_3$.

Table 6-8: Reported pH_{IEP} values for copper species

Mineral/Species	Formula/Nature	pH_{IEP}
Cuprite	CuO	9.5 ± 0.4[a]
Tenorite	Cu_2O	6.9[b]
$Cu(OH)_2$	hydrous	7.6 - 9.4[a]
	fresh	7.7[b]
	aged	7.3[b]
Malachite	$CuCO_3.Cu(OH)_2$	7.6[b]
Chrysocolla	$(Cu,Al)_2H_2Si_2O_5(OH)_4 \cdot n(H_2O)$	6.5 - 6.7[b]

[a]Parks (1965)
[b]Gonzalez (1974)

6.2.2 Effect of sulfidisation

6.2.2.1 Flotation response

Chalcopyrite responded readily to sulfidisation and nearly complete restoration of the flotation recovery was observed at a sulfidisation potential of -650 mV in the presence of the other oxidised sulfide minerals. Below this sulfidisation potential, the flotation recovery was poorer while above this sulfidisation potential, the flotation recovery of the

sulfidised chalcopyrite fell away, although not as dramatically as the other sulfide minerals present in the oxidised Nkomati ore sample.

At an Es of -500 mV, as revealed by the XPS analysis, the hydrosulfide ions removed much of the obscuring iron oxidation products and exposed the underlying surface. This surface, which was either unoxidised or Fe-deficient chalcopyrite, may have played a role in the subsequent flotation. However the significant removal of the oxidised surface products by ultrasonic treatment did not restore floatability to the level found after sulfidisation. Consequently, it is argued that sulfidisation reactions rather than surface cleaning played the dominant role in restoring the flotation recovery of oxidised chalcopyrite.

The effect of the sulfidisation potential upon the flotation response of the sulfidised oxidised chalcopyrite was similar to that observed in the sulfidisation of base-metal 'oxide' minerals where a bell-shaped flotation response was reported (Jones and Woodcock, 1978b, 1979b and Fuerstenau *et al*, 1985). Below a sulfidisation potential of -650 mV, the flotation response was related to the extent of surface sulfidisation and the availability of hydrosulfide ions to adsorb and interact with the oxidised surfaces.

As well as adsorption and sulfidisation reactions with the oxidised sulfide mineral surfaces, there are a number of competing solution reactions involving the hydrosulfide ions such as catalytic oxidation and precipitation of cations. Since solution reactions proceed more rapidly than liquid–solid reactions, these reactions would exert a greater impact on the availability of reactants, particularly at lower hydrosulfide ion concentrations. This situation was compounded by the presence of other oxidised sulfide minerals such as pyrrhotite, which is ten times more abundant than chalcopyrite in Nkomati ores. Thus, although oxidised copper species would preferentially interact with hydrosulfide ion species, below a certain threshold concentration there would be insufficient quantity of hydrosulfide ions to completely sulfidise the oxidised chalcopyrite surfaces.

Once this threshold hydrosulfide ion concentration is achieved, such as that observed at an Es of -650 mV, there was sufficient sulfidising reagent to meet the demands of most reactions, particularly the adsorption and sulfidising needs of the oxidised sulfide minerals. Consequently, at this point an optimum flotation recovery was achieved. At hydrosulfide ion concentrations above this sulfidisation potential, the flotation recovery of the sulfidised

chalcopyrite was observed to fall away. This behaviour was due to the adsorption of hydrosulfide ions and hydrosulfide ion species which are retained on the sulfidised surfaces even after the solution had been decanted and the surfaces washed prior to flotation. These species competed with the collector and prevented adsorption, thus reducing floatability.

As the electrophoretic studies found, the oxidised chalcopyrite surfaces became more negatively charged with sulfidisation potentials greater than -700 mV, which is interpreted as the strong adsorption of hydrosulfide ions. In addition, it was likely that other hydrosulfide ion species are also adsorbed, since copper forms a large range of hydrosulfide and sulfide ion ligands, which are quite stable, especially for Cu(I) (Rickard and Luther, 2006).These include $[Cu(HS)_2]^-$ (pK = 17.2 to 18.0), $[Cu_2S(HS)_2]^{2-}$ (pK = 29.9), $[Cu_2S_3]^{2-}$ (pK = 38.3), $[Cu_2(S_4)_2]^{2-}$ (pK = 17.8) and $[Cu_2(S_5)_2]^{2-}$ (pK = 20.2). With higher sulfidisation potentials, where the concentration of hydrosulfide ions was higher, these species would form either in solution and adsorb onto the oxidised chalcopyrite surfaces or directly on the sulfidised surfaces. The presence of these adsorbed hydrosulfide species would also contribute to the depression of sulfidised chalcopyrite surfaces with xanthate collector.

Based on the analyses of the XPS data, the strongest sulfidisation interaction was found at an Es of -500 mV and the abundance of the surface sulfidisation products suggests that the sulfidised chalcopyrite would have floated very strongly. Thus it was concluded that the presence of other oxidised sulfide minerals has retarded the sulfidisation process for oxidised chalcopyrite primarily by limiting the availability of hydrosulfide ions to allow complete sulfidisation of the surface.

It was possible that the polysulfides/elemental sulfur made a contribution to flotation recovery of sulfidised chalcopyrite however, as the preliminary studies indicated, a high level of collector addition was required to fully recover the chalcopyrite after sulfidisation.

6.2.2.2 Sulfidisation mechanism

Voltammetric studies of oxidised chalcopyrite surfaces confirmed that the addition of hydrosulfide ions had regenerated the oxidised surfaces and produced a similar surface to that found for the unoxidised chalcopyrite. In the presence of hydrosulfide ions, the zeta

potential of the oxidised chalcopyrite surfaces decreased and was correlated with the adsorption of hydrosulfide ions as interpreted by other researchers (Fuerstenau *et al*, 1985).

Based on these changes, hydrosulfide ions continuously adsorbed onto the oxidised chalcopyrite surfaces between Es values of -450 mV and -600 mV. More substantial hydrosulfide ion adsorption was observed between -600 and -650 mV Es. Over the range of these sulfidisation potentials, XPS studies showed that copper sulfide species had formed on the oxidised surfaces and the best flotation recoveries were achieved. Strong hydrosulfide ion adsorption also took place at sulfidisation potentials above -700mV, where an increasingly poorer flotation response was observed.

Thus it is concluded that the first stage of the sulfidisation process involved the adsorption of hydrosulfide ions onto the oxidised chalcopyrite surfaces, where the adsorbed species then interacted with oxidised copper species exhibiting some degree of solubility to form copper sulfide phases.

Analyses of the XPS data showed that upon sulfidisation, the oxidised surfaces readily formed copper sulfide-like species as well as polysulfides and elemental sulfur. As a single mineral, the sulfidisation was most effective at an Es of -500 mV, where a considerable quantity of S^{2-} was found at the surface and was closely correlated with an increase in Cu(I) species. The amount of S^{2-} was significantly more than that necessary to account for the parallel increased exposure of the unoxidised chalcopyrite signal (Cpy-S). Cu(II) and S_2^{2-} were also present in smaller quantities. Noting that covellite (CuS) may also consist of Cu(I) and S_2^{2-} as Cu_2S_2 (Fleet, 2006 and Rickard and Luther, 2006), a predominantly chalcocite-like surface (Cu_2S: $Cu(I)_2S^{2-}$) was considered to have formed in conjunction with a covellite-like phase (CuS: $Cu(I)_2S_2^{2-}$ and $Cu(II)S^{2-}$).

At this sulfidisation potential, the lower Fe-O signal, the presence of $S_2^{2-}$and the detection of a Fe-S bond also indicates the formation of a pyrite-like phase. The mechanism for the formation of this phase is discussed under pyrrhotite sulfidisation mechanisms (Section 6.3.2.2).

A large quantity of polysulfides and/or elemental sulfur was also detected on the oxidised chalcopyrite surfaces at this sulfidisation potential. The chronoamperometric studies showed that hydrosulfide ions reacted strongly with heavily oxidised chalcopyrite surfaces

in a strong cathodic reaction. This was interpreted as the oxidation of the hydrosulfide ion to produce elemental sulfur (Buckley *et al*, 1988).

Compared to the XPS analysis of the hydrolysed oxidised chalcopyrite surfaces, the presence of a substantial chalcopyrite signal was found after sulfidisation. This indicates that there was significant removal of iron oxidation products, as reflected by a significantly lower Fe-O signal. This is a feature of sulfidising reagent solutions where the potential determining ions remove oxidation products from the sulfide mineral surfaces (Luttrell and Yoon, 1984).

Under the stronger sulfidisation potential of -650 mV, a similar array of species was present however in smaller quantities. The proportion of Cu(II) had significantly increased while that of the Cu(I) had substantially decreased. Both the S^{2-} and S_2^{2-} signals were reasonably strong however the quantities of polysulfides and elemental sulfur had diminished to pre-sulfidisation levels. A small exposure of unoxidised chalcopyrite was found and also accounts for a part of the S^{2-} and Cu(I) signals. Thus it was concluded that the copper sulfide entities consisted of mainly covellite (CuS: $Cu(II)S^{2-}$ and some $Cu(I)_2S_2^{2-}$) and a smaller quantity of chalcocite (Cu_2S: Cu(I) and S^{2-}).

Most researchers have postulated that covellite was formed on sulfidised copper 'oxide' surfaces (Wright and Prosser, 1965, Bustamante and Castro, 1975 and Zhou and Chander, 1993) however without supporting evidence. Figure 6-2 shows that the covellite domain is thermodynamically favoured under less basic and reducing conditions (Garrels and Christ, 1990).

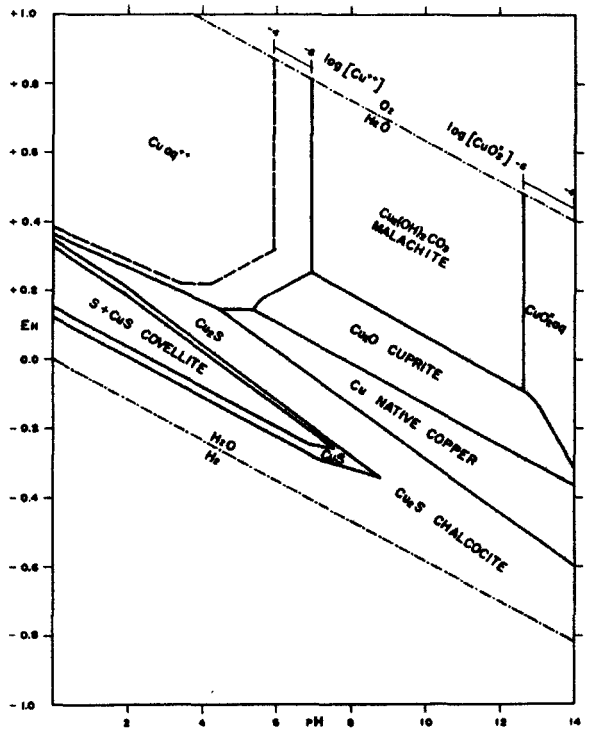

Figure 6-2: Copper sulfide species and copper 'oxide' minerals (total dissolved sulfur concentration of 10^{-1}M at 25°C) (after Garrels and Christ, 1990)

Based on Eh-pH diagrams developed by Zhang (1994), at low total sulfur concentrations (10^{-6}M) chalcocite is the dominant phase under the sulfidisation conditions at an Es of -500 mV. With increasing total sulfur concentration, the covellite domain expands and meets the chalcocite boundary at the sulfidisation conditions at an Es of -650 mV. With higher total sulfur concentrations and greater pH values, covellite continues to expand into the chalcocite domain (Garrels and Christ, 1990 and Zhang, 1994). The Eh-pH diagrams in Figure 6-3 show this relationship between the copper sulfide phases as a function of total dissolved sulfur concentration. In this research, a predominantly chalcocite-like stoichiometry was identified at a sulfidisation potential of -500 mV as well as a covellite-like phase while under more intense sulfidising conditions (Es of -650 mV), a covellite-like species had formed with lesser quantities of the chalcocite-phase.

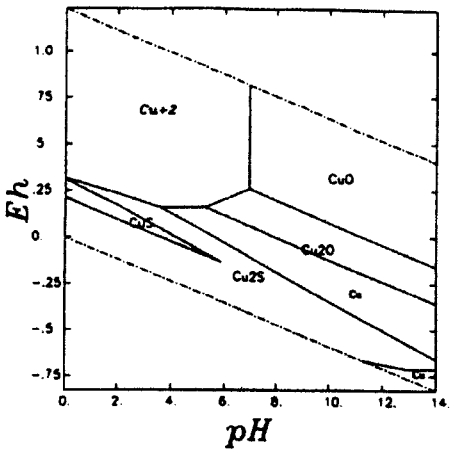

(a) 10^{-6}M (circa -600mV Es)

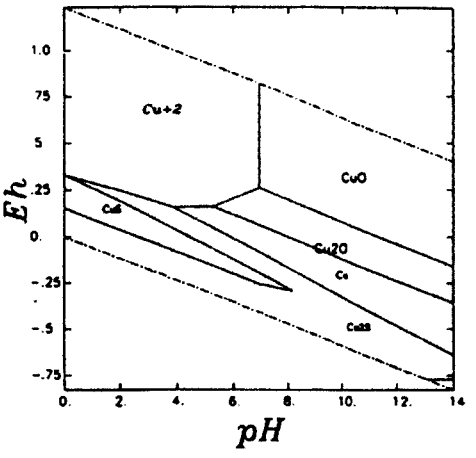

(b) 10^{-4}M (circa -700mV Es)

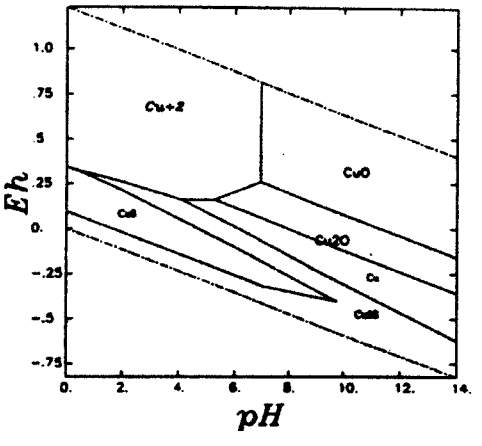

(c) 10^{-2} M (circa -800mV Es)

Figure 6-3: Growth of the covellite domain as a function of total dissolved sulfur concentration at 25°C (after Zhang,1994)

Before settling on the mechanism, a review of the thermodynamic nature of the potential sulfidisation reactions is warranted to confirm whether the proposed reactions would occur (refer to Table 6-9).

Table 6-9: Possible sulfidisation reactions for oxidised chalcopyrite at 25°C (after Roine, 2002)

Sulfidisation reactions	ΔG^o (kJ)	Log K	E^o (SHE,V)	Reaction No.
$2Cu^+ + HS^- \rightarrow Cu_2S + H^+$	-198.3	34.7	-	Cpy -1
$Cu_2O + HS^- \rightarrow Cu_2S + OH^-$	-107.7	18.9	-	Cpy -2
$2Cu(OH)_2 + HS^- + 2e^- \rightarrow Cu_2S + H_2O + 3OH^-$	-21.4	15.7	0.463	Cpy -3
$2CuO + 2HS^- + 2e^- \rightarrow Cu_2S + 2OH^- + S^{2-}$	-82.8	14.5	14.512	Cpy -4
$2CuS + H^+ + 2e^- \rightarrow Cu_2S + HS^-$	9.3	-6.9	-0.203	Cpy -5
$Cu_2O + 2HS^- \rightarrow 2CuS + H_2O + 2e^-$	-226.7	39.7	1.175	Cpy -6
$Cu^{2+} + HS^- \rightarrow CuS + H^+$	-134.2	23.5	-	Cpy -7
$Cu(OH)_2 + HS^- \rightarrow CuS + H_2O + OH^-$	-104.1	18.3	-	Cpy -8
$CuO + HS^- \rightarrow CuS + OH^-$	-97.9	17.2	-	Cpy -9
$2Cu^+ + S^{2-} \rightarrow Cu_2S$	-272.2	47.7	-	Cpy -10
$Cu_2O + S^{2-} + H_2O \rightarrow Cu_2S + 2OH^-$	-101.8	17.8	-	Cpy -11
$Cu^{2+} + S^{2-} \rightarrow CuS$	-208.1	36.5	-	Cpy -12
$Cu(OH)_2 + S^{2-} \rightarrow CuS + 2OH^-$	-98.2	17.2	-	Cpy -13
$CuO + S^{2-} + H_2O \rightarrow CuS + 2OH^-$	-91.9	16.1	-	Cpy -14

The potential sulfidisation reactions for oxidised chalcopyrite surfaces are dominated by chemical reactions and all of these chemical reactions are thermodynamically possible based on the Gibb's Free Energy function (ΔG^o). Moreover, many of the reactions have significant ΔG^o values coupled with large reaction constants. For completeness, the copper aqueous species and sulfide ion reactions have been included. Due to the abundance of the hydrosulfide ion compared to the sulfide ion under the sulfidisation conditions examined, the sulfide ions do not make a significant contribution to the sulfidisation mechanisms.

While three electrochemical reactions are possible based on ΔG^o values, only two have realistic potentials (refer to Table 6-10). Interestingly, the conversion of covellite into chalcocite (Cpy-5) is not energetically favourable. However, neither of the remaining two electrochemical reactions is feasible under the sulfidisation conditions that were employed. Thus the formation of chalcocite from the interaction of hydrosulfide ions with copper hydroxide species (Cpy-3) and the formation of covellite-like surfaces on Cu_2O with hydrosulfide ions (Cpy-6) would not occur.

Table 6-10: Calculated half-cell potentials for the electrochemical sulfidisation reactions chalcopyrite at 25°C (after Roine, 2002)

Es	Eh (V)	
(mV)	Cpy-3	Cpy-6
-800	0.7997	1.2792
-700	0.8648	1.3989
-650	0.8579	1.4500
-600	0.8565	1.4881
-500	0.8518	1.5489

Focusing on the chemical reactions presented in Table 6-9, the interaction between Cu_2O and hydrosulfide ions result in the formation of chalcocite (Cpy-2). Another source is Cu(II) ions, which would form chalcocite and precipitate onto the oxidised chalcopyrite surfaces (Cpy-1). On the other hand, two chemical reactions readily form covellite with hydrosulfide ions, namely $Cu(OH)_2$ and CuO (Cpy-8 and 9). Additionally, covellite precipitation would occur also due to the presence of Cu(II) ions in solution (Cpy-7).

In summary, the sulfidisation mechanisms initially involved the adsorption of hydrosulfide ions onto the oxidised chalcopyrite surfaces which consisted of copper oxide and hydroxide species. At a sulfidisation potential of -500 mV, the formation of chalcocite was dominant through the following interaction:

$$Cu_2O + HS^- \leftrightarrow Cu_2O.HS^-_{ads} \quad \text{.....(6-1)}$$

$$Cu_2O.HS^-_{ads} \rightarrow Cu_2S + OH^- \quad \text{.....(6-2)}$$

Covellite was formed through the following reactions :

$$Cu(OH)_2 + HS^- \leftrightarrow Cu(OH)_2.HS^-_{ads} \quad \text{.....(6-3)}$$

$$Cu(OH)_2.HS^-_{ads} \rightarrow CuS + OH^- + H_2O \quad \text{.....(6-4)}$$

$$CuO + HS^- \leftrightarrow CuO.HS^-_{ads} \quad \text{.....(6-5)}$$

$$CuO.HS^-_{ads} \rightarrow CuS + OH^- \quad \text{.....(6-6)}$$

Sulfidisation of the oxidised chalcopyrite samples was conducted under air and the formation of sulfur was assigned to the oxidation of hydrosulfide ion by dissolved oxygen, which is thermodynamically strongly favoured (HSO-1, refer to Table 6-11).

Table 6-11: Other reactions occurring during sulfidisation at 25°C (after Roine, 2002)

Other reactions	ΔG^o (kJ)	Log K	E^o (SHE,V)	Reaction No.
$HS^- \rightarrow S + H^+ + 2e^-$	-12.1	2.1	0.063	**HS -1**
$HS^- + 0.5O_2 \rightarrow S^o + OH^-$	-177.6	31.1	-	**HSO -1**

The small quantity of pyrite that was observed formed via reactions (6-7) to (6-12) as discussed in Section 6-3-2-2. Although the iron oxidation products were present in comparable amounts, the particularly strong affinity of copper for sulfur, as reflected by the copper sulfide solubility product values, has lead to the copper species dominating the sulfidisation mechanism.

Under more intense sulfidisation conditions (Es = -650mV), the same sulfidisation reactions occurred however, with Cu(II) in greater abundance, covellite would be formed in greater quantities than chalcocite. The lower surface abundances of the copper species, particularly Cu(I), at this higher sulfidisation potentials, was attributed to the formation of hydrosulfide and sulfide complexes. It is argued that in the presence of a higher concentration of hydrosulfide ions, surface dissolution occurred and the copper species were complexed into mainly solution species. These species include $Cu(HS)_2$, $[Cu_2(S_4)_2]^{2-}$,$[Cu_2(S_5)_2]^{2-}$ and particularly $Cu_2S_3^{2-}$ for the Cu(II) ion while for the Cu(I) ion they include Cu(HS), $[Cu(HS)_2]^-$, $[Cu_2S(HS)_2]^{2-}$, $[Cu(S_4)_2]^{3-}$ and $[Cu(S_4)(S_5)]^{3-}$ (Rickard and Luther, 2006). Most of these Cu(I) species have been identified exploring the solubility of Cu_2S.

6.2.2.3 Comparison with base-metal 'oxide' minerals

The sulfidisation potential at which the best flotation recovery was found for heavily thermally oxidised chalcopyrite in the presence of sulfide minerals was at an Es of -650 mV (-315 SHE) which is similar to that reported for the sulfidisation of malachite and other copper 'oxide' minerals (Jones and Woodcock, 1978b). They reported that the satisfactory sulfide ion electrode potential (SCE) range lay between -500 mV to -600 mV (-255 to -355 mV SHE).

However, as indicated by the XPS analyses, a sulfidisation potential less than these reported values would be expected since there was a lower requirement for sulfidisation. This arises due to the thin layer present on oxidised chalcopyrite surfaces compared to malachite, for example, where the entire mineral particle may become involved in

sulfidisation reactions. The sulfidisation reactions consequently reach deep into the malachite surfaces, consuming considerable quantities of hydrosulfide ions, which is reflected in higher sulfidisation potentials.

6.3 Pyrrhotite

6.3.1 Effect of oxidation

6.3.1.1 Flotation response

Before oxidation, pyrrhotite displayed the most sluggish flotation behaviour of the three sulfide minerals both in terms of natural floatability and collector-induced flotation. Nonetheless, nearly complete flotation was achieved after 10 minutes at a SIBX concentration of 1.375 x 10^{-4}M. This comparative flotation response was in agreement with that reported by other researchers (Kelebek, 1993 and Bradshaw *et al*, 1999).

Thermal oxidation had a significant impact on the flotation of pyrrhotite and the recovery fell away quickly with increasing oxidation until stabilising after 60 days to around 10%. Chemical oxidation with hydrogen peroxide had an even greater effect on the floatability of pyrrhotite and, based on flotation response, pyrrhotite was the most readily oxidised amongst the three sulfide minerals. After exposure to a 10^{-2}M H_2O_2 solution, the floatability of pyrrhotite was reduced to practically zero.

6.3.1.2 Oxidation characteristics

As the SEM images and EDX analyses of thermally oxidised Nkomati ore samples show, thermal oxidation formed a thick oxide layer consisting of mainly iron, sulfur and oxygen on the pyrrhotite particles. The layer developed quickly and with increasing exposure, the oxide layer became thicker and incorporated more oxygen and iron, thus confirming greater oxidation. The oxide layer grew in thickness from 400 nm to over 2 microns over the 121 days of thermal oxidation. No comparative data were available in the literature since previous studies on the oxidation of iron sulfide minerals were limited in terms of the extent of oxidation, which would be considered mild in the context of this research.

Table 6-12 summarises the potential oxidation reactions for pyrrhotite in air which are all thermodynamically possible. The formation of the oxidation products FeO, FeO.OH and

$FeSO_4$ are favoured and it was expected that the formation of hematite would be limited.

Table 6-12: Possible oxidation reactions for pyrrhotite at 85°C (after Roine, 2002)

Oxidation reaction	ΔG^o (kJ)	Log K
$FeS + 1.5O_{2(g)} \rightarrow FeO + SO_{2(g)}$	-440.1	64.2
$Fe_7S_8 + 11.5O_{2(g)} \rightarrow 7FeO + 8SO_{2(g)}$	-3345.3	308.0
$FeS + 2O_{2(g)} \rightarrow FeSO_4$	-701.9	102.4
$Fe_7S_8 + 15O_{2(g)} \rightarrow 7FeSO_4 + SO_{2(g)}$	-6065.8	308.0
$FeS + 1.75O_{2(g)} + 0.5H_2O_{(g)} \rightarrow FeO.OH + SO_{2(g)}$	-634.7	81.8
$Fe_7S_8 + 13.25O_{2(g)} + 3.5H_2O_{(g)} \rightarrow 7FeO.OH + 8SO_{2(g)}$	-4713.9	308.0
$2FeS + 3.5O_{2(g)} \rightarrow Fe_2O_3 + 2SO_{2(g)}$	-1121.9	163.6
$2Fe_7S_8 + 26.5O_{2(g)} \rightarrow 7Fe_2O_3 + 16SO_{2(g)}$	-8382.8	308.0

Chemical analysis of the oxide layers removed by ultrasonic treatment from oxidised Nkomati ore samples confirmed the preferential removal of iron onto the oxide layers as reported in the literature (Buckley and Woods, 1985a, Pratt *et al*, 1994, Mycroft *et al*, 1995 and Smart *et al*, 2003). Additionally, there was a significant sulfur presence in the oxidation product.

Some reactions are given in Table 6-13 for the interaction with hydrogen peroxide and pyrrhotite which all have an electrochemical nature. The dissolution of the pyrrhotite surfaces to form iron sulfate appears to be the most likely reaction.

Table 6-13: Possible reactions with hydrogen peroxide for pyrrhotite at 85°C (after Roine, 2002)

Reaction with H_2O_2	ΔGo (kJ)	Log K	Eo (SHE,V)
$8/3H_2O_2 + FeS \rightarrow Fe^{2+} + 4/3H_2O + SO_4^{2-} + 8/3H^+ + 8/3e^-$	-692.9	121.4	2.695
$2H_2O_2 + FeS \rightarrow FeSO_4 + 4H^+ + 4e^-$	-455.0	79.7	1.180
$4H_2O_2 + FeS \rightarrow Fe^{3+} + 4H_2O + SO_4^{2-} + e^-$	-1072.3	187.9	11.122

6.3.1.3 Aqueous exposure

Upon addition to water, the thermally oxidised Nkomati ore samples rapidly consumed hydroxyl ions, driving the pH down by 3.5 units, while iron and sulfate ions were found in solution. This supports the expectation that, under aqueous conditions, the oxidised pyrrhotite surfaces would be covered in base-metal hydroxides. For pyrrhotite, as shown in Figure 6-4, this was predominantly $Fe(OH)_3$, based on the $Fe/S/H_2O$ Pourbaix diagram (Garrels and Christ, 1990).

The heavily thermally oxidised Nkomati surface after hydrolysis could not be successfully analysed with XPS due to significant magnetic effects, which was also found with another sample that had been heavily chemically oxidised. Considering the XPS data for the other oxidised sulfide minerals, a hydrated Fe(III) oxy-hydroxide had formed based on the presence of iron oxy-species as well as the abundance of both hydroxyl and water on both the heavily oxidised pentlandite and chalcopyrite surfaces. This species has a significant magnetic character which explains the behaviour of the Nkomati samples under the strong magnetic field present during the XPS measurement (Cornell and Schwertmann, 1996 and Poulton *et al*, 2003). Since this behaviour was not observed after sulfidisation, the surface species had been transformed by reactions during sulfidisation. Hydrated Fe(III) oxy-hydroxides, such as ferrihydrite (generically $FeO.OH.nH_2O$), are reported to react readily with hydrosulfide ions (Poulton *et al*, 2003) and thus were likely to be the dominant species on the oxidised pyrrhotite surfaces. Iron oxides and ferric hydroxides are also probably present as secondary species.

The possible hydrolysis reactions for thermally oxidised pyrrhotite surfaces upon exposure to water are presented in Table 6-14. Of the reactions that are thermodynamically possible, two are chemical and three electrochemical.

Table 6-14: Possible hydrolysis reactions for oxidised pyrrhotite at 25°C (Roine, 2002)

Hydrolysis reaction	ΔG° (kJ)	Log K	E° (SHE,V)
$FeO + H_2O \rightarrow Fe(OH)_2$	-8.6	1.5	-
$FeO + H^+ \rightarrow Fe^{2+} + OH^-$	-3.1	0.5	-
$FeO + OH^- \rightarrow FeO.OH + e^-$	-86.2	15.1	0.894
$FeO + H_2O \rightarrow FeO.OH + H^+ + e^-$	-6.4	1.1	0.066
$FeO.OH + H^+ + e^- \rightarrow Fe(OH)_2$	-2.2	0.4	0.023
$Fe_2O_3 + H^+ + 2H_2O + 2e^- \rightarrow 2Fe(OH)_2 + OH^-$	75.1	-13.2	-0.389
$FeO.OH + H_2O + e^- \rightarrow Fe(OH)_2 + OH^-$	77.6	-13.6	-0.805
$Fe_2O_3 + H^+ + 2e^- \rightarrow 2FeO + OH^-$	92.3	-16.2	-0.479

The half-cell potentials for three electrochemical reactions are presented for the conditions measured during the hydrolysis of the heavily thermally oxidised Nkomati ore samples (refer to Table 6-15). None of the three electrochemical reactions appear to play a role in the hydrolysis of thermally oxidised pyrrhotite surfaces.

Table 6-15: Electrochemical hydrolysis reactions for oxidised pyrrhotite at 25°C

Electrochemical hydrolysis reactions	Eh (SHE,mV)			
	pH			
	4.5	5.5	6.5	7.5
Oxidised Nkomati ore	-0.020	-0.099	-0.154	-0.196
$FeO + OH^- \rightarrow FeO.OH + e^-$	1.4564	1.3972	1.3380	1.2788
$FeO + H_2O \rightarrow FeO.OH + H^+ + e^-$	-0.2004	-0.2596	-0.3188	-0.3780
$FeO.OH + H^+ + e^- \rightarrow Fe(OH)_2$	0.2894	0.3486	0.4078	0.4670

It is concluded that the two chemical reactions are the primary hydrolytic reactions and the formation of iron hydroxide as well as the release of Fe(II) ions into solution are expected. The presence of iron was observed in solution after the hydrolysis of Nkomati ore samples and the rapid fall of the pH during hydrolysis also corroborates these reactions.

Prior to oxidation, the pH_{IEP} value for pyrrhotite was 2.0 and the same as that reported by Ney (1973). As the pyrrhotite samples became more oxidised, subsequent aqueous exposure increased the pH_{IEP}, revealing surfaces of increasingly greater oxide/hydroxide character as reported by Parks (1965).

The pH_{IEP} is influenced by several factors and Parks (1965) reported the following observations concerning pH_{IEP} shifts:

(1) becomes more acidic with increased oxidation state of the metal e.g. Fe(II) to Fe(III)
(2) substitution of O^{2-} by water or hydroxyl groups leads to more basic values i.e. hydration causes an increase while dehydration results in a decrease
(3) impurities have a significant effect – structural or adsorbed anions make the pH_{IEP} more acidic while structural or adsorbed cations cause the pH_{IEP} to become more basic
(4) the nature of the species – whether crystalline, amorphous, non-stoichiometry, semi-conductive properties and structural defects

The reported pH_{IEP} values for various iron oxide and oxy-hydroxide species are summarised in Table 6-16. Based on the above comments, the acidic nature of the pH_{IEP} values found for the heavily oxidised pyrrhotite samples indicates that the surfaces would consist of Fe(III) rather than Fe(II) species, be not heavily hydrated and possibly have either structural or adsorbed cations. The pH_{IEP} values found for heavily oxidised pyrrhotite samples reflect those reported for natural goethite. Moreover, goethite is an excellent adsorbent (Cornell and Schwertmann, 1996) and the adsorption of cations or

anions (e.g. sulfate ions) from solution would affect the value of the pH_{IEP} (Parks, 1965).

Table 6-16: pH_{IEP} values for iron oxide/oxy-hydoxide species (mainly after Parks, 1965)

Mineral / Species	**Nature**	**pH_{IEP}**	
		range	**mode**
Magnetite	natural	6.5 ± 0.2	
(Fe_3O_4)	synthetic	6.5 ± 0.2	
Hematite	hydrous	4.3 - 8.6	~ 7.2
(Fe_2O_3)	+ 0.3 mole% SO_4^{2-}	ΔpH_{IEP}	-1.6
αFe_2O_3	natural	4.2 - 6.9	~ 6.7
	synthetic	6.1 - 9.0	~ 8.7
		7.2 -8.5[a]	
γFe_2O_3	synthetic	6.7 ± 0.2	
Geothite	natural	3.2	
(αFeO.OH)	synthetic	4.2 - 7.2	~ 6.7
(βFeO.OH)		6.5[b]	
Lepidocrocite	natural	7.4 ± 0.2	
(γFeO.OH)	synthetic	5.3 - 7.3	~ 5.4
'$Fe(OH)_2$'	amorphous	8.5	

[a] Fokkink, 1987
[b] Rubio and Matijevic, 1979

Based on the Fe/S/H_2O Pourbaix diagram presented in Figure 6-4, the equilibrium phases in contact with pyrrhotite surfaces are predominantly Fe(II) ions and $Fe(OH)_3$, depending upon pH. For oxidised pyrrhotite surfaces, this diagram indicates that after hydrolysis, mainly SO_4^{2-} and Fe(II) ions would be in solution.

Chemical oxidation did not produce thick oxidation layers which were probably less than 100 nm thick. The solution reaction products after chemical oxidation indicated that a similar array (Cu, Fe, Ni and SO_4^{2-}) was produced as found after hydrolysis of the thermally oxidised samples. The cyclic voltammetric studies confirmed that the heavy chemical oxidation of pyrrhotite surfaces, like that produced with heavy thermal oxidation, produced an unreactive surface.

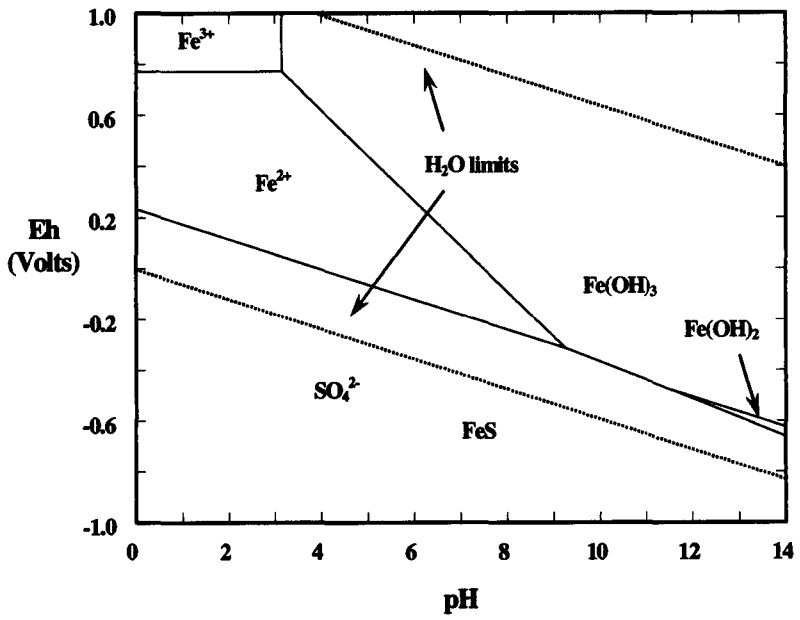

Figure 6-4: Fe-S-H_2O Eh-pH diagram at 25°C (after Roine, 2002)

6.3.2 Effect of sulfidisation

6.3.2.1 Flotation response

The pyrrhotite in the oxidised Nkomati ore sample responded well to sulfidisation and the best flotation recovery occurred at a sulfidisation potential of -650 mV. The flotation recovery of pyrrhotite at this sulfidisation potential lay between that of chalcopyrite and pentlandite.

Like the flotation response of oxidised chalcopyrite after sulfidisation, the flotation behaviour of sulfidised pyrrhotite as a function of sulfidisation potential was characterised by a bell-shape. The flotation recovery of oxidised pyrrhotite increased with increasing sulfidisation potential until the optimum value was achieved at a potential of -650 mV Es. This corresponded to the strong adsorption of hydrosulfide ions onto the pyrrhotite and Nkomati ore mineral surfaces over the sulfidisation range -600 to -650 mV Es. After this sulfidisation potential, lower flotation recoveries were found indicating some degree of depression, particularly after a sulfidisation potential of -700 mV Es, where the strong adsorption of hydrosulfide ions occurred.

The same mechanisms are operating to cause this flotation response as outlined for oxidised chalcopyrite. At values less than -650 mV (-335 mV SHE), the hydrosulfide ion

concentration required to form significant quantities of base-metal sulfides either directly at the mineral surface or from precipitation had not been reached and the flotation recovery was incomplete. Above this sulfide ion electrode potential, the surfaces of oxidised pyrrhotite strongly adsorbed hydrosulfide ions. Hydrosulfide ions are known to compete with the collector and increasing levels of adsorbed hydrosulfide ions begin to have a depressant effect on the sulfidised pyrrhotite surfaces. In addition, the formation of iron hydrosulfide ion complexes occurs as the hydrosulfide ion concentration increases. The metastable species $Fe(HS)^+$ forms readily above pH 7 (log K between 4.34 to 5.94) as do a number of other iron polysulfide species (Rickard and Luther, 2006). In spite of solution decantation and sample washing before micro-flotation, it was likely that the freshly formed sulfide surfaces retained some of the adsorbed hydrosulfide ion and ligand species. These adsorbed species hindered the adsorption of xanthate ions which subsequently decreased the flotation recovery. It was expected that the formation of these iron based hydrosulfide ligands involved the dissolution of the iron sulfide surface species, which would also have had some impact on the flotation recovery by decreasing the sulfide surface area available for interaction with the collector.

The presence of calcium ions during sulfidisation had no impact on the flotation recoveries of heavily thermally oxidised Nkomati ore samples and the individual sulfide minerals. The major reaction would have been the formation of CaS, which is soluble in water and has been used on an industrial scale to successfully sulfidise copper 'oxide' ores (Zhang, 1993).

6.3.2.2 Sulfidisation mechanism

The hydrosulfide ion is the most dominant solution species during sulfidisation and is considered to be the active species in the sulfidisation of base-metal 'oxide' minerals (Wright and Prosser, 1965 and Bustamante and Castro, 1975). It is thus considered to be the dominant sulfur species in any interaction with the oxidised sulfide mineral surfaces.

The electrophoretic testwork showed that the first stage of sulfidisation involved the strong adsorption of hydrosulfide ions before the onset of significant flotation as reported for the sulfidisation of base-metal 'oxide' minerals (Fuerstenau *et al*, 1985). Based on the sharp decrease in the zeta potential values, the oxidised surfaces of pyrrhotite strongly adsorbed hydrosulfide ions over the sulfidisation potential range of -550 mV to -650 mV. Both the

oxidised surfaces of pyrrhotite and Nkomati ore sample strongly adsorbed hydrosulfide ions at similar Es values (circa -550 mV), based on the sharp decrease in the zeta potential values. Analysis of the adsorption data indicated that the hydrosulfide ion was physically adsorbed and that increased adsorption occurred, as indicated by the electrophoretic studies, before a sulfide-like surface formed that strongly promoted a flotation response.

The XPS analysis of the sulfidised Nkomati surfaces basically reflected the surfaces of pyrrhotite. With an increase in the sulfidisation potential to -650 mV from -500 mV, there was a decrease in the abundance of hydroxyl species as well as the Fe-O signal. Both S^{2-} and S_2^{2-} were identified and their abundances followed opposite trends with increased sulfidisation potential. The disulfide ions halved in abundance while the amount of monosulfide ions doubled. Similar levels of Fe-S bonding were noted under both sulfidisation potentials. Since the S_2^{2-} signal is a feature of pyrite, it indicated that a pyrite-like species had formed while the Fe-S signal reflected the presence of a pyrrhotite-like phase. Under the conditions of sulfidisation at an Es of -650 mV (-0.3V SHE/pH 8), pyrite is thermodynamically favoured over pyrrhotite while under more reducing conditions, pyrrhotite is the dominant phase (Zhang, 1994 and Garrels and Christ, 1990) (refer to Figure 6-5). In high sulfidising reagent concentrations, cyclic voltammetric studies corroborated that an identical surface had been regenerated after sulfidisation to that of the unoxidised pyrrhotite surface.

After sulfidisation in the presence of air at an Es of -650 mV, both FeS and FeS_2 were identified on the sample surface, the later being twice as abundant. The presence of dissolved oxygen during sulfidisation had thus caused more pyrite to form, as anticipated in the literature (Berner, 1970). However, this may also arise due to the oxidation of the hydrosulfide ion, whereby the resulting polysulfide ions promoted the formation of pyrite from pyrrhotite (Schoonen and Barnes, 1991 and Wei and Osseo-Asare, 1995).

Elemental sulfur/polysulfides were found although their role in any subsequent flotation has not been determined. Glazunov *et al* (1993) proposed the formation of elemental sulfur during the sulfidisation of chrysocolla, contributing to the subsequent hydrophobicity.

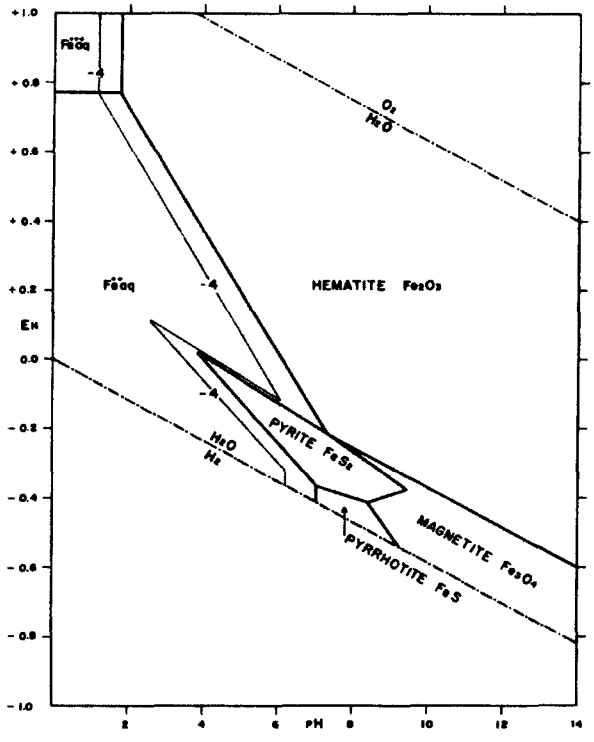

Figure 6-5: Stability domains for iron sulfide species (total dissolved sulfur concentration of 10^{-6}M at 25°C) (after Garrels and Christ, 1990)

As noted for the sulfidisation of oxidised chalcopyrite, the presence of elemental sulfide/ polysulfides on the sulfidised surfaces was considered to arise from electrochemical reactions elucidated by Buckley *et al* (1988). They reported that elemental sulfur and most likely polysulfides were preferentially deposited onto pyrite under aerated conditions. The proposed mechanism involved the anodic oxidation of the hydrosulfide ion to a polysulfide species coupled with the simultaneous cathodic reduction of dissolved oxygen.

Moreover, the amount of S_n/S^o increased significantly under the more intense sulfidisation conditions which was corroborated with results of the chronoamperometric testwork with heavily oxidised pyrrhotite surfaces. As for oxidised chalcopyrite, this was interpreted as an electrochemical cathodic reaction as presented in Table 6-11.

Table 6-17 summarises the possible sulfidisation reactions for oxidised pyrrhotite and only three are chemical (Po-2, Po-3 and Po-4). These reactions show that the interaction between hydrosulfide ions and the iron species iron hydroxide and FeO.OH would form pyrrhotite. Moreover, noting that pyrrhotite is considered the precursor to pyrite formation (Rickard, 1969 and Berner, 1970) a chemical route was also indicated for the formation of a pyrite from pyrrhotite (reaction Po-1 (Wei and Osseo-Asare, 1995)). Based on the

thermodynamics for this equation, the pyrrhotite would interact readily with elemental sulfur/polysulfides formed by the oxidation of hydrosulfide ions to form pyrite.

Table 6-17: Possible sulfidisation reactions for oxidised pyrrhotite at 25°C (after Roine, 2002)

Sulfidisation reaction	ΔG° (kJ)	Log K	E° (SHE,V)	Equation No.
$FeS + S^0 \rightarrow FeS_2$	-56.9	10.0	-	**Po-1**
$FeO + HS^- \rightarrow FeS + OH^-$	-25.6	4.5	-	**Po-2**
$Fe^{2+} + HS^- \rightarrow FeS + H^+$	-22.5	3.9	-	**Po-3**
$Fe(OH)_2 + HS^- \rightarrow FeS + OH^- + H_2O$	-17.2	3.1	-	**Po-4**
$FeO + 2HS^- \rightarrow FeS_2 + H_2O + 2e^-$	-174.4	30.6	0.904	**Po-5**
$Fe^{3+} + 2HS^- \rightarrow FeS_2 + 2H^+ + e^-$	-165.8	29.1	1.720	**Po-6**
$FeO.OH + 2HS^- \rightarrow FeS_2 + OH^- + H_2O + e^-$	-88.2	15.4	0.915	**Po-7**
$FeS + HS^- \rightarrow FeS_2 + H^+ + 2e^-$	-68.9	12.1	0.358	**Po-8**
$Fe^{3+} + 2S^{2-} \rightarrow FeS_2 + e^-$	-313.6	54.9	3.252	**Po-9**
$Fe^{2+} + 2S^{2-} \rightarrow FeS_2 + 2e^-$	-239.2	41.9	1.241	**Po-10**
$Fe(OH)_2 + 2S^{2-} \rightarrow FeS_2 + 2OH^- + 2e^-$	-153.9	27.0	0.798	**Po-11**
$Fe(OH)_3 + 2HS^- + H^+ \rightarrow FeS_2 + 3H_2O + e^-$	-185.4	32.5	1.923	**Po-12**
$FeO.OH + 2S^{2-} + H_2O \rightarrow FeS_2 + 3OH^- + e^-$	-76.3	13.4	0.791	**Po-13**
$FeS + S^{2-} \rightarrow FeS_2 + 2e^-$	-142.8	25.0	0.741	**Po-14**
$FeO.OH + HS^- + e^- \rightarrow FeS + 2OH^-$	60.6	-10.6	-0.629	**Po-15**
$FeO.OH + 2HS^- \rightarrow Fe^{2+} + S^0 + S^{2-} + H_2O + OH^- + e^-$	65.1	-11.4	-0.675	**Po-16**
$FeO.OH + HS^- \rightarrow Fe^{2+} + S^0 + 2OH^- + e^-$	71.1	-12.5	-0.737	**Po-17**
$FeO.OH + S^{2-} + H_2O \rightarrow Fe^{2+} + S^0 + 3OH^- + e^-$	77.0	-13.5	-0.799	**Po-18**
$FeO.OH + S^{2-} + H_2O + e^- \rightarrow FeS + 3OH^-$	66.6	-11.7	-0.691	**Po-19**
$2FeO.OH + HS^- + H_2O \rightarrow 2Fe^{2+} + S^0 + H_2O + 5OH^-$	234.0	-41.0	-	**Po-20**
$8FeO.OH + HS^- + 3H_2O \rightarrow 8Fe^{2+} + SO_4^{2-} + H_2O + 15OH^-$	777.3	-136.2	-	**Po-21**

The electrochemical sulfidisation reactions are evaluated under the conditions present during sulfidisation (Table 6-18). Interestingly, the widely reported interactions between FeO.OH and the sulfur species (e.g. Peiffer *et al*, 1992: reactions Po-20 and 21 and Poulton *et al*, 2003: reactions Po-15 to 17) are not thermodynamically possible. Although FeO.OH was used as a proxy for ferrihydrite (specifically reactions Po-15 to 17) and does not reflect the exact formula, similar thermodynamic outcomes would be expected. Several reactions involving the direct formation of pyrite have been investigated and only the interaction between FeO.OH and sulfide ions appears to offer any possibility. While the half-cell potential of this reaction is not the same value as the equivalent potentials calculated during sulfidisation, this reaction may partially occur at -500mV Es, although

the low sulfide ion concentration would limit the extent of the reaction.

Overall, it is concluded that electrochemical reactions do not play a major role in the sulfidisation of oxidised pyrrhotite surfaces.

Table 6-18: Electrochemical sulfidisation reactions for oxidised pyrrhotite at 25°C (after Roine, 2002)

Electrochemical sulfidisation reaction	Cell half-potential (Eh, V)					Equation No.
	Sulfidisation potential (Es, mV)					
	-500	-600	-650	-700	-800	
$FeO + 2HS^- \rightarrow FeS_2 + H_2O + 2e^-$	1.2791	1.2182	1.1799	1.1287	1.0085	Po-4
$Fe^{3+} + 2HS^- \rightarrow FeS_2 + 2H^+ + e^-$	1.9363	1.7800	1.6798	1.5525	1.1453	Po-5
$FeO.OH + 2HS^- \rightarrow FeS_2 + OH^- + H_2O + e^-$	1.2810	1.1763	1.1116	1.0216	0.8648	Po-6
$FeS + HS^- \rightarrow FeS_2 + H^+ + 2e^-$	0.3233	0.2842	0.2591	0.2273	0.1255	Po-7
$Fe^{3+} + 2S^{2-} \rightarrow FeS_2 + e^-$	4.2848	4.2066	4.1565	4.0929	3.8866	Po-8
$Fe^{2+} + 2S^{2-} \rightarrow FeS_2 + 2e^-$	0.3680	0.4461	0.4962	0.5599	0.7662	Po-9
$Fe(OH)_2 + 2S^{2-} \rightarrow FeS_2 + 2OH^- + 2e^-$	1.1092	1.0482	1.0100	0.9587	0.8359	Po-10
$FeO.OH + 2S^{2-} + H_2O \rightarrow FeS_2 + 3OH^- + e^-$	-0.3046	-0.4609	-0.5611	-0.6884	-1.0976	Po-11
$Fe(OH)_3 + 2HS^- + H^+ \rightarrow FeS_2 + 3H_2O + e^-$	3.1138	3.0094	2.9449	2.8552	2.6990	Po-12
$FeS + S^{2-} \rightarrow FeS_2 + 2e^-$	1.4364	1.3583	1.3082	1.2445	1.0382	Po-13
Es (mV)	-500	-600	-650	-700	-800	-
Equivalent Eh (SHE,V)	-0.165	-0.265	-0.315	-0.365	-0.465	-

Based on both the thermodynamic and electrochemical evaluations, only two surface species played a role in the sulfidisation reactions, namely ferric hydroxide and FeO. While both pyrite-like and pyrrhotite-like phases were found under the two sulfidising conditions, under less intense sulfidisation conditions, the pyrrhotite-like species were in greater abundance whereas at higher sulfidisation potentials, the pyrite-like phase was more dominant.

Based on the electrophoretic studies, the first stage involved the strong adsorption of hydrosulfide ions by the surface species and the formation of FeS:

$$FeO + HS^- \leftrightarrow FeO.HS^-_{ads} \quad \text{.....(6-7)}$$

$$FeO.HS^-_{ads} \rightarrow FeS + OH^- \quad \text{.....(6-8)}$$

$$Fe(OH)_2 + HS^- \rightarrow Fe(OH)_2.HS^-_{ads} \quad \text{.....(6-9)}$$

$$Fe(OH)_2.HS^-_{ads} \rightarrow FeS + OH^- + H_2O \quad \text{.....(6-10)}$$

Due to oxidation, the hydrosulfide ion supplied sulfur to the oxidised pyrrhotite surfaces which then reacted with the freshly formed pyrrhotite to form pyrite:

$$FeS + S^o \leftrightarrow FeS_2 \quad \text{.....(6-11)}$$

The iron oxide phases also provided a source of Fe(II) ions and precipitation reactions also played an important role during the sulfidisation of oxidised pyrrhotite as observed by Poulton *et al* (2003):

$$Fe^{2+} + HS^- \rightarrow FeS_{ppt} + H^+ \quad \text{.....(6-12)}$$

Both surface reactions and precipitation reactions are responsible for the formation of pyrrhotite at the lower sulfidisation potentials, however at the higher sulfidisation potentials, surface reactions would be responsible for a greater proportion due to the increased chemical potential with greater concentrations of hydrosulfide ions. At these higher concentrations, more elemental sulfur would be expected to be produced as shown in the chronoamperometric studies and thus the opportunity for more pyrite formation. When the sulfidisation was conducted under air, significantly more sulfur and pyrite were found, corroborating this mechanism.

The proposed sulfidisation mechanisms for oxidised pyrrhotite do find support in the literature, where pyrite is thermodynamically favoured over pyrrhotite under less intense sulfidising conditions and pyrrhotite dominates under more reducing conditions (Garrels and Christ, 1990).

The XPS analyses of the sulfidised oxidised Nkomati ore samples failed to identify any nickel species on the surfaces however the presence of copper in both the Cu(II) and Cu(I) forms was readily detected, although it could not be fully quantified. The proportion of Cu(I) increased markedly with more intense sulfidising conditions and is the product of the reductive conditions as observed during the sulfidisation of heterogeneite where the Co^{3+} was reduced to Co^{2+} (Bastin, *pers comm*). The reduction of Cu(II) to Cu(I) would provide an additional electronic sink for any cathodic reaction that occurred, such as the oxidation of hydrosulfide ions.

6.3.2.3 Comparison with base-metal 'oxide' minerals

The adsorption of the hydrosulfide ion on heavily thermally oxidised Nkomati ore samples

over the concentration range 10^{-3} to 10^{-5}M was described by the relationship $[HS^-] = at^{1/n}$, where a and 1/n varied from 1 x10^{-4} to 4 x10^{-4} and -0.9 to -2.1 respectively. As reported for the sulfidisation of base-metal 'oxide' minerals as well as in the precipitation of base-metal ions by sulfide species, this reaction occurred quickly and continued consumption of HS^- after the first thirty seconds indicates on-going reactions due to diffusion from within the oxide layer (Wright and Prosser, 1965 and Zhou and Chander, 1993). The Langmuir plot of this adsorption data suggested a ΔG_{ads} of -7.9 kJ/mole, which is typical of physisorption.

Adsorption studies using radio-actively labelled Na_2S with base-metal 'oxide' minerals found similar results, however many orders of magnitude higher (Mitrofanov, 1958 and Mitrofanov *et al*, 1955b and 1957). A general adsorption relationship Γ_S (mg/g) = $at^{1/n}$ was found, where 1/n varied between 0.1 and 1 (0.5 for malachite). Γ_S was typically less than 20 mg/g whereas for the heavily thermally oxidised Nkomati ore samples it was around 0.01 mg/g for the same time scale.

The flotation behaviour of oxidised pyrrhotite after sulfidisation showed similarities with that found for sulfidised oxidised chalcopyrite, and by association, to that reported for the sulfidisation of the copper 'oxide' minerals, particularly malachite. The successful sulfidisation and flotation of goethite has been reported, however the conditions are not known (Mitrofanov *et al*, 1957). It can be concluded that the response of oxidised pyrrhotite to sulfidisation appears to share similarities with that of base-metal 'oxide' minerals however with significantly less sulfidising reagent consumed.

6.4 Pentlandite

6.4.1 Background

Oxidised pentlandite as a single mineral responded very poorly to sulfidisation, yet in the presence of other oxidised sulfide minerals in the Nkomati sample, satisfactory flotation recoveries were achieved. This was corroborated with electrochemical studies and by XPS analysis. This unresponsive behaviour to sulfidisation as a single mineral was unexpected and required further investigation. The following key question arose: what is the nature of the mechanism whereby oxidised pentlandite became sulfidised in the presence of other oxidised sulfide minerals?

Based on the literature describing the reactions of ferric oxy-hydroxides species with hydrosulfide ions, it was hypothesised that the oxidised pentlandite surfaces had become sulfidised through the precipitation of base-metal sulfides. The source of the base-metal ions arose from the dissolution of the surfaces of the other oxidised sulfide minerals, principally pyrrhotite. A series of experiments was conducted to address this hypothesis and answer the key question concerning the sulfidisation mechanism. Testwork was undertaken employing the quantities of copper and iron ions during sulfidisation that were expected to be available as determined by EDTA extraction from the Nkomati ore surfaces. The formation of the base-metal sulfide precipitates could occur through two mechanisms: the conversion of surface base-metal hydroxides or direct formation on the oxidised pentlandite surfaces.

6.4.2 Effect of oxidation

6.4.2.1 Flotation response

The flotation behaviour of thermally oxidised pentlandite in the Nkomati ore sample was very similar to that observed for oxidised pyrrhotite. Even after ultrasonic treatment and conditioning with high collector strength, the flotation recovery deteriorated significantly with increased oxidation. After 60 days, the flotation response had reached a plateau and did not decrease any further.

Chemical oxidation also had a significant impact on the flotation response of pentlandite. Unlike thermal oxidation, however, the effect was not as great as that found with pyrrhotite.

6.4.2.2 Oxidation characteristics

The SEM/EDX studies showed that with increasing thermal oxidation thick layers of oxidation product formed on the surfaces of pentlandite particles. The thicknesses of the layers were similar to that identified for pyrrhotite and like the other two oxidised sulfide minerals, the oxidised layers showed an increasing content of iron and sulfur with greater oxidation.

The reactions of pentlandite with air were reported to produce iron oxides, nickel oxides/sulfates and iron deficient nickel sulfides, perhaps violarite (Buckley and Woods,

1991 and Richardson and Vaughan, 1992). Thermodynamic data for nickel species, particularly pentlandite and violarite, are limited and the results of calculations for the array of reactions presented for the other sulfide minerals are not possible. However, using the ΔG_f° data calculated for pentlandite and violarite by Warner *et al* (1996) with the HSC database (Roine, 2002) (refer to Table 6-19), the ΔG values for the most likely oxidation reactions are presented in Table 6-20.

Table 6-19: Thermodynamic data for species involved in pentlandite oxidation reactions at 25°C

Species	ΔGf° (kJ/mole)	Source
$O_{2(g)}$	-61.165	HSC (Roine, 2002)
$H_2O_{(g)}$	-298.126	HSC (Roine, 2002)
$SO_{2(g)}$	-370.82	HSC (Roine, 2002)
FeO	-284.44	HSC (Roine, 2002)
NiO	-251.052	HSC (Roine, 2002)
	-211.6	Warner *et al* (1996)
FeO.OH	-578.008	HSC (Roine, 2002)
	-488.0	Warner *et al* (1996)
$NiSO_4$	-903.109	HSC (Roine, 2002)
$FeNi_2S_4$	-346	Warner *et al* (1996)
$(Fe,Ni)_9S_8$	-813	Warner *et al* (1996)

Table 6-20: Selected pentlandite oxidation reactions in air at 25°C (after Roine, 2002)

Selected oxidation reactions	ΔG° (kJ)
$(Fe,Ni)_9S_8 + 25/2\ O_{2(g)} \rightarrow 4.5FeO + 4.5\ NiO + 8SO_{2(g)}$	-3798.7
$(Fe,Ni)_9S_8 + 7\ O_{2(g)} \rightarrow 3.5FeO + 2.5\ NiO + 4SO_{2(g)} + FeNi_2S_4$	-2211.3
$(Fe,Ni)_9S_8 + 33/2\ O_{2(g)} + 14/4\ H_2O_{(g)} \rightarrow$ $3.5FeO.OH + 2.5NiSO_4 + 1.5SO_{2(g)} + FeNi_2S_4$	-1289.9

The chemical reactions of pentlandite under acidic conditions were reported to produce iron oxides, nickel oxides/sulfates and violarite (Warner *et al*, 1996).

6.4.2.3 Aqueous exposure

Before oxidation, the pH_{IEP} of the unoxidised pentlandite was 2.0, which is similar to that reported for a synthetic millerite (NiS) sample of 2.5-3.0 (Healy and Moignard, 1976).

With thermal oxidation, unlike the other two sulfide minerals, there was unexpected difference between the two degrees of oxidation. For pH values above 6, the moderately oxidised sample had a significantly more positive surface than the heavily oxidised sample. This suggests that there were two reaction mechanisms for pentlandite producing different proportions of oxidation products and may account for the sudden fall in the flotation recoveries observed around the 50 day mark. Based on the pH_{IEP} values for thermally oxidised pentlandite samples, the pentlandite surfaces were the most heavily oxidised of all the sulfide minerals.

While chemical oxidation had a significant impact on the pH_{IEP} values, they were not as high as the values found for the thermally oxidised samples. Additionally, a graduation in pH_{IEP} values that increased with increasing levels of oxidation.

Although the electrophoretic studies indicate a significant change in the nature of the pentlandite surface and provide a clear distinction between both type and degree of oxidation for pentlandite, any interpretation was limited by the available literature. The pH_{IEP} values do not indicate that the heavily oxidised surfaces were covered in nickel hydroxide nor nickel oxide based on reported measurements (refer to Table 6-21).

Table 6-21: pH_{IEP} of selected nickel species (after Parks, 1965)

Species	pH_{IEP}
NiO	10.3 ± 0.4
$Ni(OH)_2$	11.1 ± 0.4

The cyclic voltammetric study confirmed that heavy chemical oxidation produced an unreactive surface. Based on SEM analysis, the oxidation layer was quite thin compared the thermally oxidised layers and less than 100 nm.

The XPS analysis showed that the base-metals on the oxidised pentlandite surface after contact with water appeared mainly as hydroxides and oxides, possibly oxy-hydroxides, noting the considerable amount of hydroxyl groups bound to the surface. The presence of water indicated that the hydroxides were hydrated, with Fe-O generally more abundant than Ni-O. Based on the absence of a magnetic response during XPS analysis (refer to comments for the Nkomati ore samples – Section 6.3.1.3), a Fe(III) oxy-hydroxide species was not produced in any significant quantity. Moreover, the lack of any significant sulfidisation response also confirmed that iron oxide species amenable to sulfidisation

were not present on the oxidised pentlandite surfaces. As far as sulfidisation interactions are concerned, the surface was effectively inert. Thus, for the development of the sulfidisation reactions in Section 6.4.2.2, the oxidised pentlandite surface is interpreted as consisting of NiO.OH, the nickel analogue of goethite.

Figure 6-6 presents an Eh-pH diagram for pentlandite which offers some insight into the species that may be present after the chemical oxidation of pentlandite with hydrogen peroxide. At pH values of 5 to 6, Ni(II) ions and FeO.OH are the primary oxidation products in equilibrium with a violarite (Ni_2FeS_4) surface. The chemical reactions of pentlandite under acidic conditions were reported to produce iron oxides, nickel oxides/sulfates and violarite (Warner *et al*, 1996).

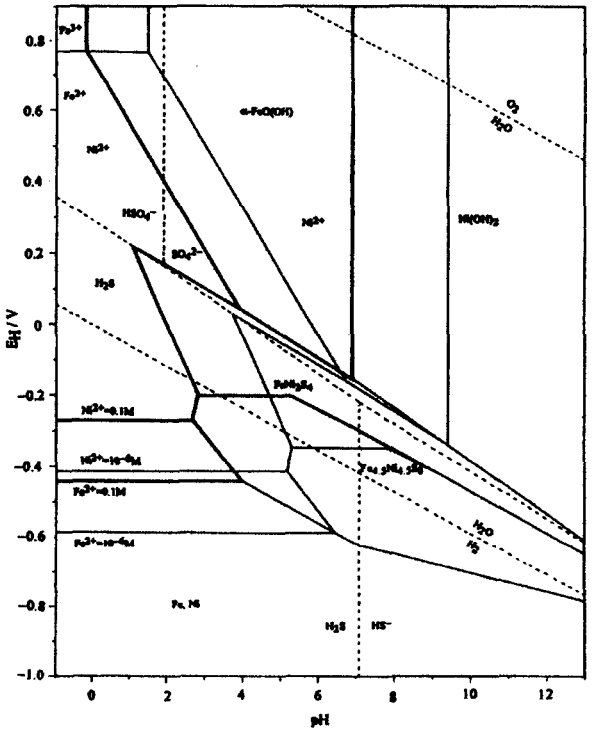

Figure 6-6: Eh-pH diagram for the Fe-Ni-S aqueous system at 25°C. Activities of the aqueous species is 10^{-6}M (fine line for nickel and iron species) (after Warner *et al*, 1996)

6.4.3 Effect of sulfidisation

6.4.3.1 Flotation response

In the presence of other oxidised sulfide minerals, oxidised pentlandite responded well to sulfidisation and, as with the other two sulfide minerals, the maximum flotation recovery

was observed at a sulfidisation potential of -650 mV. However, as a single mineral, heavily oxidised pentlandite responded poorly to sulfidisation as measured by the flotation response. Some flotation response after sulfidisation at very high sulfidisation potentials was noted. Based on the XPS data, at an Es of -800 mV there was no evidence of sulfidisation in terms of nickel or iron sulfide species. Sulfur species were found, most likely as either elemental sulfur or polysulfides, and would account for the small flotation response.

The chronoamperometric studies confirmed that hydrosulfide ions did not interact with the heavily oxidised pentlandite surface. However at high sulfidising reagent concentrations, a very small current indicated that some elemental sulfur may have been produced at the oxidised pentlandite surface through the oxidation of hydrosulfide ions. This corroborated the XPS interpretation of a small quantity of sulfur species at high sulfidisation potentials.

To test the base-metal sulfide precipitation hypothesis, testwork was conducted employing quantities of copper and iron ions during sulfidisation that were expected to be available as determined by EDTA extraction from the Nkomati surfaces.

When iron ions were added prior to sulfidisation, some improvement in the flotation of oxidised pentlandite was observed. This finding indicated that surface adsorbed iron hydroxides are amenable to sulfidisation, however the proportion of the iron hydroxide species that formed and subsequently adsorbed onto the oxidised pentlandite was not known. While this mechanism may contribute to the sulfidisation of oxidised pentlandite surfaces, it does not appear to play a dominant role.

On the other hand, iron ions added during sulfidisation at an Es of -650 mV, significantly improved the flotation of oxidised pentlandite. These results demonstrated that the surface formation of iron sulfides played a major role in the flotation recovery of oxidised pentlandite at this sulfidisation potential.

The addition of iron ions over the full sulfidisation range produced a similar flotation recovery profile for heavily thermally oxidised pentlandite to that found after sulfidisation of the heavily thermally oxidised Nkomati ore samples. The best result was obtained at -650 mV, which paralleled that found for oxidised pentlandite sulfidised in the presence of other oxidised sulfide minerals. The sulfidisation conditions at -650 mV Es (-315 SHE)

provided the best chemical conditions for the formation/ precipitation and maintenance of the surface bound iron sulfide species.

Copper ions added prior to sulfidisation were also effective, however not as significant as the addition of iron ions. Based on the quantities added, copper was considerably more effective in conferring floatability than iron, since most likely copper species are easily sulfidised. It is also possible that this reaction may proceed analogously to the activation of sphalerite surfaces by copper hydroxide species, where the copper replaces the nickel or iron in the oxidised surface species and subsequently becomes sulfidised.

As in the case of iron ions, addition during sulfidisation produced the best flotation response. The improvement in the sulfidisation response was not as great as that found for iron, solely due to the lower concentration level of copper ions employed. If employed at similar concentrations as the iron, copper would appear to be even more effective, however this requires further evaluation. This result confirmed a role for copper ions in the sulfidisation of pentlandite in oxidised Nkomati samples.

6.4.3.2 Sulfidisation mechanism

Based on the zeta potential studies, the adsorption of hydrosulfide ions by the oxidised pentlandite surfaces occurred less readily than with the other oxidised sulfide minerals. The significantly smaller drop in zeta potential indicates substantially less hydrosulfide ion adsorption and occurred at a greater sulfidising potential.

At an Es of -500 mV, both the nickel and iron oxide/hydroxides abundances were at a maximum. Only a very small Ni-S signal was detected while there was no Fe-S signal, indicating that no sulfidisation had occurred. Due to a combination of incomplete surface oxidation and surface cleaning effects, the Ni-S signal most likely reflects the underlying pentlandite surface. A moderate quantity of $S^{2-}/S_n/S^o$ was found, most probably elemental sulfur/polysulfides due to the oxidation of hydrosulfide ions.

Under more intense sulfidisation (Es = -650mV), all XPS signals except for the oxide decreased. This indicated that the increased reducing conditions had caused enhanced surface dissolution rather than sulfidisation, which would be expected if nickel hydrosulfide complexes were forming.

The electrochemical work provided strong corroborative evidence for the inability of heavily oxidised pentlandite to interact with hydrosulfide ions. Cyclic voltammetric studies showed that sulfidisation failed to regenerate an oxidised pentlandite surface while chronoamperometry showed that there was almost no interaction between the hydrosulfide ions and the oxidised pentlandite surface.

The poor interaction of oxidised pentlandite surfaces with hydrosulfide ions is puzzling for a number of reasons and independent of the oxidation method. Firstly, the formation of nickel sulfide products from nickel 'oxide' species is strongly favoured based on solubility product and thermodynamic considerations (refer to Table 6-22).

Table 6-22: Possible sulfidisation reactions for oxidised pentlandite at 25°C (after Roine, 2002)

Sulfidisation reaction	ΔG° (kJ)	Log K	E° (SHE,V)
$Ni(OH)_2 + HS^- \rightarrow NiS + OH^- + H_2O$	-10.7	7.9	-
$NiO + HS^- + e^- \rightarrow NiS + OH^-$	-43.0	7.5	-
$NiO.OH + HS^- + e^- \rightarrow NiS + 2OH^-$	-95.0	16.7	0.985
$Ni(OH)_2 + 2HS^- \rightarrow NiS_2 + 2H_2O + 2e^-$	-42.2	30.9	0.914
$Ni(OH)_2 + 2S^{2-} \rightarrow NiS_2 + 2OH^- + 2e^-$	-164.4	28.8	0.853
$NiO + 2S^{2-} + H_2O \rightarrow NiS_2 + 2OH^- + 2e^-$	-162.6	28.5	0.843
$NiO.OH + 2S^{2-} + H^+ \rightarrow NiS_2 + 2OH^- + e^-$	-267.6	51.6	3.054

At a total dissolved sulfur concentration of 10^{-5}M (circa Es = -650 mV) and particularly at a concentration of 10^{-1}M, millerite is a dominant phase (refer to Figures 6-7 and 6-8). However, in spite of these positive aspects, the interaction of hydrosulfide ions with oxidised surface species does not readily occur and the subsequent formation of nickel sulfide entities may be kinetically controlled. Another factor may be the physical nature of the oxidised pentlandite surfaces, which unlike the surfaces of the other oxidised sulfide minerals, was reported to be firmly attached and difficult to dislodge (Buckley and Woods, 1991).

While the hydrosulfide interaction is dependent on some degree of surface solubility, the contrary was found based on XPS interpretations where surface dissolution was indicated. Thus rather than forming insoluble sulfide precipitates, the oxidised nickel species may have dissolved and formed hydrosulfide and sulfide ligands, such as $Ni(HS)^+$, $Ni(HS)_2$, $[Ni_2(HS)]^{3+}$, $[Ni_3(HS)]^{5+}$, $[Ni(S_4)]$, $[Ni(S_4)]^{2+}$, $[Ni(S_5)]$ and $[Ni_2(S_5)]^{2+}$(Rickard and Luther,

2006).

Finally, the iron oxidation products present on the oxidised pentlandite surfaces would be expected to have been sulfidised and thus caused flotation. Surprisingly, both methods of oxidation produced iron oxidation species that were not apparently amenable to sulfidisation. As noted earlier, in the case of thermal oxidation followed by hydrolysis, ferric oxy-hydroxides were clearly not produced. After chemical oxidation, FeO.OH would be expected to have formed (Warner *et al*, 1996), and noting that most forms of FeO.OH interact with hydrosulfide ions and indeed goethite has been sulfidised, it was surprising that no interaction occurred.

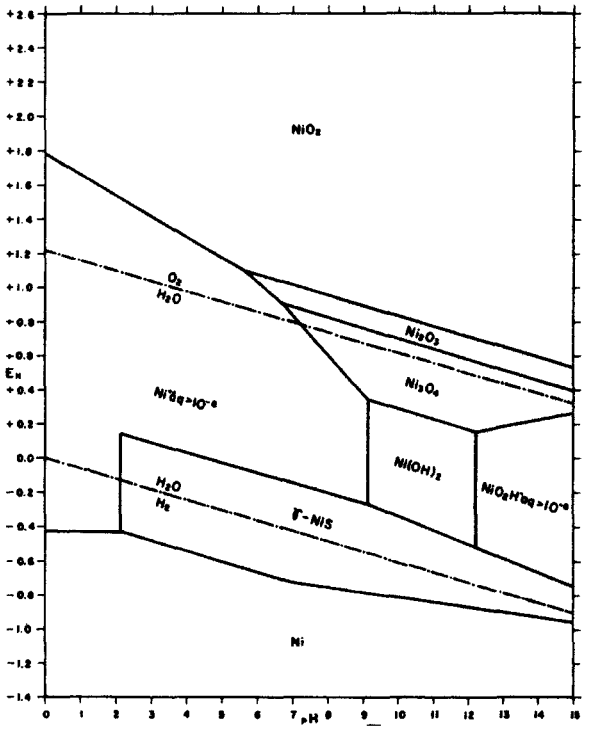

Figure 6-7: Stability relationship between nickel sulfide and nickel 'oxide' species (total dissolved sulfur of 10^{-5}M at 25°C) (after Garrels and Christ, 1990)

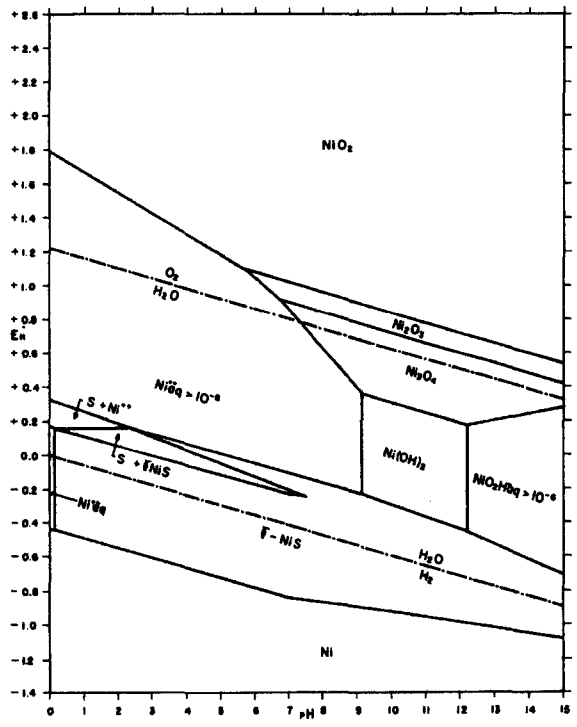

Figure 6-8: Stability relationship between nickel sulfide and nickel 'oxide' species (total dissolved sulfur of 10^{-1}M at 25°C) (after Garrels and Christ, 1990)

The proposed sulfidisation mechanism for oxidised pentlandite, particularly at sulfidisation potentials between -600 and -700 mV, is based on the formation of iron and copper sulfides on the oxidised pentlandite surfaces. This mechanism occurs as a reaction between the surface adsorbed hydrosulfide ions and iron and copper ions in solution as well as direct precipitation. The first reaction would be the reduction of the cations in solution, namely Fe(III) to Fe(II) ions and Cu(II) to Cu(I) ions, followed by surface adsorption of the hydrosulfide ions onto the oxidised surfaces as found by electrophoresis :

$$NiO.OH + HS^- \leftrightarrow NiO.OH.HS^- \quad \text{.....(6-13)}$$

$$Fe^{2+} + NiO.OH.HS^-_{ads} \rightarrow NiO.OH.FeS_{ppt} + H^+ \quad \text{.....(6-14)}$$

$$Cu^+ + NiO.OH.HS^-_{ads} \rightarrow NiO.OH.CuS_{ppt} + H^+ \quad \text{.....(6-15)}$$

As secondary mechanisms, base-metal sulfide species precipitate onto the oxidised surfaces:

$$Fe^{2+} + HS^- \rightarrow FeS_{ppt} + H^+ \quad \text{.....(6-16)}$$

$$Cu^+ + HS^- \rightarrow CuS_{ppt} + H^+ \quad \text{.....(6-17)}$$

Thermodynamically, both these latter reactions are strongly favoured (refer to Tables 6-9 and 6-17) and it is expected that reactions 6-14 and 6-15 share similar thermodynamics.

The flotation rate of the sulfidised oxidised pentlandite as a single mineral was much slower than that found after the sulfidisation in the presence of other sulfide minerals. The slower flotation rate may well be associated with the formation of a less coherent and patchier sulfide surface. In the more complex chemical environment encountered during the sulfidisation of the oxidised Nkomati ore sample, a number of complementary precipitation reactions may have enhanced both the extent and coherency of the sulfidised surfaces, resulting in faster flotation rates.

6.4.3.3 Comparison to base-metal 'oxide' minerals

There are no reported sulfidisation and flotation studies with nickel 'oxide' minerals, and although the sulfidisation of a nickel arsenide mineral was reported, no direct comparisons can be made. It is interesting to note that while nickel exists as a number of 'oxide' minerals (particularly hydroxy-carbonates), unlike the 'oxide' minerals of copper, lead and zinc, they clearly have not been of economic interest and subsequently attracted little mineral processing attention. Based on the behaviour of oxidised pentlandite, it would be expected that some difficulties would be encountered in the treatment of nickel 'oxide' minerals using sulfidisation.

6.5 Merensky ore gangue minerals

6.5.1 Effect of oxidation

The oxidation or weathering had little effect on the flotation recovery with Merensky ore gangue minerals. The small flotation response found was attributed to both the naturally floating mineral talc as well as talc-rimmed composites of pyroxene, since talc only makes up 2% of the typical mineral assemblage (Becker *et al*, 2006). This was corroborated by microscopic studies as well as X-ray diffractograms of the flotation feed and the concentrate samples (refer to Appendix D1). The latter showed that both samples were similar and consisted of both pyroxene and feldspar.

6.5.2 Effect of sulfidisation

The sulfidisation process did not have any effect on the floatability of either the unoxidised or oxidised (weathered) Merensky ore gangue minerals. This is principally due to the low reactivity of the gangue mineral surfaces and the fact that any potential surface sulfidisation product would be soluble (Na_2S or CaS).

CHAPTER 7

CONCLUSIONS

7.1 The effect of oxidation upon sulfide mineral flotation

7.1.1 Nature of the flotation response

Oxidation had a dramatic effect upon the flotation recovery of oxidised sulfide minerals. After 27 days of thermal oxidation, the flotation recovery of the Nkomati ore sample had fallen to 50% and after 121 days it was below 10%. A similar trend was found with chemical oxidation whereby increased oxidation intensity decreased the flotation recovery to 50% (1 minute @ 10^{-8} M H_2O_2) to effectively complete depression (10 minutes @ 10^{-2} M H_2O_2).

Due to differences between the sulfide minerals in terms of chemical reactivity, differences in the oxidative behaviour as measured by floatability were found. Pyrrhotite was the most significantly affected while chalcopyrite was the least. Under thermally oxidising conditions, pentlandite exhibited a similar flotation response to that of pyrrhotite. With chemical oxidation, pyrrhotite was more reactive than pentlandite. It was shown that the flotation behaviour of pentlandite, as an individual mineral, was the same after either heavy thermal or chemical oxidation.

7.2.2 Nature of the oxidation

The nature of the oxidation layer was characterised in terms of the thickness and the elemental composition as function of time for the thermally oxidised ore Nkomati samples. For oxidised pyrrhotite, the most readily detected sulfide mineral species, the oxide layer grew substantially in thickness with time and also incorporated more iron and oxygen. Similar characterisations were made for pentlandite and chalcopyrite, however in the latter case, the oxide layers were not particularly thick nor substantially enriched in iron and sulfur.

Chemically oxidised Nkomati samples were more difficult to characterise with the SEM/EDX techniques and it was concluded the oxidised layers after heavy oxidation were

less than 100 nanometers thick. After ultrasonic treatment, the thermally heavily oxidised samples also were difficult to characterise with this technique.

The degree of oxidation was characterised by the flotation response for the oxidised Nkomati ore samples. The full profile of the flotation behaviour of the Nkomati ore sample as well as the individual sulfide minerals was established as a function of the extent of surface oxidation, for both thermally and chemically oxidised samples. Subsequently, the terms 'moderate' and 'heavily' were defined based on the flotation response.

Finally, the degree of oxidation, namely unoxidised, moderate and heavy, for the oxidised Nkomati ore and the individual sulfide minerals were readily characterised by electrophoresis, where the oxidised surfaces caused the zeta potential to exhibit more positive values.

It appears that thermal oxidation and chemical oxidation produce similar surfaces, however this is not conclusive. There are conditions where differences between the two methods are found as measured by bulk surface techniques, particularly for moderately oxidised pentlandite. This is associated with the nature of the oxidation, where different mechanisms are in operation at different stages of oxidation. The surfaces of Nkomati samples, after heavy thermal oxidation, followed by ultrasonic treatment and hydrolysis, were however similar to those produced by chemical oxidation.

While similar flotation responses were obtained after sulfidisation with Nkomati ore samples for the two oxidation methods, there maybe a trade-off between the variety and quantity of oxidation products and the associated degree of solubility. It is conjectured that the chemical method may have produced fewer oxidation products but with higher solubilities while the thermal/ultrasonic treatment/hydrolysis approach may have yielded larger quantities and varieties of oxidation species with lower but adequate solubilities for successful sulfidisation.

7.3 The effect of sulfidisation upon oxidised sulfide mineral flotation

7.3.1 Nature of the sulfidisation response

Sulfidisation was found to restore the floatability of the three oxidised sulfide minerals present in the oxidised Nkomati ore, particularly between the sulfidisation potentials of -600 and -700 mV. Peak flotation recoveries for all sulfide minerals occurred at a sulfidisation potential of -650 mV, where the hydrosulfide ion concentration met all the reaction requirements of the oxidised minerals system. With increasing sulfidisation potentials, sulfide mineral flotation recoveries fell away due to the depressive effect caused the adsorption of both hydrosulfide ions and base-metal hydrosulfide complexes. For the oxidised Nkomati ore, the flotation recovery of chalcopyrite was nearly completely restored, while pyrrhotite and pentlandite exhibited satisfactory but lower recoveries.

As an individual mineral, oxidised pentlandite did not readily respond to sulfidisation. At very high sulfidisation potentials, some flotation recovery was noted, particularly for chemically oxidised samples. This was associated with the presence of elemental sulfur/polysulfides.

No significant difference in the flotation recoveries after sulfidisation was found between chemically and thermally oxidised Nkomati ore and pentlandite samples.

7.3.2 Response under Merensky ore flotation conditions

The presence of calcium ions (10^{-2} IS) during sulfidisation did not affect the sulfidisation process of the oxidised sulfide minerals as reflected by the flotation recoveries. No statistical difference in terms of individual sulfide mineral flotation recoveries with and without calcium ions was found.

7.3.3 Nature of the sulfidisation mechanism

For thermally heavily oxidised sulfide minerals after hydrolysis, hydrated base-metal oxides and oxy-hydroxides were detected on the oxidised chalcopyrite and pentlandite surfaces. In the case of oxidised pyrrhotite surfaces, it was deduced that that a hydrated Fe(III) oxy-hydroxide was the major species.

After sulfidisation, Cu_2S-like and CuS-like phases as well as elemental sulfur/polysulfides were identified on the sulfidised chalcopyrite surfaces in great abundance. For sulfidised pyrrhotite surfaces, FeS-like and FeS_2-like entities as well as elemental/polysulfides were detected in moderate amounts. However, no significant quantities of sulfidisation products were found on the sulfidised pentlandite surfaces. This was corroborated by cyclic voltammograms, where after sulfidisation, a pre-oxidation-like surface had been restored to heavily oxidised chalcopyrite and pyrrhotite samples. Sulfidisation failed to restore a pre-oxidation surface to heavily oxidised pentlandite.

The interaction between the three heavily oxidised sulfide mineral surfaces and hydrosulfide ions as measured by chronoamperometry also confirmed these observations. The order of interaction was chalcopyrite > pyrrhotite > pentlandite, with effectively no reaction occurring with heavily oxidised pentlandite surfaces. The reaction was interpreted as the oxidation of hydrosulfide ions to elemental sulfur.

The sulfidisation mechanisms for the three oxidised sulfide minerals showed similarities to those proposed for base-metal 'oxide' minerals, where an ionic exchange and precipitation are the principal mechanisms. However an electrochemical reaction made a contribution to the sulfidisation mechanisms, through the oxidation of the hydrosulfide ion species.

For oxidised chalcopyrite, the initial sulfidisation mechanism is interpreted as an anionic mechanism based on copper oxide and hydroxide to form a chalcocite-like phase. The formation of a covellite-like phase at higher sulfidisation potentials is also chemical in nature and due to the dominance of Cu(II) ions at this sulfidisation potential. The oxidation of hydrosulfide ions occurred producing elemental sulfur/polysulfides.

Two sulfidisation mechanisms occur for oxidised pyrrhotite and are dependent upon the sulfidisation intensity. The dominant one involves an ionic exchange reaction between the hydrosulfide ions and surface iron oxide and hydroxide species to form a pyrrhotite-like species. The second sulfidisation mechanism involves the interaction between the pyrrhotite-like entity with elemental sulfur to form a pyrite-like phase. Pyrite was formed in greater abundance at higher sulfidisation potentials where more elemental sulfur was available due to hydrosulfide oxidation. The release of ferrous ions during surface interaction with water subsequently results in the precipitation of a pyrrhotite-like phase onto the surfaces.

Oxidised pentlandite as a single mineral sample did not respond to sulfidisation. In the presence of other oxidised sulfide minerals, particularly oxidised pyrrhotite, it was established that the precipitation of iron and copper sulfides onto the oxidised pentlandite surfaces was the dominant mechanism. This was demonstrated with the addition of Fe(III) ion during sulfidisation, where the flotation recovery of oxidised pentlandite mirrored that found for oxidised pentlandite after the sulfidisation of oxidised Nkomati ore samples.

7.4 The effect of sulfidisation upon non-sulfide mineral flotation

Sulfidisation did not increase the floatability of either unweathered or weathered Merensky gangue minerals. This confirms that there is process selectivity between the base-metal sulfide and non-sulfide mineral types.

7.5 Further work and recommendations

It is recommended that further testwork be undertaken on pentlandite to study the effect of oxidation, sulfidisation and base-metal ions on the flotation behaviour. The nature of the oxidation mechanism as function of degree of oxidation deserves further scrutiny.

Furthermore, the application of sulfidisation should be tested upon an oxidised Merensky ore based on the conditions found in this research.

There is considerable scope to apply this approach to other Merensky type ore sources and the oxidised ores at Ngezi in the Great Dyke Zimbabwe fall into this category. These sources also include current and old tailings dams as well as slag dumps. Moreover, a more significant application may exist in the current treatment of underground Merensky ores. This arises due to the susceptibility of the base-metal sulfides to oxidation during the mining, milling and flotation stages, which would influence their recovery by flotation.

More generally, the improved understanding of the sulfidisation mechanisms for oxidised sulfide minerals should be applied to the sulfidisation of other oxidised sulfide ores, such as those that are currently stockpiled in preference to treatment of the underlying unoxidised sulfide ores (e.g. Antamina (Cu-Zn), Peru). The subsequent flotation recovery of the contained base-metal values would significantly contribute to project revenues with lower mining and milling costs and maximise the exploitation of the mineral resource.

BIBLIOGRAPHY

Abramov, A A and Avdohin, V M, 1997. Monitoring and regulation of sulfide oxidation processes during flotation. Section 8.6 in *Oxidation of sulfide minerals in benefication processes*. Translated by A Peabody, Gordon and Breach Science Publishers, Australia, pp. 273-301.

Anon, 1957. Kolwezi mill concentrates three types of copper cobalt bearings. *World Mining - San Francisco Conference, 10th February*, pp. 46-49 + 56.

Arnold, R G, 1966. Mixtures of hexagonal and monoclinic pyrrhotite and the measurement of the metal content of pyrrhotite by x-ray diffraction. *American Mineralogist*, 51, 1221-1227.

Attia, Y A, 1975. Surface chemistry of copper minerals in water. *Transactions of the Institute of Mining and Metallurgy, Section C*, 84, 221- 230.

Barker, C W, Featherstone, S F and Storey, M J, 1982. Development of flotation practice at Trojan nickel mine concentrator, Zimbabwe. *Transactions of the Institution of Mining and Metallurgy (Section C), **91***, 135-141.

Bartelds, J 1990. The Telfer CPS system: a brief overview. *AMMTEC/CSIRO Flotation Colloquium*, pp. 1-4.

Bastin, D. Personal communication.

Bastin, D, Frenay, J and Philippart, P, 2003. Ammonium sulphate as promoting agent of the the sulphidization process of Cu-Co oxides ores from the Luiswishi Deposit (DRC). In Proceedings of the *XXIInd International Mineral Processing Congress*, Editors L Lorenzen and D J Bradshaw, Cape Town, South Africa, p 434.

Becker, M. Personal communication.

Becker, M, Harris, P, Wiese, J and Bradshaw, D, 2006. The use of quantitative mineralogical data to interpret the behaviour of gangue minerals in the flotation of Merensky Reef ores. Paper presented at *Automated Mineralogy 2006*, MEI Conference, Brisbane, Australia.

Belzile, N, Chen, Y, Cai, M and Li, Y, 2004. A review on pyrrhotite oxidation. *Journal of Geochemical Exploration*. 84, 65-76.

Berner, R A, 1970. Sedimentary pyrite formation. *American Journal of Science*, 268, 1-23.

Bessiere, J, El Housni, A, and Predali, J J, 1991. Dielectric study of the activation and deactivation of malachite by sulfide ions. *International Journal of Mineral Processing*, 33, 165-183.

Billi, M and Quai, V, 1963. Developments and results obtained in the treatment of zinc oxide ores at the AMMI mines. *Proceedings of the Sixth International Mineral Processing Congress*, Cannes, pp. 631-649.

Blain, C F and Andrew, R L, 1977. Sulphide weathering and the evaluation of gossans in mineral exploration. *Minerals Science and Engineering*, 9, 119-150.

Boyard, G, 1954. Different problems posed by the flotation of lead carbonates at the washing plant of Touissit. *Review industrial minerale*, 35, 167-72.

Bradshaw, D J and O'Connor, C T, 1996. Measurement of the sub-process of bubble loading in flotation. Minerals Engineering, 9, 443-448.

Bradshaw, D J, Buswell, A M and Harris, P J, 1999. Measurement techniques for the characterisation of the flotation performance of a complex sulphide ore. Preprint no. 99 – 173, SME Annual Meeting, Denver, Colorado.

Broomhead, J A and Layers, G, 1976. Leaching studies with pentlandite and pyrrhotite. *Proceedings of the Australasian Institute of Mining and Metallurgy*, 64, 11-30.

Brunauer, S, Emmett, P H and Teller, E, 1938. Adsorption of gases in multi-molecular layers. *Journal of the Ameican Chemical Society*, 60:309-319.

Buckley, A N and Woods, R, 1984. An X-ray photoelectron spectroscopic study of the oxidation of chalcopyrite. *Australasian Journal of Chemistry*, 37, 2403-2413.

Buckley, A N and Woods, R, 1985a. X-ray photoelectron spectroscopy of oxidised pyrrhotite surfaces. Part 1- Exposure to air. *Applications in Surface Science*, 22-23, 280-287.

Buckley, A N and Woods, R, 1985b. X-ray photoelectron spectroscopy of oxidised pyrrhotite surfaces. Part 2 - Exposure to aqueous solutions. *Applications in Surface Science*, 20, 472-480.

Buckley, A N and Woods, R, 1991. Surface composition of pentlandite under flotation related conditions. *Surface and Interface Analysis*, 17, 675-680.

Buckley, A N, Woods, R and Waterlood, H J, 1988. The deposition of sulfur on pyrite and chalcopyrite from sodium sulphide solutions. *Australian Journal of Chemistry*, 41, 1003-1011.

Bulatovic, S M and Wyslouzil, D M, 1985. Selection of reagent scheme to treat massive sulphide ores. *Complex sulfides: Processing ores, concentrates and by products. (TMS/AIME Fall Extractive Meeting, TMS/AIME* San Diego :TMS. pp. 101-137.

Bustamante, H and Castro, S H, 1975. Hydrophobic effects of sodium sulphide on malachite flotation. *Transactions of the Institution of Mining and Metallurgy*, Section C, 81, 167-171.

Bustamante, H and Shergold, H L, 1983a. Surface chemistry and flotation of zinc oxide minerals. Part 1 - Flotation with dodecylamine. *Transactions of the Institution of Mining*

and Metallurgy. Sect, 92, 201-208.

Bustamante, H and Shergold, H L, 1983b. Surface chemistry and flotation of zinc oxide minerals. Part 2 - Flotation with chelating reagents. *Transactions of the Institution of Mining and Metallurgy*, Section C, 92, 208-215.

Buswell, A M and Nicol, M J, 2002. Some aspects of the electrochemisty of the flotation of pyrrhotite. *Journal of Applied Electrochemistry*, 32, 1321-1329.

Cantrell, R, 1996. The use of nitrogen in CPS flotation stage two laboratory testwork report. BOC Gases Australia Limited.

Cases, J M, Trabelsi, K, Predali, J J and Brion, D, 1979. Concentration par flottation d'un mineral d'oxyge de zinc et de plomb. In Proceedings of the *Processing of oxidized and mixed oxide-sulphide lead-zinc ores. Round Table Seminar at the XIIIth International Mineral Processing Congress*, Warsaw, Poland, Editor J Laskowski, Polish Scientific Publishers, Warsaw, pp. 95-121

Castro, S H, Gaytan, H and Goldfarb, J, 1976. The stabilizing effect of Na_2S on the collector coating of chrysocolla. *International Journal of Mineral Processing*, 3, 71-82.

Castro, S H, Soto, H, Goldfarb, F and Laskowski, J S, 1974a. Sulphidizing reactions in the flotation of oxidized copper minerals. Part 1- Chemical factors in the sulphidization of copper oxide. *International Journal of Mineral Processing*, 1, 141-149.

Castro, S H, Soto, H, Goldfarb, F and Laskowski, J S, 1974b. Sulphidizing reactions in the flotation of oxidized copper minerals. Part 2 - Role of the absorption and oxidation of sodium sulphide in the flotation of chrysocolla and malachite. *International Journal of Mineral Processing*, 1, 151-161.

Cawthorn, R, Grant, L, Christopher, A, Schouwstra, R P and Mellowship, P, 2002. Relationship between PGE and PGM in the Bushveld Complex. *Canadian Mineralogist*, 40, 311-328.

Chen, K Y and Morris, J C, 1972a. Kinetics of oxidation of aqueous sulfide by oxygen. *Environmental Science and Technology*, 6, 529-537.

Chen, K Y and Morris, J C, 1972b. Oxidation of sulfide oxygen: catalysis and inhibition. *Journal of Sanitary Engineering*, 98, 215-226.

Clark, D W and Newell, A J H, 1996. Base metal mineral flotation. *Patent AU9539027, AU691358, CA2163688, ZA9509977 and US5855770*

Clark, D W, Newell, A J H, Chilman, G F and Capps, P G, 2000. Improving flotation recovery of copper sulphide by nitrogen gas and sulphidisation conditioning. *Minerals Engineering*, 13, 1197-1206.

Clay, P, 1993. Copper and gold ore treatment at Triako Resources Ltd., Mineral Hill, NSW. In *Australian Mining and Metallurgy, The Sir Maurice Mawby Memorial Volume, Volume 1*. Editors J Woodcock and J Hamilton, Australasian Institue of Mining and

Metallurgy, Melbourne, pp 669-672.

Clesceri, L S and Greenberg, A E, 1998. Inorganic nonmetals - Sulfide. *Standard methods for the examination of water and waste water,* American Public Health Association, Washington, pp 4-162 - 4-166.

Cornell, R M and Schwertmann, U, 1996. The iron oxides: structure, properties, reactions, occurrences and uses. VCH, Weinheim, pp 112-125, 190-219, 235-266 and 313-347.

Crozier, R D, 1992. Flotation: theory, reagents and ore testing. Pergamon Press, New York, pp 107-111.

de Cuyper, J, 1981. Concentration of copper oxide ores. *International Conference on Cobalt: Metallurgy and uses.* ACTA Technica Belgica Metallurgie, Brussels, pp 27-36.

de Villiers, J, Brynard, H and Viviers, L, 1978. A mineralogical investigation of ores from the Merensky Reef and their flotation products. *Report No.1966,* National Institute for Metallurgy, Randburg, South Africa.

de Waal, S, 1978. Supergene alteration of sulphide ores. I. Literature survey, measurement, and effect on floatability and leachability. *Report No. 1962,* National Institute for Metallurgy, Randburg, South Africa.

Doniach, S and Sunjic, M, 1970. Many-electron singularity in X-ray photo-emission and X-ray line spectra from metals. *Journal of Physical Chemistry: Solid State Physics,* 3, 285–291.

Ealy, G, 1973. Concentration of copper oxides at Nacimiento. *Mining Congress Journal,* pp 63-66.

Ehm, G and Hill, G, 1992. The design, construction and operation of the Boddington Gold Mine Supergene Basement plant. *Extractive Metallurgy of Gold and Base Metals, Kalgoorlie* Australasian Institute of Mining and Metallurgy, Parkville, pp 79-94.

Fleet, M E, 2006. Phase Equilibria at High Temperatures. In *Sulfide Mineralogy and Geochemistry,* Editor D J Vaughan, *Reviews in Mineralogy and Geochemistry,* Volume 61, Chapter 7, Mineralogical Society of America, Chantilly, Virginia, pp 365-419.

Fleming, M, 1953. Effects of soluble sulphide in the flotation of secondary lead minerals. *Recent developments in mineral dressing,* Institute of Mining and Metallurgy, London, pp 521-548.

Fokkink, L G J, 1987. Ion adsorption on oxides. *Ph.D. Thesis,* Landbouwuniversiteit, Netherlands. Quoted in Grano *et al,* 1997.

Formanek, V and Lauvernier, J, 1963. Gravimetric and flotation concentration of cobalt arsenides from Bou-Azzer (Morocco). In the Proceedings of the *International Congress of the Preparation of Minerals,* Cannes, France, pp 412-34, discussion pp 434-6.

Freeman, W A, Newell, R and Quast, K B, 2000. Effect of grinding media and NaHS on copper recovery at Northparkes Mines. *Minerals Engineering*, 13, 1395-1403.

Fuerstenau, M C, Olivas, S A, Herrera-Urbina, R and Han, K N, 1987. The surface characteristics and flotation behaviour of anglesite and cerussite. *International Journal of Mineral Processing*, 20, 73-85.

Fuerstenau, D W, Sotillo, F J, and Valdivieso, A L, 1985. Sulfidisation and flotation behaviour of anglesite, cerussite and galena. In Proceedings of the *XVth International Mineral Processing Congress*, Société de L'Industrie Minérale et du Bureau de Recherches Géologiques et Minères, Cannes, France, Volume 2, pp 74-86.

Fullston, D, Fornasiero, D and Ralston, J, 1999. Zeta potential study of the oxidation of copper sulfide minerals. *Colloids and Surfaces A: Physiochemical and Engineering Aspects* , 146, 113-121.

Garrels, R M, 1953. Mineral species as function of pH and oxidation-reduction potentials, with special reference to the zone of oxidation and secondary enrichment of sulphide ore deposits. *Geochimica et Cosmochimica Acta*, 5, 15-168.

Garrels, R M and Christ, C L, 1990. *Solutions, Minerals and Equilibria.* Jones and Bartlett Publishers, Boston.

Glazunov, L, Bekturganov, N and Satayev, I, 1993. Technology of sulphidisation and flotation of non-sulphide minerals with sodium polysulphides. In the Proceedings of the *XVIIIth International Mineral Processing Congress*, Sydney, Australia, pp 607-609.

Gonzalez, G L J, 1974. The point of zero potential of oxidized copper minerals: tenorite, malachite and chrysocolla. *Electroanalytical Chemistry and Interfacial Electrochemistry*, 53, 452-456.

Gonzalez, A, Gonzalez, G L J and Laskowski, J S, 1975. Effect of ageing on the flotation response of chrysocolla. *Transactions of the Institution of Mining and Metallurgy.* Section C, 84, 154-157.

Grano, S, Sollaart, M S W, Prestidge, C and Ralston, J, 1997. Surface modifications in the chalcopyrite-sulphite ion system. I. collectorless flotation, XPS and dissolution study. *International Journal of Mineral Processing*, 50, 1-26.

Guilbert, J M and Park, C F, 1986. The geology of ore deposits. W H Freeman and Company, New York, pp 796-836.

Guy, P J and Trahar, W J, 1984. The effects of oxidation and mineral interaction on sulphide flotation. *Developments in Mineral Processing*, volume 6, pp 28-46.

Hamilton, I C and Woods. R, 1981. An investigation of surface oxidation of pyrite and pyrrhotite by linear potential sweep voltammetry. *Journal of Electroanalyical Chemistry*, 34, 13-24.

Heiskanen, K, Kirjavainen, V and Lappas, H, 1991. Possibilities of collectorless flotation in the treatment of pentlandite ores. *International Journal of Mineral Processing*, 33, 263-274.

Healy, T W and Moignard, M S, 1976. A review of electrokinetic studies of metal sulfides. In *A M Gaudin Memorial Volume, Flotation, Volume 1*, Editor M C Fuerstenau, ; American Institute of Mining, Metallurgy and Petroleum Engineers, New York, 275-97.

Helgeson, H C, 1969. Thermodynamics of hydrothermal systems at elevated temperatures and pressures. *American Journal of Science*, 267, 729-804.

Herrera-Urbina, R, Sotillo, F J and Fuerstenau, D W, 1998. Amyl xanthate uptake by natural and sulfide treated cerussite and galena. *International Journal of Mineral Processing*, 55, 113-128.

Hesse, R, Chassé, T, Streubel, P and Szargan, R, 2004. Error estimation in peak-shape analysis of XPS core-level spectra using UNIFIT 2003: how significant are the results of peak fits? *Surface and Interface Analysis*; 36; 1373-1383.

Hey, P V, 1999. The effects of weathering on the UG2 chromitite reef of the Bushveld Complex, with special reference to the platinum-group minerals. *South African Journal of Geology*; 102; 251-260.

Hodgson, M and Agar, G E, 1989. Electrochemical investigations into the flotation chemistry of pentlandite and pyrrhotite: process water and xanthate interactions. *Canadian Metallurgical Quarterly*, 28, 189-198.

Hu, Y, Liu, G and Wang, D, 1986. The study of flotation of copper-oxide with non-ionic polar collectors containing sulphur. *Nonferrous Metallurgy*, 38, 27-32. AN 8612141-0304 (Abstract).

Hunt, K, 2000. Industrial gases in flotation at the Hayden Concentrator. *AIME Spring Meeting, Arizona Section,* American Institute of Mining, Metallurgical and Petroleum Engineers, Littleton, pp 1-7.

Ishihara, T and Kagami, Y, 1964. Influence of aeration and oxidation of pyrrhotite on its flotation. *Nippon Kogyo Kaishi*, 80, 881-886. CAN 67:24091 (Abstract).

Iwasaki, I, Nakazawa, H, Malicsi, A, and Ziaowei, L, 1988. Research summary: Recovery of platinum-group metals from Gabbroic rocks. *Journal of Metals,* 40, 6, 36-39.

Janzen, M P, Nicholson, R V and Scharer, J M, 2000. Pyrrhotite reaction kinetics: reaction rates for oxidation by oxygen, ferric iron, and for non-oxidative dissolution. *Geochimica et Cosmochimica Acta*, 64, 1511-1522.

John, C I A, Sathe, R C and Kasongamulilo, V S, 1991. Improving flotation performance at the Nchanga Concentrator of Zambia Consolidated Copper Mines Limited. *Proceedings of Copper '91 International Symposium,* Ottawa, Canada, Volume 2, Pergamon Press, New York, pp 19-33.

Jones, M H, 1990. Some recent developments in the measurement and control of xanthate, perxanthate, sulphide and redox potential in flotation. *International Journal of Mineral Processing*, 33, pp 193-205.

Jones, M H and Woodcock, J T, 1978a. Evaluation of ion-selective electrode for contol of sodium sulphide additions during laboratory flotation of oxidised ores. *Transactions of the Institute of Mining and Metallurgy*, Section C, 89, 99-105.

Jones, M H and Woodcock, J T, 1978b. Optimization and control of laboratory sulphidization of oxidized copper ores with an ion selective electrode. *Proceedings of the Australasian Institution of Mining and Metallurgy*, 266, 11-19.

Jones, M H and Woodcock, J T, 1979a. Use of a sulphide ion-selective electrode in the sulphidization and flotation of oxidized copper ores. *Advances in Flotation: Proceedings of the first Latin-American Congress on Flotation*, Volume 4. University of Concepcion, pp 221-243.

Jones, M H and Woodcock, J T, 1979b. Control of laboratory sulphidization with a sulphide ion-selective electrode before flotation of oxidized lead-zinc-silver dump materials. *International Journal of Mineral Processing*, 6, 17-30.

Jones, M H, Wong, K and Woodcock, J T, 1986. Controlled potential sulphidization and rougher-cleaner flotation of an oxide sulphide copper ore. *Publication of the XIIIth CMMI Congress*, Melbourne, Australia, *Volume 4*, Australasian Institute of Mining and Metallurgy, Parkville, pp 33-40.

Jones, C F, LeCount, S, Smart, R St C and White, T J, 1992. Compositional and structural alteration of pyrrhotite surfaces in solution: XPS and XRD studies. *Applied Surface Science*, 55, 65-85.

Kelebek, S, 1993. The effect of oxidation on the flotation behaviour of nickel copper ores. In the Proceedings of the *XVIIIth International Mineral Processing Congress*, Sydney, Australia, Australasian Institute of Mining and Metallurgy, Parkville, pp 999-1005.

Kelebek S and Smith, G W, 1989. Collectorless flotation of galena and chalcopyrite: correlation between flotation rate and the amount of extracted sulphur. *Minerals and Metallurgical Processing*, 6, 123-129.

Kelly, D P and Vaughan, D J, 1983. Pyrrhotite-pentlandite ore textures: A mechanistic approach. *Mineralogical Magazine*, 47, 453-463.

Kirjavainen, V, Schreithofer, N and Heiskanen, K, 2002. Effect of some process variables on floatability in sulfide nickel ores. *International Journal of Mineral Processing*, 65, 59-72.

Klassen, V I and Mokrousov, V A, 1963. Regulating reagents containing divalent sulphur. *An Introduction to the Theory of Flotation.* Translated by J Lega and G W Poling, Butterworths. London, pp 310-349.

Kocabag, D and Smith, M R, 1985. The effect of grinding media and galvanic interactions upon the flotation of sulphide minerals. In the Proceedings of *Complex Sulfides: Processing of ores, concentrates and by-products conference.* Metallurgical Society of AIME and CIM, The Metallurgical Society Incorporated, New York, pp 55-81.

Kongolo, K, Vermaut, N and Acuna, P R, 1995. Improving the efficiency of sulphidization of oxidised copper ores by column and inert gas flotation. In the Proceedings of *Copper'95 - Copre '95 International Conference: Mineral processing and environment.* Volume 2, The Metallurgical Society of Canadian Institute of Mining and Metallurgy, pp 183-196.

Krebs, H A, 1929. The effect of heavy metals on the autoxidation of alkali sulfides and of hydrogen sulfide. *Biochemische Zeitschrift*, 204, 343-346.

Laskowski, J S and Yuan, X M, 2002. Flotation of sulfide minerals with the use of a cationic collector. *Canadian Metallurgical Quarterly*, 41, 381-390.

Lee, C A, 1996. A review of mineralisation in the Bushveld Complex and some other Layered Intrusions. *Layered Intrusions*. Editor R G Cawthorn, Elsevier Science B V, pp103-145.

Legrand, D L, Bancroft, G M and Nesbitt, H W, 1997. Surface characterization of pentlandite $(Fe,Ni)_9S_8$ by X-ray photoelectron spectroscopy. *International Journal of Mineral Processing*, 51, 217-228.

Legrand, D L, Nesbitt, H W and Bancroft, G M, 1998. X-ray photoelectron spectroscopic study of a pristine millerite (NiS) surface and the effects of air and water oxidation. *American Mineralogist*, 83, 1256-1265.

Legrand, D L, Bancroft, G M and Nesbitt, H W, 2005a. Oxidation/alteration of pentlandite and pyrrhotite surfaces at pH 9.3: Part 1. Assignment of XPS spectra and chemical trends. *American Mineralogist*, 90, 1042-1054.

Legrand, D L, Bancroft, G M and Nesbitt, H W, 2005b. Oxidation/alteration of pentlandite and pyrrhotite surfaces at pH 9.3: Part 2. Effect of xanthates and dissolved oxygen. *American Mineralogist*, 90, 1055-1061.

Leppinen, J and Mielczarski, J A, 1986. Spectroscopic study of the adsorption of thiol collectors on lead sulphide in the presence of sodium sulphide. *International Journal of Mineral Processing*, 18, 3-20.

Lewis, P J, 1990. Treatment of oxidised and primary copper/gold ores at Red Dome, Queensland, Australia. *Randol Gold Forum,* OlympicValley, California, Chapter 23, pp 4237-4243.

Lewis, A and van Hille, R, 2006. An exploration into the sulphide precipitation method and its effect on metal sulphide removal. *Hydrometallurgy*, 81, 197-204.

Licht, S and Davis, J, 1997.Disproportionation of aqueous sulfur and sulfide: kinetics of polysulfide decomposition. *Journal of Physical Chemistry B*, 101, 2540-2545.

Liebenberg, L, 1970. The sulphides in the layered sequence of the Bushveld igneous complex. In *Symposium on the Bushveld Igneous Complex and Other Layered Intrusions.* Editors G Vissler and J L Von Gruenewaldt, Geological Society of South Africa, Special Publication 1, pp 108-207.

Lord, J and Markovic, S, 1970. Control of the liquid phase composition in the differential flotation of some complex Peruvian ores. In Proceedings of the *IXth International Mineral Processing Congress.* Prague, Czechoslovakia. Institution of Mining and Metallurgy, London , pp 258-269.

Luganov, V and Bitimbaev, M, 2000. Processing of oxidized zinc-lead bearing raw materials. In Proceedings of the *XXIst International Mineral Processing Congress,* Rome, Italy. Volume B - Oral Sessions, pp B10-30 - B10-37.

Luttrell, G H and Yoon, R H, 1984. The collectorless flotation of chalcopyrite ores using sodium sulfide. *International Journal of Mineral Processing*, 13, 271-283.

Lynch, A J, Johnson, N W, Manlapig, E V and Thorne, C G, 1981. Mathematical models of flotation. In *Mineral and coal flotation circuits, their simulation and control.* Developments in Mineral Processing, Elsevier, Amsterdam, pp 57-96.

Malghan, S S, 1986. Role of sodium sulphide in the flotation of oxidized copper, lead and zinc ores. *Minerals and Metallurgical Processing*, 158-163.

Malysiak, V, O'Connor, C, Ralston, J, Gerson, A, Coetzer, L and Bradshaw, D J, 2002. Pentlandite-feldspar interaction and its effect on separation by flotation. *International Journal of Mineral Processing*, 66, 89-106.

Malysiak, V, Shackleton, N J and O'Connor, C T, 2004. An investigation into the floatability of a pentlandite-pyroxene system. *International Journal of Mineral Processing*, 74, 251-262.

Marabini, A M, Alesse, V and Garbassi, F, 1984. Role of sodium sulphide, xanthate and amine in flotation of lead zinc oxidized ores. In the Proceedings of the *Reagents in the Mineral Industry Conference.* Institution of Mining and Metallurgy, London, United Kingdom, pp 125-136.

Marabini, A M and Rinelli, G, 1986. Flotation of lead-zinc oxide ores. In the Proceedings of *Advances in Mineral Processing: Symposium honouring Nathaniel Arbiter.* Society of Mining Engineers, New Orleans, pp 269-289

McCarron, J J, Walker, G W and Buckley, A N, 1990. An X-ray photoelectron spectroscopic investigation of chalcopyrite and pyrite surfaces after conditioning in sodium sulfide solutions. *International Journal of Mineral Processing*, 30, 1-16.

McGlashan, D W, Rovig, A D and Podobnik, D M, 1969. Assessment of interfacial reactions of chalcopyrite. *Transactions American Institute of Mining, Metallurgical and Petroleum Engineers*, 224, 446-52

Migdisov, A A, Williams-Jones, A E, Lakshtanov, L Z and Alekhin, Y V V, 2002. Estimates of the second dissolution constant of the H_2S from the surface sulfidation of crystalline sulphur. *Geochimica et Cosmochimica Acta*, 66, 1713-1725.

Mitrofanov, S I, 1958. Solution of some problems concerning the theory and practice of selective flotation in the USSR. *Progress in Mineral Dressing, Transactions of the*

International Mineral Dressing Congress, Stockholm 1957. Editor S Gruvföreningen, Almquist and Wiksell Publishers, Stockholm, pp 441-478.

Mitrofanov, S I and Kushnikova, V G, 1958. Kinetics of sulfidation of smithsonite and calamine and adsorption of collector on their surface. *Tsvetnye Metally*, 31, 62-65. CAN 52:96904 (Abstract).

Mitrofanov, S I and Kushnikova, V G, 1959. Sulfidization of difficulty floated oxidised zinc minerals. *Sbornik Nauch.Trudov.,Gosudarst.Nauch.-Issledovatel Inst. Tsvetnykh Metally*, 16, 33-40. CAN 55:136454 (Abstract).

Mitrofanov, S I, Strigin, I A, Kushnikova, V G, and Rozoyskij, G S, 1955a. Sulfidization reaction of oxidised minerals. *Sbornik Nauch.Trudov.,Gosudarst.Nauch.-Issledovatel Inst. Tsvetnykh Metally*, 10, 7-29. CAN 50:88572 (Abstract).

Mitrofanov, S I, Kushnikova, V G and Frumkina, R A, 1955b. Flotation of oxidised lead minerals. *Sbornik Nauch.Trudov.,Gosudarst.Nauch.-Issledovatel Inst. Tsvetnykh Metally*, 10, 41-51. CAN 50:81553 (Abstract).

Mitrofanov, S I, Kushnikova, V G and Frumkina, R A, 1957. Flotation of anglesite and wulfenite. *Sbornik Nauch.Trudov.,Gosudarst.Nauch.-Issledovatel Inst. Tsvetnykh Metally*, 13, 5-19. CAN 55:17151 (Abstract).

Monks, A J and Weiss, N L, 1930. Concentration of oxidized lead ores at San Diego mill, Cia Minera Asarco. *Mines and Metallurgie*, 11, 455-458.

Mwema, M and Mpoyo, M, 2001. Improvements of cobalt recovery in flotation of cupro-cobaltiferous ore at Gecamines. In Proceedings of the *SAIMM Copper Cobalt Nickel & Zinc Recovery Conference, Victoria Falls, Zimbabwe*, SAIMM/IMM, pp 1-9.

Mycroft, J W, Nesbitt, H W and Pratt, A R, 1995. X-ray photoelectron and Auger electron spectroscopy of air oxidized pyrrhotite: distribution of oxidized species with depth. *Geochimica et Cosmochimica Acta*, 59, 721-733.

Nagaraj, D R and Gorken, A, 1991. Potential-controlled flotation and depression of copper sulfides and oxides using hydrosulfide in non-xanthate systems. *Canadian Metallurgical Quarterly*, 30, 79-86.

Nesbitt, H W and Muir, I J, 1994. X-ray photoelectron spectroscopic study of a pristine pyrite surface reacted with water vapour and air. *Geochimica et Cosmochimica Acta*, 58, 4667-4679.

Nesbitt H W, Schauβuss A G, Bancroft G M and Szargan R, 2002. Crystal orbital contributions to the pyrrhotite valence band with XPS evidence for weak Fe-Fe π bond formation. *Physical Chemistry of Minerals,* 29, 72–77.

Newell, A J H, Bradshaw, D J, Harris, P J, 2006. The effect of heavy oxidation upon flotation and potential remedies for Merensky type sulfides. *Minerals Engineering,* 19, 675–686.

Ney, P, 1973. Zeta-potential und Flotierbarkeit von Mineralen. *Applied Mineralogy: Technische Mineralogie,* Springer-Verlag, Vienna, pp 80-95.

O'Connor, C T, Malysiak, V, Shackleton, N J, 2006. The interaction of xanthates and amines with pyroxene activated by copper and nickel. *Minerals Engineering,* 19, 799-806.

O'Reilly, W, Hoffmann, V, Chouker, A C, Soffel, H C and Menyeh, A, 2000. Magnetic properties of synthetic analogues of pyrrhotite ore in the grain size range 1-24μm. *Geophysical Journal International,* 142, 669-683.

Orion, 1996. Instruction Manual: Model 9416 Silver/Sulfide Half Cell and Model 9616 Sure-Flow™ Combination Silver/Sulfide Electrodes, *Orion Research Incorporated.*

Orwe, D, Grano, S R and Lauder, D W, 1997. Chalcocite oxidation and its influence on fine copper recovery at the Ok Tedi Concentrator, Papua New Guinea. In Proceedings of the *Sixth Mill Operator's Conference,* Madang, Papua New Guinea, pp 85-95.

Orwe, D, Grano, S R and Lauder, D W, 1998. Increasing fine copper recovery at the Ok Tedi Concentrator, Papua New Guinea. *Minerals Engineering,* 11, 171-187.

Ozbayoglu, G, Atalay, U, and Senturk, B, 1994. Flotation of lead and zinc carbonates ore. In Proceedings of the *3rd International Recent Advances in Materials and Mineral Resources Conference*: Penang, Malaysia, pp 504-509.

Pankhurst, Q A and Pollard, R J, 1992. Structural and magnetic properties of ferrihydrite. *Clays and Clay Minerals,* 40, 268-272.

Parks, G A, 1965. The isoelectric points of solid oxides, solid hydroxides, and aqueous hydroxo complex systems. *Chemical Reviews,* 65, 177-198.

Pearce, C I, Pattrick, R A D and Vaughan, D J, 2006. Electrical and Magnetic Properties of Sulfides. In *Sulfide Mineralogy and Geochemistry,* Editor D J Vaughan, *Reviews in Mineralogy and Geochemistry,* Volume 61, Chapter 3, Mineralogical Society of America, Chantilly, Virginia, pp 127-180.

Peiffer, S, dos Santo Afonso, M, Wehrli, B and Gachter, R, 1992. Kinetics and mechanism of the reaction of H_2S with lepidocrocite. *Environmental Science and Technology,* 26, 2408-2413.

Pereira, C A and Peres, A E C, 2005. Reagents in calamine zinc ores flotation. *Minerals Engineering,* 18, 275-277.

Poulton, S W, Krom, M D, Van Rijn, J, Raiswell, R and Bows, R, 2003. Detection and removal of dissolved hydrogen sulphide in flow through systems via the sulphidation of hydrous iron (111) oxides. *Environmental Technology*, 24, 217-229.

Pratt, A R, Muir, I J and Nesbitt, H W, 1994. X-ray photoelectron and Auger electron spectroscopic studies of pyrrhotite and mechanism of air oxidation. *Geochimica et Cosmochimica Acta*, 58, 827-841.

Quast, K, Tsatouhas, G, Wong, K Y and Newell, R, 2005. The use of polysulfide as an alternative sulfidising reagent for the CPS flotation of oxide copper ores. In Proceedings of the *Centenary of Flotation Symposium*, Editor G J Jameson, Brisbane, Australia, a Joint Meeting of SME and the AusIMM, pp 1027-1032.

Queirolo, C and Castro, S, 1976. Effect of sulfidisation on the flotation of thermally activated chrysocolla. *Transactions of the Institution of Mining and Metallurgy Section C*, 85, 166-168.

Raghavan, S, Adamec, E and Lee, L, 1984. Sulfidization and flotation of chrysocolla and brochantite. *International Journal of Mineral Processing*, 12, 173-191.

Rand, D A J, 1977. Oxygen reduction on sulphide minerals. Part 111- Comparison of activities of various copper, iron, lead and nickel mineral electrodes. *Journal of Electroanalytical Chemistry*, 83, 19-32.

Rao, S R, and Hepler, L, 1977. Equilibrium constants and thermodynamics of ionization of aqueous hydrogen sulfide. *Hydrometallurgy*, 2, 293-299.

Rey, M, 1954. Flotation of oxidized ores of lead, copper, and zinc. *Bulletin - Institution of Mining and Metallurgy*, 574, 541-548.

Rey, M, Chataignon, P and Formanek, V, 1950. The influence of certain inorganic salts on the flotation of lead carbonate. *Mining Engineering*, 187, 1126.

Rey, M, De Merre, P, Mancuso, R and Formanek, V, 1961. Recent research and developments in the flotation of oxidized ores of copper, lead and zinc. *Colorado School of Mines Quarterly*, 56, 163-175.

Richardson, S and Vaughan, D J, 1989. Surface alteration of pentlandite and spectroscopic evidence for secondary violarite formation. *Mineralogical Magazine*, 53, 213-222.

Rickard, D T, 1969. The chemistry of iron sulfide formation at low temperatures. *Acta University of Stockholm*, 20, 67-95.

Rickard, D T and Luther, G L, 2006. Metal Sulfide Complexes and Clusters. In *Sulfide Mineralogy and Geochemistry,* Editor D J Vaughan, *Reviews in Mineralogy and Geochemistry*, Volume 61, Chapter 8, Mineralogical Society of America, Chantilly, Virginia, pp 421-504.

Roine, A, 2002. HSC Chemistry for Windows. Version 5.1. *Outokumpu Research Oy.*

Rosas, J E and Poling, G W, 1975. Emulsion flotation of non-sulphide copper ores. In Proceedings of the *XIth International Mineral Processing Congress*, Calvary, Canada, pp 73-98.

Rosso, K M and Vaughan, D J, 2006. Sulfide Mineral Surfaces. In *Sulfide Mineralogy and Geochemistry,* Editor D J Vaughan, *Reviews in Mineralogy and Geochemistry*, Volume 61, Chapter 9, Mineralogical Society of America, Chantilly, Virginia, pp 505-556.

Rubio, J and Matijevic, E, 1979. Interaction of metal hydroxides with chelating agents. 1. β-Fe-OOH-EDTA. *Journal of Colloid and Interfacial Science*, 68, 408-421.

Rumball, J A and Richmond, G D, 1996. Measurement of oxidation in a base metal flotation circuit by selective leaching with EDTA. *International Journal of Mineral Processing*, 48, 1-20.

Salatic, D, Puštrić, S and Djaković, D, 1975. Influence of Copper and zinc salts on the surface phenomena of galena, chalcopyrite and sphalerite and the correlation between their zeta-potential and floatability. *Special Issue – Proceedings of the XIth International Mineral Processing Congress*, Universita di Cagliari, Cagliari, pp 59-71.

Salum, M J G, de Araujo, A C and Peres, A E C, 1992. The role of sodium sulphide in amine flotation of silicate minerals. *Minerals Engineering*, 5, 411-419.

Sato, M, 1960a. Oxidation of sulfide ore bodies. I. Geochemical environments in terms of Eh and pH. *Economic Geology* , 55, 928-961.

Sato, M, 1960b. Oxidation of sulfide ore bodies II. Oxidation mechanisms of sulfide minerals at 25 degree C. *Economic Geology*, 55, 1202-1231.

Schaußuss, A G, Nesbitt, H W, Kartio, I, Laajalehto, K, Bancroft , G M and Szargan, R, 1998. Reactivity of surface chemical states on fractured pyrite. *Surface Science,* 411, 321–328.

Schindler, P W and Stumm, W, 1996. The surface chemistry of oxides, hydroxides, and oxide minerals. In *Aquatic surface chemistry*, Editor W Stumm, John Wiley and Sons, New York, pp 83-109.

Schoonen, M A A and Barnes, H L, 1991. Reactions forming pyrite and marcasite from solution. II. Via FeS precursors below 100 degree C. *Geochimica et Cosmochimica Acta*, 55, 1505-1514.

Schwarz, A, 1905. Process for concentrating ores. *USA Patent no. 807,501.*

Senior, G D, Shannon, L K and Trahar, W J, 1990. The flotation of pentlandite from pyrrhotite with particular reference to the effects of particle size. *International Journal of Mineral Processing*, 42, 169-190.

Shea, D and Helz, G R, 1988. The solubility of copper in sulfidic waters: Sulfide and polysulfide complexes in equilibrium with covellite. *Geochimica et Cosmochimica Acta*, 52, 1815-25.

Shirley, D A, 1972. High-resolution X-ray photoemission spectrum of the valence bands of gold. *Physical Reviews B,* 5, 4709–4714.

Shungu, T, Vermaut, N and Ferron, C J, 1988. Recent trends in the Gecamines copper cobalt flotation plants. *Minerals and Metallurgical Processing,* 163-170.

Skinner, W M, Nesbitt, H W and Pratt, A R, 2004. XPS identification of bulk hole defects and itinerant Fe 3d electrons in natural troilite (FeS). *Geochimica et Cosmochimica Acta,* 68, 2259–2263.

Smart, R St C, 1991. Surface layers in base metal sulphide flotation. *Minerals Engineering,* 4, 891-909.

Smart, R St C, 1994. Chemical and structural alteration in the surface layers of oxides. In *Science of Ceramic Interfaces II.* Editor J Nowotny, Elsevier Science, pp 311-339.

Smart, R St C, Amarantidis, J, Skinner, W M, Prestidge, C, La Vanier, L and Grano, S, 2003. Surface analytical studies of oxidation and collector absorption in sulfide mineral flotation. *Topics in Applied Physics,* 85, pp 3-60.

Snodgrass, R, Hay, M and Du Preez, P, 1994. Process development and design of Northam Merensky Concentrator. In Proceedings of the *XVth Commonwealth Mining and Metallurgical Institute Congress,* Johannesburg, RSA, SAIMM, Johannesburg, pp. 341-357.

Soto, H and Laskowski, J S, 1973. Redox conditions in the flotation of malachite with sulphidizing agent. *Transactions of the Institution of Mining and Metallurgy,* Section C, 82, 153-157.

Steudel, R, 2000. Sulfide and polysulfide - 1.3.1 - Hydrogen sulfide and sulfide ions. In *Environmental technologies to treat sulfur pollution, principles and engineering.* Editors P Lens and L Hulshoff Pol, IWA Publishing, London, pp 10-31.

Sutherland, K L and Wark, I W, 1955. Principles of Flotation. Australasian Institute of Mining and Metallurgy, Melbourne, pp 137-141.

Sui, C, Brienne, S H R, Rao, S R, Xu, Z and Finch, J A, 1995. Metal ion production and transfer between sulphide minerals. *Minerals Engineering,* 8, 1523-1539.

Thornber, M R, 1983. Mineralogical and electrochemical stability of the nickel-iron sulphides - pentlandite and violarite. *Journal of Applied Electrochemistry,* 13, 253-267.

Tian, J, 2003. Zinc oxide flotation process using CPS technique. In Proceedings of the *XXIInd International Mineral Processing Congress,* Editors L Lorenzen and D J Bradshaw, Cape Town, South Africa, p 369.

Tolun, R and Kitchener, J A, 1964. Electrochemical study of the galena-xanthate-oxygen flotation system. *Bulletin of Institution of Mining and Metallurgy,* 687, 313-22.

Vanthuyne, M and Maes, A, 2002. The removal of heavy metals from contaminated soil by a combination of sulfidisation and flotation. *Science of the Total Environment*, 290, 69-80.

Vaughan, D J, England, K E R, Kelsall, G H and Yin, Q, 1995. Electrochemical oxidation of chalcopyrite ($CuFeS_2$) and the related metal-enriched derivatives $Cu_4Fe_5S_8$, $Cu_9Fe_9S_{16}$ and $Cu_9Fe_8S_{16}$. *American Mineralogist*, 80, 725-731.

Velásquez, P, Leinen, D, Pascual, J, Ramos-Barrado, J R, Grez, P, Gómez, Schrebler, R, Del Rio, R and Córdova, R, 2005. A chemical, morphological, and electrochemical (XPS, SEM/EDX, CV and EIS) analysis of electrochemically modified electrode surfaces of natural chalcopyrite ($CuFeS_2$) and pyrite (FeS_2) in alkaline solutions. *Journal of Physical Chemistry B*, 109, 4977-4988.

Viljoen, M J, Theron, J, Underwood, B, Walters, B M, Weaver, J and Peyerl, W, 1986. The Amandebult section of Rustenburg Platinum Mines Limited, with reference to the Merensky Reef. *Mineral Deposits of Southern Africa*, Editors C R Anhaeusser and S Maske, Geological Society of South Africa, Volume 2, pp 1041-1060.

Walker, G W, Walters, C P and Richardson, P E, 1986. Hydrophobic effects of sulfur and xanthate on metal and mineral surfaces. *International Journal of Mineral Processing*, 18, 119-137.

Wang, H, Nakamura, H, Yao, K, Uehara, M, Nishimura, S, Maeda, H and Abe, E, 2002. Effect of polyelectrolyte dispersants on the preparation of silica-coated zinc oxide particles in aqueous media. *Journal of the American Ceramic Society*, 85, 1937-1940.

Wang, D and Qin, W, 1997. Electrochemistry of sodium sulphide - induced flotation of sulfide minerals. *Non ferrous metals-Beijing*, 45-48. English abstract.

Warner, T E, Rice, N M and Taylor, N, 1992. Electrochemical study of the dissolution of pentlandite. *Hydrometallurgy*, 31, 55-90.

Warner, T E, Rice, N M and Taylor, N, 1996. Thermodynamic stability of pentlandite and violarite and new E-pH diagrams for the iron-nickel sulphur aqueous system. *Hydrometallurgy*, 41, 107-118

Wei, D and Osseo-Asare, K, 1995. Formation of iron monosulfide : A spectroscopic study of the reaction between ferrous and sulfide ions in aqueous solutions. *Journal of Colloid and Interface Science*, 174, 273-282.

Wiese, J, Harris, P and Bradshaw, D, 2005. Investigation of the role and interactions of a dithiophosphate collector in the flotation of sulphides from the Merensky reef. *Minerals Engineering*, 18, 791-800.

Woods, R, Constable, D and Hamilton, I, 1989. A rotating ring disc electrode study of the oxidation of sulphur (-II) species on gold and sulfide minerals. *International Journal of Mineral Processing*, 27, 309-326.

Wright, A J and Prosser, A P, 1965. Study of reactions and flotation of chrysocolla with alkali-metal xanthates and sulphides. *Transactions of the Institution of Mining and Metallurgy*, 1964-1965, 259-279.

Yin, Q, Vaughan, D J, England, K E R; Kelsall and G H, Brandon, N P, 2000. Surface oxidation of chalcopyrite ($CuFeS_2$) in alkaline solutions. *Journal of the Electrochemical Society*, 147, 2945-2951.

Yin, Q, Kelsall, G H, Vaughan, D J and England, K E R, 1995. Atmospheric and electrochemical oxidation of the surface of chalcopyrite ($CuFeS_2$). *Geochimica et Cosmochimica Acta*, 59, 1091-1100.

Zachwieja, J B, McCarron, J J, Walker, G W and Buckley, A N, 1989. Correlation between surface composition and collectorless flotation of chalcopyrite. *Journal of Colloidal of Interfacial Science*, 132, 462-468.

Zhang, W, 1993. Thirty-year plant practice of sulphidisation-flotation of copper oxidised ores. In the Proceedings of the *XVIIIth International Mineral Processing Congress, Sydney,* Australia, pp 619-624.

Zhang, L, 1994. Technical Note: Electrochemical equilibrium diagrams for sulphidization of oxide copper minerals. *Minerals Engineering*, 7, 927-932.

Zhang, J Z and Millero, F J, 1994. Kinetics of oxidation of hydrogen sulfide in natural waters. *ACS Symposium Series* 550: *Environmental Geochemistry of Sulfide Oxidation*, pp 393-409.

Zhang, W and Poling, G W, 1989. Ammonium sulfate as activator in sulfidised xanthate flotation of malachite. *Canadian Institute of Mining and Metallurgical Bulletin,* 82, 35-39.

Zhang, W and Poling, G W, 1991. Sulfidisation-promoting effects of ammonium sulfate sulfidised xanthate flotation of malachite. In the *Proceedings of the XVIIth International Mineral Processing Congress*, Dresden, Germany, pp 187-197.

Zhou, R and Chander, S, 1993. Kinetics of sulphidisation of malachite in hydrosulfide and tetrasulfide solutions. *International Journal of Mineral Processing*, 37, 257-272.